ČESKÁ ZEMĚDĚLSKÁ UNIVERZITA V PRAZE
Fakulta agrobiologie, potravinových a přírodních zdrojů
Katedra pedologie a ochrany půd

Biogeochemie thallia s využitím modelové rostliny (*Sinapis alba* L.)

.....

doktorská disertační práce

Autor: **Ing., Ondřej Holubík**

Školitel: **doc. RNDr., Aleš Vaněk, Ph.D.**

Konzultant: **Prof. RNDr. Martin Mihaljevič, CSc.**

Praha 2 0 2 1

Čestné prohlášení

Prohlašuji, že jsem disertační práci (DSP) „Biogeochemie thallia s využitím modelové rostliny (*Sinapis alba* L.)“ zpracoval samostatně pod vedením svého školitele doc. RNDr, Aleše Vaňka, PhD.

V Praze dne 1.4.2021 _____

Poděkování

Rád bych touto cestou poděkoval především svému školiteli Aleši Vaňkovi, doc., RNDr., Ph.D., za příkladné vedení a spolupráci při realizaci všech výsledků DSP. Děkuji svému konzultantovi Martinu Mihaljevičovi, prof. RNDr. CSc., za podněty při řešení a měření analytických dat pomocí ICP-MS.

Děkuji Katedře pedologie a ochrany půdy ČZU za možnost studovat na katedře a podílet se na výsledcích výzkumu stabilních izotopů těžkých prvků (kovů). Děkuji oponentům DSP za věcné připomínky a kritické hodnocení mé práce. Děkuji svému zaměstnavateli a spolupracovníkům na Oddělení pedologie a ochrany půdy VÚMOP, v.v.i., za podporu a časovou úlevu z pracovních závazků. Zvláště děkuji Janu Jiříkovi za technickou podporu a pomoc při realizaci hydroponických experimentů. Závěrem musím poděkovat své rodině a dětem Karolínce, Kryštofovi a Kristýnce za jejich podporu.

OBSAH

1. Přehled o současném stavu problematiky

1.1 Úvod do biogeochemie Tl

Thallium (Tl) je prvek, který je relativně málo zastoupen v zemské kůře (~0,1-1 mg/kg, Barthelmy, 2010). Jeho důležitost v environmentálním výzkumu spočívá zejména v prokázané toxicitě pro většinu organismů včetně rostlin. Letální dávka pro člověka při perorálním užití je 20 až 60 mg solí Tl^{I} na kilogram tělesné hmotnosti během jednoho týdne (IPCS, 1996).

Thallium se vyskytuje ve dvou oxidačních stavech, Tl^{I} a Tl^{III}. Ve vodném prostředí se vyskytuje převážně jako jednomocný slabě hydratovaný ion (Sager, 1994). Díky podobnému iontovému poloměru Tl^{+} (149 pm) a K^{+} (133 pm) a analogické valenci může Tl aktivně zastupovat K v biochemických procesech a reakcích (Galván-Arzate et Santamaría, 1998).

Na fyziologické úrovni byla prokázána přímá vazba mezi toxicitou Tl a příjmem K (Sager, 1994). Je zřejmé, že podobnost iontového poloměru Tl a K může hrát důležitou roli i při vstupu Tl do rostlinných pletiv (Krasnodębska-Ostręga et al., 2012; Scheckel et al., 2004; Tremel et al., 1997; Xiao et al., 2004). Merian et Clarkson (1991) popisují také chalkofilní charakter Tl a dokládají jeho silnou afinitu k thiolovým skupinám (-SH). Tremel et al. (1997) pak na konkrétních případech popisují převládající asociaci Tl s rostlinným materiálem bohatým na S, jejichž vlivem dokáže Tl inhibovat některé enzymatické reakce. Mestek et al. (2007) ve své studii uvádí, že až 70 % Tl obsaženého v cytosolu (*Brassica napus* L.) není vázáno v komplexních sloučeninách a nemá přímou vazbu na aminokyseliny, popř. peptidy rostlin obsahující S (cystein a methionin). Většina Tl v cytosolu se vyskytuje jako volný jednomocný iont Tl^{+}. Jako významný faktor pro vznik komplexů se slabou vazebnou interakcí k Tl (ve vakuolách buněk listu) uvádějí Mestek et al. (2007) existenci volné iontové vazby.

1.2 Vstup Tl do životního prostředí a půdy

Světová komerční produkce Tl se odhaduje na 10–15 t za rok (Hammond, 1990; Merian et Clarkson, 1991). Přirozeně (tj. zvětráváním hornin) je odhadován vstup „přírodního“ Tl do životního prostředí v objemu ~2400 t/rok (Bowen, 1979). Přibližně 2000-7000 t Tl za rok je globálně mobilizováno lidskou činností (Kabata-Pendias et Pendias, 1992; Kabata-Pendias et Sadurski, 2004). Do životního prostředí vstupuje Tl z odpadních materiálů, emisí ze spalování uhlí, v důsledku těžby a zpracování rud (ZnS, PbS, FeS_2 apod.). Dalším potenciálním zdrojem antropogenního Tl souvisí s uplatněním kovových aditiv na bázi FeS_2 při výrobě cementu (Kazantzis, 2000; C Yang et al., 2009).

Komerční využití Tl souvisí zejména s výrobou anodových desek a nízkoteplotních spínačů (Hammond, 1990). Thallné soli se používají jako polovodiče pro teploměry, optické systémy, popř. infračervené detektory (Hammond, 1990). V experimentálním výzkumu se Tl využívá např. jako vysokoteplotní supravodič (Waldrop, 1988). Organokovové sloučeniny Tl se stále využívají v organické syntéze, resp. chemii cyklopentadienylových komplexů (Peter et Viraraghavan, 2005).

Sloučeniny antropogenního Tl jsou v půdách relativně dobře rozpustné a tedy i často mobilní (Kabata-Pendias et Pendias, 1992). Existuje však jen omezené množství prací (Kersten et al., 2014; Vaněk et al., 2016; Vaněk, Mihaljevič, et al., 2013; Wierzbicka et al., 2004) hodnotící vstup antropogenního Tl z půdy do rostlinné biomasy.

V půdách se Tl vyskytuje především asociované s primárními minerály se zvýšeným obsahem K (např. muskovit, orthoklas, K-živce apod.), ev. může být vázáno v sulfidech (např. v pyritu FeS_2 a sfaleritu ZnS) (Vaněk et al., 2009). V půdním systému má Tl ambivalentní (litofilní i chalkofilní) charakter (Vaněk et al., 2009, 2020). Ačkoliv nebyla dosud zcela objasněna chemická speciace Tl v půdách, předpokládá se, že je přítomno převážně v jednomocné formě. V této formě (Tl^{I}) je dominantně uvolňováno do půdního roztoku (Merian et Clarkson, 1991).

Thallium může být v půdách specificky sorbováno/fixováno na povrchu některých jílových minerálů, specifických oxidů Mn, ev. síranů (Vaněk et al., 2009). Asociace Tl byla zkoumána na povrchu illitu (Wick et al., 2018), jarositu (Voegelin et al., 2015) a zejména birnessitu δ-MnO_2 (Grösslová et al., 2015; Nielsen et al., 2013; Peacock et Moon, 2012; Vaněk et al., 2011; Vaněk, Mihaljevič, et al., 2013). Ve specifické sorpci na povrchu birnessitu se Tl vyskytuje nejen v jednomocné formě (Tl^{I}), ale také ve formě trojmocné (Tl^{III}) (Voegelin et al., 2015). Peacock et Moon (2012) popisují mechanizmus specifické

absorpce Tl na δ-MnO_2 přes Mn-vakance, kdy je Tl^I oxidováno do trojmocné formy Tl^{III} a vázáno ve vnitřní sféře Mn-komplexu. Obecně pevně vázané Tl v Mn-komplexu a Tl v půdním roztoku vykazují mezi sebou posun v izotopového složení (Peacock et Moon, 2012). Při interpretaci změny izotopické signatury Tl na povrchu Mn-komplexů hraje důležitou roli také obsah Tl „vázaného“ ve vnější sféře Mn-komplexu (Nielsen et al., 2013).

1.3 Vstup Tl do rostliny

Mechanizmus vstupu Tl z půdy do rostliny je specifický a poměrně složitý proces, kde se vzájemně prolínají faktory definované půdními podmínkami s účinky rostlin a asociovaných mikroorganismů a hub. Přístupnost Tl z půdy závisí primárně na celkovém obsahu Tl v půdě, jeho mineralogické formě, asociaci s oxidy Mn, sorpci na jílové minerály (např. illitu), obsahu karbonátů a potenciální alteraci Tl v půdě apod. (Grösslová et al., 2015; Xiao et al., 2010). Zároveň může být Tl aktivně, ale i pasivně absorbováno mikroorganismy (Skłodowska et Matlakowska, 2004). Vstup Tl do rostliny je následně ovlivněn charakterem rostlinných exudátů a stavem mikrobiologických procesů v půdě (Kunze, 1973).

Vstup Tl do rostlinných pletiv a jeho uložení v rostlině závisí především na rostlinné fyziologii (struktuře vodivých pletiv a zásobních orgánů, charakteru rostlinných exudátů), ale také na stavu enzymatických procesů v půdě (Merian et Clarkson, 1991). Tyto faktory přímo ovlivňují strategii růstu pěstované rostliny a mají významný vliv nejen na příjem Tl, ale také na jeho následnou distribuci a uložení v rostlinném pletivu (Holubík et al., 2020; Sager, 1994). Thallium je obecně relativně snadno absorbováno kořeny většiny rostlin, pravděpodobně v důsledku podobnosti s K (Sherlock et Smart, 1986). Předpokládá se, že většina biopřístupného Tl vstupuje do rostliny (aktivně/pasivně) přes protoplazmu endodermálních buněk na povrchu kořenového vlášení. Distribuce Tl v rostlině probíhá přes vodivá pletiva (xylemu) stonku. Místo samotné bioakumulace Tl v rostlinných pletivech závisí specificky na fyziologii konkrétní rostliny (Al-Najar et al., 2003, 2005; Leblanc et al., 1999; Pavlíčková et al., 2006; Sager, 1994). Pro čeledi okřehkovitých (*Lemnaceae*) a brukvovitých (*Brassicaceae*) byla významná část Tl detekována v buněčném cytosolu ve vakuolách buněk listu (Kwan et Smith, 1991; Ning et al., 2015).

Nejvyšší obsahy Tl v rostlinách byly zaznamenány u čeledi brukvovitých (*Brassicaceae*), které jsou proto často označovány za (hyper)akumulátory Tl (Al-Najar et al., 2003; Pavlíčková et al., 2005; Sherlock et Smart, 1986; van der Ent et al., 2013).

Zkoumány byly například: *Iberis intermedia* Guers. (iberka), *Biscutella laevigata* L., *Brassica oleracea acephala* L. (kapusta), *Brassica napus* L. (řepka) a *Sinapis alba* L. (hořčice bílá) (Al-Najar et al., 2005; Al-Najar et al., 2003; Madejón et al., 2007; Mazur et al., 2016; Sadowska et al., 2016; Scheckel et al., 2004; Tremel et al., 1997; Vaněk et al., 2010, 2011; Xiao et al., 2004). Některé druhy rostlin jako *Biscutella laevigata* (dvojštítek hladkoplodý), *Iberis intermedia* (iberka prostřední), *Silene latifolia* (silenka širolistá) (van der Ent et al., 2013), *Brassica oleracea acephala* (kapusta kadeřavá) (Al-Najar et al., 2003) se ukázaly jako potenciálně využitelné pro fytoremediační účely Tl.

V současnosti je zásadní veškerou snahu o uplatnění příp. fytoremediačních postupů směřovat do oblastí v Číně, Austrálii, USA a Peru, které jsou postiženy masivní expozicí Tl (Gutiérrez et al., 2016). Uvolnění Tl z běžných odpadních materiálů závisí především na celkovém obsahu biologicky dostupné formy Tl v odpadu (Harmsen, 2007). Pro fytoremediační účely je tak zásadní výběr vhodné rostliny, která je tolerantní ke specifickým podmínkám prostředí a zároveň disponuje rychlým růstem s vysokou bioakumulací polutantu v pletivu (Robinson et Anderson, 2018). Pro fytoextrakční účely je rozhodující, aby rostlina vykazovala hyperakumulační schopnost, vysokou toleranci a specifickou (pevnou) vazbu toxického prvku v rostlinném pletivu (Corzo Remigio et al., 2020). Velmi často se jedná o specifickou vazbu prvku ve formě fytochelatinů ve vakuolách buněk listu (van der Ent et al., 2013).

Existuje řada publikací popisujících biosorpci Tl z půdy (Al-Najar et al., 2003; Anderson et al., 1999; Grösslová et al., 2015; Leblanc et al., 1999; Ning et al., 2015; Pavlíčková et al., 2005; Wierzbicka et al., 2004). Na druhou stranu, existuje pouze minimum prací (Allus et al., 1987; Kim et al., 2016), které srovnávají vstupy Tl do rostliny při odlišném způsobu pěstování (v hydroponickém roztoku a v půdě).

Je dobře známo, že hydroponická kultivace může poskytnout ideální systém pro monitorování specifických reakcí na rozhraní roztok - rostlina (Fargašová, 2004; Kim et al., 2016; Smeets et al., 2008). V rámci fyziologie rostlin jsou popisovány rozdílné růstové strategie rostlin pěstovaných v půdě a při hydroponické kultivaci (Taiz et Zeiger, 2003). Lze předpokládat, že porovnání příjmu Tl rostlinou pěstovanou v hydroponii a v půdě může poskytnout zásadní informace pro uplatnění těchto rostlin pro případné fytoextrakční a fytoremediační účely.

1.4 Principy studia stabilních izotopů Tl

Studium izotopů Tl zaznamenalo v posledních 20 letech významný rozvoj, který byl umožněn především vývojem citlivé hmotnostní spektrometrie typu MC-ICP-MS (multikolektorové hmotnostní spektroskopie s indukčně vázaným plazmatem). Izotopová analýza Tl pomocí MC-ICP-MS musí být s ohledem na existenci tzv. „instrumentálního driftu" a „mass bias efektu" paralelně externě a interně korigována. Při měření izotopového složení Tl v environmentálním vzorku na MC-ICP-MS lze dosáhnout přesnosti stanovení až 0,01-0,02 % (Nielsen et al., 2004).

Thallium má dva stabilní přírodní izotopy ^{203}Tl (přirozený výskyt 29,524 %) a ^{205}Tl (70,476 %). Jejich stabilní izotopový poměr je přibližně 2,3887. Tento poměr je při měření korigován pomocí standardů Pb (NIST SRM 981) a Tl (NIST SRM 997, National Institute of Standards and Technology, USA). Izotopické složení Tl (ε^{205}Tl) se udává jako relativní odchylka od standardu NIST SRM 997 v jednotkách 10^4 (1) (Nielsen et al., 2004; Rehkämper et Halliday, 1999).

$$\varepsilon^{205}\mathrm{Tl}_{\mathrm{sample}} = 10^4 \cdot \frac{^{205}\mathrm{Tl}/^{203}\mathrm{Tl}_{\mathrm{sample}} - {}^{205}\mathrm{Tl}/^{203}\mathrm{Tl}_{\mathrm{NIST997}}}{^{205}\mathrm{Tl}/^{203}\mathrm{Tl}_{\mathrm{NIST997}}} \quad (1)$$

Izotopová signatura Tl je ovlivněna především reakční kinetikou izotopů prvků ve sledovaném systému (Wiederhold, 2015). Nejširší izotopový posun (frakcionací) se udává pro redoxní reakce. Nicméně pro komplexní popis změny izotopového složení zkoumaného prvku ve specifickém systému bývá často nutné uvažovat i o dalších typech reakcí a interakcí (zejména o reakcích komplexotvorných, srážecích, popř. enzymatických). Systémy s vyšší kinetikou jsou popisovány na pozadí tzv. Rayleighova kinetického modelu (modelu, který vychází z reakční kinetiky destilačních směsí a zanedbává zpětnou reakci v systému). Rayleighův model lze ve své podstatě využít pouze pro popis homogenních, konstantně smíšených systémů (evaporace, difúze, popř. spalovací procesy).

Obecně platí, že v uzavřeném systému nabohacení (těžších/lehčích) izotopů v reservoáru (např. v rostlině) znamená jejich ochuzení v okolním systému. Pro studium izotopové signatury jsou proto často voleny modelové podmínky ve snaze sledovat pouze jedinou změnu izotopového složení. Tento přístup byl i smyslem řešení této disertační práce, kdy byla snaha sledovat izotopové posuny Tl pouze mezi rostlinou a hydroponickým roztokem. Tento druh přeměny, který teoreticky odpovídá jednomu izotopovému přechodu z okolního rezervoáru do rostliny, se označuje jako biosignatura přechodu kovu do rostliny.

Při popisu izotopové biosignatury nelze uvažovat pouze s kinetikou definovanou podle Rayleighova kinetického modelu, ale je nutné započíst také rovnovážný efekt asociace kovu v systému (Obr. 1, Wiederhold, 2015).

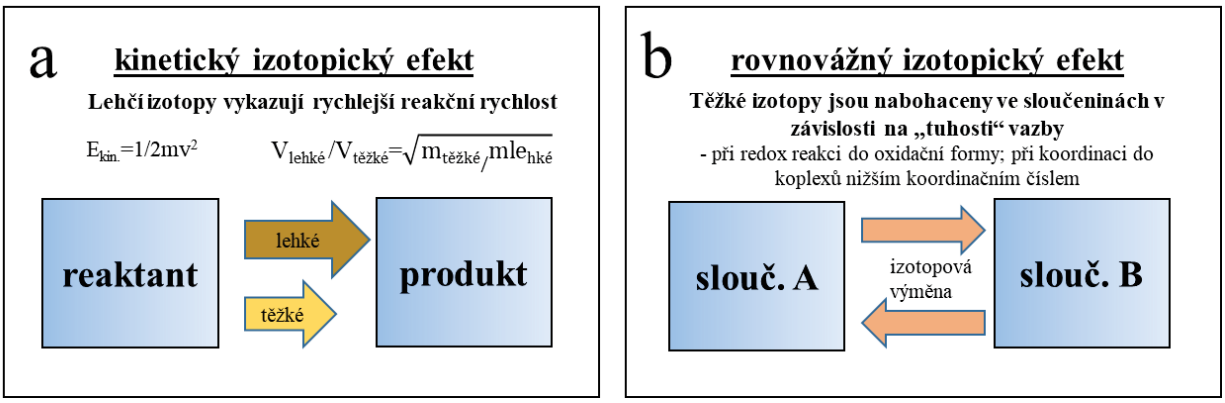

Obr. 1: Schematické znázornění kinetického (a) a rovnovážného (b) modelu stabilní izotopové frakcionace převzato z publikace Wiederhold (2015).

Kinetický efekt je popisován pro systémy s rychlou reakční rychlostí a s preferencí lehčích izotopů. Uplatňuje se v procesech evaporace, difúze a v reakční kinetice na buněčné úrovni ve vazbě enzym-substrát (E-S). Obecně jsou enzymaticky preferovány lehčí izotopy s nižší energií základního stavu atomu prvku. Kinetický efekt tak popisuje přímou reakci reaktantů v produkty a odpovídá Rayleighově modelu reakční kinetiky.

Ovšem většina reakcí v přírodním prostředí směřuje k ustavení izotopové rovnováhy. Přírodní systémy tak vykazují i zpětnou reakci (Baskaran, 2012). Tento stav popisuje rovnovážný izotopický efekt (Wiederhold, 2015). Rovnovážný efekt je nejčastěji interpretován na pozadí vzniku molekulárních vazeb, kdy izotopová rovnováha se obecně ustaluje rychleji v systému se silnější vazebnou interakcí, v systému s vyšším obsahem těžších izotopů, v systému s nižší energií molekulárních vazeb. Rovnovážný efekt se proto logicky snižuje se zvyšující se teplotou systému (Wiederhold, 2015).

Typickým příkladem popisu rovnovážného efektu je ustálení redoxní rovnováhy. Obecně platí, že těžší izotopy jsou řízeny do oxidační formy a lehčí izotopy do redukční formy. V praxi jsou velmi dobře popsány změny izotopové signatury mezi produkty tavení, pražení, spalování, loužení ideálně s výslednými produkty v jediném oxidačním stavu (Kersten et al., 2014; Vaněk et al., 2018). Obdobně lze relativně dobře popsat významný kinetický efekt pro fázové přechody (evaporace, kondenzace) nebo membránové procesy a difúze (Richter et al., 2009).

Analogicky platí pro komplexotvorné rovnováhy, že při vzniku komplexu (kov-ligand) s nižším koordinačním číslem (s kratší a silnější vazbou) dochází k nabohacení těžších izotopů v komplexní sloučenině. Zároveň při koordinaci kovu do tetraedrické a oktaedrické formy, dochází k nabohacení těžších izotopů do formy tetraedru (koordinace s nižším koordinačním číslem, kratší vazbou). V rámci koordinačních vazeb není rozhodující síla vazeb, ale její tuhost (rozdíly ve vibračních stavech atomů). Při koordinaci kovu na organický ligand pravděpodobně dochází k nabohacení těžších izotopů v organické fázi vůči roztoku, jak ukazuje Ryan et al. (2014). Ovšem zcela opačný efekt byl pozorován ve vazbě Hg na organické komplexy s thiolovou (-SH) skupinou (Wiederhold et al., 2010). Tyto předpoklady vzhledem k ambivalentnímu způsobu vazby Tl v organických komplexech (kdy vykazuje jak litofilní, tak i chalkofilní charakter) výrazně komplikují interpretaci měřených dat. Navíc při popisu vstupu Tl z půdního prostředí se velmi často uplatňují i sorpční mechanizmy a přechody z kapalné do pevné fáze.

Pro přirozené (půdní) systémy je proto velmi složité sledovat změnu dynamické rovnováhy a to i pro jednodimenzionální systémy (např. roztok-sorbent). Izotopová frakcionace je nejčastěji řízena pevností vazeb, resp. energií a délkou mezimolekulárních vazeb. Obecně platí, že pro prvky vyskytující se v kationtové formě (Fe^{2+}, Fe^{3+}, Cu^{2+}, Tl^{+} apod.) dochází k nabohacení těžších izotopů na sorpční fázi, kdežto pro prvky v aniontové formě (AsO_4^{3-}, SbO_2^{1-}, SeO_4^{2-} apod.) dochází k nabohacení o lehčí izotopy na sorbentu.

Změna izotopové signatury prvku při disociaci iontu v roztoku je nejčastěji popisována na pozadí čistě kinetického modelu. Rychlost disociace závisí na součinu rozpustnosti sloučeniny. Při disociaci iontu do roztoku je prokázána preference pro lehké izotopy v roztoku (Hofmann et al., 2012).

Sorpce v rhizosféře je řízena enzymaticky, popř. asimilačně, kdy se v závislosti na koncentraci kovu v prostředí uplatňují souběžně dva mechanizmy (aktivní a pasivní transport prvku do rostlinných pletiv, Taiz et Zeiger, 2003). Při popisu vstupu kovu do rostliny je nutné uvažovat i o možném ovlivnění typem chelatační vazby specifických rostlinných exudátů.

Samotný popis změny izotopové signatury Tl při srážení na povrchu minerální fáze (karbonátů, sulfátů, oxidů Fe/Mn, silikátů apod.), kdy dochází zároveň k nabohacení těžkými i lehkými izotopy, je za nízkých (laboratorních) teplot téměř nemožné správně interpretovat.

Při změně izotopové biosignatury (při popisu vstupu prvku do rostliny) se pravděpodobně uplatňují převážně biochemické procesy. V rámci enzymatického systému

dochází často ke specifické sorpci prvku na enzym (E-S rovnováha). Popis takového systému je tak často výsledkem jediného procesu (asimilace, oxidace, redukce, metylace, difuze apod. Beard et al., 1999). Obecně platí, že při vstupu prvku do rostliny dochází k malému nabohacení lehčích izotopů v rostlinném materiálu vůči roztoku. Tyto výsledky se potvrdily i v našich experimentech (Grösslová et al., 2015; Vaněk et al., 2019).

Téměř všechny přirozené procesy, včetně přirozeného výskytu (relativního zastoupení) stabilních izotopů jsou závislé na rozdělení hmotnosti atomů (Baskaran, 2012). Jsou tzv. hmotově závislé a vykazují MDF (mass dependent fractionation). Pouze lehké prvky (O, S) přechází do plynných stavů se stejnou molekulovou symetrií a jsou hmotově nezávislé a vykazují MIF (mass independent fractionation). Pro těžké prvky (Hg, Tl, U) je nutné v rámci popisu izotopové signatury hodnotit posun izotopového spektra vlivem „velikosti" jádra atomu – vykazují NVE (nuclear volume effect). Obecně pouze malá část efektu „velikosti" jádra (NVE) má deviaci v podobě hmotově nezávislého chování (Wiederhold, 2015). Nicméně s ohledem na přesnost stanovení izotopové signatury (faktory ε (10^4) nebo δ (10^3)) při popisu kinetického a rovnovážného efektu je nutné tyto odchylky relativisticky dopočítat (S. Yang et Liu, 2016). Pro těžké prvky (včetně Tl) může být NVE k MDF přičítán, nebo také odčítán (zvyšuje, nebo také snižuje celkovou izotopovou frakcionaci měřeného prvku).

Z dosud dostupných údajů (S. Yang et Liu, 2016) se pro redoxní systém thallia (Tl^I – Tl^{III}) oba efekty (MDF/NVE) sčítají. K celkovému popisu izotopových dat s více než 2 izotopy je potřeba hodnotit i magnetický izotopický efekt (MIE – posun izotopové signatury vlivem jaderného spinu). Při studiu Tl, které má pouze 2 stabilní izotopy ^{203}Tl a ^{205}Tl je však hodnocení MIE irrelevantní.

Pro studium přírodních procesů je izotopová signatura Tl ($\varepsilon^{205}Tl$) s výhodou využívána právě proto, že má pouze 2 stabilní izotopy. Právě díky stálému izotopovému složení Tl lze metody izotopové analýzy využít v environmentální chemii jako stopovače antropogenní zátěže, popř. kontaminace půd (Kersten et al., 2014). Nicméně samotný popis změny izotopového složení Tl je i pro relativně jednoduchý systém půdní roztok-rostlina s ohledem na fyziologií rostlin poměrně komplikovaný.

Proto je výhodné studium izotopové signatury Tl ($\varepsilon^{205}Tl$) kombinovat s pokročilými metodami separace, extrakce a izolace biologického materiálu. K dokreslení možných asociačních mechanizmů Tl v rostlině jsou využívány metody speciační analýzy.

Pro kvantitativní znalost vstupu Tl do rostliny byli v rámci DSP využívány především metody hmotnostní spektroskopie (ICP-MS), popř. optické emisní spektroskopie

(ICP-OES). Pro bližší interpretaci možné asociace Tl v rostlinném pletivu byla využita metoda XANES (rentgenová absorpční spektroskopie). K popisu (bio)geochemické interakce Tl s dalšími prvky byly modelově vyjádřeny korelační koeficienty celkové bioakumulace Tl a živin v rostlinném pletivu.

Popis Tl cyklu v přírodních podmínkách je s ohledem na široké spektrum možných reakcí, interakcí a asociací Tl poměrně komplikované. Nicméně pro možnost popisu „životního cyklu“ Tl na všech úrovních biogeochemického systému je nutné znalosti dílčích izotopových posunů (ε^{205}Tl) neustále prohlubovat. Je pravděpodobné, že během několika málo let bude výzkum izotopové signatury Tl (ε^{205}Tl) v různých (geo)materiálech prohlubován a popis chování Tl v přírodním ekosystému bude možné lépe interpretovat. Při znalosti Tl-cyklu bude možné využít vlastnosti Tl (výskytu pouze 2 stabilních izotopů ^{203,205}Tl), jako stopovače dílčích změn v životním prostředí. Jedním ze střípků této pomyslné mozaiky popisu „životního cyklu“ Tl v prostředí se mohou stát i výsledky této disertační práce.

2. Cíle a hypotézy

Cílem disertační práce (DSP) bylo na podkladech nádobových experimentů popsat vstup Tl do rostlinných pletiv modelové rostliny hořčice bílé (*Sinapis alba* L.).

2.1 Hypotézy

I. Vstup thallia do rostliny je doprovázen změnou izotopového složení.

II. Rozdílný způsob kultivace rostlin má přímý vliv na příjem živin a bioakumulaci Tl do rostlinných pletiv.

III. Vstup Tl do rostliny je doprovázeno příjmem specifického prvku.

2.2 Cíle práce

I. Detekce, kvantifikace a popis vstupu Tl do rostlinných pletiv modelové rostliny.

II. Posouzení úlohy (bio)geochemických faktorů při popisu vstupu Tl do rostlin.

III. Kvantifikace bioakumulačního potenciálu modelové rostliny k příjmu thallia.

3. Zvolené metody zpracování

Disertační práce se zabývá srovnáním příjmu Tl do rostliny s prokázanými (hyper)akumulačními schopnostmi. V rámci DSP jsou jako hlavní výsledky prezentovány 3 nezávislé nádobové „batch“ experimenty s využitím modelové rostliny hořčice bílé (*Sinapis alba* L.):

1) Experiment popisující stabilní frakcionaci izotopů Tl v rostlinách pěstovaných hydroponicky („Izotopy Tl“). Detailní popis experimentu je uveden v publikaci Vaněk et al. (2019) – PŘÍLOHA I.

2) Experiment zabývající se příjmem a bioakumulací Tl do pletiv rostlin pěstovaných v hydroponii/ umělé půdě („Bioakumulace Tl“). Detailní popis experimentu je uveden v publikaci Holubík et al. (2020) – PŘÍLOHA II.

3) Experiment sledující toleranci rostlin vůči vysoké expozici Tl při kultivaci v hydroponii/ umělé půdě („Tolerance Tl“). Detailní popis experimentu je uveden v publikaci Holubík et al. (2021) – PŘÍLOHA III.

Cílem experimentů bylo: (i) popsat místo příp. uložení Tl v rostlině a (ii) experimentálně ověřit optimální/limitní podmínky růstu rostlin při variabilní expozici Tl v roztoku. Věříme, že některé poznatky z uvedených prací najdou své uplatnění, ať již v rámci fytoextrakčních, nebo fytoremediačních postupů ve snaze o snížení celosvětové zátěže Tl v životním prostředí.

Další výsledky DSP „Izotopické stopování Tl“ (PŘÍLOHA IV.), „Izotopová signatura Tl v metalurgických odpadech“ (PŘÍLOHA V.) a „Izotopové složení Tl v půdách“ (PŘÍLOHA VI.) se zaměřily primárně na popis změny izotopové signatury Tl (ε^{205}Tl) v půdních podmínkách. Tyto práce (Vaněk et al., 2016, 2018, 2020) se zaměřují na popis izotopové signatury a izotopické frakcionace Tl ve vybraných primárních materiálech, pevných odpadech a kontaminovaných půdách. Výsledky dokreslují obraz sledování vstupu Tl na rozhraní mezi půdou a rostlinou pro případnou environmentální implementaci dosažených výsledků DSP do praxe.

3.1 Základní premisy laboratorních experimentů

Z dostupné literatury je zřejmé, že již relativně nízká koncentrace Tl v živném roztoku (~1 mg Tl/L) vede k intoxikaci rostlin (Lindsay et Doxtader, 1981). Mezi nejčastější reakce rostlin patří nízká produkce fotosyntetického pigmentu (Fargašová, 2004; Mazur et al., 2016) a omezený příjem živin (Merian et Clarkson, 1991; Tremel et al., 1997).

Připouštíme, že za reálných (půdních) podmínek se kinetika Tl může výrazně lišit od podmínek „batch" experimentů. Častým faktorem omezujícím vstup Tl do rostliny je skutečnost, že některé komplexy Tl s ligandy (oxalát, sukcinát, malonát a HPO_4^-) mají relativně nízký součin rozpustnosti (Xiong, 2009). Zároveň může být Tl v půdním prostředí sorbováno na povrchu primárních minerálů (K-živců a birnessitu, Grösslová et al., 2015; Vaněk et al., 2010) a některých sekundárních (jílových) minerálů (např. illitu, Vaněk et al., 2011; Wick et al., 2018) s různou stabilitou.

Ačkoliv speciace Tl v půdním roztoku nebyla dosud zcela objasněna (Sadowska et al., 2016; Voegelin et al., 2015), předpokládáme, že v rámci našich experimentů monovalentní ionty Tl (Tl^+) nevytváří ve sledovaném roztoku komplexy a ani se neoxidují na Tl^{3+} (Alloway, 2012; Mestek et al., 2007; Sadowska et al., 2016).

V rámci interpretace izotopických dat předpokládáme, že při vstupu Tl z roztoku do rostlinného materiálu dochází k relativnímu nabohacení lehčího izotopu ^{203}Tl v rostlině za vzniku přechodné vazby Tl na enzymatický systém (E-S). Tento aspekt popisujeme dominantně pomocí kinetického modelu (Wiederhold, 2015).

3.2 Popis experimentů

3.2.1 Způsob pěstování rostlin

Semena hořčice bílé byla sterilizována (EtOH) a inkubována v temné fázi po dobu 4 dnů při 20 °C na filtračním papíru nasáklém demi H_2O. Sazenice v růstové fázi dvou listů byly umístěny do experimentálních nádob a kultivovány při laboratorních podmínkách bez přídavného osvětlení. V rámci provedených experimentů byl rostlinám aplikován živný roztok, který odpovídal koncentraci živin v růstové fázi rostlin (resp. elektrické vodivosti, Obr. 2). Živný roztok byl připravován vždy čerstvý ze základního (Reid et York, 1958, Tab. 1) roztoku ředěním.

Tab. 1: Složení základního živného roztoku (Reid et York, 1958)

Složení Reid-Yorkova živného roztoku	
Makroelementy	koncentrace (g/L živného roztoku)
KH_2PO_4	0,136
KCl	0,373
$CaCl_2$	0,555
$MgSO_4.7H_2O$	0,443
NH_4NO_3	0,600
$FeCl_3.6H_2O$	0,049
EDTA	0,066
Mikroelementy	koncentrace (mg/L živného roztoku)
$ZnSO_4.7H_2O$	0,200
H_3BO_3	0,611
$MnCl_2.4H_2O$	0,388
$CuSO_4.5H_2O$	0,100
$Na_2MoO_4.H_2O$	0,040
$Co(NO_3)_2.6H_2O$	0,055

Pozn.: Reid et York (1958) živný roztok byl zvolen z důvodu relativné nízké asociace Tl^I s chelatačním činidlem EDTA (log Ks Tl-EDTA = 5,8, Sager, 1994).

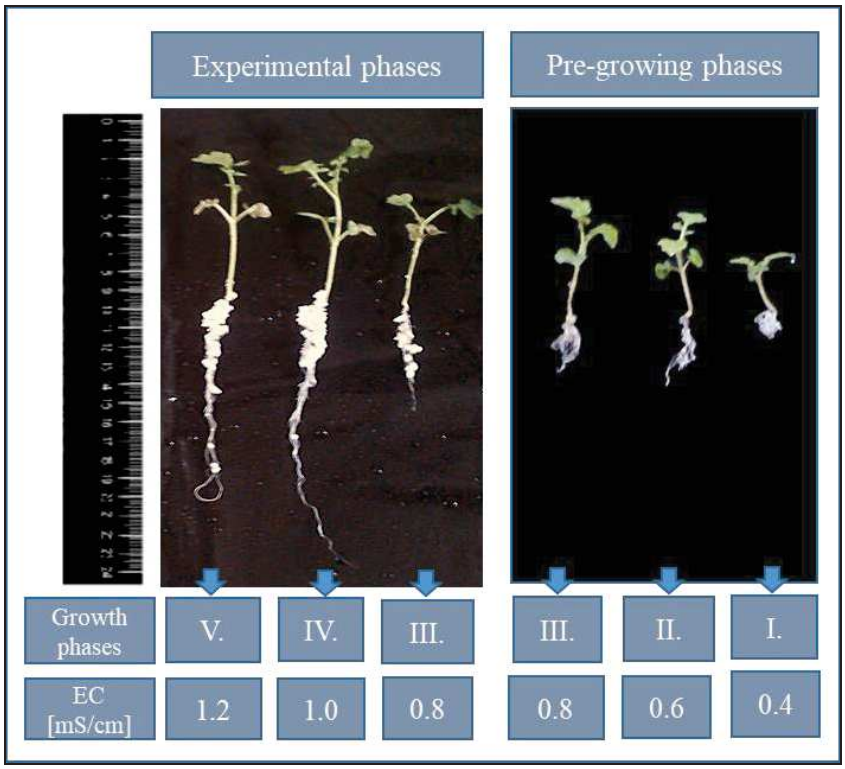

Obr. 2.: Fáze růstu modelové rostliny hořčice bílé v živném roztoku

Pro jednotlivé experimenty byla zálivka (resp. živný roztok) kontaminován specifickou dávkou Tl. Řízená kontaminace byla řešena smíšením živného roztoku a zředěného roztoku s obsahem 10mg Tl/L. Dávkování roztoku s řízenou kontaminací Tl^+ bylo podřízeno růstu rostlin na umělé půdě ve snaze o udržení ~60 % vodní kapacity v nádobách. Hodnota pH (~4,5) v živném roztoku nebyla upravována přídavnými chelatačními činidly jak popisuje Ryan et al. (2013), i když je pravděpodobné, že kyselé pH živného roztoku urychlovalo vstup Tl/živin do rostlinných pletiv.

3.2.2 Popis pěstebního substrátu

Rostliny při hydroponické kultivaci byli pěstovány v silikagelu (white, Signus SG 5, zrnitost 2-5 mm, velikost pórů 2-3 nm). Rostliny v pěstované v umělé půdě byly zasazeny do substrátu připravené podle standardu OECD (2009) z 10 % obj. rašeliny, 70 % obj. křemičitého písku (o zrnitosti 50-200 μm), a 20 % obj. podílu kaolinitického jílu (s obsahem kaolinitu nad 30 %). Doporučená úprava pH pomocí $CaCO_3$ nebyla z důvodu možné asociace Tl s ionty Ca realizována.

3.2.3 Popis experimentu „Izotopy Tl“

Experiment porovnává vstup Tl do rostlinné matrice při definované stabilní koncentraci Tl v hydroponickém roztoku. Design experimentu (Obr. 3) prezentuje 4 varianty s koncentrací Tl v roztoku: A = 0,01; B = 0,05, C = 0,1 mg/L a X = 0 mg/L. Každá varianta byla pěstována v odděleném boxu se 6 rostlinami (hořčice bílé) po dobu 21 dnů. Výměna živného roztoku s definovanou koncentrací Tl byla prováděna v pravidelném třídenním režimu.

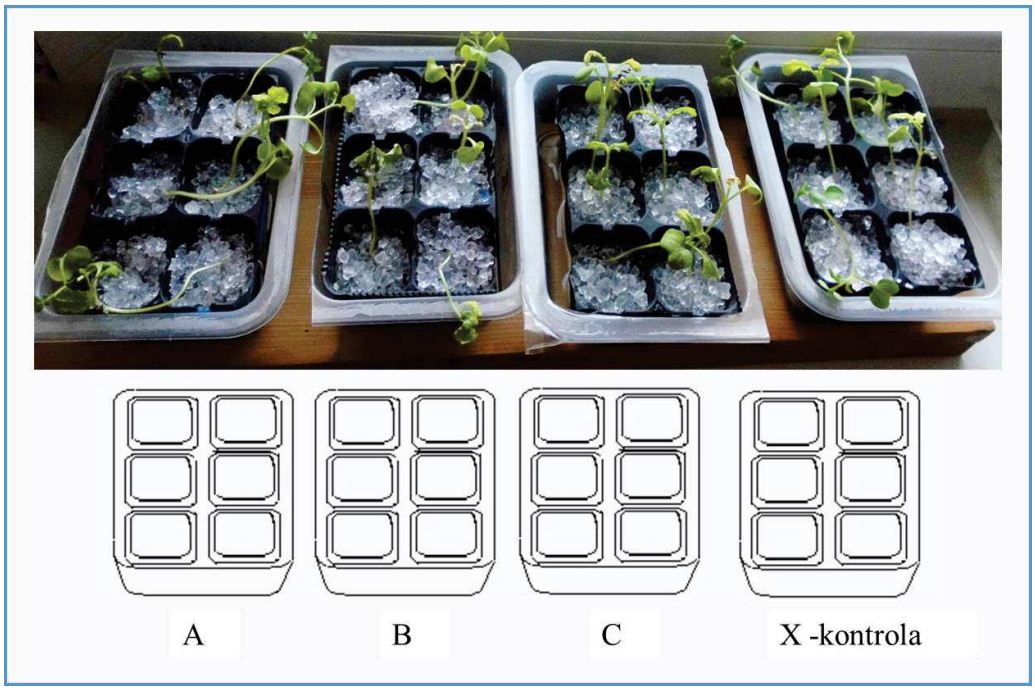

Obr. 3: Schéma nádobového pokusu „Izotopy Tl“

3.2.4 Popis experimentu „Bioakumulace Tl“

Experiment sledoval růst rostlin pěstovaných v hydroponických podmínkách (A) a v podmínkách umělé půdě (B) po dobu 21 dní. Variantní uspořádání pokusu s dávkovanou koncentrací Tl (0,01; 0,05; 0,1 a 0 mg Tl/L) ukazuje obrázek 4. Pokus byl proveden v nádobách o objemu 130 cm^3 ve 2 nezávislých opakováních. Dávkování živného roztoku bylo řízeno evapotranspirací rostlin pěstovaných v umělé půdě.

Obr. 4: Schéma nádobového pokusu „Bioakumulace Tl“

3.2.5 Popis experimentu „Tolerance Tl“

Experiment tolerance Tl sledoval reakci rostlin na extrémní dávky Tl. Rostliny byly nejprve 14 dní kultivovány v hydroponických (A) a semihydroponických (B) podmínkách bez vnosu Tl a poté vystaveny extrémní dávce Tl 1 a 2 mg Tl/L (Obr. 5). Rostlin pěstované v umělé půdě s vysokou dávkou Tl (resp. koncentrací Tl v zálivce -2 mg/L) jevily již během prvního týdne silné známky vadnutí (Obr. 5).

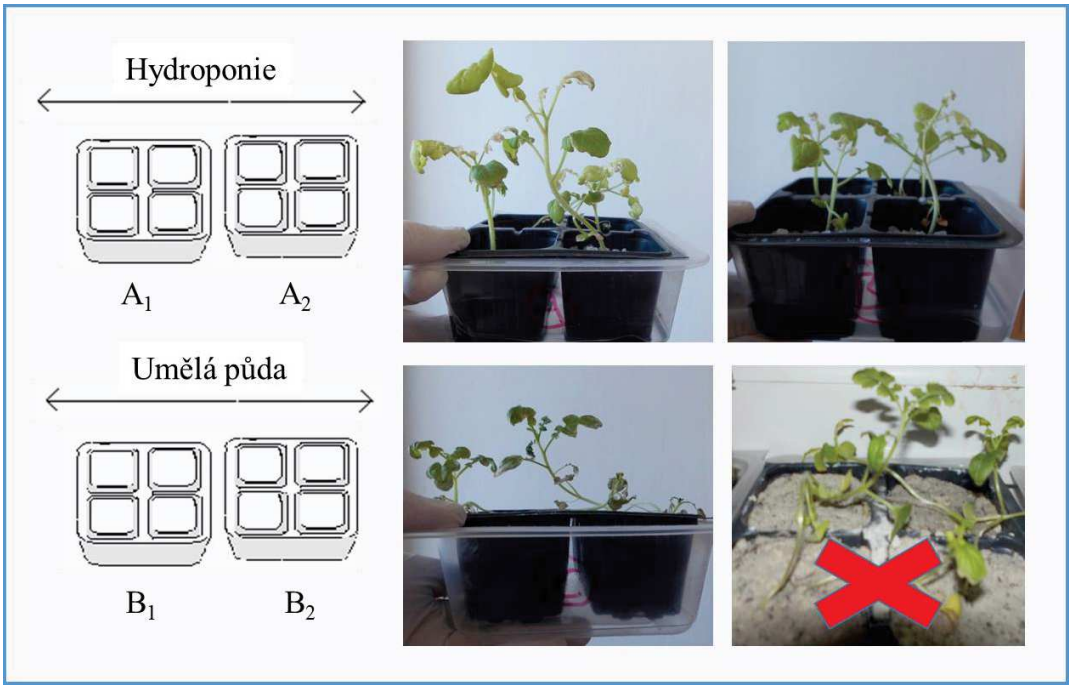

Obr. 5: Schéma nádobového pokusu Tolerance Tl

3.2.6 Způsob získávání biomasy a mineralizace rostlinného materiálu

Po provedení jednotlivých experimentů byly testované rostliny odebrány z pěstební matrice, mechanicky očištěny, promyty (několikrát v demi H_2O, poté v EtOH) a následně sušeny do konstantní hmotnosti (při teplotě 60-70 °C po dobu 24 hodin). Při získávání rostlinného materiálu byl kladen důraz na zisk celé rostliny, tj. bez půdní rhizosféry. Rostlinný materiál byl separován na kořen, stonek a list. Rostlinné tkáně byly uloženy v mrazicím boxu před dalším zpracování biomasy (mineralizací).

3.3 Analýza rostlin

3.3.1 Mineralizace rostlin

Biomasa byla mineralizována pomocí směsi HNO_3 (68%, ultrapure) a H_2O_2 (30%, suprapure) v poměru 4:1. Separované rostlinné tkáně byly rozpuštěny v celkovém objemu ~5 ml směsi (HNO_3/H_2O_2), následně vpraveny do 60 ml PTFE kádinky (Savillex, USA) a zahřívány po dobu 24 hodin na mikrovýhřevné desce při 150 °C.

3.3.2 Stanovení koncentrace živin a Tl

Koncentrace prvků (Na, Mg, K, Ca, Fe, Mn, Co, Cu, Zn, Mo a Tl) byly stanoveny pomocí optické emisní spektrometrie s ionizací prvku v indukčně vázaném plazmatu (ICP-OES, iCAP 6500, Thermo Scientific) a pomocí hmotnostní spektrometrie s indukčně vázaným plazmatem (Q-ICP-MS, Xseries II, Thermo Scientific, Německo) za standardních analytických podmínek. Ke kontrole kvality naměřených koncentrací Tl byl využit standardní referenční materiál čajových listů INCT-TL-1 (Institute of Nuclear Chemistry and Technology, Polsko).

3.3.3 Izolace a separace Tl

Izolace a separace Tl z mineralizovaného vzorku biomasy byla provedena pouze pro potřeby stanovení izotopové signatury Tl (ε^{205}Tl) v experimentu „Izotopy Tl“. Mineralizovaný materiál rostlinných pletiv byl podroben dvoustupňové chromatografické separaci na ionexu (anexu) (Bio-Rad AG1-X8) v chloridovém cyklu podle modifikovaného postupu Baker et al. (2009).

Každý vzorek biomasy (po mineralizaci) byl odpařen do úplného vysušení a poté znovu rozpuštěn v 0,1M HCI a upraven přídavkem Br_2 (1% v/v). Roztok byl ponechán volně reagovat (>12 hodin), tak aby bylo zajištěno, že veškeré jednomocné Tl bude zoxidováno na trojmocnou formu. Detailní postup separace je uveden v publikaci Vaněk et al. (2019).

3.3.4 Izotopová analýza Tl

Izotopová analýza ze separovaných vzorků byla provedena pomocí multikolektorového hmotnostního spektrometru s indukčně vázaným plazmatem (MC-ICP-MS; Neptune Plus, Thermo Scientific, Německo). Měření bylo provedeno v laboratořích Přírodovědecké fakulty Univerzity Karlovy v Praze. Všechna měření byla opakována 3x, každé v 50 cyklech. Pro korekci měření izotopického složení Tl a eliminaci např. tzv. „mass bias driftu“ byly využity standardní roztoky prvků Pb a Tl a jejich známé izotopické poměry (SRM 981- Common lead a SRM 997, Tl; NIST). Standardní roztok Tl (NIST SRM 997) byl měřen vždy před a po každém měřeném reálného vzorku. Izotopová frakcionace Tl je uváděna vždy ve vztahu k NIST SRM 997.

3.3.5 Speciační analýza Tl

Speciace Tl v rostlinném materiálu byla provedena pomocí rentgenové absorpční spektorskopie (XANES). Pro potřeby speciační analýzy experimentu „Izotopy Tl“ bylo využito směsného vzorku rostlinných pletiv rostlin pěstovaných v hydroponických podmínkách při koncentraci 2 mg Tl/L. Rostlinný materiál (kořen, stonek, list) byl po odběru, separaci a homogenizaci lyofilizován a lisován do pelet o průměru 7 mm. Pelety byly uchovány v kryostatu při teplotě 20 K. K záznamu absorpčních spekter (ve fluorescenčním spektru) byl využit křemíkový čtyřprvkový detektor driftu. Kromě měřeného spektra vzorku byla zaznamenána a porovnávána spektra Tl_2O_3, $TlAsS_2$ a Tl^I-acetátu. Spektrum vodného Tl^+ při laboratorních podmínkách bylo převzato ze studie Wick et al., (2018).

3.4 Zpracování dat

3.4.1 Výpočet bioakumulačního potenciálu Tl

Výpočet bioakumulace Tl/prvku (BAI) v rostlinném pletivu byl vyjádřen u experimentů, kde byl znám vstup Tl/živin do systému („Bioakumulace Tl“ a „Tolerance Tl“). Index bioakumulace (BAI) je principiálně založen na výpočtu faktoru biokoncentrace (BCF) (Hladun et al., 2015; Kim et al., 2016; Zayed et al., 1998). Na rozdíl od koeficientu biokoncentrace (BCF), který je vyjádřen jako podíl koncentrace prvku v rostlinné tkáni (mg/kg) vůči koncentraci prvku v systému (mg/kg), je koeficient bioakumulace (BAI) vyjádřen jako podíl hmotnosti prvku v rostlinné tkáni (g) vůči celkovému vnosu (dávce) prvku do systému (g). Index BAI tak srovnává celkovou schopnost rostliny přijmout a akumulovat Tl/živinu v rostlinném pletivu. Výpočet indexu BAI je možné využít pouze pro systémy se známými vstupy všech hodnocených prvků (včetně pozaďových hodnot použité matrice). Index bioakumulace (BAI) představuje bezrozměrný faktor podílu hmotnosti prvku v pletivu ($X_{\text{kořen, stonek, list}}$) a v systému ($Y_{\text{total}}$) vyjádřený v [%].

Výpočet BAI byl proveden podle vzorce (2):

$$BAI_{(\text{kořen, stonek, list})} = X_{(\text{kořen, stonek, list})} / Y_{\text{total}} * 100\ [\%] \quad (2)$$

Celkový index bioakumulace (BAI_{tot}) je následně vyjádřen jako suma BAI pro každé pletivo podle rovnice (3):

$$BAI_{tot} = \sum BAI_{kořen} + BAI_{stonek} + BAI_{list} [\%] \quad (3)$$

Distribuční faktor (DF) konkrétního prvku (včetně Tl) je vyjádřen jako podíl indexu bioakumulace v jednotlivém pletivu ($BAI_{kořen, stonek, list}$) vůči bioakumulaci prvku v celé rostlině (BAI_{tot}), obdobně jako je vyjádřen indexu translokace prvku (TLI %) při hodnocení indexu BCF (Kim et al., 2016).

3.4.2 Statistická analýza

Veškeré výsledky měření jsou vyjádřeny jako aritmetický průměr ($\bar{x}$) s definovanou mírou variability pomocí směrodatné odchylky (SD) z definovaného počtu opakování (n). Pokročilejších metod statistického vyhodnocení výsledků bylo využito u experimentu „Bioakumulace Tl“. Přesto, že design experimentu „Bioakumulace Tl“ nebyl primárně koncipován ke statistické analýze (nebyl volen plně faktoriální design pokusu) bylo možné s ohledem na nezávislé pozorování v rámci pokusu provést základní testování vědeckých hypotéz. Výběrový soubor měřených dat (s nízkou repeticí) logicky nevykazoval normální rozdělení (testováno Shapiro-Wilkovým testem). Proto bylo přistoupeno k analýze výběrového souboru pomocí neparametrických (robustních) testů. Vztahy mezi variabilitou proměnných byly testovány pomocí Friedmanova testu (neparametrické jednofaktorové analýzy rozptylu pro závislé vzorky). Srovnání rozptylů mezi 2 variantami bylo hodnoceno párovým Wilcoxonovým testem.

Pro determinaci možného asociativního chování Tl a dalších prvků byl vyjádřen Spearmanův koeficient pořadové korelace (r_s). V rámci vyhodnocení indexu bioakumulace (BAI) bylo pro seřazená data možné využít i Pearsonových korelačních koeficientů (r). Pro sestavení lineárních modelů asociace Tl s dalšími prvky byla využita technika krokové regresní analýzy (top-down analýzy). Význam jednotlivých členů lineárního modelu byl hodnocen na základě koeficientu determinace (R^2) a testován pomocí Sheffeho testu v rámci post-hoc analýzy. Všechna měření byla testována na hladině významnosti ($\alpha = 0,05$) pomocí softwaru Statistica 10 (StatSoft, 2012).

4. Publikované práce

4.1 Izotopy Tl

V experimentu „Izotopy Tl“ bylo cílem (i) změřit variace izotopové signatury Tl v závislosti na stabilní koncentraci Tl v hydroponickém roztoku, (ii) popsat změnu izotopové signatury Tl při vstupu do rostlinných pletiv a (iii) diskutovat změnu izotopové signatury Tl v kontextu se speciací Tl v rostlinném pletivu. Výsledky experimentu směřovaly k pochopení mechanizmu nabohacení Tl v biomase a k popisu „životního cyklu“ Tl v životním prostředí (PŘÍLOHA I.).

Vaněk, A., Holubík, O., Oborná, V., Mihaljevič, M., Trubač, J., Ettler, V., Pavlů, L., Vokurková, P., Penížek, V., Zádorová, T., Voegelin, A., 2019. Thallium stable isotope fractionation in white mustard: Implications for metal transfers and incorporation in plants. Journal of Hazardous Materials. 369, 521–527.
https://doi.org/10.1016/j.jhazmat.2019.02.060

4.2 Bioakumulace Tl

Smyslem experimentu „Bioakumulace Tl“ bylo: (i) popsat jak experimentální podmínky a počáteční koncentrace Tl ovlivňují bioakumulaci Tl do pletiv hořčice bílé, (ii) na podkladě matematických modelů popsat cestu Tl do rostliny v asociaci s příjmem dalších prvků a živin. Koncepce výzkumu směřovala k nastavení optimálních podmínek pro růst modelové rostliny (hořčice bílé) k fytoremediačním a fytoextrakčním účelům (PŘÍLOHA II.).

Holubík, O., Vaněk, A., Mihaljevič, M., Vejvodová, K., 2020. Higher Tl bioaccessibility in white mustard (hyper-accumulator) grown under the soil than hydroponic conditions: A key factor for the phytoextraction use. Journal of Environmetal Management. 255, 109880. https://doi.org/10.1016/j.jenvman.2019.109880

4.3 Tolerance Tl

Experiment „Tolerance Tl“ měl za cíl určit limity růstu hořčice bílé při extrémní expozici Tl v půdním/hydroponickém roztoku. Výsledky mohou sloužit k nastavení podmínek růstu hořčice bílé pro fytoremediační, popř. fytoextrakční účely (PŘÍLOHA III.).

Holubík, O., Vaněk, A., Mihaljevič, M., Vejvodová, K., 2021. Thallium uptake/tolerance in a model (hyper)accumulating plant: Effect of extreme contaminant loads. Soil and Water Research. 16, 129–135. https://doi.org/10.17221/167/2020-SWR

4.4 Další publikace

4.4.1 Izotopické trasování Tl

Práce se zabývá stopováním izotopové signatury Tl v kontaminovaných půdách v oblasti na pomezí česko-německo-polských hranic (tzv. “Black Triangle“). Půdy této oblasti byly v minulosti ovlivněny emisemi ze spalování uhlí z elektráren Turów a Hirschfelde. Výsledky prezentují v kontrastu sledování lesních a lučních půd důkazy o antropogenním vstupu Tl do půdního prostředí (PŘÍLOHA IV.).

Vaněk, A., Grösslová, Z., Mihaljevič, M., Trubač, J., Ettler, V., Teper, L., Cabala, J., Rohovec, J., Zádorová, T., Penížek, V., Pavlů, L., Holubík, O., Němeček, K., Houška, J., Drábek, O., Ash, C., 2016. Isotopic Tracing of Thallium Contamination in Soils Affected by Emissions from Coal-Fired Power Plants. Environmental Science & Technology. 50, 9864–9871. https://doi.org/10.1021/acs.est.6b01751

4.4.2 Izotopová signatura Tl v metalurgických odpadech

Práce se zabývá hodnocením izotopů Tl v půdách kontaminovaných expozicí odpadu po těžbě Zn a odpadů z metalurgického zpracování Zn-rudy. V práci jsou navrhovány metody sledování změn izotopové signatury Tl na pozadí možné redistribuce izotopů Tl v popisovaném půdním systému (PŘÍLOHA V.).

Vaněk, A., Grösslová, Z., Mihaljevič, M., Ettler, V., Trubač, J., Chrastný, V., Penížek, V., Teper, L., Cabala, J., Voegelin, A., Zádorová, T., Oborná, V., Drábek, O., Holubík, O., Houška, J., Pavlů, L., Ash, C., 2018. Thallium isotopes in metallurgical wastes/contaminated soils: A novel tool to trace metal source and behavior. Journal of Hazardous Materials. 343, 78–85. https://doi.org/10.1016/j.jhazmat.2017.09.020

4.4.3 Izotopové složení Tl v půdách

Práce se věnuje sledování změny izotopového složení Tl v půdách přirozeně bohatých na obsah Tl oblasti Erzmatt (Švýcarsko). Publikace se pokouší popsat vznik těchto silně hydrotermálně mineralizovaných dolomitických půd na pozadí sledování izotopového složení Tl z extrahovatelných podílů půd v kombinaci se speciační analýzou půdních vzorků (PŘÍLOHU VI.).

Vaněk, A., Voegelin, A., Mihaljevič, M., Ettler, V., Trubač, J., Drahota, P., Vaňková, M., Oborná, V., Vejvodová, K., Penížek, V., Pavlů, L., Drábek, O., Vokurková, P., Zádorová, T., Holubík, O., 2020. Thallium stable isotope ratios in naturally Tl-rich soils. Geoderma 364, 114183. https://doi.org/https://doi.org/10.1016/j.geoderma.2020.114183

5. Diskuze

5.1 Izotopová frakcionace Tl při vstupu do rostlin

Výsledky provedeného experimentu Vaněk et al. (2019) (Tab. 2) ukazují celkově nižší produkci biomasy u rostlin pěstovaných v kontaminovaných roztocích vůči kontrolní variantě. Při vyšší koncentraci Tl v roztoku (specificky 0,1 mg Tl/L) byl zaznamenán vyšší příjem Ca a K do kořene a listu vůči kontrole (Tab. 2).

Tab. 2: Koncentrace živin (K, Ca, Mg a Fe) v biomase při různé expozici Tl

konc. Tl v roztoku (mg Tl/L)	pletivo	hmotnost biomasy (g)	K (g /kg)	Ca (g /kg)	Mg (g /kg)	Fe (g /kg)
0,1	kořen	0,006	6,3	13,6	4	3,5
	stonek	0,024	32,6	10,8	5,9	0,8
	list	0,048	33	30,2	9,7	1,2
0,05	kořen	0,01	2,2	10,1	2,6	6,6
	stonek	0,015	34,1	16,9	7,1	2,5
	list	0,06	15,3	20,8	5,9	0,9
0,01	kořen	0,013	2,1	9,3	2,7	3,8
	stonek	0,02	34,2	14,4	9,6	1,2
	list	0,054	15,4	15,1	4,3	0,6
0 (kontrola)	kořen	0,027	1,4	3,8	1	0,8
	stonek	0,029	29,6	13,1	7,1	0,6
	list	0,09	11,5	11,5	4,3	0,7

Pozn.: koncentrace byly měřeny ICP-MS ze směsných vzorků (n = 6)

Zvýšenou poptávku rostliny po živinách a nižší produkci biomasy je možné vysvětlit reakcí rostlin na stresové podmínky způsobené příjmem Tl (Merian et Clarkson, 1991). Navzdory skutečnosti, že se v rámci experimentu nepodařilo prokázat přímou vazbu mezi vstupem Tl a K, existuje mnoho publikací asociativní chování K a Tl ukazují (Krasnodębska-Ostręga et al., 2012; Sadowska et al., 2016; Scheckel et al., 2004; Tremel et al., 1997; Vaněk et al., 2010; Xiao et al., 2004). Na základě výsledků prací Alloway (2012) a Sager, (1994) jsme předpokládali, že Na^{+}/K^{+}-ATPáza hraje důležitou roli pro vnitřní přenosy Tl v rostlině.

I když přesný mechanismus bioakumulace Tl v rostlině není znám, z výzkumu Ning et al. (2015) vyplývá, že až 80 % z celkového Tl obsaženého v listové hmotě se nachází

v buněčném cytosolu vakuol. Zároveň je v publikacích Hall (2002) a Ning et al. (2015) na modelové rostlině hlávkového zelí (*Brassica oleracea var. Capitata*) popisována fytochelatace Tl v cytosolu na peptidy obsahujícími thiolovou (-SH) skupinu. Tento mechanizmus může hrát významnou roli i při toleranci rostlin čeledi Brukvovité (*Brasicaceae*) vůči stresu vyvolaného kontaminací Tl.

Z naměřených koncentrací Tl v jednotlivých pletivech (Tab. 3) vyplývá, že významná část Tl se nachází ve stonku modelové rostliny (hořčice bílé). Obdobné trendy prezentují také předešlé studie Krasnodębska-Ostręga et al. (2012) a Vaněk et al. (2010).

Tab. 3: Celková koncentrace a izotopová frakcionace Tl (ε^{205}Tl) v biomase

konc. Tl v roztoku (mg Tl/L)	pletivo	Tl (mg /kg)	obsah Tl (µg v biomase)	ε^{205}Tl ± 0.7
0,1	roztok			-2,76
	kořen	6,37 ± 0,41	0,04	-2,78
	stonek	9,47 ± 0,65	0,23	-4,23
	list	6,68 ± 0,39	0,32	-3,46
	prýt		0,55	-3,53
	celá rostlina		0,59	-3,72
0,05	roztok			-2,05
	kořen	1,73 ± 0,12	0,02	-5,92
	stonek	7,42 ± 0,35	0,11	-1,81
	list	1,81 ± 0,08	0,11	-3,6
	prýt		0,22	-2,48
	celá rostlina		0,24	-2,97
0,01	roztok			-2,36
	kořen	0,25 ± 0,01	0,003	-10,64
	stonek	0,86 ± 0,04	0,02	-2,7
	list	0,52 ± 0,04	0,03	-4,88
	prýt		0,05	-3,79
	celá rostlina		0,053	-4,39
INCT-Tl-1	Standard - čajové listy	0,06 ± 0,01		-6,21

Pozn.: Nejistoty pro celkové koncentrace Tl jsou uváděny na úrovni dvojnásobné směrodatné odchylky. Data ε^{205}Tl zobrazují průměrné hodnoty pro 6 vzorků s chybou ± 0,9 od standardního referenčního materiálu INCT-Tl-1 (Institute of Nuclear Chemistry and Technology, Polsko).

Výsledky měření izotopové signatury Tl (ε^{205}Tl, Tab. 3) naznačují preferenci příjmu lehkého izotopu ^{203}Tl ze živného roztoku do rostliny. Nejvyšší obohacení izotopů ^{203}Tl bylo pozorováno ve variantě s nejnižší koncentrací Tl v hydroponickém roztoku (0,01 mg Tl/L, Tab. 3).

Wiggenhauser et al. (2016) naznačili, že frakcionace izotopů mezi stonkem a listem (i když pro izotopy Cd) je způsobena kombinovaným účinkem speciace, adsorpce a asimilace prvku v listu. Wiggenhauser et al. (2016) dále popisují mechanizmus ovlivněný vodivými pletivy ve stonku (konkrétně xylemu), kde se projevuje transpirační efekt (s preferencí lehkých izotopů). Výsledný transport prvku (Cd) v rostlině tak možná kombinuje efekt spojený s chelatací prvku ve vakuolách listu (s preferencí těžkých izotopů) s transpiračním efektem (spojeným s preferencí lehčích izotopů). Rozdíly v izotopové signatuře Tl (Tab. 3) mohou odrážet také vývoj rostliny, kdy jsou druhotné listy mladší než stonek a kořenové části rostliny. Krasnodębska-Ostręga et al. (2012) vysvětlují nabohacení lehkými izotopy ^{203}Tl v kořeni vůči stonku možným výskytem Tl^{III} komplexů. Hall (2002), Wiederhold et al. (2010) a Ning et al. (2015) popisují, že nabohacení může souviset s fyziologickou oxidací Tl v pletivu, popř. s chelatací lehkého izotopu ^{203}Tl na peptidy s thiolovou (-SH).

Z provedených výsledků speciační analýzy (XANES) se však žádný z těchto předpokladů neprokázal (Graf 1). Výsledky speciační analýzy vykazují vzájemnou podobnost spektra kořenu, stonku a listu. Možný vznik Tl^{III} – komplexů v pletivech stonku jak popisují Krasnodębska-Ostręga et al. (2012) se v naší práci nepotvrdil. Obdobně ani spektra $TlAsS_2$, která simulovala možnou koordinaci Tl na skupiny s atomem S, se neshodovala s měřenými spektry rostlinných pletiv (Graf 1). Výsledky speciační analýzy rostlin (Graf 1) prezentují podobnost se spektry Tl^{I} -acetátu a volného Tl^{+} iontu. Toto zjištění je v souladu s výsledky Scheckel et al. (2004) pro měření XANES v čerstvém vzorku iberky (*Iberis intermedia)*.

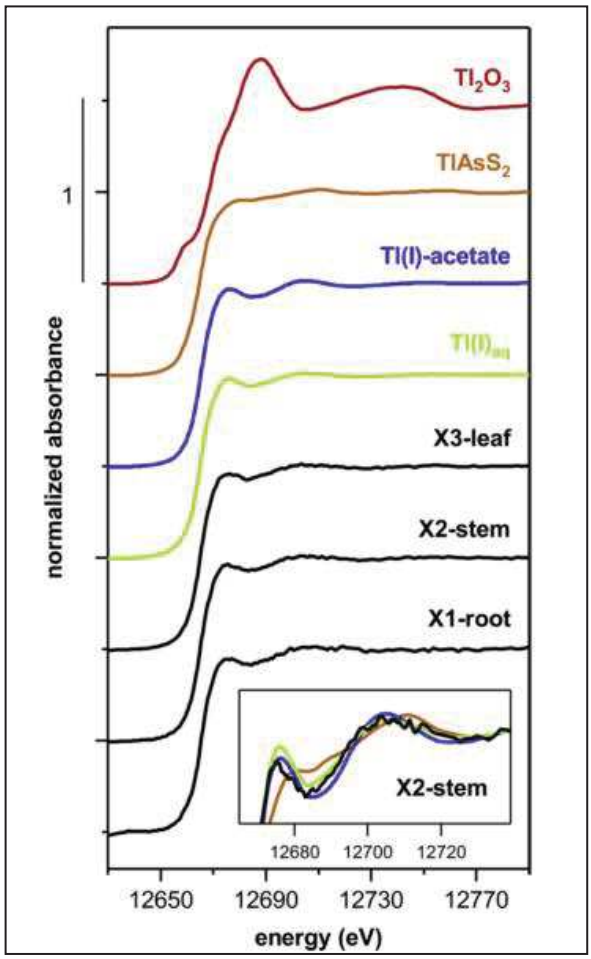

Graf 1: Výsledky spektra XANES převzato z publikace Vaněk et al. (2019)

Výsledky experimentu Vaněk et al. (2019) ukazují, že při absorpci Tl vegetací dochází k výrazné izotopové transformaci s preferencí lehkých izotopů ^{203}Tl do rostlinných pletiv. Vstup Tl do rostliny se dá v hydroponických podmínkách popsat v dimenzích kinetického efektu (Rayleighova modelu). Dílčí posuny vedoucí ke zpětnému nabohacení těžších izotopů v rostlině mohou indikovat místo se změnou reakční kinetiky a detekovat pravděpodobné místo akumulace Tl v rostlinném pletivu.

5.2 Bioakumulace Tl v rostlině

Thallium je stopový prvek, jehož obvyklá koncentrace v rostlině se pohybuje kolem 0,05 mg/kg (Adriano, 2001). Fytotoxická hladina Tl v rostlinách se pohybuje kolem 20 mg/kg (Kabata-Pendias et Pendias, 1992). V práci Holubík et al., (2020) sice měřená koncentrace Tl v biomase (Tab. 4) mírně převyšuje běžné koncentrace Tl v rostlině (Adriano, 2001), ale nedosahuje fytotoxické hladiny (Kabata-Pendias et Pendias, 1992).

Nejvyšší hodnoty koncentrace Tl v biomase dosahovaly maximálně polovičních limitů fytotoxicity. V rámci experimentu byla snaha minimalizovat možnou asociaci/precipitaci Tl v matrici pěstebního substrátu. Proto věříme, že naměřené hodnoty (Tab. 4) ukazují přímou závislost zvýšení koncentrace Tl v rostlinném pletivu v závislosti na vstupní dávce.

Tab. 4: Koncentrace Tl v rostlinném pletivu při pěstování v hydroponii a umělé půdě

konc. Tl v roztoku	pletivo	Hydroponie			Umělá půda		
(mg Tl/L)		průměr	±	SD	průměr	±	SD
0,01	list	0,62	±	0,02	2,24	±	0,70
0,05		2,02	±	0,47	6,81	±	1,37
0,1		6,70	±	2,06	7,28	±	2,62
0 (kontrola)		0,61	±	0,07	3,19	±	0,98
0,01	stonek	1,38	±	1,03	3,76	±	0,29
0,05		3,38	±	0,49	10,94	±	3,69
0,1		5,27	±	0,53	12,53	±	4,26
0 (kontrola)		0,59	±	0,12	4,51	±	1,62
0,01	kořen	0,09	±	0,04	1,92	±	0,79
0,05		1,82	±	1,22	6,88	±	3,17
0,1		1,07	±	0,63	9,92	±	4,17
0 (kontrola)		0,23	±	0,02	0,71	±	0,26

Pozn.: data ukazují průměr ± SD (směrodatnou odchylku) pro (n=2) zcela nezávislé systémy pěstování rostlin

Bylo překvapivé, že rostliny pěstované hydroponicky vykazovaly nižší koncentrace Tl v pletivu, než rostliny pěstované v umělé půdě (Tab. 4). Obdobné výsledky prezentují Allus et al. (1987) pro řepku (*Brassica napus* L.) a ječmen (*Hordeum vulgare*). Pro popis efektu je možné uvažovat o akceleraci příjmu Tl vlivem obecně vyšší biologické aktivity půdních variant, jak ukazují Al-Najar et al. (2003) a Pavlíčková et al. (2006). Nicméně domníváme se, že v podmínkách umělé půdy může být tento efekt relativně malý. Myslíme si, že důležitou roli v příjmu Tl může hrát odlišná strategie růstu rostliny pěstované v hydroponii a v půdě, jak popisují Taiz et Zeiger (2003). Při hydroponickém uspořádání jsou zdroje živin pro rostlinu snadněji dostupné. Rostlina tak může významnou část prvků přijímat do rostlinných pletiv pomocí pasivního transportu. Obecně rostliny pěstované v hydroponickém roztoku disponují rychlejším růstem nadzemních částí a málo rozvětveným kořenovým systémem (Taiz et Zeiger 2003). Naopak u rostlin pěstovaných v půdním prostředí, kdy je rostlina nucena prvky získávat aktivním příjmem často v chelátové formě (za pomocí kořenových výměšků), byla zaznamenána mnohem rozvinutější architektura kořenového systému (Taiz et Zeiger 2003).

Měřená data základních živin (Tab. 5) naznačují u rostlin pěstovaných v umělé půdě prokazatelně vyšší příjem K a Mg vůči hydroponii. Naopak v hydroponickém systému je akcelerován příjem Ca (Tab. 5). Naše výsledky společně s pracemi Ning et al. (2015), Scheckel et al. (2004) a Xiao et al. (2004) ukazují, že Ca může hrát důležitou roli při bioakumulaci Tl a může ovlivnit toleranci rostliny vůči vysoké expozici kontaminantu v prostředí.

Tab. 5: Index celkové biologické dostupnosti (BAI_{tot})

prvek	Hydroponie BAI_{tot} [%] průměr ± SD	Umělá půda BAI_{tot} [%] průměr ± SD
Tl	**1,3 ± 1,1**	**2,8 ± 1,6**
K	7,8 ± 4,5	11,2 ± 1,4
Ca	6,5 ± 2,9	4,8 ± 1,0
Mg	7,0 ± 3,9	8,3 ± 1,2
Fe	5,1 ± 2,9	5,3 ± 1,8
Na	59,7 ± 26,7	20,2 ± 3,8
Cu	0,7 ± 0,3	0,2 ± 0,1
Zn	0,4 ± 0,2	0,1 ± 0,1
Mn	1,2 ± 0,8	1,2 ± 0,4
Mo	7,5 ± 4,7	7,4 ± 2,5
Co	1,0 ± 0,6	0,4 ± 0,1

Pozn.: $BAI_{to} = BAI_{list} + BAI_{stonek} + BAI_{kořen}$, každého prvku z hodnocených prvků; data prezentují průměr ± směrodatná odchylka (SD); pro Tl (n = 6) a pro ostatní prvky (n = 8) opakování

Zajímavým ukazatelem je celkový index bioakumulace Tl v rostlině ($BAI_{tot.Tl}$, Graf 2), který prezentuje pro každou z měřených variant téměř dvojnásobnou bioakumulaci Tl v modelových rostlinách pěstovaných v umělé půdě, vůči hydroponii. Zároveň naše výsledky pro juvenilní stádia hořčice ukazují, že nižší dávka Tl v systému vede k vyšší bioakumulaci prvku v rostlině (Graf 2).

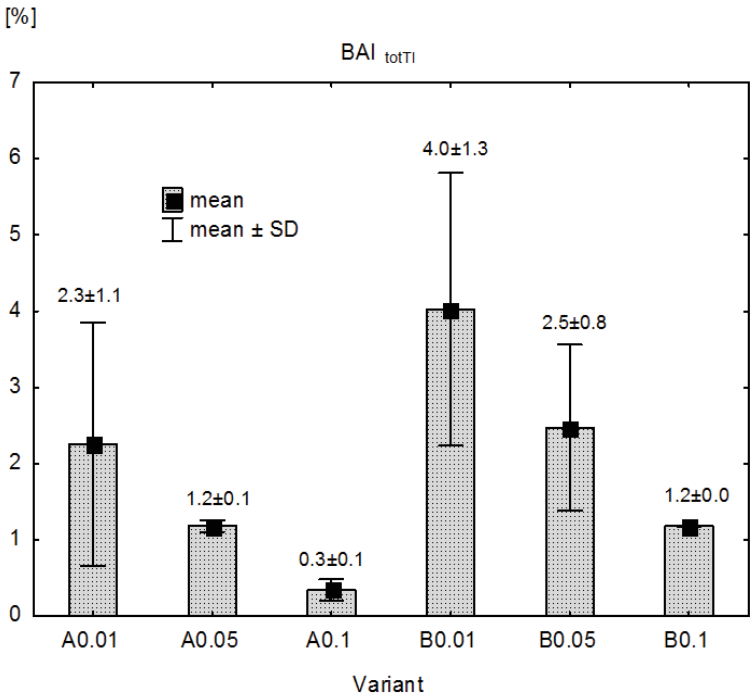

Graf 2: Index celkové biologické dostupnosti (BAI_{tot}) thallia v rostlinách pěstovaných v hydroponii (A) a v umělé půdě (B).

Pozn.: data prezentují průměr ± směrodatná odchylka (SD); pro 2 nezávislé systémy sledování na variantu

Z výsledků statistické analýzy BAI (Tl/živin, Tab. 6) se zdá, že Tl je skutečně v rámci příjmu do rostliny specificky doprovázeno některými prvky. Rozdílná strategie růstu může ovlivnit příjem Tl do kořenů, nebo i jeho krátkodobé uložení v xylemu stonku, popř. může ovlivnit i následnou depozici Tl v buněčném cytosolu a vakuole listu, jak uvádí Ning et al. (2015). Předpokládáme, že vstup Tl^+ a iontů dalších prvků prochází protoplazmou endodermálních buněk na povrchu kořenového vlášení, kde jsou jednotlivé ionty tříděny a dále transportovány jak popisují Taiz et Zeiger (2003). Kwan et Smith (1991) následně popisují, že se až 80 % dostupného Tl hromadí v cytoplazmatické membráně listu navázané na specifický nízkomolekulární peptid s neprokázanou vazbou na thiolovou (-SH) skupinu.

Tab. 6: Index biologické dostupnosti (BAI) do rostlinného pletiva

pletivo	list			stonek			kořen		
kultivace	Hydrop. BAI [%]	Umělá půda BAI [%]	Wilcox. Test A-B	Hydrop. BAI [%]	Umělá půda BAI [%]	Wilcox. test A-B	Hydrop. BAI [%]	Umělá půda BAI [%]	Wilcox. Test A-B
prvek	$\bar{x} \pm SD$	$\bar{x} \pm SD$	p - value	$\bar{x} \pm SD$	$\bar{x} \pm SD$	p - value	$\bar{x} \pm SD$	$\bar{x} \pm SD$	p - value
Tl	0,6 ± 0,4	1,8 ± 1,1	**0,043**	0,6 ± 0,6	0,8 ± 0,4	0,686	0,0 ± 0,0	0,2 ± 0,1	**0,043**
K	5,1 ± 2,5	8,8 ± 1,0	0,075	2,5 ± 1,9	2,1 ± 0,3	0,753	0,2 ± 0,1	0,3 ± 0,2	0,601
Ca	3,9 ± 1,6	3,6 ± 0,7	0,463	2,2 ± 1,1	1,0 ± 0,2	**0,028**	0,4 ± 0,2	0,3 ± 0,1	0,116
Mg	4,3 ± 2,2	6,6 ± 0,8	0,173	2,4 ± 1,5	1,4 ± 0,3	**0,028**	0,4 ± 0,2	0,3 ± 0,1	0,075
Fe	2,5 ± 1,2	2,8 ± 0,4	0,917	1,4 ± 0,8	1,3 ± 0,6	0,463	1,2 ± 1,0	1,2 ± 0,8	0,463
Na	35,0 ± 9,1	15,4 ± 2,5	0,109	22,4 ± 16,5	4,2 ± 1,1	**0,028**	2,2 ± 1,1	0,7 ± 0,3	**0,028**
Cu	0,2 ± 0,1	0,1 ± 0,0	**0,028**	0,1 ± 0,1	0,1 ± 0,1	0,345	0,3 ± 0,1	0,1 ± 0,0	**0,028**
Zn	0,1 ± 0,1	0,1 ± 0,0	**0,028**	0,1 ± 0,1	0,0 ± 0,0	0,345	0,2 ± 0,1	0,0 ± 0,0	**0,028**
Mn	0,8 ± 0,6	1,0 ± 0,4	0,463	0,3 ± 0,1	0,1 ± 0,0	**0,028**	0,1 ± 0,0	0,0 ± 0,0	**0,028**
Mo	5,3 ± 3,6	6,6 ± 2,3	0,463	1,6 ± 0,8	0,7 ± 0,2	**0,028**	0,6 ± 0,3	0,1 ± 0,0	**0,028**
Co	0,7 ± 0,5	0,4 ± 0,1	**0,046**	0,2 ± 0,1	0,1 ± 0,0	**0,028**	0,1 ± 0,0	0,0 ± 0,0	**0,028**

Pozn.: Data jsou uvedeny jako průměr $\bar{x} \pm$ směrodatná odchylka (SD); pro Tl (n = 6) opakování pro ostatní prvky (n = 8) opakování; Tučně je značena statisticky významná hodnota (p) Wilcoxonova párového testu na hladině významnosti ($\alpha = 0,05$).

Z výsledků indexu bioakumulace (BAI) pro jednotlivá pletiva (Tab. 6) byly v rámci experimentu „Bioakumulace Tl“ sestaveny hypotetické modely, které měly za cíl sledovat vstup Tl v asociaci s dalšími prvky do jednotlivých pletiv. Bylo zjištěno, že biologická dostupnost Tl (BAI) v listové biomase rostlin pěstovaných v hydroponii významně korelovala (r = 0,90) s bioakumulací Ca. Hydroponický model akumulace Tl v listu BAI_{Tl} = - 0,28 + 0,21 BAI_{Ca} vysvětluje výskyt Tl z 69 % (p = 0,01). Tyto závěry korespondují s publikacemi Ning et al. (2015) a Scheckel et al. (2004), které obdobně prezentují, že Ca hraje důležitou roli v toleranci rostlin vůči intoxikaci thalliem. Naproti tomu při pěstování v umělé půdě se tento trend nepotvrdil. Biologická dostupnost (BAI) Tl v listu je pro model umělé půdy vysvětlována vyšším zastoupení Mn. Tento modelový přístup by mohl vést k možnému vysvětlení, že Tl je v půdním systému nejen asociováno na Mn, ale také že je s ním společně ukládáno do fytochelatinů v listu ve vazbě se silně aniontovým lipidem jak prezentuje Günther et Umland (1988).

Příjem Tl do stonku je v rámci hydroponického systému doprovázen především vyšším zastoupením Na (model BAI_{Tl} = -0,334 + 0,034 BAI_{Na} vysvětluje vstup Tl z 89 %). Tento trend je při hydroponickém uspořádání pravděpodobně asociován dominantním příjmem Na v rámci pasivního transportu (Zijiang, 2016). Naopak vstup Tl do xylemových pletiv stonku je v „půdním“ systému řízen spíše stresovými mechanismy spojenými s

nedostatkem živin, jak ukazuje Xiao et al. (2010). Tyto předpoklady potvrzují vysoké korelace bioakumulace Tl se vstupy Mg a K (r = 0,94, resp. 0,99). Biogenní prvky K a Mg mají specifickou roli v aktivačních enzymech zapojených do dýchání a vytváření chlorofylu (Taiz et Zeiger, 2003). Zvýšený příjem K a Mg, tak může indikovat stresovou reakci rostlin.

Z pohledu praktického uplatnění hydroponického systému (např. k fytoextrakci Tl z kalů po důlní těžbě) je pozitivním zjištěním, že příjem Tl do kořenů rostlin je prakticky nulový (Tab. 6). Naproti tomu obsah Tl v kořenech rostlin pěstovaných v umělé půdě je poměrně významný až 20 % (Tab. 6). Bioakumulace Tl v kořenovém systému rostlin pěstovaných na umělé půdě je až z ~90 % vysvětlována v asociaci s příjmem K (BAI_{Tl} = 0,125 + 0,256 * BAI_K).

5.3 Tolerance rostlin vůči extrémní dávce Tl

Různí autoři se pokoušeli odhadnout mezní/prahovou koncentraci Tl v rostlinách s prokázanou (hyper)akumulačními schopností k příjmu Tl. Van Der Ent et al. (2013) v rešeršní práci predikují koncentraci 100 mg Tl/kg, Leblanc et al. (1999) ukazují limity růstu iberky (*Iberis intermedia*) při koncentraci 500 mg Tl/kg a Krämer (2010) prezentuje limitní koncentraci až 1 000 mg Tl/ kg.

Výsledky měřených koncentrací Tl v rostlinách experimentu Holubík et al. (2021) (Tab. 7) nedosahují tak vysokých hodnot jak ukazuje např. Krämer (2010), nicméně překračují limity fytotoxicity thallia 20 mg/kg (Kabata-Pendias et Pendias, 1992). Je zřejmé, že celková koncentrace Tl v rostlině pěstované v řízených podmínkách nádobového pokusu po dobu 21 dní nebude dosahovat koncentrací v rostlinách pěstovaných v zatížených oblastech, jak uvádí např. Xiao et al. (2012) pro brukev *(Brassica oleracea)* v oblast Lanmuchang (Čína) ~340 mg Tl/kg.

Věříme, že velmi důležitým parametrem, který může ovlivnit růst rostlin s (hyper)akumulační schopností, je aktuální koncentrace Tl v půdním/hydroponickém roztoku (Holubík et al., 2020). Při akutní expozici Tl může docházet k blokování příjmu biogenních prvků (Merian et Clarkson, 1991; Tremel et al., 1997), vadnutí a ztrátě pigmentu (Mazur et al., 2016). Právě tyto příznaky vykazovaly v našem experimentu všechny rostliny pěstované v umělé půdě. Rostliny intoxikované roztokem Tl v dávce 66 µg Tl/den (var. B_2, Obr. 5) vykazovaly symptomy akutní toxicity již po prvním týdnu kultivace. Pro všechny varianty pěstované v umělé půdě byl pozorován velmi nízký příjem biogenních prvků (Tab.

7). Prvními projevy rostlin pěstovanými v umělé půdě byl zvýšený příjem K a Mg jak ukazuje Holubík et al. (2020). Tyto prvky rostlina využívá při enzymatických procesech nutných k dýchání a k tvorbě chlorofylu (Taiz et Zeiger, 2003). Naopak rostliny pěstované v hydroponii nejevily v průběhu celého experimentu sebemenší známky vadnutí. Vitalitu pěstovaných rostlin při hydroponické kultivaci dokreslují hodnoty koncentrace základních živin v rostlině (Tab. 7).

Tab. 7: Koncentrace živin v pletivech rostlin

pletivo	varianta	K (g /kg)	Mg (g /kg)	Ca (g /kg)	Fe (g /kg)
list	A_1	26,8	3,8	15,0	0,3
	A_2	12,1	2,9	11,7	0,3
	B_1	2,9	1,4	9,9	0,7
stonek	A_1	22,5	5,5	14,1	0,5
	A_2	19,6	4,1	10,3	0,5
	B_1	4,9	1,7	7,6	2,0
kořen	A_1	20,8	3,9	14,1	0,4
	A_2	11,7	3,9	10,6	0,2
	B_1	1,8	1,0	3,8	0,7

Pozn.: data kumulují hodnoty replikace 4 rostlin na variantu

Při srovnání variant se stejnou expozicí Tl (A_1 a B_1, Tab. 8), je zřejmá preference příjmu Tl do kořene a stonku ve variantách umělé půdy vůči hydroponické kultivaci. Z výsledků experimentu Holubík et al. (2021) (Tab. 8, DF) plyne pozitivní zjištění, že při hydroponické kultivaci je 95-99% akumulovaného Tl uloženo v nadzemních částech rostlin.

Tab. 8: Koncentrace Tl v pletivu a distribuční faktor (DF) pěstované hořčice bílé při různých dávkách Tl.

varianta	pletivo	biomasa (mg)	konc. Tl (mg /kg)	DF (%)
A_1 (Hydrop.)	list	96	39,39	56,9
	stonek	74	31,20	34,8
	kořen	47	11,76	8,3
	celá rostlina	217	30,61	--
A_2 (Hydrop.)	list	106	87,20	61,9
	stonek	74	66,53	33,0
	kořen	43	17,57	5,1
	celá rostlina	223	66,91	--
B_1 (Umělá půda)	list	72	40,52	43,0
	stonek	43	53,84	34,1
	kořen	55	28,32	22,9
	celá rostlina	170	39,94	--

Pozn.: koncentrace Tl v celé rostlině byla vypočtena jako vážený průměr koncentrací jednotlivých pletiv a biomasy; data kumulují hodnoty replikace 4 rostlin na variantu.

Výsledky experimentu Holubík et al. (2021) potvrzují hypotézu, že vstup Tl do rostlinné matrice je při hydroponické kultivaci doprovázen vyšším příjmem jednomocných prvků Na a K (Tab. 9). Tento efekt pravděpodobně souvisí s uplatněním pasivního příjmu a biogenních prvků jak ukazují Taiz et Zeiger (2003). Výsledky příjmu Tl u rostlin pěstovaných na umělé půdě nejsou s ohledem na pozorované známky vadnutí zcela objektivním pozorováním.

Tab. 9: Index biologické akumulace prvků/Tl (BAI) do pletiv

varianta	pletivo	**$BAI_{Tl\ (\%)}$**	BAI_{Na} (%)	BAI_{Mg} (%)	BAI_{K} (%)	BAI_{Ca} (%)	BAI_{Mn} (%)	BAI_{Fe} (%)
A_1	list	**0,54**	59	4,2	5,6	3,7	1,0	1,4
	stonek	**0,33**	29	2,5	1,9	2,2	0,4	1,1
	kořen	**0,08**	5	0,8	0,3	1,2	0,3	1,7
	celá rostlina	**0,95**	93	7,5	7,8	7,1	1,7	4,2
A_2	list	**0,66**	46	4,9	4,8	3,8	1,2	2,1
	stonek	**0,35**	31	3,4	1,9	2,0	0,5	0,8
	kořen	**0,05**	3	0,5	0,2	0,4	0,2	1,6
	celá rostlina	**1,07**	80	8,8	6,8	6,2	1,9	4,4
B_1	list	**0,42**	16	4,6	3,5	2,6	0,5	1,9
	stonek	**0,33**	9	2,1	1,8	1,1	0,2	1,0
	kořen	**0,22**	3	1,1	0,6	1,1	0,2	5,6
	celá rostlina	**0,97**	27	7,7	5,9	4,8	0,9	8,5

Pozn.: Index Bio-akumulace pro celou rostlinu (BAI_{tot}) je počítán jako suma BAI jednotlivých pletiv; data kumulují hodnoty replikace 4 rostlin na variantu

Z literatury je známo, že některé rostliny s (hyper)akumulačními vlastnostmi dokáží do svých pletiv absorbovat až 19 g Tl/kg (sušiny) dvojštítek (*Biscutella laevigata*), 13 g Tl/kg (sušiny) iberka (*Iberis intermedia*) (Scheckel et al., 2004). Výsledky experimentu „Tolerance Tl" ukazují při kultivaci na půdě mnohem nižší prahovou hodnotu příjmu Tl hořčicí bílou (*Sinapis alba* L.) ~0,05 g Tl/kg (sušiny). Pro další směřování a potenciální využití modelové rostliny hořčice bílé k fytoremediačním účelům je limitní obsah přístupné formy Tl^+ v půdním roztoku ~1 mg Tl/L, který odpovídá akutnímu příjmu Tl^+ ~30 µg Tl/den.

5.4 Sledování izotopové signatury Tl v půdních podmínkách

Popis poměru stabilních izotopů $^{203/205}$Tl v půdě na pozadí speciační analýzy Vaněk et al. (2020) ukazuje, že v přírodním prostředí se na izotopickém posunu podílejí i další geochemické procesy (včetně zvětrávání). Tyto procesy mohou vést k akumulaci těžkého izotopu ^{205}Tl v půdách. Při zvětrávání půd dochází k častým projevům dynamické půdní rovnováhy. Pro popis izotopového složení jsou zásadní především projevy redoxní rovnováhy. Při popisu změny izotopového složení Tl jsou však nezanedbatelné i posuny spojené se specifickou sorpcí Tl na fáze illitu a birnessitu, příp. interakce na sorpčním komplexu s půdní organickou hmotou. V rámci popisu přirozeného zvětrávání je tak velmi složité odlišit prokázaný kinetický efekt (nabohacení o lehčí izotop ^{203}Tl během příjmu Tl rostlinou) a rovnovážný efekt (nabohacení o těžší izotop ^{205}Tl vlivem ustanovení dynamické půdní rovnováhy).

O mnoho jednodušší je pozorovat změny izotopové signatury Tl (ε^{205}Tl) v půdách ovlivněných emisemi z uhelných elektráren jak popisujeme v práci Vaněk et al. (2016). Emise antropogenního Tl mají s ohledem na spalovací proces typicky nízkou hodnotu ε^{205}Tl ($\leq 2{,}5$). Proto je určení tohoto druhu znečištění v půdě poměrně snadno prokazatelné a lehké izotopové frakce (^{203}Tl) mohou v půdě fungovat jako dobré stopovače antropického znečištění. Ve studii Vaněk et al. (2016) jsme na pomezí česko-německo-polských hranic (v oblasti tzv. „Black triangle") prokázali ovlivnění půd antropogenními vstupy Tl z více než 50%.

Antropogenní vstupy Tl z těžební a hutní činnosti pochází dominantně ze sulfidických rud (pyritu FeS_2, sfaleritu ZnS a galenitu PbS, Corzo Remigio et al., 2020;

Vaněk, Chrastný, et al., 2013; Xiao et al., 2004). Průměrný obsah Tl ve svrchních vrstvách půd zasažených oblastí obvykle překračuje 10 mg Tl/kg (Xiao et al., 2004). Vliv antropogenní zátěže (průmyslových odpadů z těžby Zn v oblasti Oklusz Polsko) byl sledován i práci Vaněk et al., (2018). I když rozsah kontaminace Tl (1-500 mg/kg) v jednotlivých odpadních materiálech byl široký, izotopové signatury Tl (ε^{205}Tl) pro fáze popílku (ε^{205}Tl ~-4,1) a strusky (ε^{205}Tl ~-3,3) vykazovaly typické signatury (Vaněk et al., 2018). Výsledky studie ukazují, že zdroje popílku či strusky jsou v půdách oblasti Oklusz patrné i po 30 letech od masivní depozice těchto materiálů. Výsledky frakcionace izotopů Tl v oblasti Oklusz (Vaněk et al., 2018) představily reálnou možnost využití ε^{205}Tl pro sledování historické zátěže průmyslové depozice rizikových prvků v životním prostředí.

6. Závěr

Disertační práce je souborem výzkumných prací, které se pokusily odpovědět na základní otázky: (i) jakým způsobem vstupuje Tl do pletiv rostlin a zda je tento vstup doprovázen změnou izotopového složení, (ii) zda má různý způsob kultivace rostlin přímý vliv na příjem živin a zda může ovlivnit příjem Tl rostlinou, (iii) zda je vstup Tl do rostliny řízen v asociaci s dalšími prvky.

K možnosti odpovědět na tyto otázky byly sestaveny tři nezávislé nádobové pokusy s modelovou rostlinou hořčicí bílou (*Sinapis alba* L.). Sledování izotopické signatury Tl ukazuje nabohacení lehčími izotopy ^{203}Tl v rostlině vůči hydroponickému roztoku. Bylo prokázáno, že intenzita frakcionace ε^{205}Tl se zvyšovala v závislosti na tom, jak se snižovala dostupná zásoba Tl v živném roztoku. Při popisu ε^{205}Tl v rostlině byl zaznamenán mírný posun k nabohacení těžších izotopů ^{205}Tl v nadzemních částech rostlin, vůči kořenům. Toto zjištění nás vede k domněnce, že v nadzemních částech rostlin může docházet k vnitřním reakcím a k částečné vazebné akumulaci Tl v rostlině. Vznik komplexů Tl^{I} s vazbou na S (popř. na thiolovou skupinou -SH) se však na základě speciační analýzy (XANES) nepotvrdila. Speciační analýza nezávisle na vzorkované části rostlin ukázala dominantní přítomnost volného Tl v rostlině a částečnou koordinaci Tl^{I} na karboxylovou skupinu (-COOH).

Pro praktické využití výsledků disertační práce je podstatné zjištění, že příjem Tl do rostlin je maximální při koncentraci okolo 0,01 mg Tl/L v roztoku. Zároveň se ukazuje, že

při koncentracích Tl do 0,1 mg Tl/L v roztoku je až dvakrát efektivnější kultivace rostlin v půdě, kdy předpokládáme aktivní příjem Tl a biogenních prvků z půdního roztoku vůči hydroponické kultivaci. Vstup Tl do rostliny je při hydroponické kultivaci spojen s příjmem monovalentních iontů (Na/K), které zřejmě nesouvisí s reakcí rostliny na stresové podmínky vyvolané expozicí Tl. Samotné uložení Tl v rostlinném pletivu je až z 95 % řízeno do stonku a následně do listu, kde je pravděpodobně ukládáno ve vakuole společně s Ca. Při kultivaci v umělé půdě se můžeme domnívat, že zvýšený příjem K a Mg může být spojován s reakcí rostlin na stresové podmínky vyvolané intoxikací prostředí ionty Tl. Pro růst modelové rostliny (*Sinapis alba* L.) v půdním prostředí byla detekována limitní koncentrace ~1 mg Tl/L v půdním roztoku. Pro případné fytoextrakční využití modelové rostliny (hořčice bílé) je pozitivní, že ani dvounásobná koncentrace Tl (~2 mg Tl/L) v hydroponickém roztoku nepůsobí rostlinám fyziologický stres a neovlivňuje příjem základních živin.

Výsledky práce ukazují reálnou možnost sledovat metodami izotopového složení Tl parametry historické zátěže životního prostředí. Kombinací poznatků získaných v modelovaných podmínkách (nádobových experimentů) a poznatků spojených s hodnocením izotopové signatury Tl v reálných půdních podmínkách mohou přispět k popisu biogeochemických procesů na pomezí mezi půdou a rostlinou.

7. Seznam příloh

- PŘÍLOHA I. - Izotopy Tl

Vaněk, A., Holubík, O., Oborná, V., Mihaljevič, M., Trubač, J., Ettler, V., Pavlů, L., Vokurková, P., Penížek, V., Zádorová, T., Voegelin, A., 2019. Thallium stable isotope fractionation in white mustard: Implications for metal transfers and incorporation in plants. Journal of Hazardous Materials. 369, 521–527. https://doi.org/10.1016/j.jhazmat.2019.02.060

- PŘÍLOHA II. - Bioakumulace Tl

Holubík, O., Vaněk, A., Mihaljevič, M., Vejvodová, K., 2020. Higher Tl bioaccessibility in white mustard (hyper-accumulator) grown under the soil than hydroponic conditions: A key factor for the phytoextraction use. Journal of Environmetal Management. 255, 109880. https://doi.org/10.1016/j.jenvman.2019.109880

- PŘÍLOHA III. - Tolerance Tl

Holubík, O., Vaněk, A., Mihaljevič, M., Vejvodová, K., 2021. Thallium uptake/tolerance in a model (hyper)accumulating plant: Effect of extreme contaminant loads. Soil and Water Research. 16, 129–135. https://doi.org/10.17221/167/2020-SWR

- PŘÍLOHA IV. - Izotopické trasování Tl

Vaněk, A., Grösslová, Z., Mihaljevič, M., Trubač, J., Ettler, V., Teper, L., Cabala, J., Rohovec, J., Zádorová, T., Penížek, V., Pavlů, L., Holubík, O., Němeček, K., Houška, J., Drábek, O., Ash, C., 2016. Isotopic Tracing of Thallium Contamination in Soils Affected by Emissions from Coal-Fired Power Plants. Environmental Science & Technology. 50, 9864–9871. https://doi.org/10.1021/acs.est.6b01751

- PŘÍLOHA V. - Izotopová signatura Tl v metalurgických odpadech

Vaněk, A., Grösslová, Z., Mihaljevič, M., Ettler, V., Trubač, J., Chrastný, V., Penížek, V., Teper, L., Cabala, J., Voegelin, A., Zádorová, T., Oborná, V., Drábek, O., Holubík, O., Houška, J., Pavlů, L., Ash, C., 2018. Thallium isotopes in metallurgical wastes/contaminated soils: A novel tool to trace metal source and behavior. Journal of Hazardous Materials. 343, 78–85. https://doi.org/10.1016/j.jhazmat.2017.09.020

- PŘÍLOHU VI. - Izotopové složení Tl v půdách

Vaněk, A., Voegelin, A., Mihaljevič, M., Ettler, V., Trubač, J., Drahota, P., Vaňková, M., Oborná, V., Vejvodová, K., Penížek, V., Pavlů, L., Drábek, O., Vokurková, P., Zádorová, T., Holubík, O., 2020. Thallium stable isotope ratios in naturally Tl-rich soils. Geoderma 364, 114183. https://doi.org/https://doi.org/10.1016/j.geoderma.2020.114183

8. Seznam použité literatury

Adriano, D. C. 2001. Trace Elements in Terrestrial Environments. NY. Springer New York. ISBN: 978-1-4684-9505-8.

Al-Najar, H., Kaschl, A., Schulz, R., Römheld, V. 2005. Effect of thallium fractions in the soil and pollution origins on Tl uptake by hyperaccumulator plants: a key factor for the assessment of phytoextraction. International Journal of Phytoremediation. 7 (1). 55–67. doi: 10.1080/16226510590915837.

Al-Najar, H., Schulz, R., Römheld, V. 2003. No Title. Plant and Soil. 249 (1). 97–105. doi: 10.1023/A:1022544809828.

Alloway, B. J. 2012. Heavy Metals in Soils. Springer; Softcover reprint of the original 2nd ed. 1995 Springer (Verlag). p. 368. ISBN: 9789401045865.

Allus, M. A., Martin, M. H., Nickless, G. 1987. Comparative toxicity of thallium to two plant species. Chemosphere. 16 (4). 929–932. doi: 10.1016/0045-6535(87)90026-9.

Anderson, C. W. N., Brooks, R. R., Chiarucci, A., Lacoste, C. J., Leblanc, M., Robinson, B. H., Simcock, R., Stewart, R. B. 1999. Phytomining for nickel, thallium and gold. In: Journal of Geochemical Exploration. Vol. 67. p. 407–415. Elsevier.

Barthelmy, D. Mineral Species containing Thallium. In: Mineralogy database [online]. 2010 [cit. 2015-08-12]. Dostupné z: <http://webmineral.com/>.

Baker, R. G. A., Rehkämper, M., Hinkley, T. K., Nielsen, S. G., Toutain, J. P. 2009. Investigation of thallium fluxes from subaerial volcanism-Implications for the present and past mass balance of thallium in the oceans. Geochimica et Cosmochimica Acta. 73 (20). 6340–6359. doi: 10.1016/j.gca.2009.07.014.

Baskaran, M. 2012. Handbook of environmental isotope geochemistryHandbook of Environmental Isotope Geochemistry. Vol. 1–2. p. 1-951. ISBN: 9783642106378.

Beard, B. L., Johnson, C. M., Cox, L., Sun, H., Nealson, K. H., Aguilar, C. 1999. Iron isotope biosignatures. Science (New York, N.Y.). 285 (5435). 1889–1892. doi: 10.1126/science.285.5435.1889.

Bowen, H.J.M. 1979. Environmental chemistry of the elements. Academic Press, London. p. 333. ISBN: 0121204502.

Corzo Remigio, A., Chaney, R. L., Baker, A. J. M., Edraki, M., Erskine, P. D., Echevarria, G., van der Ent, A. 2020. Phytoextraction of high value elements and contaminants from mining and mineral wastes: opportunities and limitations. Plant and Soil. 449 (1–2). 11–37. doi: 10.1007/s11104-020-04487-3.

Fargašová, A. 2004. Toxicity comparison of some possible toxic metals (Cd, Cu, Pb, Se, Zn) on young seedlings of Sinapis alba L. Plant, Soil and Environment. 50 (1). 33–38.

Galván-Arzate, S., Santamaría, A. 1998. Thallium toxicity. Toxicology Letters. 99 (1). 1–13.

Grösslová, Z., Vaněk, A., Mihaljevič, M., Ettler, V., Hojdová, M., Zádorová, T., Pavlů, L., Penížek, V., Vaněčková, B., Komárek, M., Chrastný, V., Ash, C. 2015. Bioaccumulation of thallium in a neutral soil as affected by solid-phase association. Journal of Geochemical Exploration. 159 . 208–212. doi: 10.1016/j.gexplo.2015.09.009.

Günther, K., Umland, F. 1988. Speziesanalytik von Cadmium und Thallium in nativen Rapspflanzen (Brassica napus). Fresenius' Zeitschrift Für Analytische Chemie. 331 (3–4). 302–309. doi: 10.1007/BF00481900.

Gutiérrez, M., Mickus, K., Camacho, L. M. 2016. Abandoned Pb Zn mining wastes and their mobility as proxy to toxicity: A review. Science of The Total Environment. 565 . 392–400. doi: 10.1016/j.scitotenv.2016.04.143.

Hall, J. L. 2002. Cellular mechanisms for heavy metal detoxification and tolerance. Journal of Experimental Botany. 53 (366). 1–11. Retrieved from http://www.ncbi.nlm.nih.gov/pubmed/11741035

Hammond, C. R. 1990. The elements. In: CRC handbook of chemistry and physics, 71st ed. p. 2324. ISBN: 0-8493-0471-7.

Harmsen, J. 2007. Measuring Bioavailability: From a Scientific Approach to Standard Methods. Journal of Environmental Quality. 36 (5). 1420–1428. doi: 10.2134/jeq2006.0492.

Hladun, K. R., Parker, D. R., Trumble, J. T. 2015. Cadmium, Copper, and Lead Accumulation and Bioconcentration in the Vegetative and Reproductive Organs of Raphanus sativus: Implications for Plant Performance and Pollination. Journal of Chemical Ecology. 41 (4). 386–395. doi: 10.1007/s10886-015-0569-7.

Hofmann, A. E., Bourg, I. C., Depaolo, D. J. 2012. Ion desolvation as a mechanism for kinetic isotope fractionation in aqueous systems. PNAS. 109 (46). 18689–18694. doi: 10.1073/pnas.1208184109.

Holubík, O., Vaněk, A., Mihaljevic, M., Vejvodová, K. 2021. Thallium uptake/tolerance in a model (hyper)accumulating plant: Effect of extreme contaminant loads. Soil and Water Research. 2021 (2). 129–135. doi: 10.17221/167/2020-SWR.

Holubík, O., Vaněk, A., Mihaljevič, M., Vejvodová, K. 2020. Higher Tl bioaccessibility in white mustard (hyper-accumulator) grown under the soil than hydroponic conditions: A key factor for the phytoextraction use. Journal of Environmental Management. 255 (November 2019). 109880. doi: 10.1016/j.jenvman.2019.109880.

IPCS 1996. Thallium. International Program on Chemical Saftey. Environmental Health Criteria. 182. Geneva, Switzerland, World Health Organization.

Kabata-Pendias, A., Pendias, H. 1992. Trace elements in soils and plants. 2nd Editio. Boca Raton. CRC Press. p. 365. ISBN: 0849366437.

Kabata-Pendias, A., Sadurski, W. 2004. Trace elements and compounds in soil. Elements and Their Compounds in the Environment. 79–99. doi: 10.1002/9783527619634.ch5.

Kazantzis, G. 2000. Thallium in the Environment and Health Effects. Environmental Geochemistry and Health. 22 (4). 275–280. doi: 10.1023/A:1006791514080.

Kersten, M., Xiao, T., Kreissig, K., Brett, A., Coles, B. J., Rehkämper, M. 2014. Tracing anthropogenic thallium in soil using stable isotope compositions. Environmental Science & Technology. 48 (16). 9030–6. doi: 10.1021/es501968d.

Kim, D. J., Park, B. C., Ahn, B. K., Lee, J. H. 2016. Thallium uptake and translocation in barley and sunflower grown in hydroponic conditions. International Journal of Environmental Research. 10 (4). 575–582. doi: 10.22059/ijer.2016.59686.

Krämer, U. 2010. Metal Hyperaccumulation in Plants. Annual Review of Plant Biology. 61 (1). 517–534. doi: 10.1146/annurev-arplant-042809-112156.

Krasnodębska-Ostręga, B., Sadowska, M., Ostrowska, S. 2012. Thallium speciation in plant tissues—Tl(III) found in Sinapis alba L. grown in soil polluted with tailing sediment containing thallium minerals. Talanta. 93 . 326–329. doi: 10.1016/j.talanta.2012.02.042.

Kunze, M. 1972. Sensitivity of Staphylococcus aureus and Staphylococcus epidermidis to thallium. Zentralbl Bakteriol Parasitenkd Infektionskr Hyg Abt. I Orig. Reihe A. 222(4). 548–551.

Kwan, K. H. M., Smith, S. 1991. Some aspects of the kinetics of cadmium and thallium uptake by fronds of Lemna minor L. New Phytologist. 117 (1). 91–102. doi: 10.1111/j.1469-8137.1991.tb00948.x.

Leblanc, M., Petit, D., Deram, A., Robinson, B. H., Brooks, R. R. 1999. The phytomining and environmental significance of hyperaccumulation of thallium by Iberis intermedia from southern France. Economic Geology. 94 (1). 109–113. doi: 10.2113/gsecongeo.94.1.109.

Lindsay, W. L., Doxtader, K. G. 1981. Environmental Chemistry of the Elements. Journal of Environmental Quality. 10 (2). 249–249. doi: 10.2134/jeq1981.00472425001000020030x.

Madejón, P., Murillo, J. M., Marañón, T., Lepp, N. W. 2007. Factors affecting accumulation of thallium and other trace elements in two wild Brassicaceae spontaneously growing on soils contaminated by tailings dam waste. Chemosphere. 67 (1). 20–28. doi: 10.1016/j.chemosphere.2006.10.008.

Mazur, R., Sadowska, M., Kowalewska, Ł., Abratowska, A., Kalaji, H. M., Mostowska, A., Garstka, M., Krasnodębska-Ostręga, B. 2016. Overlapping toxic effect of long term thallium exposure on white mustard (Sinapis alba L.) photosynthetic activity. BMC Plant Biology. 16 (1). 191. doi: 10.1186/s12870-016-0883-4.

Merian, E., Clarkson, T. W. 1991. Metals and their compounds in the environment : occurrence, analysis, and biological relevance. Weinheim, VCH, 1991. 1438 p. ISBN: 352726521X

Mestek, O., Polák, J., Juříček, M., Karvánková, P., Koplík, R., Šantrůček, J., Kodíček, M. 2007. Trace element distribution and species fractionation in Brassica napus plant. In: Applied Organometallic Chemistry. Vol. 21. p. 468–474. John Wiley & Sons, Ltd.

Nielsen, S. G., Rehkämper, M., Baker, J., Halliday, A. N. 2004. The precise and accurate determination of thallium isotope compositions and concentrations for water samples by MC-ICPMS. Chemical Geology. 204 (1–2). 109–124. doi: 10.1016/j.chemgeo.2003.11.006.

Nielsen, S. G., Wasylenki, L. E., Rehk??mper, M., Peacock, C. L., Xue, Z., Moon, E. M. 2013. Towards an understanding of thallium isotope fractionation during adsorption to manganese oxides. Geochimica et Cosmochimica Acta. 117 . 252–265. doi: 10.1016/j.gca.2013.05.004.

Ning, Z., He, L., Xiao, T., Márton, L. 2015. High Accumulation and Subcellular Distribution of Thallium in Green Cabbage (Brassica Oleracea L. Var. Capitata L.). International Journal of Phytoremediation. 17 (11). 1097–1104. doi: 10.1080/15226514.2015.1045133.

OECD 2001. OECD guidelines for the testing of chemicals - 303A Activated sludge units. Available in: http://www.oecd.org/env/ehs/testing/34898616.pdf. Draft Docu (November). 1–53. doi: 10.1787/9789264203785-en.

Pavlíčková, J., Zbíral, J., Smatanová, M., Habarta, P., Houserová, P., Kubáň, V. 2006. Uptake of thallium from artificially contaminated soils by kale (Brassica oleracea L. var. acephala). Plant, Soil and Environment. 52 (12). 544–549. doi: 10.17221/3545-PSE.

Pavlíčková, J., Zbíral, J., Smatanová, M., Houserová, P., Čižmárová, E., Havlíková, Š., Kubáň, V. 2005. Uptake of Thallium from Artificially and Naturally Contaminated Soils into Rape (*Brassica napus* L.). Journal of Agricultural and Food Chemistry. 53 (8). 2867–2871. doi: 10.1021/jf048042k.

Peacock, C. L., Moon, E. M. 2012. Oxidative scavenging of thallium by birnessite: Explanation for thallium enrichment and stable isotope fractionation in marine ferromanganese precipitates. Geochimica et Cosmochimica Acta. 84 . 297–313. doi: 10.1016/j.gca.2012.01.036.

Peter, A. L. J., Viraraghavan, T. 2005. Thallium: A review of public health and environmental concerns. Environment International. 31 (4). 493–501. doi: 10.1016/j.envint.2004.09.003.

Rehkämper, M., Halliday, A. N. 1999. The precise measurement of Tl isotopic compositions by MC-ICPMS: Application to the analysis of geological materials and meteorites. Geochimica et Cosmochimica Acta. 63 (6). 935–944. doi: 10.1016/S0016-7037(98)00312-3.

Reid, P. H., York, E. T. 1958. Effect of Nutrient Deficiencies on Growth and Fruiting Characteristics of Peanuts in Sand Cultures1. Agronomy Journal. 50 (2). 63. doi: 10.2134/agronj1958.00021962005000020002x.

Richter, F. M., Dauphas, N., Teng, F. 2009. Non-traditional fractionation of non-traditional isotopes : Evaporation , chemical diffusion and Soret diffusion. Chemical Geology. 258 . 92–103. doi: 10.1016/j.chemgeo.2008.06.011.

Robinson, B., Anderson, C. 2018. Element Case Studies: Thallium and Noble Metals. . p. 253–261. Springer, Cham.

Ryan, B. M., Kirby, J. K., Degryse, F., Harris, H., Mclaughlin, M. J., Scheiderich, K. 2013. Copper speciation and isotopic fractionation in plants: Uptake and translocation mechanisms. New Phytologist. 199 (2). 367–378. doi: 10.1111/nph.12276.

Ryan, B. M., Kirby, J. K., Degryse, F., Scheiderich, K., McLaughlin, M. J. 2014. Copper isotope fractionation during equilibration with natural and synthetic ligands. Environmental Science and Technology. 48 (15). 8620–8626. doi: 10.1021/es500764x.

Sadowska, M., Biaduń, E., Krasnodębska-Ostręga, B. 2016. Stability of Tl(III) in the context of speciation analysis of thallium in plants. Chemosphere. 144. 1216–1223. doi: 10.1016/j.chemosphere.2015.09.079.

Sager, M. 1994. Thallium. Toxicological & Environmental Chemistry. 45 (1–2). 11–32. doi: 10.1080/02772249409358067.

Sherlock, J. C., Smart, G. A. 1986. Thallium in foods and the diet. Food Additives and Contaminants. 3 (4). 363–370. doi: 10.1080/02652038609373603.

Scheckel, K. G., Lombi, E., Rock, S. A., McLaughlin, M. J. 2004. In vivo synchrotron study of thallium speciation and compartmentation in Iberis intermedia. Environmental Science and Technology. 38 (19). 5095–5100. doi: 10.1021/es049569g.

Skłodowska, A., Matlakowska, R. 2004. The role of microorganisms in dispersion of thallium compounds in the environment. Polish Journal of Microbiology. 53 (4). 273–278.

Smeets, K., Ruytinx, J., Van Belleghem, F., Semane, B., Lin, D., Vangronsveld, J., Cuypers, A. 2008. Critical evaluation and statistical validation of a hydroponic culture system for Arabidopsis thaliana. Plant Physiology and Biochemistry. 46 (2). 212–218. doi: 10.1016/j.plaphy.2007.09.014.

Taiz, L., Zeiger, E. 2003. Plant physiology. 3rd edn.Annals of Botany. Sinauer Associates; 3 edition. p. 690. ISBN: 0878938230.

Tremel, A., Masson, P., Sterckeman, T., Baize, D., Mench, M. 1997. Thallium in French agrosystems - I. Thallium contents in arable soils. Environmental Pollution. 95 (3). 293–302. doi: 10.1016/S0269-7491(96)00145-5.

van der Ent, A., Baker, A. J. M., Reeves, R. D., Pollard, A. J., Schat, H. 2013. Hyperaccumulators of metal and metalloid trace elements: Facts and fiction. Plant and Soil. 362 (1–2). 319–334. doi: 10.1007/s11104-012-1287-3.

Vaněk, A., Grösslová, Z., Mihaljevič, M., Ettler, V., Trubač, J., Chrastný, V., Penížek, V., Teper, L., Cabala, J., Voegelin, A., Zádorová, T., Oborná, V., Drábek, O., Holubík, O., Houška, J., Pavlů, L., Ash, C. 2018. Thallium isotopes in metallurgical wastes/contaminated soils: A novel tool to trace metal source and behavior. Journal of Hazardous Materials. 343 . 78–85. doi: 10.1016/j.jhazmat.2017.09.020.

Vaněk, A., Grösslová, Z., Mihaljevič, M., Trubač, J., Ettler, V., Teper, L., Cabala, J., Rohovec, J., Zádorová, T., Penížek, V., Pavlů, L., Holubík, O., Němeček, K., Houška, J., Drábek, O., Ash, C. 2016. Isotopic Tracing of Thallium Contamination in Soils Affected by Emissions from Coal-Fired Power Plants. Environmental Science and Technology. 50 (18). 9864–9871. doi: 10.1021/acs.est.6b01751.

Vaněk, A., Holubík, O., Oborná, V., Mihaljevič, M., Trubač, J., Ettler, V., Pavlů, L., Vokurková, P., Penížek, V., Zádorová, T., Voegelin, A. 2019. Thallium stable isotope fractionation in white mustard: Implications for metal transfers and incorporation in plants. Journal of Hazardous Materials. 369 (December 2018). 521–527. doi: 10.1016/j.jhazmat.2019.02.060.

Vaněk, A., Chrastný, V., Komárek, M., Penížek, V., Teper, L., Cabala, J., Drábek, O. 2013. Geochemical position of thallium in soils from a smelter-impacted area. Journal of Geochemical Exploration. 124 . 176–182. doi: 10.1016/j.gexplo.2012.09.002.

Vaněk, A., Chrastný, V., Mihaljevič, M., Drahota, P., Grygar, T., Komárek, M. 2009. Lithogenic thallium behavior in soils with different land use. Journal of Geochemical Exploration. 102 (1). 7–12. doi: 10.1016/j.gexplo.2008.10.004.

Vaněk, A., Komárek, M., Chrastný, V., Bečka, D., Mihaljevič, M., Šebek, O., Panušková, G., Schusterová, Z. 2010. Thallium uptake by white mustard (Sinapis alba L.) grown on moderately contaminated soils—Agro-environmental implications. Journal of Hazardous Materials. 182 (1–3). 303–308. doi: 10.1016/J.JHAZMAT.2010.06.030.

Vaněk, A., Komárek, M., Vokurková, P., Mihaljevič, M., Šebek, O., Panušková, G., Chrastný, V., Drábek, O. 2011. Effect of illite and birnessite on thallium retention and bioavailability in contaminated soils. Journal of Hazardous Materials. 191 (1–3). 170–176. doi: 10.1016/J.JHAZMAT.2011.04.065.

Vaněk, A., Mihaljevič, M., Galušková, I., Chrastný, V., Komárek, M., Penížek, V., Zádorová, T., Drábek, O. 2013. Phase-dependent phytoavailability of thallium – A synthetic soil experiment. Journal of Hazardous Materials. 250–251 . 265–271. doi: 10.1016/j.jhazmat.2013.01.076.

Vaněk, A., Voegelin, A., Mihaljevič, M., Ettler, V., Trubač, J., Drahota, P., Vaňková, M., Oborná, V., Vejvodová, K., Penížek, V., Pavlů, L., Drábek, O., Vokurková, P., Zádorová, T., Holubík, O. 2020. Thallium stable isotope ratios in naturally Tl-rich soils. Geoderma. 364 . 114183. doi: https://doi.org/10.1016/j.geoderma.2020.114183.

Voegelin, A., Pfenninger, N., Petrikis, J., Majzlan, J., Plötze, M., Senn, A.-C., Mangold, S., Steininger, R., Göttlicher, J. 2015. Thallium Speciation and Extractability in a Thallium- and Arsenic-Rich Soil Developed from Mineralized Carbonate Rock. Environmental Science & Technology. 49 (9). 5390–5398. doi: 10.1021/acs.est.5b00629.

Waldrop, M. M. 1988. Thallium superconductor reaches 125-K. Science. 239 (4845). 1243-1243.

Wick, S., Baeyens, B., Marques Fernandes, M., Voegelin, A. 2018. Thallium Adsorption onto Illite. Environmental Science & Technology. 52 (2). 571–580. doi: 10.1021/acs.est.7b04485.

Wiederhold, J. G. 2015. Metal stable isotope signatures as tracers in environmental geochemistry. Environmental Science and Technology. 49 (5). 2606–2624. doi: 10.1021/es504683e.

Wiederhold, J. G., Cramer, C. J., Daniel, K., Infante, I., Bourdon, B., Kretzschmar, R. 2010. Equilibrium Mercury Isotope Fractionation between Dissolved Hg(II) Species and Thiol-Bound Hg. Environmental Science & Technology. 44 (11). 4191–4197. doi: 10.1021/es100205t.

Wierzbicka, M., Szarek-Łukaszewska, G., Grodzińska, K. 2004. Highly toxic thallium in plants from the vicinity of Olkusz (Poland). Ecotoxicology and Environmental Safety. 59 (1). 84–88. doi: 10.1016/j.ecoenv.2003.12.009.

Wiggenhauser, M., Bigalke, M., Imseng, M., Müller, M., Keller, A., Murphy, K., Kreissig, K., Rehkämper, M., Wilcke, W., Frossard, E. 2016. Cadmium isotope fractionation in soil-wheat systems. Environmental Science and Technology. 50 (17). 9223–9231. doi: 10.1021/acs.est.6b01568.

Xiao, T., Guha, J., Boyle, D., Liu, C.-Q., Chen, J. 2004. Environmental concerns related to high thallium levels in soils and thallium uptake by plants in southwest Guizhou, China. Science of The Total Environment. 318 (1–3). 223–244. doi: 10.1016/S0048-9697(03)00448-0.

Xiao, T., Rehkämper, M., Yang, Z. 2010. Thallium isotope fractionation in the soil-plant interfaceEarth Science. Retrieved from https://goldschmidtabstracts.info/2010/1155.pdf

Xiao, T., Yang, F., Li, S., Zheng, B., Ning, Z. 2012. Thallium pollution in China: A geo-environmental perspective. Science of the Total Environment. 421–422 . 51–58. doi: 10.1016/j.scitotenv.2011.04.008.

Yang, C., Chen, Y., Peng, P., Li, C., Chang, X., Wu, Y. 2009. Trace element transformations and partitioning during the roasting of pyrite ores in the sulfuric acid industry. Journal of Hazardous Materials. 167 (1–3). 835–845. doi: 10.1016/j.jhazmat.2009.01.067.

Yang, S., Liu, Y. 2016. Nuclear field shift effects on stable isotope fractionation: a review. Acta Geochimica. 35 (3). 227–239. doi: 10.1007/s11631-016-0109-3.

Zayed, A., Gowthaman, S., Terry, N. 1998. Phytoaccumulation of Trace Elements by Wetland Plants: I. Duckweed. Journal of Environment Quality. 27 (3). 715. doi: 10.2134/jeq1998.00472425002700030032x.

Zijiang, Y. Dynamic model for nutrient uptake by tomato plant in hydroponics. (D. R. L. Karel Keesman, Ed.) (2016). Wageningen University. ISBN: 920926-980-090. Retrieved from http://edepot.wur.nl/389817

Použité programy:

StatSoft ČR, 2012. STATISTICA version 10.0. www.statsoft.com.

9. Přílohy

- PŘÍLOHA I. - Izotopy Tl

Vaněk, A., Holubík, O., Oborná, V., Mihaljevič, M., Trubač, J., Ettler, V., Pavlů, L., Vokurková, P., Penížek, V., Zádorová, T., Voegelin, A., 2019. Thallium stable isotope fractionation in white mustard: Implications for metal transfers and incorporation in plants. Journal of Hazardous Materials. 369, 521–527.
https://doi.org/10.1016/j.jhazmat.2019.02.060

Journal of Hazardous Materials 369 (2019) 521–527

Contents lists available at ScienceDirect

Journal of Hazardous Materials

journal homepage: www.elsevier.com/locate/jhazmat

Thallium stable isotope fractionation in white mustard: Implications for metal transfers and incorporation in plants

Aleš Vaněk[a,*], Ondřej Holubík[a], Vendula Oborná[a], Martin Mihaljevič[b], Jakub Trubač[b], Vojtěch Ettler[b], Lenka Pavlů[a], Petra Vokurková[a], Vít Penížek[a], Tereza Zádorová[a], Andreas Voegelin[c]

[a] Department of Soil Science and Soil Protection, Faculty of Agrobiology, Food and Natural Resources, Czech University of Life Sciences Prague, Kamýcká 129, 165 00 Prague 6, Czech Republic
[b] Institute of Geochemistry, Mineralogy and Mineral Resources, Faculty of Science, Charles University, Albertov 6, 128 43 Prague 2, Czech Republic
[c] Eawag, Swiss Federal Institute of Aquatic Science and Technology, Ueberlandstrasse 133, CH-8600 Duebendorf, Switzerland

GRAPHICAL ABSTRACT

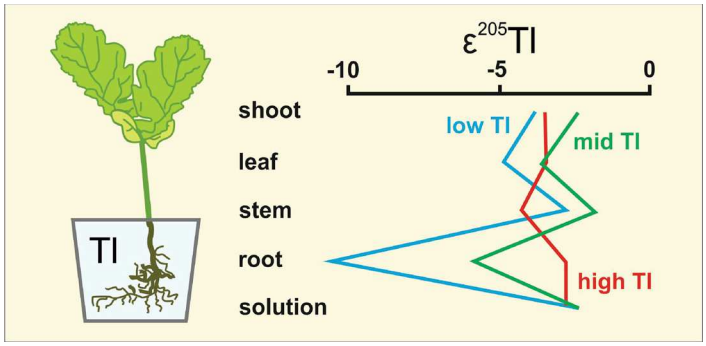

ARTICLE INFO

Keywords:
Thallium
Isotopes
Plant
Isotope fractionation

ABSTRACT

We studied thallium (Tl) isotope fractionation in white mustard grown hydroponically at different Tl doses. Thallium isotope signatures in plants indicated preferential incorporation of the light ^{203}Tl isotope during Tl uptake from the nutrient solution. Negative isotope fractionation was even more pronounced in dependence on how much the available Tl pool decreased. This finding corresponds to the concept of isotope overprinting related to a high contamination level in the growing media (solution or soil). Regarding Tl translocation in plants, we observed a large Tl isotope shift with an enrichment in the heavy ^{205}Tl isotope in the shoots relative to the roots in treatments with low/moderate solution Tl concentrations (0.01/0.05 mg Tl/L), with the corresponding $\alpha^{205/203}$Tl fractionation factors of ˜1.007 and 1.003, respectively. This finding is probably a consequence of specific (plant) reactions of Tl replacing K in its cycle. The formation of the S-coordinated Tl(I) complexes, potentially affecting both Tl accumulation and Tl isotope fractionation in plants, however, was not proven in our plants, since we did not have indication for that on the basis of X-ray absorption spectroscopy, suggesting that Tl was mainly present as free/hydrated Tl^+ ion or chemically bound to O-containing functional groups.

* Corresponding author.
E-mail address: vaneka@af.czu.cz (A. Vaněk).

https://doi.org/10.1016/j.jhazmat.2019.02.060
Received 18 December 2018; Received in revised form 7 February 2019; Accepted 15 February 2019
Available online 18 February 2019
0304-3894/

1. Introduction

Limited information is available on thallium (Tl) isotopes in biological materials. This kind of data is essential for complex understanding of Tl enrichment in biota and/or cycling in the environment. For example, the aspects of the degree to which the Tl isotope signature in biota can resemble the primary Tl source or whether Tl isotopes can better serve as a proxy for physiological processes and Tl speciation changes both remain unclear. Similarly, isotope data could be a promising tool for discrimination between soil substrate versus atmospheric deposition as important Tl sources in the biosphere.

Briefly, there is evidence that *Brassicaceae* can accumulate Tl with the following species reported to have high Tl levels in their tissues: *Iberis intermedia* Guers. (candytuft), *Biscutella laevigata* L., *Brassica oleracea acephala* L. (kale), *Brassica napus* L. (rape) and *Sinapis alba* L. (white mustard) [1–14]. The authors systematically highlighted the analogy of Tl(I) and K(I), reflecting similar ionic radii of Tl^+/K^+, which probably promotes an active role of Tl in the K biochemical cycle in plants [1,4,5,7,11]. Tremel et al. [1] also pointed out the predominant association of Tl with S-rich plants. To the contrary, Mestek et al. [15] documented that the S-containing compounds of plants (e.g., amino acids and peptides), considered to be the Tl-binding compounds in plant tissues, are of lesser importance in Tl complexation and transfer (i.e., Tl is mainly present as a free ion and/or a labile complex). Similarly, Kowalska et al. [6] did not identified any S-coordinated Tl complexes or even Tl-free compounds (i.e., phytochelatins) in mustard plants, potentially reducing the toxic effect of Tl. It is evident from this summary that the mechanisms of Tl uptake by plants, including isotopes [16], have not yet been fully elucidated and result from a set of processes such as soil Tl association, Tl speciation, nutrient availability, internal reactions related to K (and S?) biochemistry, etc.

Here, we tested Tl isotope variations during biological uptake and the transfer in a Tl-accumulating plant (white mustard) grown hydroponically, i.e., under well-defined/controlled conditions, to better understand Tl redistribution processes during contamination. Furthermore, the aspect of the degree to which the Tl isotope fractionation can reflect Tl incorporation into the plant or can be overprinted by the available Tl pool was considered in this study.

2. Experimental

2.1. Hydroponic experiment

White mustard (*Sinapis alba* L.) was grown hydroponically in a Reid-York nutrient solution (pH ~4.5) [17]. The solution was obtained from diluted stock solution (Supplementary material, Table S1) to ensure appropriate nutrient levels for the individual growth phases: (i) 7 days representing a preparatory (Tl-free) period where 10-fold diluted Reid-York solution was used and (ii) a 21 day period with Tl-spiked hydroponic media diluted 5-fold. The experiment was conducted under standard laboratory conditions (room temperature ~21 °C, humidity 40–55%, etc.). Thallium(I) sulfate (analytical grade; Fluka, Germany) dissolved in deionized water was used for Tl contamination. Briefly, the growing scheme was as follows: (i) mustard seeds were incubated on filter paper soaked in deionized H_2O for 4 days at ~20 °C; (ii) the two-leaf seedlings were placed on top of seed boxes filled with SignUS SG 5 silica gel (Sivomatic, the Netherlands) (Supplementary material, Table S2) saturated with the nutrient (Tl-free) solution; (iii) the plants were grown at different Tl levels corresponding to 0.01, 0.05 and 0.1 mg Tl/L. The Tl-free treatment was used as a control. Six plants were grown separately for each Tl solution, which was periodically replaced every 3 days to ensure approximate nutrient and contaminant homogeneity of the substrate. At the end of the 21-day period, the plants were carefully washed twice using deionized H_2O and ethanol to ensure complete removal of Tl from the plant surface. They were then divided into individual plant parts (root, stem and leaf; n = 6) and collected for further use and analyses. Finally, all the biomass was dried at 70 °C to constant weight prior to mineralization.

To determine the Tl/element contents and the Tl isotope composition, the biomass (0.01-0.09 g) was decomposed using a mixture of ultrapure/suprapure HNO_3/H_2O_2 (Merck, Germany) in a ratio of 4:1 which was added to the sample in a total volume of ~1–3 mL and then left in a closed 60-mL PTFE beaker (Savillex, USA) on a hot plate (150 °C) for 24 h. The concentrations of the major/trace elements (K, Ca, Mg, Fe, Mn, Pb and Tl) in the total digests and the hydroponic solutions were determined using either inductively coupled plasma optical emission spectrometry (ICP-OES, iCAP 6500, Thermo Scientific, UK) or quadrupole based inductively coupled plasma mass spectrometry (Q-ICP-MS, Xseries II, Thermo Scientific, Germany) under standard analytical conditions. The standard reference material INCT-TL-1 (tea leaves) (Institute of Nuclear Chemistry and Technology, Poland) was used for QC of quantitative analyses of trace elements (Supplementary material, Table S3).

2.2. Thallium speciation analysis

The speciation of Tl in plant material (root, stem, leaf) of white mustard was analyzed by X-ray absorption near-edge structure (XANES) spectroscopy at the Tl L_{III}-edge at the SAMBA beamline at the Soleil synchrotron (Gif-sur-Yvette, France). To ensure precise analysis with a sufficient amount of Tl in the plant tissue, the growth media contained 2 mg Tl/L for this experimental part. The experimental conditions, including the nutrient concentrations, were analogous to the treatments with lower Tl doses (0.01, 0.05 and 0.1 mg Tl/L). The speciation trial was thus represented by the additional plant group. The Tl concentrations related to the leaf, stem and root were 87, 66 and 28 mg Tl/kg, respectively. The freeze-dried plant materials were pressed into 7-mm diameter pellets, which were analyzed in a cryostat at 20 K. The monochromator was calibrated by setting the first maximum of the first derivative of the absorption edge of elemental Se to 12,658 eV A 4-element silicon drift detector was used to record the absorption spectra in the transmission mode. In addition to the sample spectra, the spectra of Tl_2O_3, $TlAsS_2$ and Tl(I)-acetate were recorded. The spectrum of aqueous Tl^+ at room temperature was available from an earlier study [18].

2.3. Thallium isolation

In order to isolate Tl from the sample matrix (i.e., digested biomass sample or hydroponic solution), a two-stage chromatographic separation with an anion exchange resin (Bio-Rad AG1-X8, 200–400 mesh, Cl^- cycle) was performed according to the modified procedure of Baker et al. [19]. The sample was evaporated to complete dryness and then redissolved in 0.1 M HCl. Subsequently, Br_2 was added so that the reagent had a final concentration of 1% (v/v) in the sample solution (0.1 M HCl). The solution was then left overnight (> 12 h) to ensure that all the Tl(I) was oxidized to Tl(III). For Tl separation, the whole sample or its aliquot was taken so that, in general, < 500 ng of total Tl was present. The first stage of the chromatography utilized a 10-mL Poly-Prep-column (Bio-Rad, USA) filled with 2 mL of resin, followed by steps with reagent mixtures and volumes as follows: (i) 5 × 1 mL 0.1 M HCl-SO_2 + 5 × 1 mL 0.1 M HCl, resin cleaning; (ii) 5 × 1.5 mL 0.1 M HCl-1% Br_2, resin treatment; (iii) sample loading (0.1 M HCl-1% Br_2); (iv) 10 × 2 mL 0.01 M HCl-1% Br_2; (v) 6 × 2 mL 0.5 M HNO_3-1% Br_2; (vi) 6 × 2 mL 2 M HNO_3-1% Br_2; (vii) 6 × 2 mL 0.1 M HCl-1% Br_2; (viii) 15 × 2 mL 0.1 M HCl-SO_2, Tl/Pb fraction elution. The obtained Tl/Pb fraction was evaporated and redissolved in 200 µL 0.1 M HCl-1% Br_2 (> 12 h), in preparation for the next part of the Tl purification. A PP 1.2-mL micro-column filled with 250 µL of resin was used for the second chromatographic stage. Resin cleaning and treatment, as well as sample loading, were performed in the same way, with correspondingly lower volumes of the individual reagent mixtures. Once the final Tl fraction

was obtained, the Tl sample was evaporated and diluted in 5 mL 2% HNO_3. The thallium and Pb concentrations were monitored after sample dissolution and Tl separation using Q-ICP-MS; the Pb concentrations were systematically below 0.01% in relation to the Tl levels in the final Tl fraction. Chemicals of ultrapure/suprapure quality (Merck, Germany) and deionized water (MilliQ+, Millipore, USA) were used for the separation techniques.

2.4. Thallium isotope measurement

Thallium isotope analyses were carried out using MC-ICP-MS (Neptune Plus, Thermo Scientific, Germany) with desolvating nebulizer (Aridus II, CETAC, Thermo Scientific, Germany) at the Mass Spectrometry Laboratories of the Faculty of Science, Charles University in Prague (M. Mihaljevič, J. Trubač – operators), under the following analytical conditions: The detector configuration was: ^{202}Hg-L3, ^{203}Tl-L2, ^{204}Pb-L1, ^{205}Tl-C, ^{206}Pb-H1, ^{207}Pb-H2, ^{208}Pb-H3. All the solutions were measured in 3 runs of 50 cycles. Mass bias drift was eliminated using external normalization and standard sample bracketing (NIST SRM 997). The solutions were doped with NIST SRM 981 to obtain Pb/Tl 2-3. For inter-element correction, the ^{208}Pb/^{206}Pb ratio was related to the raw ^{205}Tl/^{203}Tl data by the exponential mass dependent fractionation law. The NIST SRM 997 standard was measured directly before and after each sample and the final data were interpolated between bracketing standards. The thallium isotope composition was reported with an ε notation relative to the NIST SRM 997 standard (Eq. (1)):

$$\varepsilon^{205}Tl = \frac{^{205}Tl/^{203}Tl_{sample} - ^{205}Tl/^{203}Tl_{NIST997}}{^{205}Tl/^{203}Tl_{NIST997}} \times 10^4 \quad (1)$$

The NIST SRM 997 standard was used as the ε^{205}Tl = 0 standard throughout. Repeated analyses of the Sigma-Alrich standard solution (for ICP analysis) confirmed the consistency with the reported value of ε^{205}Tl = -0.81 ± 0.33 (2 SD, n = 133) [20], reaching an ε^{205}Tl interval between -0.75 and -0.90 for the means of the measurement cycles (n = 4). The total procedural Tl blank was < 15 pg Tl, corresponding to less than 0.1% of the indigenous element budget. An external reproducibility test of the Tl isotope analyses carried out in our laboratories yielded a value of ± 0.9 ε^{205}Tl (2 SD), which is based on the multiple separate analyses (n = 6) of standard reference material – INCT-TL-1 (Tea leaves, Institute of Nuclear Chemistry and Technology, Poland). This value represents the estimated error for the presented dataset because this uncertainty value accounts for all the possible sources of error including sample dissolution, ion exchange chromatography, mass spectrometric procedures, etc. The fractionation factor, indicating the degree of Tl isotope fractionation between two samples (A and B) [21], is expressed in terms of α throughout this study, according to the following equation (Eq. (2)):

$$\alpha_{A-B} \sim \frac{(\varepsilon^{205}Tl_A + 10^4)}{(\varepsilon^{205}Tl_B + 10^4)} \quad (2)$$

3. Results and discussion

3.1. Plant biomass and Tl distribution

The average dry weight yields of mustard are given in Table 1. We detected variations in plant growth between the Tl treatments and the (Tl-free) control when the total above-ground biomass was considered. Moreover, there was an apparent change in the nutrient uptake. Potassium, Ca and Mg all predominated in the roots and leaves for the trial with maximum Tl concentration in the hydroponic solution (0.1 mg Tl/L, compared to less contaminated plants (0.05 and 0.01 mg Tl/L in solutions) or the control (Table 1). This finding points to the stress response and associated increased nutrient demand of Tl-affected plants. The Tl concentrations in mustard tissues corresponded well to

Table 1
Macronutrient concentrations (K, Ca, Mg and Fe) in mustard grown hydroponically at different Tl doses.

Tl level (mg Tl/L)	Sample	Biomass (g)	K (g/kg)	Ca (g/kg)	Mg (g/kg)	Fe (g/kg)
0.1	Root	0.006	6.3	13.6	4.0	3.5
	Stem	0.024	32.6	10.8	5.9	0.8
	Leaf	0.048	33.0	30.2	9.7	1.2
0.05	Root	0.010	2.2	10.1	2.6	6.6
	Stem	0.015	34.1	16.9	7.1	2.5
	Leaf	0.060	15.3	20.8	5.9	0.9
0.01	Root	0.013	2.1	9.3	2.7	3.8
	Stem	0.020	34.2	14.4	9.6	1.2
	Leaf	0.054	15.4	15.1	4.3	0.6
0 (control)	Root	0.027	1.4	3.8	1.0	0.8
	Stem	0.029	29.6	13.1	7.1	0.6
	Leaf	0.090	11.5	11.5	4.3	0.7

The concentration data are means with RSD < 5%.

the degree of the Tl contamination in the nutrient solutions, with the following plant Tl distribution order: stem (≤9.5 mg/kg), leaf (≤6.7 mg/kg) and root (≤6.4 mg/kg) (Table 2). Despite the fact that we did not find any correlation between the Tl and K contents in our samples, the tendency of Tl(I) to enter K(I) reactions in the *Brassicaceae* species (including mustard) and/or the processes taking place at the soil-plant interface was systematically demonstrated elsewhere [1,4,7,8,11,14,22]. It is thought that Na^+/K^+-ATPase, i.e., its formation, is an important control for internal Tl transfers [23,24]. In connection with the high Tl concentration in the stems, analogous behavior was identified for mustard grown on Tl-spiked soils, suggesting that this tissue has the greatest potential for Tl accumulation [8,11]. Scheckel et al. [4] report extremely high Tl levels throughout the vascular system of *I. intermedia* with average Tl concentrations in leaves and cotyledons of 8000 and 15,000 mg/kg (DW), respectively, using synchrotron X-ray differential absorption-edge computed microtomography. Again, this anomaly was simply interpreted in terms of the Tl(I)-K similarity. Although we do not know the exact mechanism of Tl accumulation (and stabilization) in plants, Tl complexation (or possibly coprecipitation) within the tissue(s) (e.g. in veins) could be involved. Ning et al. [25] who studied the subcellular distribution of Tl in green cabbage leaves, discovered important Tl compartmentalization, with the Tl concentration decreasing in the order cytosol and vacuole (~80% of total leaf Tl) > > cell wall > cell organelles. This specific subcellular fractionation appeared to facilitate detoxification of Tl by keeping it away from sensitive cellular organelles in the plant cell. The complexation of Tl in the cytosol by thiol-containing peptides such as phytochelatins was previously predicted to play an important role in Tl detoxification and plant tolerance to Tl stress [26]. However, this process has not been proven in this study, i.e., with regard to the obtained Tl speciation data better mimicking the K biochemistry (see Section 3.4). The finding is thus consistent with the data of Kowalska et al. [6], demonstrating that the role of the S-coordinated Tl complexes, including those with Tl(III), is probably negligible in plant Tl fixation, as they were not detected in any tested mustard tissue by the authors using the MS-based HPLC techniques.

3.2. Thallium isotope fractionation during uptake

The Tl isotope signatures for whole mustard plants indicated preferential incorporation of the light isotope (^{203}Tl) during Tl uptake from a nutrient solution having ε^{205}Tl ~-2.4 on an average; the observed isotope variability within individual media, although limited, probably resulted from Tl redistribution in vegetation boxes (resulting from e.g. partial Tl adsorption) and/or the instrumental error. In any case, our finding is consistent with the results reported previously for Cu and Cd,

Table 2
Total Tl concentrations, Tl isotope compositions (ε^{205}Tl) and respective fractionation factors (α) in mustard grown hydroponically at different Tl doses.

Tl level (mg Tl/L)	Sample	Tl (mg/kg)	Tl amount (μg/biomass)	ε^{205}Tl ± 0.9	$\alpha_{\text{ROOT-SOLUTION}}$	$\alpha_{\text{STEM-ROOT}}$	$\alpha_{\text{LEAF-STEM}}$	$\alpha_{\text{SHOOT-ROOT}}$	$\alpha_{\text{WHOLE PLANT-SOLUTION}}$
0.1	Solution			−2.76#					
	Root	6.37 ± 0.41	0.04	−2.78	1.0000	n.d.	n.d.	n.d.	n.d.
	Stem	9.47 ± 0.65	0.23	−4.23	n.d.	0.9999	n.d.	n.d.	n.d.
	Leaf	6.68 ± 0.39	0.32	−3.46	n.d.	n.d.	1.0001	n.d.	n.d.
	Shoot		0.55	−3.53	n.d.	n.d.	n.d.	0.9999	n.d.
	Whole Plant		0.59	−3.72	n.d.	n.d.	n.d.	n.d.	0.9999
0.05	Solution			−2.05#					
	Root	1.73 ± 0.12	0.02	−5.92	0.9996	n.d.	n.d.	n.d.	n.d.
	Stem	7.42 ± 0.35	0.11	−1.81	n.d.	1.0004	n.d.	n.d.	n.d.
	Leaf	1.81 ± 0.08	0.11	−3.60	n.d.	n.d.	0.9998	n.d.	n.d.
	Shoot		0.22	−2.48	n.d.	n.d.	n.d.	1.0003	n.d.
	Whole Plant		0.24	−2.97	n.d.	n.d.	n.d.	n.d.	0.9999
0.01	Solution			−2.36#					
	Root	0.25 ± 0.01	0.003	−10.64	0.9992	n.d.	n.d.	n.d.	n.d.
	Stem	0.86 ± 0.04	0.02	−2.70	n.d.	1.0008	n.d.	n.d	n.d.
	Leaf	0.52 ± 0.04	0.03	−4.88	n.d.	n.d.	0.9998	n.d.	n.d.
	Shoot		0.05	−3.79	n.d.	n.d.	n.d.	1.0007	n.d.
	Whole Plant		0.053	−4.39	n.d.	n.d.	n.d.	n.d.	0.9998
INCT-Tl-1*	Tea leaves	0.06 ± 0.01		−6.21*					

The uncertainties for total Tl concentrations are reported at the 2 SD level. The ε^{205}Tl data depict the average values for 6 specimens with an assigned error of ± 0.9 ε^{205}Tl (2 SD), which is based on multiple separate analyses (n = 6)* of standard reference material INCT-Tl-1 (Tea Leaves, Institute of Nuclear Chemistry and Technology, Poland), involving sample digestion, column chemistry and mass spectrometry. The isotope fractionation factors between two samples (respective plant parts) were estimated using the following equation: $\alpha_{A\text{-}B} \approx (\varepsilon^{205}Tl_A + 10{,}000)/(\varepsilon^{205}Tl_B + 10{,}000)$. The shoot and whole-plant ε^{205}Tl values were calculated using the mass balance equation: $\varepsilon^{205}Tl = \Sigma F_i \times \varepsilon^{205}Tl_i$; where F_i is the Tl portion in plant part and $\varepsilon^{205}Tl_i$ is its isotope composition. #This isotope variability resulted from the Tl redistribution in vegetation boxes and/or the instrumental error.

indicating that lighter isotopes could be preferentially taken up by plants/trees (oat, tomato, *Solanum nigrum* L., *Ricinus communis* L., pine) [27–29]. The greatest ^{203}Tl enrichment was found in mustard with a low Tl concentration in solution (0.01 mg Tl/L), with an ε^{205}Tl factor for the whole plant of −4.4. In contrast, larger ε values without a significant difference in the isotope signature were identified in plants affected by high and moderate Tl doses (0.1/0.05 mg Tl/L), with $\varepsilon^{205}Tl_{\text{WHOLE PLANT}}$ values of −3.7 and −3, respectively, and identical $\alpha_{\text{WHOLE PLANT-SOLUTION}}$ factors of ˜0.9999 (Table 2). This α factor was thus larger than the parameter obtained for the low-contaminated mustard (˜0.9998), suggesting increasing isotope fractionation with a decrease in the Tl concentration. According to Weiss et al. [30], who studied Zn isotope fractionation during the uptake by different plant species (rice, tomato and lettuce), the light isotope enrichment in plants could be related to lower proportion of free metal ions available in solution. This also means that some kind of Tl speciation changes should be considered as the control. Nevertheless, e.g. Tl chelation in solution is not probable, taking into account the very low stability of both organic (including EDTA) [31] and inorganic complexes with Tl(I) [32]. With reference to the results from our previous study [33], where speciation modelling was applied to different (synthetic) rhizosphere Tl solutions, the vast majority of the metal was predicted to be Tl(I) present as the free Tl^+ ion. Therefore, this aspect needs to be further tested.

Since we do expect that Tl uptake by mustard is promoted by its analogy with K, both having stable (dominant) oxidation (I) states in their species, reductive uptake similar to that, e.g. for Cu and Cd, is not possible. The Tl isotope fractionation for the whole plant was rather limited, compared to the isotope changes taking place during Tl translocation between individual plant parts (see Section 3.3), suggesting that isotope kinetics related to different (specific) physiological processes is the controlling factor. In other words, the light ^{203}Tl isotope presumably tends to react faster and thus it can participate preferentially in specific biochemical reactions.

3.3. Thallium isotope fractionation during translocation

Mustard exhibited large fractionation of Tl isotopes during translocation between different tissues impacted by low/moderate solution Tl levels, with a ε^{205}Tl variation of up to -8 units (Table 2). Here we identified significant enrichment in the heavy ^{205}Tl isotope in the shoots (ε^{205}Tl ≤-2.5) relative to the roots (ε^{205}Tl ≤-5.9), with corresponding $\alpha_{\text{SHOOT-ROOT}}$ factors of ˜1.0003–1.0007. This behavior was even more pronounced when the Tl fractionation for the stem-root interface was considered, as indicated by the $\alpha_{\text{STEM-ROOT}}$ factors ˜1.0004–1.0008. In terms of the results for the root-solution interface from an identical sample group, the heavy Tl isotope was depleted from the roots, with an $\alpha_{\text{ROOT-SOLUTION}}$ value of ≤0.9996 (Table 2). For the most contaminated mustard (0.1 mg Tl/L), both the $\alpha_{\text{SHOOT-ROOT}}$ and $\alpha_{\text{STEM-ROOT}}$ parameters had the same values, ˜0.9999, suggesting small (or limited) variability of Tl isotopes during translocation. Moreover, it is important to stress that this plant maintained a relatively consistent Tl isotope signature among the individual organs with the maximum ε^{205}Tl variation < −1.4 unit (Table 2).

While the ε^{205}Tl value for the whole plant results from the isotope fractionation during Tl uptake alone, ε^{205}Tl in the shoots (stem and leaf) depends on both the Tl isotope signature for the whole plant and the isotope fractionation during translocation. This fact also means that preferential translocation of the heavy ^{205}Tl isotope, if present, results in the Tl remaining in the original tissue being isotopically lighter. For this reason, Tl potentially tends to be more enriched in the light isotope in the roots as more total Tl is translocated to the shoots. This was clearly demonstrated by the α factors related to the root-solution and shoot-root interfaces (i.e., with 0.01 and 0.05 mg Tl/L in the media). A similar trend, although principally not comparable, was detected in the leaves with more negative ε^{205}Tl values (≤ −3.6) than those of the stems (≤ −1.8), suggesting that the ^{203}Tl isotope accumulated as Tl was translocated from the stems to the leaves (Table 2). Wiggenhauser et al. [34] suggested that the isotope fractionation between the stems and the leaves, although for Cd, is caused by a combined effect of ion speciation, adsorption and assimilation in the leaves relative to the stems. The authors report that xylem-related processes, i.e., associated

with transpiration, generally prefer light isotopes, i.e., similarly as it was demonstrated for Ni [35]. In contrast, vacuolar sequestration usually leads to heavy isotope enrichment [34]. The difference in the isotopic composition between these plant parts may further reflect the complete history of Tl uptake. Firstly, the secondary leaves are younger than the stems or the primary leaves, suggesting that the Tl isotope shift may be linked with previous Tl uptake and/or root-shoot Tl translocation, resulting in the isotopic alteration within the plant itself. Secondly, as the plant growth progresses, an excess of Tl is stored in the roots, whereas Tl transfer in the above-ground parts is further regulated. This concept was proposed for Cu [27]. In any case, the Tl isotope fractionation between the stems and leaves may be fully understood only by using an appropriate experimental design, involving complex organic and isotope analyses within the respective parts, as well as plant solutions related to specific cell compartments.

At this point, it should be pointed out that sorption/precipitation reactions linked with the redox Tl(I)→(III) shift are probably the most important way in which the heavy isotope fraction, if dissolved, could be accumulated in environmental systems. In contrast, the Tl isotope effects resulting from the reaction kinetics, involving reactants and products with predominant Tl(I), are potentially of less importance. Redox Tl processes linked with large heavy Tl isotope enrichments in mineral matrices were periodically reported for sedimentary systems, where the associated sorption and oxidation of Tl(I) on Mn(III,IV) oxide (s) took place [36–38]. This specific Tl behavior was mechanistically interpreted for birnessite (δ-MnO_2) by Nielsen et al. [21] and Peacock and Moon [39]. A similar trend was indicated for the Tl-contaminated soils with an apparent ε^{205}Tl increase in soil horizons containing higher portions of the oxalate-extractable Mn, indicative of secondary Mn oxides [16,40,41]. Even though we do not have detailed data on soluble Tl species in any mustard tissue, Krasnodebska-Ostrega et al. [11] demonstrated traces of Tl(III) complexes in plant extracts from mustard grown in Tl(I)-rich soils, using coupled HPLC and ICP-MS analysis, indicating the ability of the plant to oxidize some (limited) amount of Tl. Therefore, the heavy isotope enrichment in the mustard shoots relative to the roots might theoretically reflect this redox shift. On the other hand, we think that the process, if present, would play only a minor role in total isotope fractionation. Firstly, Tl(I) is thermodynamically more stable, compared to its trivalent form. Secondly, there is evidence for an extremely fast spontaneous reduction of Tl(III) to Tl(I) which is generally much faster than potential complexation of Tl(III) [14]. Besides the predicted important (dominant?) role of the K^+ channel in the Tl cycle, Tl(I) complexation by specific organic ligands, preferring the heavy ^{205}Tl isotope, might be another explanation for heavy Tl isotope enrichment during translocation (e.g., in xylem sap). However, this concept clearly needs further research, since we did not have any indication for such an association, including the S-coordinated Tl(I) (amino acids/peptides), in our tissues on the basis of XANES (see next chapter).

3.4. Thallium speciation by Tl L_{III}-edge XANES spectroscopy

In Fig. 1, the Tl L_{III}-edge spectra of the roots, stems and leaves of mustard plants grown in a concentrated Tl solution are shown in comparison to the reference spectra. The spectra of all the plant tissues were similar. Comparison with the reference spectra indicated that Tl (III) did not represent a substantial fraction (i.e., identifiable) of the plant Tl. In addition, the spectrum of $TlAsS_2$, which served as a proxy for S-coordinated Tl(I), did not closely match the plant Tl spectra. On the other hand, the plant Tl spectra most closely matched the spectra of Tl(I)-acetate and aqueous Tl^+. This suggested that Tl was predominantly O-coordinated Tl(I) as free/hydrated Tl^+ or was coordinated to O-containing functional groups, analogously to that of K(I) species. This finding was in accordance with the results of an earlier XANES study on Tl speciation in fresh leaves of *Iberis intermedia* [4]. Even though the solution Tl concentration (2 mg Tl/L) for the speciation trial did not match the trials where Tl isotopes were studied (0.01-0.1 mg Tl/L), we think that at least the principal mechanisms of Tl incorporation were similar, since we did not observe any special changes in plant growth or intoxication indications. Nevertheless, we realize that the detoxification mechanisms (Tl sequestration in non-active organs or cell vacuoles, complexation, etc.) might be promoted in plants affected by a higher Tl load.

4. Environmental implications

Our results indicate a clear shift towards the isotopically lighter Tl fraction observed during Tl uptake by an accumulating plant cultivated in hydroponics at variable Tl doses. Based on previous studies devoted to isotope fractionation of other metals [27,28,34,42], we expect that similar bulk enrichment in the light ^{203}Tl isotope will also be valid for other growing substrates (soil) and plant species (including trees). However, an enrichment of the heavy ^{205}Tl isotope in the shoots relative to the roots affected by moderate/low solution Tl doses indicates that the speciation and other specific reactions (e.g., Tl substitution for K in the plant K cycle) may play a key role in isotope shifts during Tl translocation.

In fact, there are at least three variables affecting complex Tl isotope dynamics in the substrate-plant systems *sensu lato*. Firstly, Tl(I) in soil is present in various phases/minerals exhibiting different solubility; possibly incongruent leaching of Tl from the host material will result in the isotope shift of dissolved Tl as compared to the bulk Tl pool. Secondly, abiotic transformation of Tl(I) to less mobile Tl(III) species as a result of

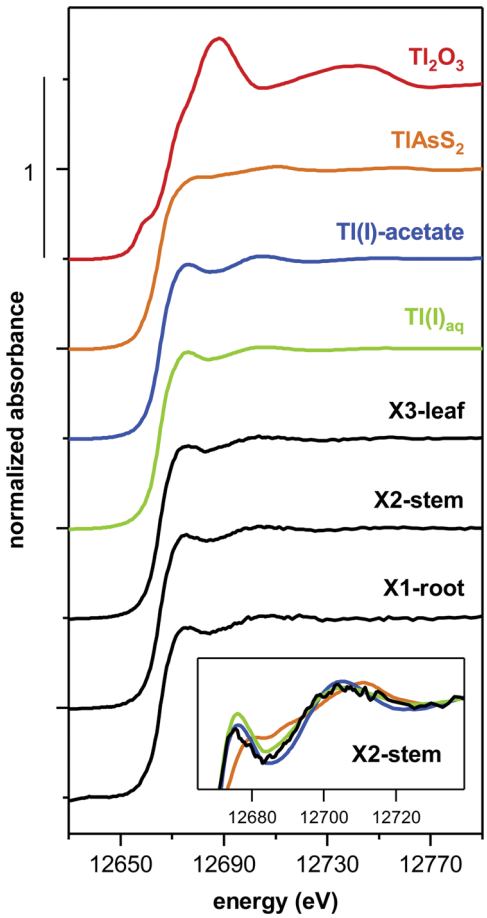

Fig. 1. Tl LIII-edge XANES spectra of freeze-dried root (X1), stem (X2) and leaf (X3) tissue of mustard (grown in 2 mg Tl/L-solution) compared with reference spectra for Tl_2O_3, $TlAsS_2$, Tl(I)-acetate and aqueous Tl^+. The inset shows an overlay plot of the spectra of $TlAsS_2$, Tl(I)-acetate and aqueous Tl^+ and the plant stem for direct comparison.

sorption to Mn (or potentially Fe) oxide minerals can generate significant post-depositional Tl isotope fractionations in soil, generally complicating the discrimination of the contamination (primary) source [16]. Thirdly, there is a good chance that Tl may passively enter the vegetation via leaves, i.e., plant surface, leading to similar isotope signature in the impacted biomass relative to the primary Tl source, as there is not a significant effect of biochemical processes within the line of root-stem-leaf.

In summary, our findings indicate that the application of Tl isotopes is a suitable tool for tracing Tl transfers between the substrate and plants, but similarly to other trace metals [27,34,42], Tl speciation seems to play an important role in the strategies of Tl uptake/avoidance by plant. All the above mentioned accompanying processes/mechanisms must be verified by further experiments with other plant species, more complex substrates and using more sophisticated approach depicting effects of individual physiological processes on Tl isotope shifts among individual plant parts.

Acknowledgements

This research was funded by a grant from the Czech Science Foundation (17-03211S). Part of the equipment used for this study was purchased from the Operational Programme Prague – Competitiveness (Project CZ.2.16/3.1.00/21516). The Charles University team was partly supported by institutional funding from the Center for Geosphere Dynamics (UNCE/SCI/006). The Soleil synchrotron light source (Gif-sur-Yvette, France) is acknowledged for allocation of beamtime at the SAMBA beamline and Gautier Landrot is thanked for his assistance during data collection. Dr. Madeleine Štulíková (a native speaker) is thanked for revision of the English manuscript. We would also like to cordially thank the two anonymous reviewers and Prof. Gerasimos Lyberatos (Editor of Journal of Hazardous Materials) for their suggestions/comments which improved the quality of the original manuscript.

Appendix A. Supplementary data

Supplementary material related to this article can be found, in the online version, at doi:https://doi.org/10.1016/j.jhazmat.2019.02.060.

References

[1] A. Tremel, P. Masson, H. Garraud, O.F.X. Donard, D. Baize, M. Mench, Thallium in French agrosystems–II. Concentration of thallium in field-grown rape and some other plant species, Environ. Pollut. 97 (1997) 161–168, https://doi.org/10.1016/S0269-7491(97)00060-2.

[2] H. Al-Najar, R. Schulz, V. Römheld, Plant availability of thallium in the rhizosphere of hyperaccumulator plants: a key factor for assessment of phytoextraction, Plant Soil 249 (2003) 97–105, https://doi.org/10.1023/A:1022544809828.

[3] H. Al-Najar, A. Kaschl, R. Schulz, V. Römheld, Effect of thallium fractions in the soil and pollution origins on Tl uptake by hyperaccumulator plants: a key factor for the assessment of phytoextraction, Int. J. Phytoremediat. 7 (2005) 55–67, https://doi.org/10.1080/16226510590915837.

[4] K.G. Scheckel, E. Lombi, S.A. Rock, M.J. McLaughlin, In Vivo synchrotron study of thallium speciation and compartmentation in Iberis intermedia, Environ. Sci. Technol. 38 (2004) 5059–5100, https://doi.org/10.1021/es049569g.

[5] K.G. Scheckel, R. Hamon, L. Jassogne, M. Rivers, E. Lombi, Synchrotron X-ray absorption-edge computed microtomography imaging of thallium compartmentalization in Iberis intermedia, Plant Soil 290 (2007) 51–60, https://doi.org/10.1007/s11104-006-9102-7.

[6] J. Kowalska, K. Kińska, M. Sadowska, M. Biesaga, B. Krasnodębska-Ostręga, The role of phytochelatins in Sinapis alba L. response to stress caused by two toxic elements As and Tl, Int. J. Environ. Anal. Chem. 95 (2015) 1148–1156, https://doi.org/10.1080/03067319.2015.1085527.

[7] T. Xiao, J. Guha, D. Boyle, C.Q. Liu, J. Chen, Environmental concerns related to high thallium levels in soils and thallium uptake by plants in southwest Guizhou, China, Sci. Total Environ. 318 (2004) 223–244, https://doi.org/10.1016/S0048-9697(03)00448-0.

[8] A. Vaněk, M. Komárek, V. Chrastný, D. Bečka, M. Mihaljevič, O. Šebek, G. Panušková, Z. Schusterová, Thallium uptake by white mustard (*Sinapis alba* L.) grown on moderately contaminated soils-Agro-environmental implications, J. Hazard. Mater. 182 (2010) 303–308, https://doi.org/10.1016/j.jhazmat.2010.06.030.

[9] A. Vaněk, M. Komárek, P. Vokurková, M. Mihaljevič, O. Šebek, G. Panušková, V. Chrastný, O. Drábek, Effect of illite and birnessite on thallium retention and bioavailability in contaminated soils, J. Hazard. Mater. 191 (2011) 190–196, https://doi.org/10.1016/j.jhazmat.2011.04.065.

[10] A. Vaněk, M. Mihaljevič, I. Galušková, V. Chrastný, M. Komárek, V. Penížek, T. Zádorová, O. Drábek, Phase-dependent phytoavailability of thallium – a synthetic soil experiment, J. Hazard. Mater. 250–251 (2013) 265–271, https://doi.org/10.1016/j.jhazmat.2013.01.076.

[11] B. Krasnodębska-Ostręga, M. Sadowska, S. Ostrowska, Thallium speciation in plant tissues-Tl(III) found in Sinapis alba L. grown in soil polluted with tailing sediment containing thallium minerals, Talanta 93 (2012) 326–329, https://doi.org/10.1016/j.talanta.2012.02.042.

[12] Y. Jia, T. Xiao, G. Zhou, Z. Ning, Thallium at the interface of soil and green cabbage (*Brassica oleracea* L. *var. capitata* L.): soil-plant transfer and influencing factors, Sci. Total Environ. 450–451 (2013) 140–147, https://doi.org/10.1016/j.scitotenv.2013.02.008.

[13] J. Liu, X. Luo, J. Wang, T. Xiao, D. Chen, G. Sheng, M. Yin, H. Lippold, C. Wang, Y. Chen, Thallium contamination in arable soils and vegetables around a steel plant-A newly-found significant source of Tl pollution in South China, Environ. Pollut. 224 (2017) 445–453, https://doi.org/10.1016/j.envpol.2017.02.025.

[14] M. Sadowska, E. Biaduń, B. Krasnodębska-Ostręga, Stability of Tl(III) in the context of speciation analysis of thallium in plants, Chemosphere 144 (2016) 1216–1223, https://doi.org/10.1016/j.chemosphere.2015.09.079.

[15] O. Mestek, J. Polák, M. Juříček, P. Karvánková, R. Koplík, J. Šantrůček, M. Kodíček, Trace element distribution and species fractionation in *Brassica napus* plant, Organometal. Chem. 21 (2007) 468–474, https://doi.org/10.1002/aoc.1237.

[16] M. Kersten, T. Xiao, K. Kreissig, A. Brett, B.J. Coles, M. Rehkämper, Tracing anthropogenic thallium in soil using stable isotope compositions, Environ. Sci. Technol. 48 (2014) 9030–9036, https://doi.org/10.1021/es501968d.

[17] P.H. Reid, E.T. York Jr., Effect of nutrient deficiencies on growth and fruiting characteristics of peanuts in sand cultures, Agric. J. 2 (1958) 63–67, https://doi.org/10.2134/agronj1958.00021962005000020002x.

[18] S. Wick, B. Baeyens, M. Marques Fernandes, A. Voegelin, Thallium adsorption onto illite, Environ. Sci. Technol. 52 (2) (2018) 571–580, https://doi.org/10.1021/acs.est.7b04485.

[19] R.G.A. Baker, M. Rehkämper, T.K. Hinkley, S.G. Nielsen, J.P. Toutain, Investigation of thallium fluxes from subaerial volcanism–Implications for the present and past mass balance of thallium in the oceans, Geochim. Cosmochim. Acta 73 (2009) 6340–6359, https://doi.org/10.1016/j.gca.2009.07.014.

[20] J. Prytulak, S.G. Nielsen, T. Plank, M. Barker, T. Elliot, Assessing the utility of thallium and thallium isotopes for tracing subduction zone inputs to the Mariana arc, Chem. Geol. 345 (2013) 139–149, https://doi.org/10.1016/j.chemgeo.2013.03.003.

[21] S.G. Nielsen, L.E. Wasylenki, M. Rehkämper, C.L. Peacock, Z. Xue, E.M. Moon, Towards an understanding of thallium isotope fractionation during adsorption to manganese oxides, Geochim. Cosmochim. Acta 117 (2013) 252–265, https://doi.org/10.1016/j.gca.2013.05.004.

[22] B.Z. Siegel, S.M. Siegel, Effect of potassium on thallium toxicity in cucumber seedlings: further evidence for potassium-thallium ion antagonism, Bioinorg. Chem. 6 (1976) 341–345, https://doi.org/10.1016/S0006-3061(00)80019-8.

[23] R. Edwards, N.W. Lepp, K.C. Jones, Other less abundant elements of potential environmental significance, in: B.J. Alloway (Ed.), Heavy Metals in Soils, Blackie Academic and Professional, London, UK, 1995, pp. 306–352.

[24] M. Sager, Thallium, Toxicol. Environ. Chem. 45 (1994) 11–32, https://doi.org/10.1080/02772249409358067.

[25] Z. Ning, L. He, T. Xiao, L. Márton, High accumulation and subcellular distribution of thallium in green cabbage (*Brassica Oleracea* L. *Var. Capitata* L.), Int. J. Phytoremediat. 17 (2015) 1097–1104, https://doi.org/10.1080/15226514.2015.1045133.

[26] J. Hall, Cellular mechanisms for heavy metal detoxification and tolerance, J. Exp. Bot. 53 (2002) 1–11, https://doi.org/10.1093/jexbot/53.366.1.

[27] B.M. Ryan, J.K. Kirby, F. Degryse, H. Harris, M.J. McLaughlin, K. Scheiderich, Copper speciation and isotopic fractionation in plants: uptake and translocation mechanisms, New Phytol. 199 (2013) 367–378, https://doi.org/10.1111/nph.12276.

[28] M. Mihaljevič, A. Jarošíková, V. Ettler, A. Vaněk, V. Penížek, B. Kříbek, V. Chrastný, O. Sracek, J. Trubač, M. Svoboda, I. Nyambe, Copper isotopic record in soils and tree rings near a copper smelter, Copperbelt, Zambia, Sci. Total Environ. 621 (2018) 9–17, https://doi.org/10.1016/j.scitotenv.2017.11.114.

[29] R. Wei, Q. Guo, G. Yu, J. Kong, S. Li, Z. Song, J. Hu, L. Tian, X. Han, C.P. Okoli, Stable isotope fractionation during uptake and translocation of cadmium by tolerant *Ricinus communis* and hyperaccumulator *Solanum nigrum* as influenced by EDTA, Environ. Pollut. 236 (2018) 634–644, https://doi.org/10.1016/j.envpol.2018.01.103.

[30] D.J. Weiss, T.F.D. Mason, F.J. Zhao, G.J.D. Kirk, B.J. Coles, M.S.A. Horstwood, Isotopic discrimination of zinc in higher plants, New Phytol. 165 (2005) 703–710, https://doi.org/10.1111/j.1469-8137.2004.01307.x.

[31] J. Zembrzuska, B. Karbowska, Identification of complexes involving thallium(I) and thallium(III) with EDTA and DTPA ligands by electrospray ionization mass spectrometry, Rapid Commun. Mass Spectrom. 31 (2017) 1785–1792, https://doi.org/10.1002/rcm.7962.

[32] D.I. Kaplan, S.V. Mattigod, Aqueous geochemistry of thallium, in: J.O. Nriagu (Ed.), Thallium in the Environment, John Wiley & Sons, Inc., New York, 1998, pp. 15–29.

[33] A. Vaněk, V. Chrastný, M. Komárek, I. Galušková, P. Drahota, T. Grygar, V. Tejnecký, O. Drábek, Thallium dynamics in contrasting light sandy soils-Soil vulnerability assessment to anthropogenic contamination, J. Hazard. Mater. 173 (2010) 717–723, https://doi.org/10.1016/j.jhazmat.2009.08.144.

[34] M. Wiggenhauser, M. Bigalke, M. Imseng, M. Müller, A. Keller, K. Murphy, K. Kreissig, M. Rehkämper, W. Wilcke, E. Frossard, Cadmium isotope fractionation in soil-wheat systems, Environ. Sci. Technol. 50 (2016) 9223–9231, https://doi.org/10.1021/acs.est.6b01568.

[35] T.H. Deng, C. Cloquet, Y.T. Tang, T. Sterckeman, G. Echevarria, N. Estrade, J.L. Morel, R.L. Qiu, Nickel and zinc isotope fractionation in hyperaccumulating and nonaccumulating plants, Environ. Sci. Technol. 48 (2014) 11926–11933, https://doi.org/10.1021/es5020955.

[36] M. Rehkämper, M. Frank, J.R. Hein, D. Porcelli, A. Halliday, J. Ingri, V. Liebetrau, Thallium isotope variations in seawater and hydrogenetic, diagenetic, and hydrothermal ferromanganese deposits, Earth Planet. Sci. Lett. 197 (2002) 65–81, https://doi.org/10.1016/S0012-821X(02)00462-4.

[37] M. Rehkämper, M. Frank, J.R. Hein, A. Halliday, Cenozoic marine geochemistry of thallium deduced from isotopic studies of ferromanganese crusts and pelagic sediments, Earth Planet. Sci. Lett. 219 (2004) 77–91, https://doi.org/10.1016/S0012-821X(03)00703-9.

[38] S. Howarth, J. Prytulak, S.H. Little, S.J. Hammond, W. Widdowson, Thallium concentration and thallium isotope composition of lateritic terrains, Geochim. Cosmochim. Ac. 239 (2018) 446–462, https://doi.org/10.1016/j.gca.2018.04.017.

[39] C.L. Peacock, E.M. Moon, Oxidative scavenging of thallium by birnessite: Explanation for thallium enrichment and stable isotope fractionation in marine ferromanganese precipitates, Geochim. Cosmochim. Ac. 84 (2012) 297–313, https://doi.org/10.1016/j.gca.2012.01.036.

[40] A. Vaněk, Z. Grösslová, M. Mihaljevič, V. Trubač, V. Ettler, L. Teper, J. Cabala, J. Rohovec, T. Zádorová, V. Penížek, L. Pavlů, O. Holubík, K. Němeček, J. Houška, O. Drábek, C. Ash, Isotopic tracing of thallium contamination in soils affected by emissions from coal-fired power plants, Environ. Sci. Technol. 50 (2016) 9864–9871, https://doi.org/10.1021/acs.est.6b01751.

[41] A. Vaněk, Z. Grösslová, M. Mihaljevič, V. Ettler, J. Trubač, V. Chrastný, V. Penížek, L. Teper, J. Cabala, A. Voegelin, T. Zádorová, V. Oborná, O. Drábek, O. Holubík, J. Houška, L. Pavlů, C. Ash, Thallium isotopes in metallurgical wastes/contaminated soils: a novel tool to trace metal source and behavior, J. Hazard. Mater. 343 (2018) 78–85, https://doi.org/10.1016/j.jhazmat.2017.09.020.

[42] D. Jouvin, D.J. Weiss, T.F.M. Mason, M.N. Bravin, P. Louvat, F. Zhao, F. Ferec, P. Hinsinger, M.F. Benedetti, Stable isotopes of Cu and Zn in higher plants: evidence for Cu reduction at the root surface and two conceptual models for isotopic fractionation process, Environ. Sci. Technol. 46 (2012) 2652–2660, https://doi.org/10.1021/es202587m.

- PŘÍLOHA II. - Bioakumulace Tl

Holubík, O., Vaněk, A., Mihaljevič, M., Vejvodová, K., 2020. Higher Tl bioaccessibility in white mustard (hyper-accumulator) grown under the soil than hydroponic conditions: A key factor for the phytoextraction use. Journal of Environmetal Management. 255, 109880. https://doi.org/10.1016/j.jenvman.2019.109880

Journal of Environmental Management 255 (2020) 109880

Contents lists available at ScienceDirect

Journal of Environmental Management

journal homepage: http://www.elsevier.com/locate/jenvman

Research article

Higher Tl bioaccessibility in white mustard (hyper-accumulator) grown under the soil than hydroponic conditions: A key factor for the phytoextraction use

Ondřej Holubík [a,b,*], Aleš Vaněk [a], Martin Mihaljevič [c], Kateřina Vejvodová [a]

[a] Department of Soil Science and Soil Protection, Faculty of Agrobiology, Food and Natural Resources, Czech University of Life Sciences Prague, Kamýcká 129, 165 21, Praha 6, Czech Republic

[b] Research Institute for Soil and Water Conservation, Department of Soil Science and Soil Conservation, Prague, Žabovřeská 250, 156 27, Praha 5-Zbraslav, Czech Republic

[c] Institute of Geochemistry, Mineralogy and Mineral Resources, Faculty of Science, Charles University, Albertov 6, 128 43, Prague 2, Czech Republic

ARTICLE INFO

Keywords:
Plant thallium uptake
Artificial soil
Hydroponic
Plant physiology
Phytoremediation

ABSTRACT

The paper deals with the thallium (Tl) access into the white mustard (*Sinapis alba* L.). We were comparing two approaches: A - hydroponic, B - semi-hydroponic (artificial soil). The kinetics of Tl plant uptake at different available Tl doses (0.1, 0.05 and 0.01 mg L^{-1}) was tested. It was revealed that the hydroponic arrangement did not accelerate the plant uptake of Tl. The concentration of plant Tl was surprisingly roughly double under the semi-hydroponic (artificial soil) conditions as compared to the hydroponic system; the highest Tl concentrations were detected in stems, proving an important role of plant grown strategy on Tl bioaccessibility. We found that almost independently of the initial dose of Tl the juvenile stadium of the mustard can preserve1-2% of the total Tl pool. Up to 95% of this Tl dose is stored in the shoots. The different strategy of the plant growing may strongly affect the path of Tl incorporation. The total Tl input into the leaf tissue in hydroponics may be from 69% ($p = 0.01$) explained by parallel assimilation of Ca. In contrast, the Tl entry into the leaf grown on the artificial soil could be limited by Mn path ($R^2 = 0.91$, $p = 0.01$).

1. Introduction

The phytoavailability of Tl (as a global pollutant) depends on plant species (Al-Najar et al., 2003; Leblanc et al., 1999; Pavlíčková et al., 2006; Sager, 1994). Some of them have proved potentially useful in soil clean-up as hyperaccumulator plants (Al-Najar et al., 2003; Van Der Ent et al., 2013). Among plants with a high accumulation potential of Tl in plant tissues, it is possible to arrange: *Iberis intermedia* Guers. (candy-tuft), *Biscutella laevigata* L., *Brassica oleracea acephala* L. (kale), *Brassica napus* L. (rape) and *Sinapis alba* L. (white mustard) (Al-Najar et al., 2005, 2003; Madejón et al., 2007; Mazur et al., 2016; Sadowska et al., 2016; Scheckel et al., 2004; Tremel et al., 1997; Vaněk et al., 2011, 2010; Xiao et al., 2004). But the *Brassicaceae* family exhibited 1000 times more Tl uptake rate than the others (Sager, 1994).

There are a relatively large number of publications describing the Tl uptake into the biomass from the soil (Al-Najar et al., 2003; Anderson et al., 1999; Grösslová et al., 2015; Leblanc et al., 1999; Ning et al., 2015; Pavlíčková et al., 2005; Wierzbicka et al., 2004), but just a limited number with a hydroponic way (Allus et al., 1987; D. J. Kim et al., 2016) and only review papers describe soil and hydroponic system comparison (Sager, 1994). It is well known, that a hydroponic system can provide an ideal system to monitor specific treatment on the plant nutrient solution interface (Fargašová, 2004; D J Kim et al., 2016; Smeets et al., 2008). But the plant-nutrient interface of both growing systems will certainly be different. Therefore, we think that just the comparison of the specific Tl uptake into the plant in hydroponic and "soil" arrangements makes sense to better understand the white mustard (hyper)accumulation potential and efficiency (Al-Najar et al., 2005).

Under physiological conditions, Tl occurs as single-charged, a weakly hydrated cation with an ionic radius similar to K^+ (Sager, 1994). Therefore it is often stated that Tl mimics K in biochemical processes (Galván-Arzate and Santamaría, 1998). Contrary to K, Tl has a strong

* Corresponding author. Department of Soil Science and Soil Protection, Faculty of Agrobiology, Food and Natural Resources, Czech University of Life Sciences Prague, Kamýcká 129, 165 21, Praha 6, Czech Republic.
E-mail address: holubik.ondrej@vumop.cz (O. Holubík).

https://doi.org/10.1016/j.jenvman.2019.109880
Received 19 July 2019; Received in revised form 6 November 2019; Accepted 16 November 2019
Available online 25 November 2019
0301-4797/

attraction to sulfhydryl groups and thereby inhibits an enzymatic system (Tremel et al., 1997). There is a direct link between Tl toxicity and K-cycles in terms of molecular and cellular biology (Sager, 1994).

The majority of up-taken Tl run along nutrient paths into the cell cytosol and vacuole storage (Kwan and Smith, 1991; Ning et al., 2015). However the physicochemical form (Tl speciation) has not yet been fully elucidated (Sadowska et al., 2016; Voegelin et al., 2015) we suppose, that the monovalent Tl ions (Tl^{+}) do not complex with other precursors and are not transformed into trivalent ions (Tl^{3+}) (Alloway, 2012; Mestek et al., 2007; Sadowska et al., 2016). Even at a relatively low concentration 1 mg Tl l^{-1} in the soil solution leads to the intoxication of *Brassicaceae* plant species; often resulting in low photosynthetic pigments production (Fargašová, 2004; Mazur et al., 2016) and limited nutrient intake (Tremel et al., 1997). Nevertheless, it may be an understanding of some mechanisms essential for the future application of white mustard due to the clean-up of contaminated soils (Van Der Ent et al., 2013). In any case, a biogeochemical process of Tl tissue uptake has not yet been fully explained (Ning et al., 2015). Finally, the results of this study can support phytoremediation processes (in-situ/ex-situ) with partially hydroponic conditions.

This paper focused on 21 days of experimental verification of white mustard Tl uptake and bioaccumulation. The goal of the experiment was to find out: (i) how the experimental conditions and initial concentration affected the Tl uptake by the plant, (ii) what is the distribution of Tl in the plant tissue, (iii) by which elements are Tl accompanied when entering specific plant tissue.

2. Materials and methods

2.1. Experimental description

Sixteen initial plants of white mustard (*Sinapis alba* L.) were exposed to a specific dose of Tl (Fig. 1) for a total of 21-days. We compared 2 specific experimental conditions: hydroponic (A) and semi-hydroponic (B) with Tl and nutrient dose control.

We followed 3 juvenile phases of white mustard growth for 21 days. Duplicate treatments including a Tl-free variant were weekly run in the specific growing phase solution electrical conductivity (EC: 0.4, 0.6, 0.8 mS/cm). For each growth phases, fresh standard Reid-York nutrition solutions (Reid and York, 1958) alter spiked/not by Tl were prepared. The counted volume of solution (30–50 ml) was added at 2–3 day regime to reach ∽60% of water holding capacity. A total dose of Tl applied into each pot during the 21-day long experiment was 0.13μgTl ($A/B_{0.01}$); 0.65μgTl ($A/B_{0.05}$); 1.30 μgTl ($A/B_{0.1}$). The nutrient dose of each element from the solution was counted (see supplementary material, Table S1).

The pH of the solution (∽4.5) was not corrected following Ryan et al. (2013). The Reid-York nutrient solution was chosen because the Tl-EDTA complex has low chelating effects on Tl (I) uptake (log $K_{Tl\text{-}EDTA}$ = 5.8, Sager, 1994). Thallium was added to the solution from the freshly prepared stock solution of Tl_2SO_4 (p.a.) solid phase, solvated with deionized water.

2.2. Plant growing and harvesting

Seeds of white mustard were sterilized and incubated (in a dark box for 4 days at 20 °C) on filter paper soaked with deionized water. The two leaf seedlings were each placed in their own (130 ml) pot; filled with silica gel and artificial soil. For the hydroponic system (variant A) a silica gel (white, Signus SG 5) grain size (2–5 mm), active surface (approx. 800 m^2 g^{-1}), mean of pore (2.0–3.0 nm), volume porosity (0.35–0.45 ml g^{-1}) with 99.7% of SiO2.n (H_2O) amorphous phase were used. For the preparation of artificial soil (variant B), a mixture of 10% Sphagnum-peat, 70% quartz sand (50–200 μm) and 20% of china clay (with approx. 30% kaolinite content) was prepared according to the (OECD, 2009) standard.

All the plants were harvested on day 21; separated into leaves, stems, and roots and washed in Milli-Q water and EtOH. Plant tissues were oven-dried at 60 °C for 24 h and homogenized. The biomass was decomposed using a mixture of ultrapure/suprapure HNO_3/H_2O_2 (Merck, Germany) in a ratio of 4:1 which were added to the sample in a total volume of ∼5 mL, then left in a closed 60-mL PTFE beaker (Savillex, USA) on a hot plate (150 °C) for 24 h.

The weight of dry biomass in hydroponics was 20.3 ± 3.6 mg and in artificial soil 21.7 ± 1.8 mg. The largest part of the mass is contained in leaves 56% (var. A), resp. 63% (var. B); in the stem 27% (var. A), resp. 17% (var. B); the rest of mass in the roots is 16% (var. A) and 20% (var. B).

2.3. Determination of Tl/element concentrations

The concentrations of the major/trace elements (Na, Mg, K, Ca, Fe, Mn, Co, Cu, Zn, Mo and Tl) in the total digests solution were determined using a quadrupole based inductively coupled plasma mass spectrometry (Q-ICP-MS, Xseries II, Thermo Scientific, Germany) under standard analytical conditions. The standard reference material INCT-TL-1 (tea

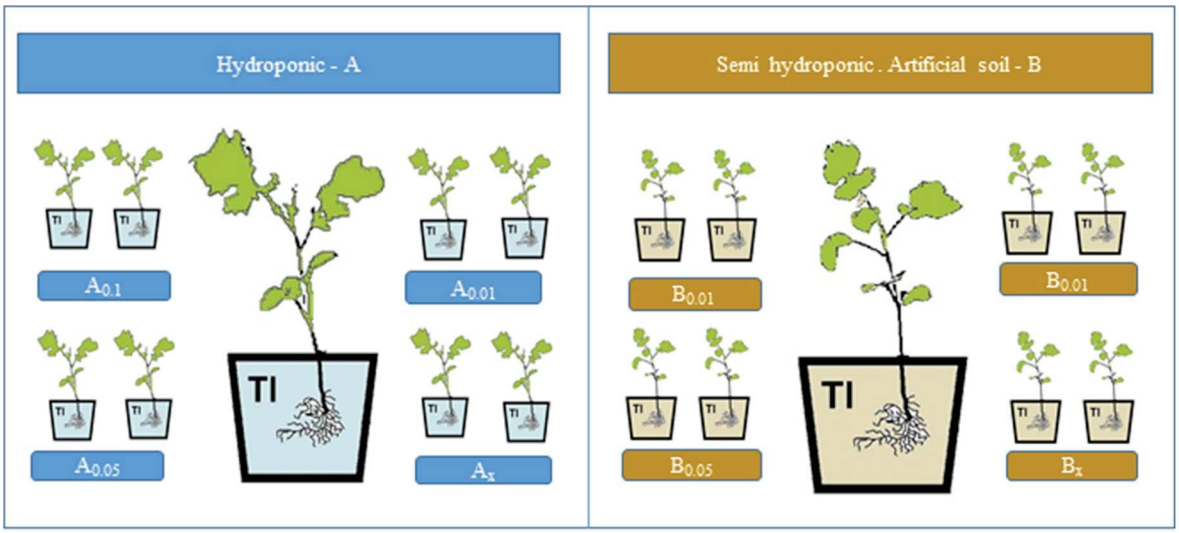

Fig. 1. Design of experiment. A – hydroponic, B-semi-hydroponic (artificial soil) experiment; index 0.01, 0.05, 0.1 represents a conc. of Tl (mg l^{-1}) applied in the nutrient solution; index x - marked (Tl free) control.

leaves) (Institute of Nuclear Chemistry and Technology, Poland) was used for QC of quantitative analyses of trace elements.

2.4. Calculation of Tl bioaccessibility

The Bio-Accessibility Index (BAI) is based on the bioconcentration factor (BCF) definition as Hladun et al. (2015); Kim et al. (2016); Zayed et al. (1998) described. But unlike the BCF, the BAI is expressed as the sum of a dose of the element. The BAI is expressed as the dose of the element in a specific tissue (X_{tissue})/sum of element doses (Y_{total}) entering the system (solution) according to the formula: $BAI = X_{tissue}/Y_{total} * 100$ [%].

The total Bio-Accessibility Index (BAI_{tot}) for each element is expressed as a sum of BAI of a specific tissue. This expression could be chosen because we exactly know an input dose of Tl and elements into the pot system.

2.5. Statistical analyses

The data of Tl and nutrients tissue concentrations were processed by Friedman ANOVA and tested by Wilcox pair-wise test and Kruskal – Wallis non-parametric analysis. For the Tl Bio-Accessibility relationship finding a Pearson correlation and step by step (top-down), multiple linear regression model was used. The significance of the linear model was tested through ANOVA. All measurements were statistically evaluated at the level of confidence ($\alpha = 0.05$) by Statistica 10 software (StatSoft 2012).

3. Results and discussion

3.1. Plant tissue concentration of Tl

Thallium is the trace element, where the usual concentration in the plant ranges about 0.05 mg kg^{-1} (Adriano, 2001). However, the accumulation of Tl in plant biomass was many times higher in our experiments (see Table 1), these results correspond with Madejón et al. (2007) (5 mg kg^{-1}) and our previous Grösslová et al. (2015). The data of semi-hydroponic way showed a limited Tl - kaolinite association compare to Grösslová et al. (2015) study (Tl – birnessite), that we believe that the data (Table 1) show "clear" concentration-dose dependence (Table 1).

3.2. Thallium tissue distribution

The aim of this study was to compare the Tl and nutrient uptake by the plant in the hydroponic (A) and artificial soil (B) arrangement. It was interesting and strange at the same time, that the results of Tl concentration demonstrate basically lower concentration through the hydroponic cultivation against the artificial soil arrangement (Fig. 2). However, these results were already recorded in Allus et al. (1987) study for the rape plant (*Brassica napus* L.) and barley (*Hordeum Vulgare cv Proctor*). There are many possibilities to explain this phenomenon. First of all, we must admit the contribution of artificial soil nutrient composition (with 6.1% of total organic carbon, 0.05% of total nitrogen, 0.02% of total phosphorus). Even if some $CaCl_2$/DTPA extracted nutrients from OECD artificial soil (especially Fe, Mn and Mg) can highly contribute to plant nutrient availability (see supplementary material, Table S1). The influence of artificial soil on the controlled dosage of Tl is negligible. Higher plant Tl uptake from the soil may be more related to Tl - rhizosphere binding and Tl – SOM association as shown by Al-Najar et al. (2003) or higher biological activity as shown by Pavlíčková et al. (2006). The effect of chelation, as another mobilization mechanism, cannot also be omitted. Nevertheless, its efficiency is strictly dependent on the type and solubility of organic substances (Vaněk et al., 2013, 2012) contained in peat. However, we tend to believe, that the dominant effect of significantly higher uptake of Tl by white mustard in soil was caused by the different strategy of growth as Taiz and Zeiger (2003) described.

Table 1
Mean thallium concentration (mg kg^{-1}) of 2 individual pot measurements.

Level Tl (mg kg^{-1}) *Tissue*	Hydroponic				Artificial soil			
	$A_{0.01}$	$A_{0.05}$	$A_{0.1}$	A_x	$B_{0.01}$	$B_{0.05}$	$B_{0.1}$	B_x
leaf	0.62	2.02	6.70	0.61	2.24	6.81	7.28	3.19
stem	1.38	3.38	5.27	0.59	3.76	10.94	12.53	4.51
root	0.09	1.82	1.07	0.23	1.92	6.88	9.92	0.71

Note: A total dose of Tl applied into the 100 ml pot system during 21 days was 0.13 μg ($A/B_{0.01}$); 0.65 μg ($A/B_{0.05}$); 1.30 μg ($A/B_{0.1}$).

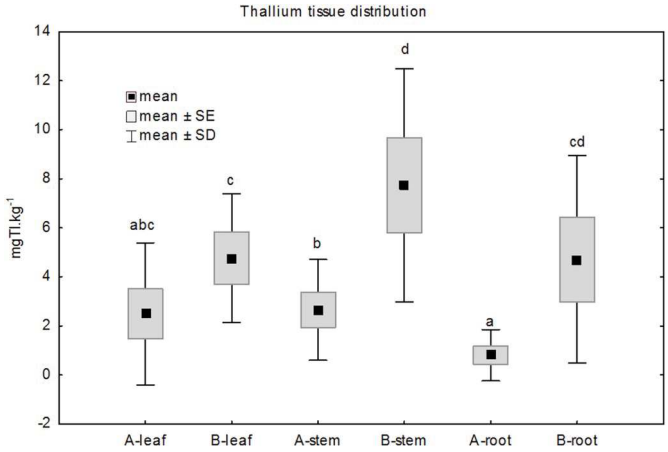

Fig. 2. Thallium concentration (mg kg^{-1}) for the different part of the white mustard on the A-hydroponic (n = 6) and B-semi-hydroponic (n = 4) system. Differ letter (a, b) present a Wilcox pair-wise test (A–B) p-value at the level of confidence ($\alpha = 0.05$): Leaf: $p = 0.0747$, Stem and Root: $p = 0.0277$.

As follows, Fig. 2 present the significantly higher measured concentration of Tl in the shoot of plants cultivated in artificial soil (B), similar to Allus et al. (1987). Highest stem concentrations of Tl have been already described in Grösslová et al. (2015); Vaněk et al. (2010).

3.3. Plant nutrition uptake

Different plant nutrition uptake manifested the different growth strategies (in the hydroponic and "soil" systems) of plants. The kinetics and assimilation of some essential elements (K and Mg) are significantly higher in the plant leaf material grown on artificial soil (Figs. 3 and 4). On the contrary, the Ca content is higher in the hydroponic arrangement (Fig. 5).

Our results confirm the Xiao et al. (2004) findings on Tl-polluted soil, where the crop growing generally corresponds to Ca and Mg elevation. Similarly, Scheckel et al., 2004 described a positive correlation between Tl and Ca in the main vein of the basal leaves (*Iberis intermedia*). Therefore, following Ning et al. (2015) and Scheckel et al. (2004), we assumed that Ca play an important role in the Tl accumulation and tolerance in green parts of white mustard.

3.4. The total bio-accessibility of Tl

The mean efficiency of white mustard Tl accessibility is ranged from 1.2 to 4.0% for the semi-hydroponic system, resp. from 0.3 to 2.3% for a hydroponic way with great variability (Fig. 6). Despite this, it was interesting that the lower dose of Tl leads to higher bioaccumulation (BAI). However, the total bio-accessibility (BAI_{totTl}) for each dose of Tl is still roughly twice in the „soil"arrangement against the pure hydroponics nursery. Ultimately, the total Bio-Accessibility index is most

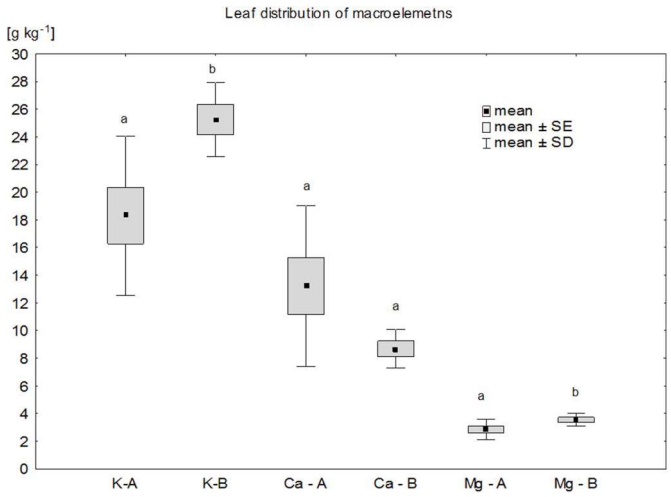

Fig. 3. The distribution and comparison of (K, Ca and Mg) leaf concentration (g kg^{-1}); n = 10 (var. A), resp. n = 8 (var. B). Differ letter (a, b) present a Wilcox pair-wise test (A–B) p-value at the level of confidence (α = 0.05); K: p = 0.0464; Ca: p = 0.1158 and for Mg: p = 0.0464.

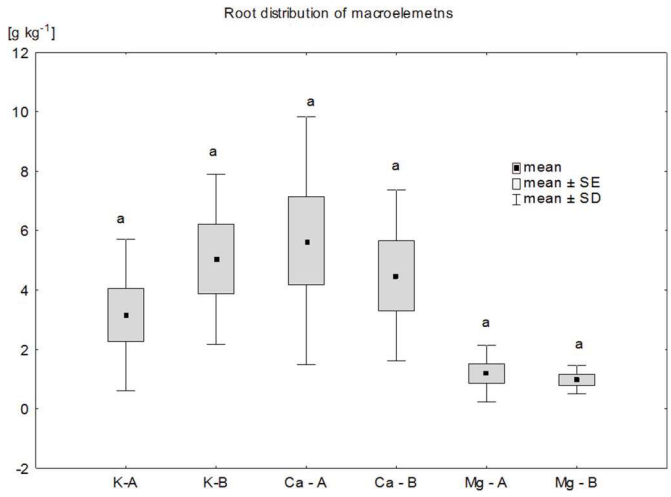

Fig. 5. The distribution and comparison of (K, Ca and Mg) root concentration (g kg^{-1}); n = 10 (var. A), resp. n = 8 (var. B). Differ letter (a) present a no significant p-value of Wilcox pair-wise test (A–B) at the level of confidence (α = 0.05); K: p = 0.1729; Ca: p = 0.3454 and for Mg: p = 0.0600.

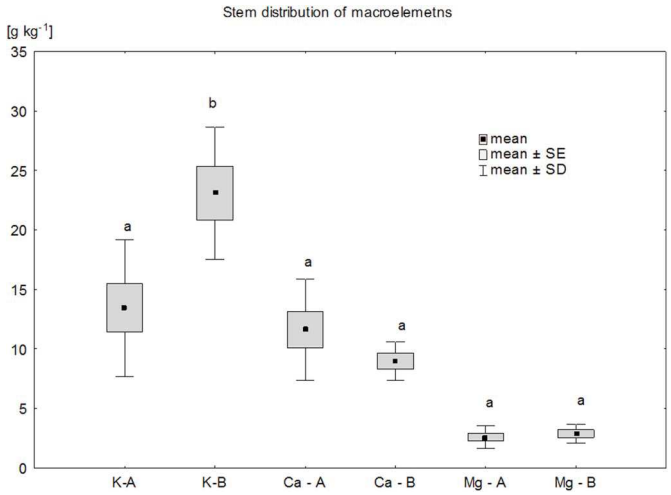

Fig. 4. The distribution and comparison of (K, Ca and Mg) stem concentration (g kg^{-1}); n = 10 (var. A), resp. n = 8 (var. B). Differ letter (a, b) present a Wilcox pair-wise test (A–B) p-value at the level of confidence (α = 0.05); K: p = 0.0464; Ca: p = 0.4630 and for Mg: p = 0.1729.

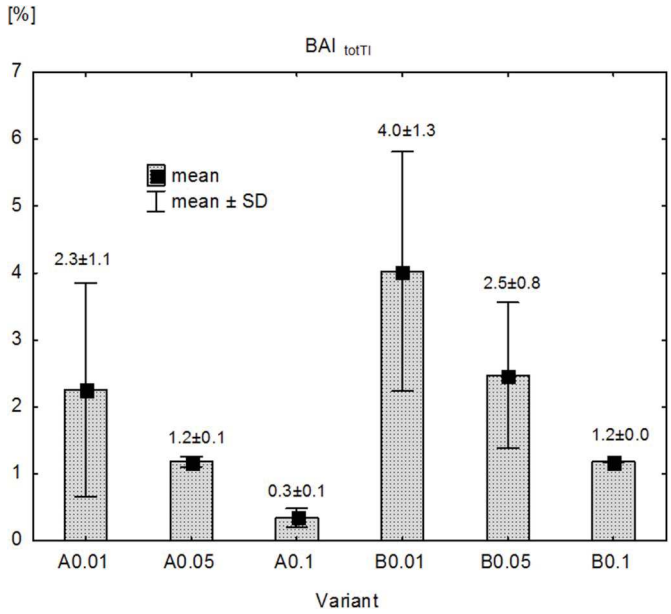

Fig. 6. The total Bio-Accessibility Index of Tl ($BAI_{tot\ Tl}$) = ∑ BAI (leaf + stem + root); the results were presented as mean ± standard deviation (SD); each slope represents the mean ± SD of 2 repetitions; variant B_x and A_x calculate with zero input concentration.

affected by the dry mass of biomass distribution than the pure concentration analyses.

When we have compared the total BAI of Tl across the variant (Table 2) the lower efficiency of Tl intake by the plant grown in hydroponic is evident. At the same time, some trends as an insignificantly higher intake of K and Mg in artificial soil variants (B) and higher intake of Na and Ca in hydroponics (A) can be related as well.

In detail (Table 3) significantly higher access of Tl into the leaf through var. B (artificial soil) was evident. At the same time, there were described partial trends of significantly lower access of the Cu, Co and Zn elements into the leaf. An element which was dominantly attacking the plant in a hydroponic system was Na. On the contrary, the soil system greatly buffers the Na ions entering into the stem. Interestingly, a difference of hydroponic and artificial soil cultivation was recorded for the Ca and Mg in the stem and K in the leaf.

3.5. The thallium plant tissue pathway models

Generally, it seems, that the Tl is really accompanied by the macronutrient on their biochemical path to the cell cytosol and the vacuole as Ning et al. (2015) described. We believed, similarly as Kwan and Smith (1991), that the entrance of Tl and other elements goes through the protoplasm of the endodermis cells, where they are sorted and transported. We suppose that in the cytoplasmatic fraction a greater proportion of Tl (80%) accumulates within the plasma membrane (Kwan and Smith, 1991; Sager, 1994) and bounds to specific low-molecular weight peptide without sulphureous phytochelatins nor the metallothioneins (Günther and Umland, 1988). We estimate that the path of Tl was based on the similarity of occurrence with individual elements in the specific plant tissue. But we had recognized that there was no evidence of Tl entering the plant. Our estimation was based on the correlation and linear regression models. Although the design of our experiment does not have robust test parameters. Yet, we tried to

Table 2
The total Bio-Accessibility Index (BAI_{tot}) = $\sum BAI_{(leaf+stem+root)}$ of each element and Tl. All data are means ± SD; for Tl: (n = 6), elements (n = 8).

Element	Hydroponic			Artificial soil		
	BAI tot [%]			BAI tot [%]		
	mean	±	SD	mean	±	SD
Tl	1.3	±	1.1	2.8	±	1.6
K	7.8	±	4.5	11.2	±	1.4
Ca	6.5	±	2.9	4.8	±	1.0
Mg	7.0	±	3.9	8.3	±	1.2
Fe	5.1	±	2.9	5.3	±	1.8
Na	59.7	±	26.7	20.2	±	3.8
Cu	0.7	±	0.3	0.2	±	0.1
Zn	0.4	±	0.2	0.1	±	0.1
Mn	1.2	±	0.8	1.2	±	0.4
Mo	7.5	±	4.7	7.4	±	2.5
Co	1.0	±	0.6	0.4	±	0.1

uncover the Tl path into the plant tissue.

To express the "hydroponic leaf model", correlation dependencies of all variables were examined using the Pearson (r) correlation coefficient. The bioaccessibility of Tl (Table 3, $BAI_{Tl\ leaf}$) significantly correlated from 90% with the $BAI_{Ca\ leaf}$ and insignificantly with Mg (r = 0.86). The linear regression model (with step by step pre-analysis) described the Tl leaf bioaccessibility by a single variable, occurrence of Ca. The hydroponic leaf model $BAI_{Tl\ leaf}$ = - 0.28 + 0.21 $BAI_{Ca\ leaf}$ significantly (p = 0.01) explained the Tl occurrence from 69%. These conclusions correspond to the works (Ning et al., 2015; Scheckel et al., 2004), which suggested that Ca has an important role in Tl plant tolerance.

While for the soil system, the Tl bioaccessibility (Table 3, $BAI_{Tl\ leaf}$) strongly correlated to Mn, Mo and Co variables (r = 0.94–0.95), the "soil leaf model" showed the significant linear similarity with Mn only: $BAI_{Tl\ leaf} = -1.05 + 2.68\ BAI_{Mn\ leaf}$ ($r^2 = 0.91$, p = 0.01). This model approach could result in a possible explanation, that part of Mn is co-precipitated and associated with Tl in the soil system (Vaněk et al., 2010). At the same time, the model results supported the theory, that the Tl that has been transported in association with typical elements (Mn - soil, Ca - hydroponic) into their vacuoles and may be stored by strongly anionic lipid as Günther and Umland (1988) described.

The Na seems to be the dominant element in the "hydroponic stem model". The Tl bio-accessibility by stem correlated from 89% with Na. The linear model of Tl accumulation into the stem tissue is from 89% described as $BAI_{Tl\ stem} = -0334 + 0.034\ BAI_{Na\ stem}$. It seems that the Tl followed the Na sorption into the stem xylem. The similarity of both elements uptake may be caused by increasing the passively accepted elements in a hydroponic system (D. J. Kim et al., 2016).

The plant Tl access into the stem of the artificial soil could be affected by plant defence mechanisms associated with nutrient deficiency as shown by Xiao et al. (2004). The Pearson correlation coeff. was strongest for K and Mg (r = 0.94, resp. 0.99) and relatively strong for Cu, Zn, (r = 0.63) and Mn, Mo (r = 0.78) and Co (r = 0.79) as well. But the linear multi-regression model of BAI_{Tlstem} could be explained from 98% by Mg variable only: $BAI_{Tl\ stem} = -0.81 + 1.17\ BAI_{Mg\ stem}$. Magnesium and potassium has a specific role in activation enzymes involved respiration and builds chlorophyll (Taiz and Zeiger, 2003). The higher levels of Tl in the stem can be dir/indirectly related to higher nutrients uptake (K, Mg), which may/may not be a reaction to the stress of Tl intake (Sager, 1994).

The hydroponic way of Tl intake by the roots is practically zero (see Fig. 3). The Tl regression coefficients were similar to the other tissue uptake and tissue distribution. Potassium and sodium correlated with Tl from 75%, respectively with 79%. We anticipate a passive element intake to explain.

On the other hand, the Tl entering by the root in the soil system could be a much more complex system. We supposed the combined effects of a plant stress reaction (through K and Mg accompaniment) and possible (Ca–Tl cytosol incorporation) as the white mustard tolerance reaction.

Table 3
The Bio-Accessibility Index for the plant tissue (BAI) = the Tl (element) dose measured in the tissue/total Tl (element) dose added into the system (during whole experiment) * 100 [%]; the data are means ± SD; for Tl: (n = 6), A-elements: (n = 8); the bold font presents a significant (p – value) of Wilcox pair-wise test for A-B comparison at the level of confidence (α = 0.05).

Tissue	LEAF							STEM							ROOT						
Element	Hydroponic BAI [%]			Artificial soil BAI [%]			Wilcox. Test A-B	Hydroponic BAI [%]			Artificial soil BAI [%]			Wilcox. Test A-B	Hydroponic BAI [%]			Artificial soil BAI [%]			Wilcox. Test A-B
	mean	±	SD	mean	±	SD	p - value	mean	±	SD	mean	±	SD	p - value	mean	±	SD	mean	±	SD	p - value
Tl	0.63	±	0.42	1.83	±	1.09	**0.043**	0.59	±	0.62	0.81	±	0.42	0.686	0.04	±	0.02	0.20	±	0.05	**0.043**
K	5.07	±	2.48	8.80	±	0.96	0.075	2.49	±	1.92	2.10	±	0.33	0.753	0.20	±	0.10	0.26	±	0.16	0.600
Ca	3.94	±	1.56	3.57	±	0.66	0.463	2.21	±	1.14	0.98	±	0.23	**0.028**	0.39	±	0.15	0.25	±	0.08	0.116
Mg	4.25	±	2.21	6.62	±	0.77	0.173	2.37	±	1.51	1.43	±	0.34	**0.028**	0.39	±	0.17	0.27	±	0.10	0.075
Fe	2.51	±	1.16	2.76	±	0.37	0.917	1.40	±	0.81	1.28	±	0.62	0.463	1.16	±	0.97	1.24	±	0.76	0.463
Na	35.03	±	9.12	15.35	±	2.47	0.109	22.43	±	16.48	4.22	±	1.10	**0.028**	2.21	±	1.09	0.68	±	0.26	**0.028**
Cu	0.21	±	0.09	0.12	±	0.02	**0.028**	0.13	±	0.13	0.07	±	0.06	0.345	0.33	±	0.13	0.05	±	0.02	**0.028**
Zn	0.12	±	0.05	0.07	±	0.01	**0.028**	0.07	±	0.07	0.04	±	0.04	0.345	0.18	±	0.07	0.03	±	0.01	**0.028**
Mn	0.84	±	0.58	1.04	±	0.36	0.463	0.25	±	0.13	0.11	±	0.03	**0.028**	0.10	±	0.04	0.02	±	0.01	**0.028**
Mo	5.26	±	3.63	6.56	±	2.27	0.463	1.55	±	0.82	0.67	±	0.18	**0.028**	0.64	±	0.26	0.14	±	0.04	**0.028**
Co	0.70	±	0.48	0.35	±	0.11	**0.046**	0.19	±	0.11	0.05	±	0.02	**0.028**	0.10	±	0.04	0.02	±	0.01	**0.028**

All the Pearson's corr. coef. Tl with Ca (r = 0.90), K and Mg (r = 0.95), Na (r = 0.93) are significantly high. Some significant correlation was also found with Co (r = 0.90), Mn and Mo (r = 0.78). But the resulting linear "soil root model" of Tl bioaccessibility was significantly (r^2 = 0.89) described as $BAI_{Tl\ root} = 0.125 + 0.256 * BAI_{K\ root}$ just for the one independent variable K.

Finally, the linear regression model of Tl bioaccessibility (Table 2, $BAI_{Tl\ tot}$) showed $BAI_{Tl\ tot} = 0.08 + 0.22 * BAI_{K\ tot} - 0.01\ BAI_{Na\ tot}$. The total bioaccessibility of Tl could be (from 67%) explained by two independent values K and Na fluxes. All of these model results could indicate some Tl uptake, transport and storage in the plant. But the "real" mechanisms of Tl accompaniment with other elements have not been described. For this purpose, additional knowledge needs to be added.

4. Environmental implications

Our results indicate the higher Tl bio-accessibility under the lowest dose of a contaminant. We find out that the hydroponic cultivation leads to roughly half-plant Tl access than the semi-hydroponic cultivation (on the same level of Tl dose). Based on our previous study findings (Vaněk et al., 2019) the XANES spectra show, that Tl was predominantly O-coordinated as free/hydrated ion at an analogy to K(I) species in hydroponic. But this study showed that the Tl bio-access is positively/negatively affected by the other elements as well; related to the Ca and Na content in hydroponic and possibly limited by the Mn association in the soil. These findings lead us to suggest, that the plant grown strategy can play a crucial role in future phytoextraction use of white mustard.

We assumed that in hydroponic, the root tip selection and mainly passive transport (simple diffusion) of monovalent ions (Na/K) through protoplasm membrane (channel/carrier protein) affected the Tl transportation as Taiz and Zeiger (2003) described. But under the semi-hydroponic (artificial soil) conditions, the passive transport is probably accompanied by active transport (ATPase pump) and the income of Tl is higher. The active transport can be caused by plant stress reaction and associated with higher K and Mg addition. Some correlation of our study showed the positive effect of Ca intake along with Tl. The content of Ca cell phytochelatin formation may increase plant tolerance to Tl.

In summary, our findings indicate that in acidic solution the juvenile phase of white mustard (*Sinapis Alba* L.) plant can accept roughly 1–2% of the Tl pool depending on the cultivation system and plant growth strategy. A dominant part of this amount is accumulated into the shoots (97% in hydroponic, resp. 93% in soil). These results correspond to our previous study (Vaněk et al., 2019), where was observed a large Tl isotope shift with an enrichment in the heavy ^{205}Tl isotope in the shoots relative to the roots. These results show that for the Tl white mustard phytoremediation use is sufficient to harvest aboveground biomass.

While we admit that under "real" soil conditions the kinetics of Tl may be more different from our experiments. Frequent factor limiting Tl plant uptake and soil clean-up use is the fact, that Tl is relatively insoluble in soils; associated with a number of various primary/secondary minerals of different stability strongly with birnessite (Grösslová et al., 2015; Vaněk et al., 2010). Our previous study Grösslová et al. (2015) shows that even 85% of the soil Tl pools should be releasable in the reducible fraction (0.5.M NH_2OH.HCL-extractable). Thus, a dramatical reduction in pH is required. In addition, the carbonate-rich soil is an important precursor for further contaminant mobilization. Higher Ca concentration can be used for higher plant tolerance against Tl. On the contrary the higher content of Mn(III,IV) oxides present in soils dramatically reduce the plant Tl uptake. We hope that this contribution can help better understanding of fate/behaviour of Tl when enriches the plant and can open the door for the further white mustard implementation as a Tl hyperaccumulator.

Acknowledgements

This research was supported by the Czech Science Foundation [17-03211S]; the Ministry of Agriculture of the Czech Republic grant [RO0218]; the Center for Geosphere Dynamics [UNCE/SCI/006]. We also would like to thank Jan Jiřík for brainstorming, discussion, as well as the help with hydroponic experiments.

Appendix A. Supplementary data

Supplementary data to this article can be found online at https://doi.org/10.1016/j.jenvman.2019.109880.

References

Adriano, D.C., 2001. Trace Elements in Terrestrial Environments. Springer New York, New York, NY. https://doi.org/10.1007/978-0-387-21510-5.

Al-Najar, H., Kaschl, A., Schulz, R., Römheld, V., 2005. Effect of thallium fractions in the soil and pollution origins on Tl uptake by hyperaccumulator plants: a key factor for the assessment of phytoextraction. Int. J. Phytoremediation 7, 55–67. https://doi.org/10.1080/16226510590915837.

Al-Najar, H., Schulz, R., Römheld, 2003. Plant availability of thallium in the rhizosphere of hyperaccumulator plants: a key factor for assessment of phytoextraction. Plant Soil 249, 97–105. https://doi.org/10.1023/A:1022544809828.

Alloway, B.J., 2012. Heavy Metals in Soils, second ed., vol. 1995. Springer; Softcover reprint of the original, Springer (Verlag.

Allus, M.A., Martin, M.H., Nickless, G., 1987. Comparative toxicity of thallium to two plant species. Chemosphere 16, 929–932. https://doi.org/10.1016/0045-6535(87)90026-9.

Anderson, C.W.N., Brooks, R.R., Chiarucci, A., Lacoste, C.J., Leblanc, M., Robinson, B.H., Simcock, R., Stewart, R.B., 1999. Phytomining for nickel, thallium and gold. In: Journal of Geochemical Exploration. Elsevier, pp. 407–415. https://doi.org/10.1016/S0375-6742(99)00055-2.

Fargašová, A., 2004. Toxicity comparison of some possible toxic metals (Cd, Cu, Pb, Se, Zn) on young seedlings of Sinapis alba L. Plant Soil Environ. 50, 33–38.

Galván-Arzate, S., Santamaría, A., 1998. Thallium toxicity. Toxicol. Lett. 99, 1–13.

Grösslová, Z., Vaněk, A., Mihaljevič, M., Ettler, V., Hojdová, M., Zádorová, T., Pavlů, L., Penížek, V., Vaněčková, B., Komárek, M., Chrastný, V., Ash, C., 2015. Bioaccumulation of thallium in a neutral soil as affected by solid-phase association. J. Geochem. Explor. 159, 208–212. https://doi.org/10.1016/j.gexplo.2015.09.009.

Günther, K., Umland, F., 1988. Speziesanalytik von Cadmium und Thallium in nativen Rapspflanzen (Brassica napus). Fresenius' Z. für Anal. Chem. 331, 302–309. https://doi.org/10.1007/BF00481900.

Hladun, K.R., Parker, D.R., Trumble, J.T., 2015. Cadmium, copper, and lead accumulation and bioconcentration in the vegetative and reproductive organs of raphanus sativus: implications for plant performance and pollination. J. Chem. Ecol. 41, 386–395. https://doi.org/10.1007/s10886-015-0569-7.

Kim, D.J., Park, B.C., Ahn, B.K., Lee, J.H., 2016. Thallium uptake and translocation in barley and sunflower grown in hydroponic conditions. Int. J. Environ. Res. 10, 575–582. https://doi.org/10.22059/ijer.2016.59686.

Kwan, K.H.M., Smith, S., 1991. Some aspects of the kinetics of cadmium and thallium uptake by fronds of Lemna minor L. New Phytol. 117, 91–102. https://doi.org/10.1111/j.1469-8137.1991.tb00948.x.

Leblanc, M., Petit, D., Deram, A., Robinson, B.H., Brooks, R.R., 1999. The phytomining and environmental significance of hyperaccumulation of thallium by Iberis intermedia from southern France. Econ. Geol. 94, 109–113. https://doi.org/10.2113/gsecongeo.94.1.109.

Madejón, P., Murillo, J.M., Marañón, T., Lepp, N.W., 2007. Factors affecting accumulation of thallium and other trace elements in two wild Brassicaceae spontaneously growing on soils contaminated by tailings dam waste. Chemosphere 67, 20–28. https://doi.org/10.1016/j.chemosphere.2006.10.008.

Mazur, R., Sadowska, M., Kowalewska, Ł., Abratowska, A., Kalaji, H.M., Mostowska, A., Garstka, M., Krasnodębska-Ostręga, B., 2016. Overlapping toxic effect of long term thallium exposure on white mustard (Sinapis alba L.) photosynthetic activity. BMC Plant Biol. 16, 191. https://doi.org/10.1186/s12870-016-0883-4.

Mestek, O., Polák, J., Juříček, M., Karvánková, P., Koplík, R., Šantrůček, J., Kodíček, M., 2007. Trace element distribution and species fractionation in Brassica napus plant. In: Applied Organometallic Chemistry. John Wiley & Sons, Ltd, pp. 468–474. https://doi.org/10.1002/aoc.1237.

Ning, Z., He, L., Xiao, T., Márton, L., 2015. High accumulation and subcellular distribution of thallium in green cabbage (Brassica oleracea L. Var. Capitata L.). Int. J. Phytoremediation 17, 1097–1104. https://doi.org/10.1080/15226514.2015.1045133.

OECD, 2009. OECD guidelines for the testing of chemicals. Oecd/Ocde 220 Draft Docu 1–22. https://doi.org/10.1787/9789264203785-en.

Pavlíčková, J., Zbíral, J., Smatanová, M., Habarta, P., Houserová, P., Kubáň, V., 2006. Uptake of thallium from artificially contaminated soils by kale (Brassica oleracea L. var. acephala). Plant Soil Environ. 52, 544–549.

Pavlíčková, J., Zbíral, J., Smatanová, M., Houserová, P., Čižmárová, E., Havlíková, Š., Kubáň, V., 2005. Uptake of thallium from artificially and naturally contaminated soils into rape (Brassica napus L.). J. Agric. Food Chem. 53, 2867–2871. https://doi.org/10.1021/jf048042k.

Reid, P.H., York, E.T., 1958. Effect of nutrient deficiencies on growth and fruiting characteristics of peanuts in sand Cultures1. Agron. J. 50, 63. https://doi.org/10.2134/agronj1958.00021962005000020002x.

Ryan, B.M., Kirby, J.K., Degryse, F., Harris, H., Mclaughlin, M.J., Scheiderich, K., 2013. Copper speciation and isotopic fractionation in plants: uptake and translocation mechanisms. New Phytol. 199, 367–378. https://doi.org/10.1111/nph.12276.

Sadowska, M., Biaduń, E., Krasnodębska-Ostręga, B., 2016. Stability of Tl(III) in the context of speciation analysis of thallium in plants. Chemosphere 144, 1216–1223. https://doi.org/10.1016/j.chemosphere.2015.09.079.

Sager, M., 1994. Thallium. Toxicol. Environ. Chem. 45, 11–32. https://doi.org/10.1080/02772249409358067.

Scheckel, K.G., Lombi, E., Rock, S.A., McLaughlin, M.J., 2004. In vivo synchrotron study of thallium speciation and compartmentation in Iberis intermedia. Environ. Sci. Technol. 38, 5095–5100. https://doi.org/10.1021/es049569g.

Smeets, K., Ruytinx, J., Van Belleghem, F., Semane, B., Lin, D., Vangronsveld, J., Cuypers, A., 2008. Critical evaluation and statistical validation of a hydroponic culture system for Arabidopsis thaliana. Plant Physiol. Biochem. 46, 212–218. https://doi.org/10.1016/j.plaphy.2007.09.014.

Taiz, L., Zeiger, E., 2003. Plant Physiology, third ed. https://doi.org/10.1093/aob/mcg079

Tremel, A., Masson, P., Sterckeman, T., Baize, D., Mench, M., 1997. Thallium in French agrosystems - I. Thallium contents in arable soils. Environ. Pollut. 95, 293–302. https://doi.org/10.1016/S0269-7491(96)00145-5.

Van Der Ent, A., Baker, A.J.M., Reeves, R.D., Pollard, A.J., Schat, H., Van Der Ent, A., Baker, A.J.M., Pollard, A.J., Schat, H., 2013. Hyperaccumulators of metal and metalloid trace elements: facts and fiction. Plant Soil 362, 319–334. https://doi.org/10.1007/s11104-012-1287-3.

Vaněk, A., Holubík, O., Oborná, V., Mihaljevič, M., Trubač, J., Ettler, V., Pavlů, L., Vokurková, P., Penížek, V., Zádorová, T., Voegelin, A., 2019. Thallium stable isotope fractionation in white mustard: implications for metal transfers and incorporation in plants. J. Hazard Mater. 369, 521–527. https://doi.org/10.1016/j.jhazmat.2019.02.060.

Vaněk, A., Komárek, M., Chrastný, V., Bečka, D., Mihaljevič, M., Šebek, O., Panušková, G., Schusterová, Z., 2010. Thallium uptake by white mustard (Sinapis alba L.) grown on moderately contaminated soils—agro-environmental implications. J. Hazard Mater. 182, 303–308. https://doi.org/10.1016/J.JHAZMAT.2010.06.030.

Vaněk, A., Komárek, M., Chrastný, V., Galušková, I., Mihaljevič, M., Šebek, O., Drahota, P., Tejnecký, V., Vokurková, P., 2012. Effect of low-molecular-weight organic acids on the leaching of thallium and accompanying cations from soil - a model rhizosphere solution approach. J. Geochem. Explor. 112, 212–217. https://doi.org/10.1016/j.gexplo.2011.08.010.

Vaněk, A., Komárek, M., Vokurková, P., Mihaljevič, M., Šebek, O., Panušková, G., Chrastný, V., Drábek, O., 2011. Effect of illite and birnessite on thallium retention and bioavailability in contaminated soils. J. Hazard Mater. 191, 170–176. https://doi.org/10.1016/J.JHAZMAT.2011.04.065.

Vaněk, A., Mihaljevič, M., Galušková, I., Chrastný, V., Komárek, M., Penížek, V., Zádorová, T., Drábek, O., 2013. Phase-dependent phytoavailability of thallium - a synthetic soil experiment. J. Hazard Mater. 250–251, 265–271. https://doi.org/10.1016/j.jhazmat.2013.01.076.

Voegelin, A., Pfenninger, N., Petrikis, J., Majzlan, J., Plötze, M., Senn, A.-C., Mangold, S., Steininger, R., Göttlicher, J., 2015. Thallium speciation and extractability in a thallium- and arsenic-rich soil developed from mineralized carbonate rock. Environ. Sci. Technol. 49, 5390–5398. https://doi.org/10.1021/acs.est.5b00629.

Wierzbicka, M., Szarek-Łukaszewska, G., Grodzińska, K., 2004. Highly toxic thallium in plants from the vicinity of Olkusz (Poland). Ecotoxicol. Environ. Saf. 59, 84–88. https://doi.org/10.1016/j.ecoenv.2003.12.009.

Xiao, T., Guha, J., Boyle, D., Liu, C.-Q., Chen, J., 2004. Environmental concerns related to high thallium levels in soils and thallium uptake by plants in southwest Guizhou, China. Sci. Total Environ. 318, 223–244. https://doi.org/10.1016/S0048-9697(03)00448-0.

Zayed, A., Gowthaman, S., Terry, N., 1998. Phytoaccumulation of trace elements by wetland plants: I. Duckweed. J. Environ. Qual. 27, 715. https://doi.org/10.2134/jeq1998.00472425002700030032x.

- PŘÍLOHA III. - Tolerance Tl

Holubík, O., Vaněk, A., Mihaljevič, M., Vejvodová, K., 2021. Thallium uptake/tolerance in a model (hyper)accumulating plant: Effect of extreme contaminant loads. Soil and Water Research. 16, 129–135. https://doi.org/10.17221/167/2020-SWR

https://doi.org/10.17221/167/2020-SWR

Thallium uptake/tolerance in a model (hyper)accumulating plant: Effect of extreme contaminant loads

Ondřej Holubík[1,2], Aleš Vaněk[1], Martin Mihaljevič[3], Kateřina Vejvodová[1]*

[1]*Department of Soil Science and Soil Protection, Faculty of Agrobiology, Food and Natural Resources, Czech University of Life Sciences Prague, Prague, Czech Republic*

[2]*Department of Soil Science and Soil Conservation, Research Institute for Soil and Water Conservation, Prague, Czech Republic*

[3]*Institute of Geochemistry, Mineralogy and Mineral Resources, Faculty of Science, Charles University, Prague, Czech Republic*

**Corresponding author: holubik.ondrej@vumop.cz*

Citation: Holubík O., Vaněk A., Mihaljevič M., Vejvodová K. (2021): Thallium uptake/tolerance in a model (hyper)accumulating plant: Effect of extreme contaminant loads. Soil & Water Res., 16: 129–135.

Abstract: Thallium (Tl) is a toxic trace element with a highly negative effect on the environment. For phytoextraction purposes, it is important to know the limitations of plant growth. In this study, we conducted experiments with a model Tl-hyperaccumulating plant (*Sinapis alba* L., white mustard) to better understand the plant tolerance and/or associated detoxification mechanisms under extreme Tl doses (accumulative 0.7/1.4 mg Tl, in total). Both the hydroponic/semi-hydroponic (artificial soil) cultivation variants were studied in detail. The Tl bioaccumulation potential for the tested plant reached up to 1% of the total supplied Tl amount. Furthermore, it was revealed that the plants grown in the soil-like system did not tolerate Tl concentrations in nutrient solutions higher than ~1 mg/L, i.e., wilting symptoms were evident. Surprisingly, for the plants grown in hydroponic solutions, the tolerable Tl concentration was by contrast at least 2-times higher (≥ 2 mg Tl/L), presumably mimicking the K biochemistry. The obtained hydroponic/semi-hydroponic phytoextraction data can serve, in combination, as a model for plant-assisted remediation of soils or mining/processing wastes enriched in Tl, or possibly for environmental cycling of Tl in general.

Keywords: artificial soil; bioaccumulation; hydroponic; phytoextraction; Tl; uptake

Currently, the best-known plant species with the ability to accumulate thallium (Tl), being a highly toxic (global) pollutant, include *Biscutella laevigata*, *Iberis intermedia* and *Brassica oleracea acephala* L. (Al-Najar et al. 2003; Ning et al. 2015), *Brassica napus* L. (Pavlíčková et al. 2006; Madejón et al. 2007; Mestek et al. 2007; Liu et al. 2020) and *Sinapis alba* L. (Fargašová 2004; Krasnodębska-Ostręga et al. 2012; Vaněk et al. 2013; Grösslová et al. 2015; Mazur et al. 2016). World production of Tl is estimated at 10–15 t/year (Merian & Clarkson 1991). On the other hand, up to ~2 000–7 000 t of Tl per year is mobilized globally by human activities (Kabata-Pendias & Pendias 1992; Kabata-Pendias & Sadurski 2004) as solid/liquid emissions from coal combustion, ferrous/non-ferrous mining/smelting, or eventually cement production (Kazantzis 2000; Yang et al. 2009). Targets for the use of phytoextraction techniques

Supported by the Czech Science Foundation (Project 20-08717S), by the Ministry of Agriculture of the Czech Republic (Grant No. RO0218), and by the European Regional Development Fund (Project CZ.02.1.01/0.0/0.0/16_019/0000845). Part of the equipment used for this study was purchased from the Operational Programme Prague – Competitiveness (Project CZ.2.16/3.1.00/21516).

https://doi.org/10.17221/167/2020-SWR

are potentially linked with the process of wastewater treatments (Vácha et al. 2015; Gutiérrez et al. 2016). The Tl transfer mechanism from the waste materials into the plant tissue generally depends on the total bioavailable element fraction in soil (Harmsen 2007) and plant physiology (Sager 1994).

An advantage of phytoextraction processes using the hyperaccumulating plants could be the natural selection of trace elements (Čechmánková et al. 2011; Corzo Remigio et al. 2020), though, the Tl/element transfer under the laboratory trial has several limitations, such as the number of suitable plants with a high accumulation potential tolerance for specific soil/climatic conditions. The bioavailability of Tl in soil depends on the specific sorption, mainly onto specific Mn oxide, birnessite (δ-MnO_2) and illite [$(K,H_3O)Al_2(Al,Si)_4O_{10}(OH)_2$], being probably the most important Tl scavengers and the general stability of Tl-host phase (Al-Najar et al. 2003; Vaněk et al. 2013; Grösslová et al. 2015). Possibly incongruent leaching of Tl from the soil to the biological/plant material may refer to the Mn-Tl association (Vaněk et al. 2019). The physiological availability of Tl into the plant depends mostly on the crop species, storage organ structure, accessibility of plant exudates, state of enzymatic processes, and plant growing strategy (Merian & Clarkson 1991). It is supposed that the majority of the up-taken Tl run along nutrient paths into the cell cytosol and vacuole storage (Kwan & Smith 1991; Ning et al. 2015).

This paper aims to evaluate and to understand the limitations of white mustard, and possibly analogous *Brassicaceae* species, to absorb/accumulate Tl, i.e., as affected by extreme Tl loads. Two growth strategies, hydroponic and semi-hydroponic (artificial soil), were investigated in detail, both being in line with the Tl remediation planning of contaminated soils (wastes) in the future. Furthermore, the results are also important from the view of general knowledge of environmental Tl cycling.

MATERIAL AND METHODS

Plant growing. Sixteen plants (in total) of white mustard (*Sinapis alba* L.) (14 days pre-cultivated grown-up) were exposed to extreme concentrations of Tl (1 and 2 mg Tl/L) for 21 days. Two different plant growing systems were compared: A – hydroponic and B – semi-hydroponic (artificial soil) system (Figure 1). A total dose of Tl applied through lower concentration during 21 days was 0.7 mg Tl (A_1 and B_1) and 1.4 mg Tl for higher concentration (A_2 and B_2). Five growth phases (Figure 2) of the mustard plant with controlled Tl and nutrition dose exposure was monitored.

Nutrient solution control. Five (fresh) nutrient solutions with specific electrical conductivity (EC) (Figure 2) were prepared every week. The solution was Tl-contaminated with the dissolved Tl_2SO_4 (Fluka, Germany, p.a.) for the whole experiment. All the plants were cultivated in the Reid and York (1958) nutrient solution: 0.136 g/L KH_2PO_4, 0.373 g/L KCl, 0.555 g/L $CaCl_2$, 0.443 g/L $MgSO_4{\cdot}7H_2O$, 0.600 g/L NH_4NO_3, 0.049 g/L $FeCl_3{\cdot}6H_2O$, 0.066 g/L Na_2-EDTA, 0.200 mg/L $ZnSO_4{\cdot}7H_2O$, 0.611 mg/L H_3BO_3, 0.388 mg/L $MnCl_2{\cdot}4H_2O$, 0.100 mg/L $CuSO_4{\cdot}5H_2O$, 0.040 mg/L $Na_2MoO_4{\cdot}H_2O$, 0.055 mg/L $Co(NO_3)_2{\cdot}6H_2O$. The 100 ml of Tl and nutrient solution was dosed into the containers (volume approx. 600 ml) according to variants at a 2–3-day regime. For the hydroponic

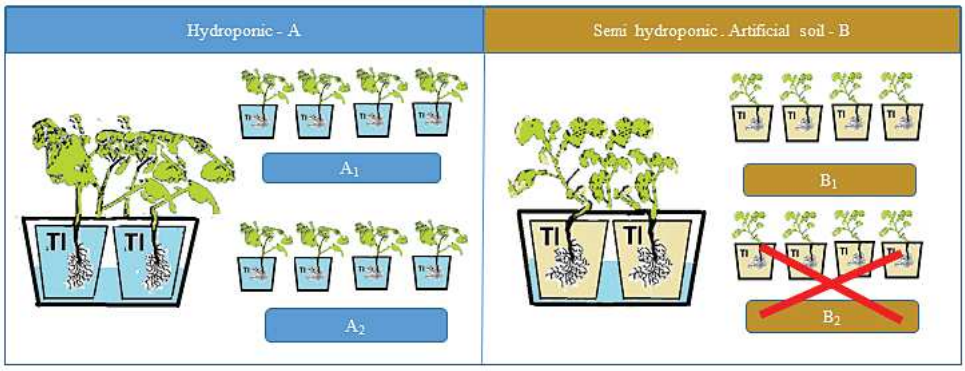

Figure 1. Experimental design of the 4-pots variants affected by (controlled) thallium (Tl) expositions; variant A – hydroponic cultivation; variant B – artificial soil cultivation; the Tl solution concentration was as follows: 1 mg Tl/L (A_1/B_1), 2 mg Tl/L (A_2/B_2); the total Tl dose for the 21-day-long experiment was 0.7 mg Tl (A_1/B_1) and 1.4 mg Tl ($A_2/_{B2}$), respectively; the B_2 variant was excluded, due to the significant wilting symptoms during the first 5 days

https://doi.org/10.17221/167/2020-SWR

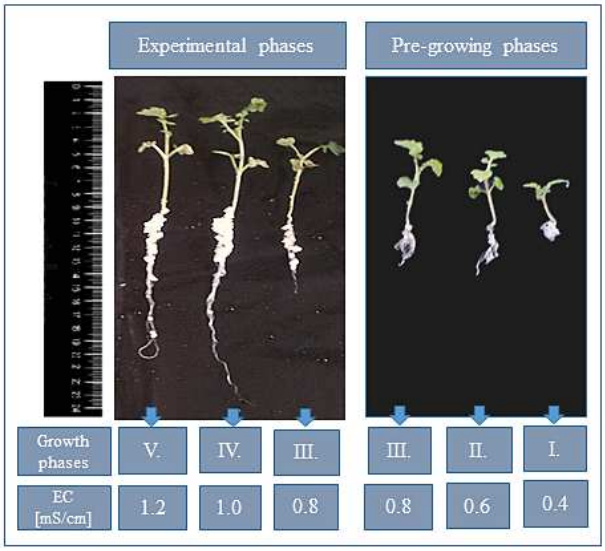

Figure 2. Growing phases of the tested plant (white mustard) and corresponding nutrient solution conductivity (EC)

system (A), a silica gel (white, Signus SG 5) grain size (2–5 mm) was used. The artificial soil variant (B) was prepared as 10% Sphagnum-peat, 70% quartz (SiO_2) sand (50–200 µm), and 20% of china clay (with ~30% kaolinite ($Al_2(OH)_4Si_2O_5$) content) were prepared according to the OECD (2009) standard.

Harvesting and digestion of plant materials. All the plants were harvested after a 21-day long experiment (on day 35 of their life); separated into leaves, stems, and roots; washed in deionized water and ethanol. Plant tissues were oven-dried at 60 °C for 24 h and homogenized. The biomass was decomposed using a mixture of concentrated (65%) HNO_3 (suprapure) with H_2O_2 (suprapure) (Merck, Germany) in a ratio of 4 : 1 which were added to the sample in a total volume of ~5 and 10 mL, then left in a closed 60-mL PTFE beaker (Savillex, USA) on a hot plate (150 °C) for 24 h.

Determination of Tl and element concentrations. The concentrations of the major/trace elements (Na, Mg, K, Ca, Mn, Fe, and Tl) in the total digests solution (of plant tissue) were determined using either inductively coupled plasma optical emission spectrometry (ICP-OES, iCAP 6500, Thermo Scientific, UK) or quadrupole based inductively coupled plasma mass spectrometry (Q-ICP-MS, Xseries II, Thermo Scientific, Germany) under standard analytical conditions. The standard reference material INCT-TL-1 (tea leaves, Institute of Nuclear Chemistry and Technology, Poland) was used for QC of quantitative analyses of Tl/major elements; the detected relative Tl recovery was ≥ 90% of the certified concentration (n = 3).

Calculation of bioaccessibility index BAI. The bio-accessibility index (BAI) is thought to be based on publications (Zayed et al. 1998; Hladun et al. 2015; Kim et al. 2016) where the bioconcentration factor (BCF) is expressed. The calculation of BAI presents a different approach. While BFC is expressed as a proportion of the concentration of the metal in the plant's tissue (mg/kg)/metal concentration in the soil (mg/kg), the BAI was expressed as the sum of the element in a specific plant tissue (g) (X_{tissue})/ sum of the total element dose (g) applied into the pot system during the whole experiment (Y_{total}), according to the formula:

$$BAI = X_{tissue}/Y_{total} \times 100\ (\%)$$

The total bio-accessibility index (BAI_{tot}) is expressed as a sum of BAI (%). The distribution factor (DF) of the trace element is counted as BAI/BAI_{tot}.

RESULTS AND DISCUSSION

Thallium uptake and distribution in plant. The usual Tl concentration in the plant tissue is ≤ 0.05 mg/kg (Adriano 2001; Krasnodębska-Ostręga et al. 2012). The phytotoxic level of Tl for plants varies ~20 mg/kg (Kabata-Pendias & Pendias 1992). The authors estimated the threshold of Tl hyperaccumulation in a whole plant as either 100 mg/kg (Van Der Ent et al. 2013), 500 mg/kg (Leblanc et al. 1999), or up to 1 000 mg/kg (Krämer 2010). Our results slightly exceed the physiological limit of Tl intoxications, as determined by Kabata-Pendias and Pendias (1992). The plant concentrations of Tl varied from 30 to 60 mg/kg within our experiment (Table 1). It is a much lower concentration than ~340 mg Tl/kg recorded by Xiao et al. (2012) in the green cabbage in "Lanmuchang" Tl-polluted area.

We assume that more important than the total concentration of Tl in a plant itself is its actual Tl content in soil (or hydroponic) solution. The initial concentrations of 2 mg Tl/L were lethal for plants incubated in the artificial soil (variant B_2). All the plants growing under the semi-hydroponic conditions signalled from the 2nd week of their life wilting symptoms: blockade of the biogenic element (Merian & Clarkson 1991; Tremel et al. 1997) and pigment loss (Mazur et al. 2016). On the other hand, not even a high concentration of Tl under the hydroponic cultivation caused signs of wilting.

https://doi.org/10.17221/167/2020-SWR

Table 1. Total thallium (Tl) concentration and distribution factor (DF) of white mustard at different Tl doses and growing systems; data cumulate 4 plants replicate as a variant

Variant	Sample	Biomass (mg)	Tl level (mg/kg)	DF (%)
A_1	leaf	96	39.39	56.9
	stem	74	31.20	34.8
	root	47	11.76	8.3
	Σ whole plant	217	30.61	–
A_2	leaf	106	87.20	61.9
	stem	74	66.53	33.0
	root	43	17.57	5.1
	Σ whole plant	223	66.91	–
B_1	leaf	72	40.52	43.0
	stem	43	53.84	34.1
	root	55	28.32	22.9
	Σ whole plant	170	39.94	–

A – hydroponic system; B – semi-hydroponic (artificial soil) system; the whole plant level of Tl was calculated as weighted means of individual tissue concentrations; the DF was expressed as a specific plant tissue bio-accessibility index (BAI)/total plant (BAI_{tot}); the Tl concentration data are means with SD < 15%

When comparing the variants with the same Tl exposition (A_1 and B_1, Table 1), the preference of Tl bioconcentration into the root and stem in artificial soil variant is evident. At the same time, plants growing in the artificial soil (semi-hydroponics) demonstrate comparable (or slightly higher) Tl inputs into the whole plant. Despite that, the Tl bioconcentration in the soil-like system could be affected by the weak interaction with the clay/kaolinite as Grösslova et al. (2015) estimated as 0.6 ± 0.02 mg Tl/kg for the background phases with kaolinite. In hydroponic cultivation, Tl is concentrated predominantly in the shoots, negligibly in the root of the plants. This aspect, together with the higher tolerance of white mustard to Tl exposure in hydroponic systems could be crucial for the phytoremediation use.

In general, our experiment confirmed different Tl bioaccumulation into the specific plant tissues depending on the cultivation media which does correspond to our previous findings (Holubík et al. 2020). Most of the total received Tl was accumulated into the shoots of white mustard (regardless of the method of cultivation). The distribution factor (DF) of the bioaccumulated Tl into the foliar mass ranged from ~50 to 60% for the hydroponic cultivation (Table 1); the entry of Tl into root tissues is minimal in hydroponic cultivation (from ~5 to 8%). Under the semi-hydroponic (soil-like) cultivation almost 20% of Tl remained in the roots, 30% were shifted to the stem, and 40% to the leaf (Table 1). Higher root development in plants grown in the soil and higher development of green parts in hydroponic systems corresponds to a different plant growth strategy (Taiz & Zeiger 2003; Holubík et al. 2020).

Thallium bioaccumulation and nutrient control. It turns out that the Tl entrance into the plant was related to monovalent ion intake (mainly of K) within the hydroponic cultivation (Table 2). It is known, that under physiological conditions Tl tends to mimic K(I) in biochemical processes (Sager 1994; Galván-Arzate & Santamaría 1998). Our data clearly indicate reduced inputs of major/nutrient elements for plants grown in artificial soil. Despite minimal differences of BAI of main nutrients into the specific plant tissues (Table 3), we tried to relate which elements may accompany Tl on the way to the plant by linear regression relationship. Irrespective of cultivation and Tl spiked concentration the potassium follows the thallium into the plant due to: $BAI_{Tl} = 7.1\ BAI_K$ ($R^2 = 0.90$); similarly magnesium: $BAI_{Tl} = 8.0\ BAI_{Mg}$ ($R^2 = 0.96$), calcium as $BAI_{Tl} = 6.0\ BAI_{Ca}$ ($R^2 = 0.91$) and manganese as $BAI_{Tl} = 1.5\ BAI_{Mn}$ ($R^2 = 0.82$). The total plant Tl uptake (BAI_{tot}) was 0.99 ± 0.05% (Table 3). The hydroponic cultivation prefers Tl bioaccumulation in the shoot (0.9–1% of total Tl pool) and only a minimal proportion was accumulated

Table 2. The nutrient concentrations (g/kg) of the grow-up plants ($n = 4$)

Tissue	Variant	K	Mg	Ca	Fe
		(g/kg)			
Leaf	A_1	26.8	3.8	15.0	0.3
	A_2	12.1	2.9	11.7	0.3
	B_1	2.9	1.4	9.9	0.7
Stem	A_1	22.5	5.5	14.1	0.5
	A_2	19.6	4.1	10.3	0.5
	B_1	4.9	1.7	7.6	2.0
Root	A_1	20.8	3.9	14.1	0.4
	A_2	11.7	3.9	10.6	0.2
	B_1	1.8	1.0	3.8	0.7

A – hydroponic system; B – semi-hydroponic (artificial soil) system; the nutrient concentration data are means with SD < 20%

https://doi.org/10.17221/167/2020-SWR

Table 3. The bio-accessibility index (BAI) of the tested plant (white mustard) grown under different thallium (Tl) doses and growing systems; all the data cumulate the 4-plant replicates

Variant	Sample	BAI_{Tl}	BAI_{Na}	BAI_{Mg}	BAI_{K}	BAI_{Ca}	BAI_{Mn}	BAI_{Fe}
		(%)						
A_1	leaf	0.54	59	4.2	5.6	3.7	1.0	1.4
	stem	0.33	29	2.5	1.9	2.2	0.4	1.1
	root	0.08	5	0.8	0.3	1.2	0.3	1.7
	Σ whole plant	0.95	93	7.5	7.8	7.1	1.7	4.2
A_2	leaf	0.66	46	4.9	4.8	3.8	1.2	2.1
	stem	0.35	31	3.4	1.9	2.0	0.5	0.8
	root	0.05	3	0.5	0.2	0.4	0.2	1.6
	Σ whole plant	1.07	80	8.8	6.8	6.2	1.9	4.4
B_1	leaf	0.42	16	4.6	3.5	2.6	0.5	1.9
	stem	0.33	9	2.1	1.8	1.1	0.2	1.0
	root	0.22	3	1.1	0.6	1.1	0.2	5.6
	Σ whole plant	0.97	27	7.7	5.9	4.8	0.9	8.5

BAI was expressed as the sum of total element content in a specific plant tissue (g) (X_{tissue})/sum of the total element dose (g) applied during the whole experiment (Y_{total}), according to the formula: $BAI = X_{tissue}/Y_{total} \times 100$ (%); the total bio-accessibility index for the whole plant (BAI_{tot}) is expressed as a sum of specific tissue BAI (%)

into the roots (0.05–0.1 %). On the other hand, in the artificial soil system, a considerable portion of Tl (0.2%) was accumulated by root tissue. The different growth strategies (in soil/hydroponic) may affect individual nutrient uptake. Higher bioaccumulation of K and Na in the hydroponic system was observed (see Table 3), possibly due to the passive transport mechanism(s). For the semi-hydroponic cultivation, the Fe-Tl association was observed, which could have resulted from the active transport of Fe from the nutrient solution.

Environmental applications. Average levels in topsoils contaminated with Tl typically exceed 10 mg/kg (Xiao et al. 2004). Scheckel et al. (2004) demonstrated on Tl-spiked soils, that the Tl uptake mainly depends on the soil Tl concentration; the studied *Iberis intermedia* absorbed more than 13 mg Tl/g. Clearly, our results show a much lower absolute uptake of Tl into the white mustard plant tissue, reaching of ~0.05 mg/g (dry weight). Nevertheless, this behaviour could likely be compensated by a higher amount of biomass. We assume that the soil solution Tl concentration for phytoremediation cannot exceed 1 mg Tl/L. An important finding is that the concentration of 2 mg Tl/L is not limiting for hydroponic cultivation, being in contrast to Sager (1994) who reports for soybean plants (*Glycine max.*) ≤ 0.6 mg Tl/L (provoked leaf chlorosis), and ≤ 1 mg Tl/L (provoked leaf necrosis).

Our results demonstrate that the Tl plant uptake is primarily dependent on the concentration and speciation of Tl in the primary Tl pool, but for successful (efficient) phytoremediation use, it is also important to know the maximum available Tl load(s) and Tl distribution within respective plant organs/tissues. For practical use, it is still necessary to verify the experiment on an operational scale.

CONCLUSION

Based on our experiments, the tested mustard plant (*Sinapis alba* L.) could absorb up to 1% of the total supplied Tl amount, regardless of the method of cultivation. On the contrary, the distribution of Tl/element into specific tissue cytosol cell or vacuole storages depended on the cultivation strategy. For the hydroponic cultivation, up to 95% of the plant Tl was translocated into the shoots, and only ≤ 8% remained in the roots; the plants indicated by contrast a ~20% Tl root accumulation within the semi-hydroponics (soil-like system). In other words, we assume that Tl within the hydroponic system entered the plant tissues along the paths of the monovalent elements (mainly K), and contrarily to our/common expectations, for the semi-hydroponic system, the Tl introduction could have also been affected by the uptake of Fe. It should be noted that the higher Tl contamination in the soil/nutrient solution may

https://doi.org/10.17221/167/2020-SWR

decrease the uptake of biogenic elements. This aspect was evident for the soil-like cultivation at critical Tl doses (>1 mg Tl/L), where the plants suffered from wilting symptoms, which, by contrast, were negligible or absent for simple hydroponics and the same Tl load.

REFERENCES

Adriano D.C. (2001): Trace Elements in Terrestrial Environments. New York, Springer New York.

Al-Najar H., Schulz R., Römheld V. (2003): Plant availability of thallium in the rhizosphere of hyperaccumulator plants: A key factor for assessment of phytoextraction. Plant and Soil, 249: 97–105.

Čechmánková J., Vácha R., Skála J., Havelková M. (2011): Heavy metals phytoextraction from heavily and moderately contaminated soil by field crops grown in monoculture and crop rotation. Soil and Water Research, 6: 120–130.

Corzo Remigio A., Chaney R.L., Baker A.J.M., Edraki M., Erskine P.D., Echevarria G., van der Ent A. (2020): Phytoextraction of high value elements and contaminants from mining and mineral wastes: opportunities and limitations. Plant and Soil, 449: 11–37.

Fargašová A. (2004): Toxicity comparison of some possible toxic metals (Cd, Cu, Pb, Se, Zn) on young seedlings of *Sinapis alba* L. Plant, Soil and Environment, 50: 33–38.

Galván-Arzate S., Santamaría A. (1998): Thallium toxicity. Toxicology Letters, 99: 1–13.

Grösslová Z., Vaněk A., Mihaljevič M., Ettler V., Hojdová M., Zádorová T., Pavlů L., Penížek V., Vaněčková B., Komárek M., Chrastný V., Ash C. (2015): Bioaccumulation of thallium in a neutral soil as affected by solid-phase association. Journal of Geochemical Exploration, 159: 208–212.

Gutiérrez M., Mickus K., Camacho L.M. (2016): Abandoned Pb Zn mining wastes and their mobility as proxy to toxicity: A review. Science of the Total Environment, 565: 392–400.

Harmsen J. (2007): Measuring bioavailability: From a scientific approach to standard methods. Journal of Environmental Quality, 36: 1420–1428.

Hladun K.R., Parker D.R., Trumble J.T. (2015): Cadmium, copper, and lead accumulation and bioconcentration in the vegetative and reproductive organs of *Raphanus sativus*: Implications for plant performance and pollination. Journal of Chemical Ecology, 41: 386–395.

Holubík O., Vaněk A., Mihaljevič M., Vejvodová K. (2020): Higher Tl bioaccessibility in white mustard (hyper-accumulator) grown under the soil than hydroponic conditions: A key factor for the phytoextraction use. Journal of Environmental Management, 255: 109880.

Kabata-Pendias A., Pendias H. (1992): Trace Elements in Soils and Plants. 2nd Ed., Boca Raton, CRC Press.

Kabata-Pendias A., Sadurski W. (2004): Trace elements and compounds in soil. In: Merian E., Anke M., Ihnat M., Stoeppler M. (eds.): Elements and their Compounds in the Environment. 2nd Ed. Weinheim, Wiley-VCH: 79–99.

Kazantzis G. (2000): Thallium in the environment and health effects. Environmental Geochemistry and Health, 22: 275–280.

Kim D.J., Park B.C., Ahn B.K., Lee J.H. (2016): Thallium uptake and translocation in barley and sunflower grown in hydroponic conditions. International Journal of Environmental Research, 10: 575–582.

Krämer U. (2010): Metal hyperaccumulation in plants. Annual Review of Plant Biology, 61: 517–534.

Krasnodębska-Ostręga B., Sadowska M., Ostrowska S. (2012): Thallium speciation in plant tissues—Tl(III) found in *Sinapis alba* L. grown in soil polluted with tailing sediment containing thallium minerals. Talanta, 93: 326–329.

Kwan K.H.M., Smith S. (1991): Some aspects of the kinetics of cadmium and thallium uptake by fronds of *Lemna minor* L. New Phytologist, 117: 91–102.

Leblanc M., Petit D., Deram A., Robinson B.H., Brooks R.R. (1999): The phytomining and environmental significance of hyperaccumulation of thallium by *Iberis intermedia* from southern France. Economic Geology, 94: 109–113.

Liu J., Wei X., Zhou Y., Tsang D.C.W., Yin M., Lippold H., Yuan W., Wang J., Feng Y., Chen D. (2020): Thallium contamination, health risk assessment and source apportionment in common vegetables. Science of the Total Environment, 703: 135547.

Madejón P., Murillo J.M., Marañón T., Lepp N.W. (2007): Factors affecting accumulation of thallium and other trace elements in two wild Brassicaceae spontaneously growing on soils contaminated by tailings dam waste. Chemosphere, 67: 20–28.

Mazur R., Sadowska M., Kowalewska Ł., Abratowska A., Kalaji H.M., Mostowska A., Garstka M., Krasnodębska-Ostręga B. (2016): Overlapping toxic effect of long term thallium exposure on white mustard (*Sinapis alba* L.) photosynthetic activity. BMC Plant Biology, 16: 191.

Merian E., Clarkson T.W. (1991): Metals and their Compounds in the Environment : Occurrence, Analysis, and Biological Relevance. Weinheim, Wiley-VCH.

Mestek O., Polák J., Juříček M., Karvánková P., Koplík R., Šantrůček J., Kodíček M. (2007): Trace element distribution and species fractionation in *Brassica napus* plant. Applied Organometallic Chemistry, 21: 468–474.

Ning Z., He L., Xiao T., Márton L. (2015): High accumulation and subcellular distribution of thallium in green cab-

https://doi.org/10.17221/167/2020-SWR

bage (*Brassica oleracea* L. var. *capitata* L.). International Journal of Phytoremediation, 17: 1097–1104.

OECD (2009): OECD Guidelines for the Testing of Chemicals. Oecd/Ocde 220 Draft Documents. Available at https://www.oecd.org/chemicalsafety/testing/44098118.pdf

Pavlíčková J., Zbíral J., Smatanová M., Habarta P., Houserová P., Kubáň V. (2006): Uptake of thallium from artificially contaminated soils by kale (*Brassica oleracea* L. var. *acephala*). Plant, Soil and Environment, 52: 544–549.

Reid P.H., York E.T. (1958): Effect of nutrient deficiencies on growth and fruiting characteristics of peanuts in sand cultures. Agronomy Journal, 50: 63.

Sager M. (1994): Thallium. Toxicological & Environmental Chemistry, 45: 11–32.

Scheckel K.G., Lombi E., Rock S.A., McLaughlin M.J. (2004): In vivo synchrotron study of thallium speciation and compartmentation in *Iberis intermedia*. Environmental Science & Technology, 38: 5095–5100.

Taiz L., Zeiger E. (2003): Plant Physiology. 3rd Ed. Sunderland, Sinauer Associates, Inc. Publishers

Tremel A., Masson P., Sterckeman T., Baize D., Mench M. (1997): Thallium in French agrosystems – I. Thallium contents in arable soils. Environmental Pollution, 95: 293–302.

Vácha R., Skála J., Čechmánková J., Horváthová V., Hladík J. (2015): Toxic elements and persistent organic pollutants derived from industrial emissions in agricultural soils of the Northern Czech Republic. Journal of Soils and Sediments, 15: 1813–1824.

Van Der Ent A., Baker A.J.M., Reeves R.D., Pollard A.J., Schat H. (2013): Hyperaccumulators of metal and metalloid trace elements: Facts and fiction. Plant and Soil, 362: 319–334.

Vaněk A., Mihaljevič M., Galušková I., Chrastný V., Komárek M., Penížek V., Zádorová T., Drábek O. (2013): Phase-dependent phytoavailability of thallium – A synthetic soil experiment. Journal of Hazardous Materials, 250–251: 265–271.

Vaněk A., Holubík O., Oborná V., Mihaljevič M., Trubač J., Ettler V., Pavlů L., Vokurková P., Penížek V., Zádorová T., Voegelin A. (2019): Thallium stable isotope fractionation in white mustard: Implications for metal transfers and incorporation in plants. Journal of Hazardous Materials, 369: 521–527.

Xiao T., Guha J., Boyle D., Liu C.-Q., Chen J. (2004): Environmental concerns related to high thallium levels in soils and thallium uptake by plants in southwest Guizhou, China. Science of the Total Environment, 318: 223–244.

Xiao T., Yang F., Li S., Zheng B., Ning Z. (2012): Thallium pollution in China: A geo-environmental perspective. Science of the Total Environment, 421–422: 51–58.

Yang C., Chen Y., Peng P., Li C., Chang X., Wu Y. (2009): Trace element transformations and partitioning during the roasting of pyrite ores in the sulfuric acid industry. Journal of Hazardous Materials, 167: 835–845.

Zayed A., Gowthaman S., Terry N. (1998): Phytoaccumulation of trace elements by wetland plants: I. Duckweed. Journal of Environmental Quality, 27: 715.

Received: November 26, 2020
Accepted: February 17, 2021
Published online: March 16, 2021

- PŘÍLOHA IV. - Izotopické trasování Tl

Vaněk, A., Grösslová, Z., Mihaljevič, M., Trubač, J., Ettler, V., Teper, L., Cabala, J., Rohovec, J., Zádorová, T., Penížek, V., Pavlů, L., Holubík, O., Němeček, K., Houška, J., Drábek, O., Ash, C., 2016. Isotopic Tracing of Thallium Contamination in Soils Affected by Emissions from Coal-Fired Power Plants. Environmental Science & Technology. 50, 9864–9871. https://doi.org/10.1021/acs.est.6b01751

Environmental Science & Technology

Article

pubs.acs.org/est

Isotopic Tracing of Thallium Contamination in Soils Affected by Emissions from Coal-Fired Power Plants

Aleš Vaněk,*[,†] Zuzana Grösslová,[†] Martin Mihaljevič,[‡] Jakub Trubač,[‡] Vojtěch Ettler,[‡] Leslaw Teper,[§] Jerzy Cabala,[§] Jan Rohovec,[∥] Tereza Zádorová,[†] Vít Penížek,[†] Lenka Pavlů,[†] Ondřej Holubík,[†] Karel Němeček,[†] Jakub Houška,[†] Ondřej Drábek,[†] and Christopher Ash[†]

[†]Department of Soil Science and Soil Protection, Faculty of Agrobiology, Food and Natural Resources, Czech University of Life Sciences Prague, Kamýcká 129, 165 21 Praha 6, Czech Republic

[‡]Institute of Geochemistry, Mineralogy and Mineral Resources, Faculty of Science, Charles University in Prague, Albertov 6, 128 43 Praha 2, Czech Republic

[§]Department of Economic Geology, Faculty of Earth Sciences, University of Silesia, Bedzinska 60, Sosnowiec 41-200, Poland

[∥]Institute of Geology of the CAS, v.v.i., Rozvojová 269, 165 00 Praha 6, Czech Republic

Supporting Information

ABSTRACT: Here, for the first time, we report the thallium (Tl) isotope record in moderately contaminated soils with contrasting land management (forest and meadow soils), which have been affected by emissions from coal-fired power plants. Our findings clearly demonstrate that Tl of anthropogenic (high-temperature) origin with light isotope composition was deposited onto the studied soils, where heavier Tl (ε^{205}Tl ∼ −1) naturally occurs. The results show a positive linear relationship (R^2 = 0.71) between 1/Tl and the isotope record, as determined for all the soils and bedrocks, also indicative of binary Tl mixing between two dominant reservoirs. We also identified significant Tl isotope variations within the products from coal combustion and thermodesorption experiments with local Tl-rich coal pyrite. Bottom ash exhibited the heaviest Tl isotope composition (ε^{205}Tl ∼ 0), followed by fly ash (ε^{205}Tl between −2.5 and −2.8) and volatile Tl fractions (ε^{205}Tl between −6.2 and −10.3), suggesting partial Tl isotope fractionations. Despite the evident role of soil processes in the isotope redistributions, we demonstrate that Tl contamination can be traced in soils and propose that the isotope data represent a possible tool to aid our understanding of postdepositional Tl dynamics in surface environments for the future.

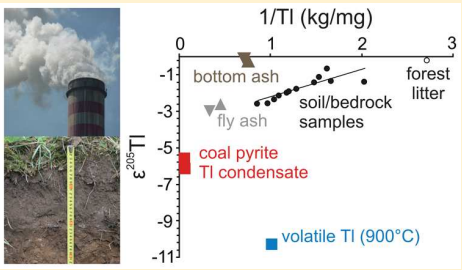

INTRODUCTION

A limited amount of data on the behavior and fate of thallium (Tl) in the environment is available, compared to other trace metals/metalloids. The environmental impact of Tl has also received little attention, although lately interest in this element is growing, probably due to both the extreme toxicity of Tl for most living organisms and the successful development and expansion of powerful analytical mass spectrometric (MS) techniques. The recent developments of multiple-collector inductively coupled mass spectrometry (MC-ICP-MS) represent a new and unconventional tool in the geochemical research of Tl, as ^{205}Tl/^{203}Tl isotope ratio in environmental samples can be accurately determined by this technique.[1]

Solid wastes and emissions from coal combustion, metal mining and metallurgy, and cement production all represent potential anthropogenic sources of Tl,[2−5] primarily resulting from the abundance of Tl within specific sulfides (e.g., pyrite, sphalerite), which are (co)processed. Since most Tl compounds are volatile at high temperatures, they are not efficiently retained by the emission-control facilities, such as electrostatic precipitators, and a large metal portion may readily enter the atmosphere, as well as surrounding environments. Compared to the geogenic Tl range of 0.01−1 mg/kg,[3] anthropogenic Tl levels in soils (or sediments) in such affected areas commonly exceed 1−10 mg/kg.[5−8] It should be highlighted that, apart from the chalcophile nature of Tl, this element also tends to compete for K(I) or Rb(I) in K-silicates (feldspars, micas, etc.).[9,10] Efficient "scavengers" of Tl in soils/sediments include Mn(III,IV) oxides (mainly, birnessite, δ-MnO_2) and illite.[11−15] The geochemical behavior in soils/sediments is thus efficiently controlled by specific Tl adsorption and/or Tl−K replacement within the mineral (inter)layers. Moreover, specific association of Mn phases with Tl comes from the surface oxidation of Tl(I) to Tl(III), which is then tightly adsorbed or precipitated onto the oxide as Tl_2O_3.[16] Recent investigations of Tl-rich soils using μ-X-ray absorption spectroscopy (XAS) documented the presence of both species, i.e., Tl(III)-δ-MnO_2 and Tl_2O_3.[15]

A number of works focused on Tl geochemistry linked with specific geological processes and isotope effects, such as

Received: April 8, 2016
Revised: July 21, 2016
Accepted: August 18, 2016
Published: August 18, 2016

DOI: 10.1021/acs.est.6b01751
Environ. Sci. Technol. 2016, 50, 9864−9871

Table 1. Physico−Chemical Characteristics of the Studied Forest (F) and Meadow (M) Soil Profiles[a]

soil profile/GPS position	soil type	horizon	depth (cm)	clay content (%)	pH KCl	pH H_2O	CEC (cmol/kg)[b]	TOC (%)[b]	S_{tot} (mg/kg)[b]	Fe_{ox} (g/kg)[b]	Mn_{ox} (g/kg)[b]	Al_{ox} (g/kg)[b]
F/N50.8688°	Dystric Cambisol	L	20−15	n.d.	3.4	3.7	106	37.6	0.11	1.57	0.18	1.23
E15.0407°		F + H	15−0	n.d.	3.4	3.9	50.5	16.7	0.09	6.46	0.03	5.60
		A	0−5	19.1	3.5	4.1	25.8	4.16	0.09	8.95	0.04	2.77
		AB	5−25	6.0	4.2	4.4	24.3	3.07	0.06	8.00	0.17	9.29
		Bw	25−45	9.3	4.4	4.5	18.8	0.70	0.05	4.92	0.09	8.37
		C	45−65	11.2	4.4	4.5	11.8	0.06	0.05	3.85	0.07	5.73
M/N50.8693°	Dystric Cambisol	A1	0−5	4.6	4.8	5.8	23.0	2.95	0.06	5.27	0.22	3.40
E15.0399°		A2	5−25	4.8	5.0	6.1	17.3	1.13	0.05	5.18	0.15	3.28
		AB	25−40	10.2	4.9	6.3	12.3	0.47	0.08	3.26	0.26	3.82
		Bw	40−60	9.3	4.8	6.1	10.3	0.31	0.07	4.15	0.29	3.57
		C	60−80	9.4	4.5	5.7	9.5	0.34	0.05	2.55	0.15	3.21

[a]Fe_{ox}, Mn_{ox}, and Al_{ox}: oxalate-extractable Fe, Mn, and Al concentrations. n.d.: not determined. [b]The data are means (n = 3) with RSD ≤ 10%.

transport/deposition of geomaterials, redox variations at low temperature (marine, fluvial, and terrestrial) geosystems, and paleoclimate dynamics.[17−19] On the other hand, only one pioneering environmental study devoted to the isotope tracing of anthropogenic Tl in contaminated soils is currently available in the literature, and it clearly demonstrates stable isotope variations (i) between Tl of geogenic and industrial origin and (ii) Tl at the soil−plant interface.[5]

Whereas isotope fractionation of other metals during high-temperature processes has been reported for smelters[20,21] and coal-fired power plants,[22−24] to date, we do not know to what extent Tl may isotopically fractionate from the primary source (ore, coal) during these industrial processes. Moreover, the role of composition and processes occurring in soils in the postdepositional Tl isotope fractionation is not known. Thus, it is evident that, in order to better understand Tl mobility, enrichment, and processes affecting its cycling in the environment, these Tl-isotope fractionation data are needed. Here, for the first time, we report the Tl isotope record in moderately contaminated forest and meadow soils, which have been affected by emissions from coal-fired power plants in the "Black Triangle" area, Central Europe.

EXPERIMENTAL SECTION

Study Area, Soil Sampling, and Characterization. The area, situated approximately 100 km N of Prague, the capital of the Czech Republic (Figure S1), covers a part of the so-called "Black Triangle", an area listed among the historically most polluted regions in Central Europe. The site has been polluted predominantly by extensive combustion of local brown coal (lignite) since the 1960s. The coal-fired power stations "Turów" (2000 MW, Poland; in operation since 1962) and "Hirschfelde" (330 MW, Germany; in operation 1911−1992), located close to the Czech−Polish−German tripoint, represent the former point pollution sources of the surroundings.

Regarding coal combustion technologies, pulverized fuel (PF) boilers operating at high temperatures (1100−1400 °C) were installed in both power plants, for practically all of the operation time at Hirschfelde power station. In 2005, the PF boilers in Turów power plant were completely replaced by circulating fluidized bed (CFB) units, with an optimum bed temperature of ∼850 °C. The air pollution control (APC) facilities, primarily consisting of bag and electrostatic filters, which have only limited flue gas cleaning efficiency, have undergone complex modernization since 1994. More efficient electrostatic precipitators, flue gas desulfurization, urea/catalytic denitrification units, etc. are now involved in APC to provide conformity to valid emission standards.

Since the study area is affected by prevailing NW winds (besides S winds) (Figure S1), former dry/wet deposition has led to increased SO_2, NO_x, and trace metal/metalloid (Pb, Cr, Cu, Ni, Hg, Tl, As) input in the northern part of the Czech Republic.[25] The median Tl concentration in topsoil in the area (the EuroRegion Neisse) reaches ∼0.5 mg/kg[26] and is consistent with increased Tl amounts reported for local lignite (<0.2−2.4 mg/kg).[27] The area can also be characterized by an anomalous Tl background level, resulting from Paleozoic methamorphics enriched in Tl (<1 mg/kg). Surprisingly, all of the tested coals represented by three different types of lignite from Turów coal mine (sedimentary rock collection of the University of Silesia), as well as feed coal, were very low in total Tl contents (0.001−0.02 mg/kg), probably due to the lack of sulfides.

For tracing Tl sources in soils, both industrial (waste) and natural samples were investigated for Tl isotopes: (i) fly and bottom ashes derived by two energy blocks (A and B), with CFB units from the Turów power station; (ii) Tl-rich coal pyrite, Turów coal mine (mineral collection of the Czech University of Life Sciences Prague); (iii) model high-temperature pyrite evaporates with Tl fractions volatilized at 700 and 900 °C/oxidizing conditions/10 min each and total Tl condensed (300−900 °C, 60 min) on the inner wall of a quartz tube, all obtained from a closed (quartz) system consisting of a laboratory programmable induction oven followed by a glass bubbler (0.1 M HCl) in a synthetic air atmosphere (Figure S2); (iv) appropriate bedrock and biomass samples. The main difference between blocks A and B comes from the coal cocombustion with ∼10 and ∼4 t/h of biomass and with external and internal separation of solids, respectively. Moreover, there is a slight difference in the steam temperature of ∼540 and ∼565 °C for blocks A and B, respectively.

In this study, two contrasting profiles of forest (F) and meadow (M) soils were sampled approximately 12 km SE of the coal-fired power plants; the GPS coordinates of soil profiles were as follows: (F) N50.8688°, E15.0407° and (M) N50.8693°, E15.0399°. In order to preserve uniform bedrock composition for both soil profiles, the distance between individual sampling sites was minimized to ∼50 m.

DOI: 10.1021/acs.est.6b01751
Environ. Sci. Technol. 2016, 50, 9864−9871

Muscovite−biotite orthogneiss represents the bedrock type for both profiles. The soils were sampled from 1 × 1 m-wide pits according to the natural development of soil horizons, down to the bottom horizon C, and classified as Dystric Cambisols.[28] Composite samples of fresh needles and wood biomass of Norway spruce (*Picea abies* L.) collected at the forest sampling site (<5 m from the pit) simulated the primary organic matter (OM) for profile F. All soils were air-dried, homogenized, and sieved through a 2 mm stainless-steel sieve prior to further use or analyses. Complex data on the physicochemical properties of the soils are summarized in Table 1 and were determined as described further. Soil pH was measured in a 1:5 (v/v) ratio of soil and water or 1 M KCl solution using a Handylab pH 11 multimeter (Schott, Germany). The amounts of total organic carbon (TOC) and sulfur (S_{tot}) were determined by catalytic oxidation (1350 °C) using a combination of Metalyt CS 500 and Metalyt CS 530 (ELTRA, Germany) elemental analyzers. The cation exchange capacity (CEC) was computed after saturation of the soil sample with 0.1 M $BaCl_2$ followed by Ba^{2+} release using $MgSO_4$.[29] Acid oxalate extraction (0.2 M ammonium oxalate/oxalic acid at pH 3), used to indicate the presence of amorphous/poorly crystalline Fe, Mn, and Al (hydr)oxides, was performed according to Pansu and Gautheyrou.[30] Clay content was estimated by the hydrometer method.[31] The exchangeable fraction of Tl in soil samples was determined by means of a single (2 h) extraction at a solid-to-liquid ratio of 1:2.5 using 1 M NH_4NO_3.[32]

The bulk mineralogy of both profiles was dominated by quartz, K/Na feldspars ($K/NaAlSi_3O_8$), amphibole ($Ca_2(Mg,Fe,Al)_5(Si,Al)_8O_{22}(OH)_2$), and muscovite ($KAl_2(AlSi_3O_{10})(F,OH)_2$), as determined using X-ray diffraction analysis (XRD). The indicated clay phases consisted of illite ($(K,H_3O)Al_2(Si,Al)_4O_{10}(OH)_2$), and clinochlore ($(Mg,Al)_6(Si,Al)_4O_{10}(OH)_8$). XRD analysis was performed using an X'Pert Pro diffractometer (PANalytical, The Netherlands) under the following conditions: Cu Kα radiation, 40 kV, 30 mA, and step scanning at 0.02°/150 s in the range of 3−80° 2θ.

Prior to determining total metal concentrations and Tl isotopes, soils, bedrocks, biomass, and reference/waste samples were carefully homogenized and then finely ground in an agate mill (Pulverisette 0, Fritsch, Germany). Subsequently, a mass of 0.5 g of each sample was totally decomposed using a hot acid mixture; in the case of coal, an aliquot of 1 g was treated. Concentrated HNO_3 and HF acids (Merck Ultrapure, Germany) mixed in the ratio of 1:1 or 2:1 were added to the sample in a total volume of 5−20 (30) mL and then left in a closed 60 mL PTFE beaker (Savillex, USA) on a hot plate (150 °C) for 48 h. If any organic residue persisted, 1−2 mL of H_2O_2 was added and left overnight at room temperature. The standard reference materials, NIST 2711 (Montana Soil) (National Institute of Standards and Technology, USA) and INCT-TL-1 (Tea Leaves) (Institute of Nuclear Chemistry and Technology, Poland) were used for QC of quantitative analyses (Table S1).

Element Concentrations. Concentrations of the main cations (Al, Ca, Fe, K, Mg, Mn, Na) and trace metals/metalloids (As, Cd, Co, Cu, Pb, V, Tl, Zn, Sc, Zr) in the total digests of soils, rocks, and industrial (waste) and biomass samples, as well as in various soil extracts were determined in triplicate using either inductively coupled plasma optical emission spectrometry (ICP-OES, iCAP 6500, Thermo Scientific, UK) or quadrupole based inductively coupled plasma mass spectrometry (Q-ICP-MS, Xseries II, Thermo Scientific, Germany) under standard analytical conditions.

Sample Purification. In order to isolate Tl from the sample matrix, a two-stage chromatographic separation with an anion exchange resin (Bio-Rad AG1-X8, 200−400 mesh, Cl^- cycle) was performed according to the modified procedure of Baker et al.[33] The sample was evaporated to complete dryness and then redissolved in 0.1 M HCl. Subsequently, Br_2 was added so that the reagent had a final concentration of 1% (v/v) in the sample solution (0.1 M HCl). The solution was then left overnight (>12 h) to ensure that all Tl(I) was oxidized to Tl(III). For Tl separation, a sample aliquot was taken so that generally 100−500 ng of total Tl is present. The first stage of chromatographic chemistry utilized a glass 8 mL Econo-column (Bio-Rad, USA) filled with 2 mL of resin, followed by steps with reagent mixtures and volumes as described further: (i) 5 × 1 mL of 0.1 M HCl-SO_2 + 5 × 1 mL of 0.1 M HCl, resin cleaning; (ii) 5 × 1.5 mL of 0.1 M HCl-1% Br_2, resin treatment; (iii) sample loading (0.1 M HCl-1% Br_2); (iv) 10 × 2 mL of 0.01 M HCl-1% Br_2; (v) 6 × 2 mL of 0.03 M HBr-0.5 M HNO_3-1% Br_2; (vi) 6 × 2 mL of 0.03 M HBr-2 M HNO_3-1% Br_2; (vii) 6 × 2 mL of 0.1 M HCl-1% Br_2; (viii) 13 × 2 mL of 0.1 M HCl-SO_2, Tl/Pb fraction elution. The obtained Tl/Pb fraction was evaporated and redissolved in 200 μL of 0.1 M HCl-1% Br_2 (>12 h), in preparation for the next part of Tl purification. For the second chromatographic stage, a PP 1.2 mL microcolumn filled with 250 μL of resin was used. Resin cleaning and treatment, as well as sample loading, were performed in the same way, with corresponding lower volumes of individual reagent mixtures. Once the Tl fraction was obtained, the Tl sample was evaporated and diluted in 5 mL of 2% HNO_3. Thallium and Pb concentrations were monitored using Q-ICP-MS after sample dissolution and Tl separation. In cases when some Pb in the final solution remained (~0.1% of the original Pb concentration), the microcolumn chemistry was repeated. Chemicals of ultrapure and suprapure quality (Merck, Germany) and deionized water (Milli-Q+, Millipore, USA) were used for separation techniques.

Thallium Isotope Measurements. Thallium isotope analyses were carried out using MC-ICP-MS (Neptune Plus, Thermo Scientific, Germany) with desolvating nebulizer (Aridus II, CETAC, Thermo Scientific, Germany) at the Laboratories of Mass Spectrometry of the Faculty of Science, Charles University in Prague, under the following analytical conditions: The detector configuration was: ^{202}Hg−L3, ^{203}Tl−L2, ^{204}Pb−L1, ^{205}Tl−C, ^{206}Pb−H1, ^{207}Pb− H2, and ^{208}Pb−H3. All solutions were measured in 3 runs of 50 cycles. Mass bias drift was eliminated using external normalization and standard sample bracketing (NIST SRM 997). Solutions with Tl concentration were doped with NIST SRM 981 to obtain Pb/Tl 2−3. For interelement correction, the ratio ^{208}Pb/^{206}Pb was related to the raw ^{205}Tl/^{203}Tl data by the exponential mass dependent fractionation law. The NIST SRM 997 was measured directly before and after each sample, and final data were interpolated between bracketing standards. Thallium isotope composition was reported with an ε notation relative to the NIST SRM 997 (eq 1).

$$\varepsilon^{205}\mathrm{Tl} = \frac{^{205}\mathrm{Tl}/^{203}\mathrm{Tl}_{\mathrm{sample}} - ^{205}\mathrm{Tl}/^{203}\mathrm{Tl}_{\mathrm{NIST997}}}{^{205}\mathrm{Tl}/^{203}\mathrm{Tl}_{\mathrm{NIST997}}} \times 10^4 \quad (1)$$

DOI: 10.1021/acs.est.6b01751
Environ. Sci. Technol. 2016, 50, 9864−9871

Table 2. Total and Exchangeable Tl Concentrations, Tl Isotope Compositions (Expressed as ε^{205}Tl), and Tl/Zr and Tl/Sc Ratios in the Studied Soils, Bedrocks, Biomass, and Reference/Waste Samples, i.e., Local Brown Coal, Coal Pyrite, Model Volatile Tl Fractions/Condensate and Fly/Bottom Ashes[a]

soil profile/sample	horizon	total Tl (mg/kg)	exchangeable Tl (mg/kg)	ε^{205}Tl ± 0.7	Tl/Zr (×10^2)	Tl/Sc (×10^2)
F	L	0.37 ± 0.08	0.04 ± 0	−0.16	1.90	27.5
	F + H	0.92 ± 0.15	0.07 ± 0.02	−2.08	1.49	19.5
	A	0.97 ± 0.11	0.05 ± 0	−2.30	1.25	21.8
	AB	0.84 ± 0.20	0.02 ± 0	−1.86	1.04	17.0
	Bw	0.78 ± 0.27	0.02 ± 0	−1.72	0.87	14.6
	C	0.66 ± 0.03	0.02 ± 0	−1.07	0.69	12.6
	Bedrock 1	0.50 ± 0.19	n.d.	−1.33	1.12	16.2
M	A1	1.18 ± 0.16	0.04 ± 0	−2.53	1.64	27.6
	A2	1.04 ± 0.26	0.03 ± 0	−2.51	1.37	24.6
	AB	0.85 ± 0.17	0.02 ± 0	−1.93	1.02	16.5
	Bw	0.62 ± 0.18	0.02 ± 0	−0.61	0.75	11.3
	C	0.60 ± 0.15	0.02 ± 0	−1.29	0.73	11.7
	Bedrock 2	0.68 ± 0.11	n.d.	−1.36	0.84	12.4
brown coal/lignite		0.001−0.02	n.d.	n.d.	0.14	1.26
coal pyrite		24.5 ± 10.0	n.d.	−5.54	15.4	b.d.l.
volatile Tl fraction (700 °C)		∼0.25	n.d.	−6.16	n.d.	n.d.
volatile Tl fraction (900 °C)		∼0.98	n.d.	−10.3	n.d.	n.d.
Tl condensate (300−900 °C)		∼19.0	n.d.	−6.19	n.d.	n.d.
fly ash (block A)		2.25 ± 0.27	n.d.	−2.50	3.98	44.4
bottom ash (block A)		1.33 ± 0.28	n.d.	−0.16	2.14	23.2
fly ash (block B)		2.94 ± 0.41	n.d.	−2.82	2.50	94.3
bottom ash (block B)		1.40 ± 0.10	n.d.	0.23	2.61	12.0
wood (*Picea abies* L.)		0.02 ± 0	n.d.	−1.60	2.43	7.13
needles (*Picea abies* L.)		0.04 ± 0	n.d.	−3.66	5.22	4.87

[a]Exchangeable Tl concentrations were determined using a 1 M NH_4NO_3 extraction procedure. n.d.: not determined; b.d.l.: below detection limit (Sc). The uncertainties for total/exchangeable Tl concentrations are reported at the 2 SD level, on the basis of triplicate sample analysis. The ε^{205}Tl data are assigned an error of ±0.7 ε^{205}Tl (2 SD), on the basis of the reproducibility of multiple (6) separate analyses (including sample dissolution, column chemistry, and mass spectrometry) of USGS standard reference material AGV-2 (Table S2).

The NIST SRM 997 was used as ε^{205}Tl = 0 standard throughout. Repeated analyses of the Sigma-Alrich standard solution (for ICP analysis) confirmed very good consistency with reported ε^{205}Tl = −0.81 ± 0.33 (2 SD, n = 133),[34] corresponding to a value of ε^{205}Tl = −0.85 ± 0.38 (2 SD, n = 3). The total procedural Tl blank was <15 pg Tl, corresponding to less than 0.1% of the indigenous element budget (3−25 ng/mL). Thallium isotope analysis, which was carried out for six separate dissolutions of USGS standard reference material AGV-2 of known Tl isotope composition (Table S2), yielded an external reproducibility of ±0.7 ε^{205}Tl (2 SD). This value represents an estimated error for our data set because such an uncertainty accounts for all possible sources of error including sample dissolution, ion exchange chromatography, and mass spectrometric procedures.

RESULTS AND DISCUSSION

Thallium in Reference/Waste Samples. All tested lignite samples were unexpectedly low in Tl (≤0.02 mg/kg), and thus, the Tl isotope composition of local coal could not be accurately determined using the MC-ICP-MS. The overall Tl isotope composition expressed as ε^{205}Tl for the studied samples and Tl-rich coal pyrite (24.5 mg/kg) varied from −10.3 for the model volatile Tl fraction (900 °C) to 0.23 for the bottom ash (Table 2). Regarding the comparison of Tl isotope composition between fly ash and bottom ash, there is evidence of isotopically lighter Tl of the former (Table 2). An analogous observation has been reported by Bigalke et al.[20] for Zn isotopes in fly ash (δ^{66}Zn, −0.41‰) in relation to heavier Zn in slag or solid waste from the Cu metallurgy (0.18‰ and 0.25‰, respectively), implying that kinetic isotope fractionation during Zn evaporation could be a controlling process.

Considering the ε^{205}Tl values for coal pyrite (−5.5) and fly ash (−2.5 and −2.8, blocks A and B, respectively), the Tl isotope signature for the potential primary source is substantially lighter than for the secondary product. Ochoa Gonzalez and Weiss[22] have identified similar behavior for Zn isotopes during coal combustion; the authors suggested that the presence of heavier Zn in fly ash, relative to both coal and vapor phase, results from the preferential adsorption (condensation) of heavier isotopes onto the surface of emitted microparticles. However, the Tl isotope composition for the bulk coal reservoir in the study area is unknown and must be heterogeneous. Therefore, the use of pyrite as a contaminant proxy for the combusted coal is somewhat questionable. On the other hand, sulfides (mainly, FeS_2 and ZnS) are known for their ability to accumulate high Tl concentrations,[2−5] as compared to organic matter. We assume that pyrite, if abundant in feed coal, possibly (temporarily) enhanced an overall trend toward the isotopically lighter fraction for Tl emissions.

In the following text, we will briefly comment on potential pathways of emitted Tl during coal combustion. The model thermo-desorption experiment with sulfide proved substantial (semiquantitative) vaporization of Tl (Tl recovery ∼83%), with an average ε^{205}Tl value of −6.4. This value reflects the ε^{205}Tl data and mass proportionality of the model pyrite evaporates, which were as follows: −6.16/1% Tl−volatile Tl fraction at 700 °C; −10.3/4% Tl−volatile Tl fraction at 900 °C; −6.19/78%

DOI: 10.1021/acs.est.6b01751
Environ. Sci. Technol. 2016, 50, 9864−9871

Tl−Tl condensate at 300−900 °C (Table 2). On this basis, it can be hypothesized that a part of the total/historical Tl emissions was freely mobilized in a volatile form, having very low ε^{205}Tl, i.e., close to that of pyrite. Nevertheless, the exact contribution of volatile Tl fraction(s) in the total process of historical contamination in the area remains unclear. In fact, Tl concentrations and isotope data related to the tested fly ashes and the soil profiles fit better to each other and favor the tendency of Tl to enter particulate emissions, having ε^{205}Tl ≤ −2.5 (see Variations of Tl Isotope Composition in Soils). We assume that, during the coal combustion for the period when high-temperature PF boilers were operated, enhanced Tl vaporization resulted in an intensive Tl release, leading to analogous signatures of Tl present in coal feed and emissions.

On the basis of thermodynamic data available for different Tl species,[35,36] Tl(I) chloride is assumed to be a major component of volatile Tl species (boiling temperature, 806 °C) present in the coal-derived flue gas, respecting the well-known affinity of Tl to Cl^- anion, similar to Pb.[5] The Tl_2O species is possibly more associated with the bottom ash. The formation of Tl(I) species is favored mainly due to the fact that Tl(III) compounds need highly oxidative conditions to arise, and they also have low or limited thermal stability.[37] For example, $TlCl_3$ tends to degrade from its melting point (150−160 °C), leading to the formation of more stable TlCl. Similarly, Tl_2O_3 decomposes in the range of 100−500 °C with Tl_2O as a final product.[38] In our opinion, temperatures of ∼800−1400 °C, typical for the oxidation zone in mechanical or CFB boilers in coal-fired power stations, allow such a simple interpretation.

Distribution of Tl in Soils. A comparable trend in Tl concentrations showing a slight depth dependent decrease was observed in both forest (F) and meadow (M) soil profiles. Although the maximum Tl amount for profile F was present in the subsurface (organo-mineral) horizon A, a moderate Tl input (presumably from an anthropogenic source) into the soils is apparent in both profiles (Table 2, Figure 1). Moreover, Tl values normalized by Zr or Sc (Table 2), representing geogenic elements with extremely low levels for industrial wastes, support this statement. As far as the exchangeable fraction of Tl (NH_4NO_3 extractable) is considered, preferential accumulation of "labile" Tl in the TOC-rich soil layers was recorded (Tables 1 and 2), indicating an unspecified interaction of Tl containing phases with soil organic matter (SOM). The ability of SOM to contribute to Tl release from mineral solids has been already reported[39] and possibly results from the acidic attack of the SOM. Nevertheless, Ettler et al.[40] highlighted that not only H^+-promoted reactions but also the nature of simple organic acids and fulvic or humic substances are critical for enhanced reactivity of anthropogenic dust microparticles (e.g., fly ash), followed by trace element release in the organic soils. For most organic ligands (log K ∼ 0.5−2.0) and fulvic acids (∼3.3−4.8), weak complexation with Tl is predicted;[41] therefore, formation of strong organic complexes with Tl, as well as its intensive adsorption onto the SOM, is not likely.[11] There is only one exception; the −SH functional groups have a potential to bind Tl to some extent, although other cations such as Fe or Al may better compete for these sorption sites.[12] Therefore, we assume that the overall retention capacity of the SOM for Tl is much lower, as compared to its role in trace element mobilization, which tends to prevail.[42] All organic, organo-mineral, and mineral horizons of profiles F and M were logically abundant in Tl of geogenic origin, presumably entrapped in soil silicates (K-feldspar, muscovite, and illite),

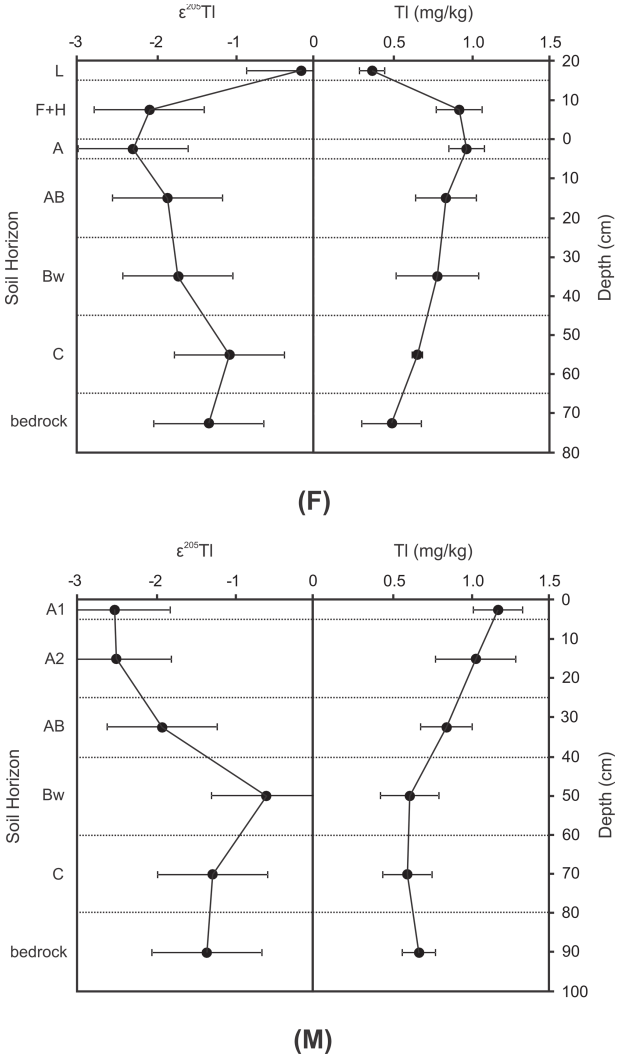

Figure 1. Vertical evolution of Tl isotope composition (ε^{205}Tl) and Tl concentration in forest (F) and meadow (M) soil profiles. The ε^{205}Tl data are assigned an error of ±0.7 ε^{205}Tl (2 SD), on the basis of the reproducibility of multiple (6) separate analyses (including sample dissolution, column chemistry, and mass spectrometry) of USGS standard reference material AGV-2 (Table S2). The concentration values depict means ±2 SD (n = 3).

which were detected by XRD. However, the Tl distribution among these phases is unclear; we only hypothesize that Tl could be more concentrated in secondary illite.[14,42] Crystalline Mn(III,IV) oxides, responsible for efficient Tl retention and/or redox changes of Tl (Tl(III)/Tl(I) couple; Eh ∼ 1.25 V) in soils and sediments,[15,41] were not detected in any of the tested samples. Only a slight enrichment of oxalate-extractable Mn was observed in profile M, i.e., in the soil horizons AB and Bw (Table 1), which might imply the presence of poorly crystalline or amorphous Mn (hydr)oxides. In any case, the vertical shift of Tl through the colloidal (or microparticle) transport, as can be expected again by illite and Mn oxides, cannot be omitted and potentially contributes to the total process of trace element movement in the studied soils.

Variations of Tl Isotope Composition in Soils. There exists only limited information concerning Tl isotopes in soils, even when the pioneering study of Kersten et al.[5] is taken into

DOI: 10.1021/acs.est.6b01751
Environ. Sci. Technol. 2016, 50, 9864−9871

account. We identified a significant difference in Tl isotope compositions (ε^{205}Tl) between upper and lower soil horizons (Table 2, Figure 1), with ε^{205}Tl values generally increasing with profile depth. Except for the L horizon (profile F), the variation of Tl isotope composition typical for organic and organo-mineral layers (ε^{205}Tl ≤ -1.9) clearly reflected isotopically lighter Tl of anthropogenic origin, represented by appropriate reference samples (i.e., fly ash ± volatile Tl fraction(s)), all having ε^{205}Tl below −2.5 (Table 2). Nevertheless, the lighter Tl derived from vegetation also cannot be omitted and probably contributed to some extent to a ε^{205}Tl decrease in topsoils, although this Tl portion (i.e., associated with the primary biomass) is unclear from the long-term point of view. The Tl isotope signatures of mineral horizons (Bw and C) in both profiles agreed with those associated with bedrock samples, corresponding to the ε^{205}Tl value of ∼−1.3 (Table 2).

The shift in ε^{205}Tl toward the isotopically heavier fraction detected in raw litter (horizon L, profile F), up to −0.2, is questionable. This Tl isotope deviation cannot reflect the input of organic matter enriched in heavy Tl, due to both very low contents of Tl (≤0.04 mg/kg) and more negative ε^{205}Tl values (≥−3.7) of appropriate primary biomass (tree needles and wood) (Table 2). Therefore, this isotope deviation seems to be somehow associated with the SOM-controlled processes, despite the fact that the SOM does not exhibit a strong retention capacity for Tl as demonstrated earlier.[11] Regarding an example of Cu isotopes, Bigalke et al.[20,43] suggested that the SOM, composed mainly of humic substances, is likely responsible for heavier Cu adsorption linked with lighter Cu entering the soil solution and migrating downward. Although Tl does not represent a trace element with a special affinity toward organic substances and the role of organic matter in the complex process of Tl dynamics seems to be limited, the equilibrium fractionation of Tl between dissolved and adsorbed Tl species in a highly organic environment (TOC > 30 wt %, CEC > 100 cmol/kg, Table 1) might be a possible explanation for mobilization of Tl with a low ε^{205}Tl value. Therefore, this model could also be suitable for explaining the isotopically heavier Tl remaining in the top section of the forest floor. Such a prediction is favored by the Tl concentration pattern of profile F, which shows Tl accumulation in the subsurface organic layers, as well as its normalization by strictly geogenic elements (Zr, Sc) (Table 2).

An increase in ε^{205}Tl was also detected in the Bw horizon (profile M) (Figure 1). Its origin might be theoretically ascribed to Tl sorption onto secondary soil minerals (e.g., oxides). For example, Nielsen et al.[44] document a systematic increase in Tl isotope composition during Tl sorption onto the Mn(III,IV) oxide, namely, hexagonal birnessite, using model sorption experiments; the magnitude of fractionation (α) accounted for ∼1.0002 to 1.0015. The authors hypothesized that this isotope fractionation comes from the combined effect of the oxidation of Tl(I) to Tl(III), which is then adsorbed over the Mn vacancy sites in the phyllomanganate sheets of birnessite. Nevertheless, it must be highlighted that only oxalate-extractable increases in Mn and Fe, with no apparent change in total Tl content for the investigated soil layer, have been detected (Tables 1 and 2).

Environmental Implications. The mobilization of Tl following coal combustion is well-known; this activity is potentially responsible for more than 1/4 of global anthropogenic Tl inputs worldwide, which are estimated to be ∼0.6 Gg/year.[4] The recent energy concept, especially in Asia and Europe, supports both modernization of existing power stations and installation of new units, of course besides safe nuclear engineering or alternative energy sources. In fact, there is an effort to minimize the amounts of dust microparticles and gaseous emissions released during electricity production, based on a combined approach of installation of efficient coal-fired boilers and improvement of APC technologies. Nevertheless, Tl belongs to the group of highly volatile elements (e.g., Br, Hg, I), which tend to be concentrated in the vapor/gas phase and are often depleted in most solid phases,[45] resulting in reduced or complicated recovery of the APC systems for the trace element. In contrast, relative Tl abundance has been observed by solids in electrostatic precipitators in systems of sulfide roasting reactors, probably due to high Tl concentration in primary ores (>50 mg/kg) and thus also a logically higher Tl portion in most waste (solid) products.[46] As Tl is included in the US EPA list of priority toxic pollutants, brown/hard coals used for electricity production, expected to be rich in Tl-containing sulfides, and also derived wastes should be monitored and alternatively recommended for special treatment.

Unfortunately, we were not able to calculate both Tl mass and Tl isotope mass balances for active CFB boilers in the Turów power plant to estimate Tl emission factors in detail, due to enormous heterogeneity in the Tl distribution in feed coal (controlled by sulfide content) and missing bulk isotope coal data. However, our findings clearly demonstrate a historical input of anthropogenic (high-temperature) Tl into the studied soils, primarily in the organic/organo-mineral horizons, as evidenced by Tl isotope tracing. The complex Tl results presented in Figure 2 show a good (positive) linear relationship

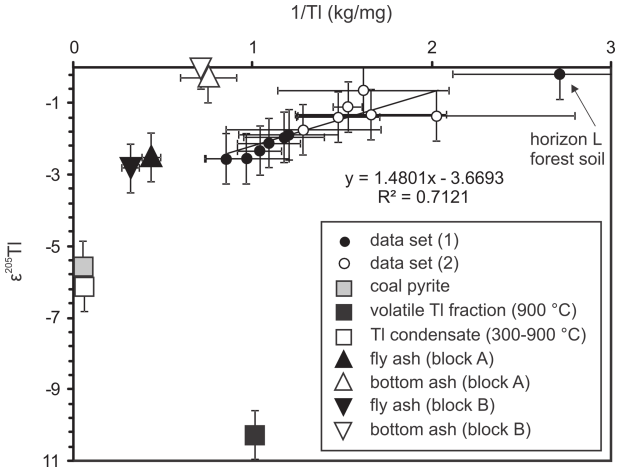

Figure 2. Tl isotope compositions of soils, bedrocks, and waste/model samples expressed as ε^{205}Tl values against 1/Tl concentrations. The data set (1) consists of organic and organo-mineral soil horizons: L, F + H, A, and AB; the data set (2) consists of mineral horizons: Bw, C, and bedrocks of appropriate soil profiles F and M, respectively. The linearity and the R^2 value were calculated from the soil and bedrock data only (except horizon L). The Tl isotope data are assigned an estimated error of ±0.7 ε^{205}Tl (2 SD). Thallium concentrations depict means ±2 SD (n = 3).

(R^2 = 0.71) between 1/Tl and the isotope record, determined for all the tested soils and bedrocks, also indicative of binary Tl mixing between two dominant reservoirs. If we consider that the Tl occurring in the upper soil layers (0−45 cm) is a mixture of anthropogenic Tl with typically low ε^{205}Tl values (≤−2.5) and geogenic Tl having ∼−1, without any postdepositional

DOI: 10.1021/acs.est.6b01751
Environ. Sci. Technol. 2016, 50, 9864−9871

isotope redistribution effects, the calculated coal-derived Tl load corresponds to up to more than half of its total soil content. Surprisingly, Tl isotope compositions detected in our soils reflected the Tl signature of the prevailing pollution source, regarding "only" a moderate level of contamination. One reason could be that the deposition of Tl continues, although the total amount of the contaminant being emitted in the area is unclear.

Considering the presented data set, further isotope research focusing on specific Tl pathways, such as sorption onto different organic and mineral constituents of soils/sediments or its uptake by biota, is needed for a more detailed insight into Tl dynamics in surface environments and remains a challenge for the future.

■ ASSOCIATED CONTENT

Supporting Information

The Supporting Information is available free of charge on the ACS Publications website at DOI: 10.1021/acs.est.6b01751.

Location of the study area and the soil sampling sites; a model setup used for temperature-controlled volatilization of Tl; compilation of measured and reference Tl concentrations and Tl isotope data for standard reference materials (PDF)

■ AUTHOR INFORMATION

Corresponding Author

*Phone: +420 224 382 752; fax: +420 234 381 836; e-mail: vaneka@af.czu.cz.

Notes

The authors declare no competing financial interest.

■ ACKNOWLEDGMENTS

We kindly thank both Julie Prytulak (Imperial College London) and Sune Nielsen (Woods Hole Oceanographic Institution) for offering specific advice on Tl isotope analysis using MC-ICP-MS, as well as data interpretations. The authors would also like to thank Eng. Tomasz Ozimowski, the head of the laboratory of the Turów power plant, for his help with industrial sample collection. The research was funded by the grant of Czech Science Foundation (14-01866S). Part of the equipment used for the study was purchased from the Operational Programme Prague – Competitiveness (Project CZ.2.16/3.1.00/21516).

■ REFERENCES

(1) Rehkämper, M.; Halliday, A. N. The precise measurement of Tl isotopic compositions by MC-ICPMS: Application to the analysis of geological materials and meteorites. *Geochim. Cosmochim. Acta* **1999**, *63* (6), 935–944.

(2) Xiao, T.; Yang, F.; Li, S.; Zheng, B.; Ning, Z. Thallium pollution in China: A geo-environmental perspective. *Sci. Total Environ.* **2012**, *421–422*, 51–58.

(3) Kazantzis, G. Thallium in the environment and health effects. *Environ. Geochem. Health* **2000**, *22* (4), 275–280.

(4) Peter, A. L. J.; Viraraghavan, T. Thallium: a review of public health and environmental concerns. *Environ. Int.* **2005**, *31* (4), 493–501.

(5) Kersten, M.; Xiao, T.; Kreissig, K.; Brett, A.; Coles, B. J.; Rehkämper, M. Tracing anthropogenic thallium in soil using stable isotope compositions. *Environ. Sci. Technol.* **2014**, *48* (16), 9030–9036.

(6) Vaněk, A.; Chrastný, V.; Komárek, M.; Penížek, V.; Teper, L.; Cabala, J.; Drábek, O. Geochemical position of thallium in soils from a smelter-impacted area. *J. Geochem. Explor.* **2013**, *124*, 176–182.

(7) Jakubowska, M.; Pasieczna, A.; Zembrzuski, W.; Swit, Z.; Lukaszewski, Z. Thallium in fractions of soil formed on floodplain terraces. *Chemosphere* **2007**, *66* (4), 611–618.

(8) Karbowska, B.; Zembrzuski, W.; Jakubowska, M.; Wojtkowiak, T.; Pasieczna, A.; Lukaszewski, Z. Translocation and mobility of thallium from zinc–lead ores. *J. Geochem. Explor.* **2014**, *143*, 127–135.

(9) Jović, V. Thallium. In *Encyclopedia of Geochemistry*; Marshall, C. P., Fairbridge, R. W., Eds.; Kluwer Academic Publishers: Dordrecht, Germany, 1998; pp 622–623.

(10) Tremel, A.; Masson, P.; Sterckeman, T.; Baize, D.; Mench, M. Thallium in French agrosystems–I. thallium contents in arable soils. *Environ. Pollut.* **1997**, *95* (3), 293–302.

(11) Jacobson, A. R.; McBride, M. B.; Baveye, P.; Steenhuis, T. S. Environmental factors determining the trace-level sorption of silver and thallium to soils. *Sci. Total Environ.* **2005**, *345* (1–3), 191–205.

(12) Jacobson, A. R.; Klitzke, S.; McBride, M. B.; Baveye, P.; Steenhuis, T. S. The desorption of silver and thallium from soils in the presence of a chelating resin with thiol functional groups. *Water, Air, Soil Pollut.* **2005**, *160* (1–4), 41–54.

(13) Vaněk, A.; Mihaljevič, M.; Galušková, I.; Chrastný, V.; Komárek, M.; Penížek, V.; Zádorová, T.; Drábek, O. Phase-dependent phytoavailability of thallium – A synthetic soil experiment. *J. Hazard. Mater.* **2013**, *250–251*, 265–271.

(14) Vaněk, A.; Komárek, M.; Vokurková, P.; Mihaljevič, M.; Šebek, O.; Panušková, G.; Chrastný, V.; Drábek, O. Effect of Illite and birnessite on thallium retention and bioavailability in contaminated soils. *J. Hazard. Mater.* **2011**, *191* (1–3), 170–176.

(15) Voegelin, A.; Pfenninger, N.; Petrikis, J.; Majzlan, J.; Plötze, M.; Senn, A. C.; Mangold, S.; Steininger, R.; Göttlicher, J. Thallium speciation and extractability in a thallium- and arsenic-rich soil developed from mineralized carbonate rock. *Environ. Sci. Technol.* **2015**, *49* (9), 5390–5398.

(16) Bidoglio, G.; Gibson, P. N.; O'Gorman, M.; Roberts, K. J. X-ray absorption spectroscopy investigation of surface redox transformations of thallium and chromium on colloidal mineral oxides. *Geochim. Cosmochim. Acta* **1993**, *57* (10), 2389–2394.

(17) Rehkämper, M.; Frank, M.; Hein, J. R.; Halliday, A. Cenozoic marine geochemistry of thallium deduced from isotopic studies of ferromanganese crusts and pelagic sediments. *Earth Planet. Sci. Lett.* **2004**, *219* (1–2), 77–91.

(18) Nielsen, S. G.; Rehkämper, M.; Porcelli, D.; Andersson, P.; Halliday, A. N.; Swarzenski, P. W.; Latkoczy, C.; Günther, D. Thallium isotope composition of the upper continental crust and rivers–An investigation of the continental sources of dissolved marine thallium. *Geochim. Cosmochim. Acta* **2005**, *69* (8), 2007–2019.

(19) Nielsen, S. G.; Mar-Gerrison, S.; Gannoun, A.; LaRowe, D.; Klemm, V.; Halliday, A. N.; Burton, K. W.; Hein, J. R. Thallium isotope evidence for a permanent increase in marine organic carbon export in the early Eocene. *Earth Planet. Sci. Lett.* **2009**, *278* (3–4), 297–307.

(20) Bigalke, M.; Weyer, S.; Kobza, J.; Wilcke, W. Stable Cu and Zn isotope ratios as tracers of sources and transport of Cu and Zn in contaminated soil. *Geochim. Cosmochim. Acta* **2010**, *74* (23), 6801–6813.

(21) Mattielli, N.; Petit, J. C. J.; Deboudt, K.; Flament, P.; Perdrix, E.; Taillez, A.; Rimetz-Planchon, J.; Weis, D. Zn isotope study of atmospheric emissions and dry depositions within a 5 km radius of a Pb–Zn refinery. *Atmos. Environ.* **2009**, *43* (6), 1265–1272.

(22) Ochoa Gonzalez, R.; Weiss, D. Zinc isotope variability in three coal-fired power plants: A predictive model for determining isotopic fractionation during combustion. *Environ. Sci. Technol.* **2015**, *49* (20), 12560–12567.

(23) Sun, R.; Sonke, J. E.; Heimbürger, L.-E.; Belkin, H. E.; Liu, G.; Shome, D.; Cukrowska, E.; Liousse, C.; Pokrovsky, O. S.; Streets, D. G. Mercury stable isotope signatures of world coal deposits and

DOI: 10.1021/acs.est.6b01751
Environ. Sci. Technol. 2016, 50, 9864–9871

historical coal combustion emissions. *Environ. Sci. Technol.* **2014**, *48* (13), 7660−7668.
(24) Sun, R.; Heimbürger, L.-E.; Sonke, J. E.; Liu, G.; Amouroux, D.; Berail, S. Mercury stable isotope fractionation in six utility boilers of two large coal-fired power plants. *Chem. Geol.* **2013**, *336*, 103−111.
(25) Suchara, I.; Sucharová, J. Distribution of sulphur and heavy metals in forest floor humus of the Czech Republic. *Water, Air, Soil Pollut.* **2002**, *136* (1), 289−316.
(26) Heim, M.; Wappelhorst, O.; Markert, B. Thallium in terrestrial environments − Occurrence and effects. *Ecotoxicology* **2002**, *11* (5), 369−377.
(27) Bojakowska, I.; Lech, D. Variability of trace elements in the brown coal deposits of Poland. *Biuletyn Państwowego Instytutu Geologicznego* **2012**, *448* (1), 209−214.
(28) *World Reference Base for Soil Resources: A framework for international classification, correlation and communication*; Food and Agriculture Organization of the United Nations (FAO): Rome, Italy, 2006; ftp://ftp.fao.org/agl/agll/docs/wsrr103e.pdf.
(29) *Standard of Soil Quality − Determination of effective cation exchange capacity and base saturation level using barium chloride solution* (ISO 11260:1994); International Organization of Standardization: Geneva; 1994; http://www.iso.org/iso/iso_catalogue/catalogue_tc/catalogue_detail.htm?csnumber=19238.
(30) Pansu, M.; Gautheyrou, J. *Handbook of Soil Analysis: Mineralogical, Organic and Inorganic Methods*; Springer-Verlag: Berlin, Heidelberg, Germany, 2006.
(31) Gee, G. W.; Bauder, J. W. Particle-size analysis. In *Methods of Soil Analysis, Part I: Physical and Mineralogical Methods*; Klute, A., Ed.; American Society of Agronomy-Soil Science Society of America: Madison, WI, 1986; pp 383−412.
(32) *Standard of Soil Quality − Extraction of trace elements from soil using ammonium nitrate solution* (ISO 19730:2008); Beuth Verlag: Berlin, 2009; https://www.beuth.de/de/norm/din-iso-19730/117095524.
(33) Baker, R. G. A.; Rehkämper, M.; Hinkley, T. K.; Nielsen, S. G.; Toutain, J. P. Investigation of thallium fluxes from subaerial volcanism−Implications for the present and past mass balance of thallium in the oceans. *Geochim. Cosmochim. Acta* **2009**, *73* (20), 6340−6359.
(34) Prytulak, J.; Nielsen, S. G.; Plank, T.; Barker, M.; Elliott, T. Assessing the utility of thallium and thallium isotopes for tracing subduction zone inputs to the Mariana arc. *Chem. Geol.* **2013**, *345*, 139−149.
(35) Lide, D. R., Ed. *CRC Handbook of Chemistry and Physics*, 90th, ed.; CRC Press (Taylor and Francis Group): Boca Raton, FL, 2009.
(36) Phillips, S. L., Perry, D. L., Eds. *Handbook of Inorganic Compounds*; CRC Press: Boca Raton, FL, 1995.
(37) Holleman, A. F.; Wiberg, E.; Wiberg, N. *Lehrbuch der Anorganischen Chemie*; Walter de Gruyter & Co.: Berlin, NY, 1995.
(38) Brauer, G. *Handbuch der Präparativen Anorganischen Chemie*; F. Enke Verlag: Stuttgart, Germany, 1954.
(39) Vaněk, A.; Chrastný, V.; Mihaljevič, M.; Drahota, P.; Grygar, T.; Komárek, M. Lithogenic thallium behavior in soils with different land use. *J. Geochem. Explor.* **2009**, *102* (1), 7−12.
(40) Ettler, V.; Vrtišková, R.; Mihaljevič, M.; Šebek, O.; Grygar, T.; Drahota, P. Cadmium, lead and zinc leaching from smelter fly ash in simple organic acids−Simulators of rhizospheric soil solutions. *J. Hazard. Mater.* **2009**, *170* (2−3), 1264−1268.
(41) Kaplan, D. I.; Mattigod, S. V. Aqueous geochemistry of thallium. In *Thallium in the Environment*; Nriagu, J. O., Ed.; John Wiley & Sons, Inc.: New York, 1998; pp 15−29.
(42) Vaněk, A.; Chrastný, V.; Komárek, M.; Galušková, I.; Drahota, P.; Grygar, T.; Tejnecký, V.; Drábek, O. Thallium dynamics in contrasting light sandy soils−Soil vulnerability assessment to anthropogenic contamination. *J. Hazard. Mater.* **2010**, *173* (1−3), 717−723.
(43) Bigalke, M.; Weyer, S.; Wilcke, W. Copper isotope fractionation during complexation with insolubilized humic acid. *Environ. Sci. Technol.* **2010**, *44* (14), 5496−5502.
(44) Nielsen, S. G.; Wasylenki, L. E.; Rehkämper, M.; Peacock, C. L.; Xue, Z.; Moon, E. M. Towards an understanding of thallium isotope fractionation during adsorption to manganese oxides. *Geochim. Cosmochim. Acta* **2013**, *117*, 252−265.
(45) López Antón, M. A.; Spears, D. A.; Díaz Somoano, M.; Martínez Tarazona, M. R. Thallium in coal: Analysis and environmental implications. *Fuel* **2013**, *105*, 13−18.
(46) Liu, J.; Wang, J.; Chen, Y.; Xie, X.; Qi, J.; Lippold, H.; Luo, D.; Wang, C.; Su, L.; He, L.; Wu, Q. Thallium transformation and partitioning during Pb−Zn smelting and environmental implications. *Environ. Pollut.* **2016**, *212*, 77−89.

DOI: 10.1021/acs.est.6b01751
Environ. Sci. Technol. 2016, 50, 9864−9871

- PŘÍLOHA V. - Izotopová signatura Tl v metalurgických odpadech

Vaněk, A., Grösslová, Z., Mihaljevič, M., Ettler, V., Trubač, J., Chrastný, V., Penížek, V., Teper, L., Cabala, J., Voegelin, A., Zádorová, T., Oborná, V., Drábek, O., Holubík, O., Houška, J., Pavlů, L., Ash, C., 2018. Thallium isotopes in metallurgical wastes/contaminated soils: A novel tool to trace metal source and behavior. Journal of Hazardous Materials. 343, 78–85. https://doi.org/10.1016/j.jhazmat.2017.09.020

Journal of Hazardous Materials 343 (2018) 78–85

Contents lists available at ScienceDirect

Journal of Hazardous Materials

journal homepage: www.elsevier.com/locate/jhazmat

Thallium isotopes in metallurgical wastes/contaminated soils: A novel tool to trace metal source and behavior

Aleš Vaněk[a,*], Zuzana Grösslová[a], Martin Mihaljevič[b], Vojtěch Ettler[b], Jakub Trubač[b], Vladislav Chrastný[c], Vít Penížek[a], Leslaw Teper[d], Jerzy Cabala[d], Andreas Voegelin[e], Tereza Zádorová[a], Vendula Oborná[a], Ondřej Drábek[a], Ondřej Holubík[a], Jakub Houška[a], Lenka Pavlů[a], Christopher Ash[a]

[a] Department of Soil Science and Soil Protection, Faculty of Agrobiology, Food and Natural Resources, Czech University of Life Sciences Prague, Kamýcká 129, 165 21 Praha 6, Czech Republic
[b] Institute of Geochemistry, Mineralogy and Mineral Resources, Faculty of Science, Charles University, Albertov 6, 128 43 Praha 2, Czech Republic
[c] Department of Environmental Geosciences, Faculty of Environmental Sciences, Czech University of Life Sciences Prague, Kamýcká 129, 165 21 Praha 6, Czech Republic
[d] Department of Applied Geology, Faculty of Earth Sciences, University of Silesia, Bedzinska 60, 41-200 Sosnowiec, Poland
[e] Eawag, Swiss Federal Institute of Aquatic Science and Technology, Ueberlandstrasse 133, CH-8600 Duebendorf, Switzerland

HIGHLIGHTS

- Thallium isotopes in industrial wastes from zinc metallurgy.
- Thallium contamination in soils can be traced using isotopes.
- Thallium isotope fractionation may occur in soil.
- Sorption and/or precipitation processes are responsible for isotope redistribution.

GRAPHICAL ABSTRACT

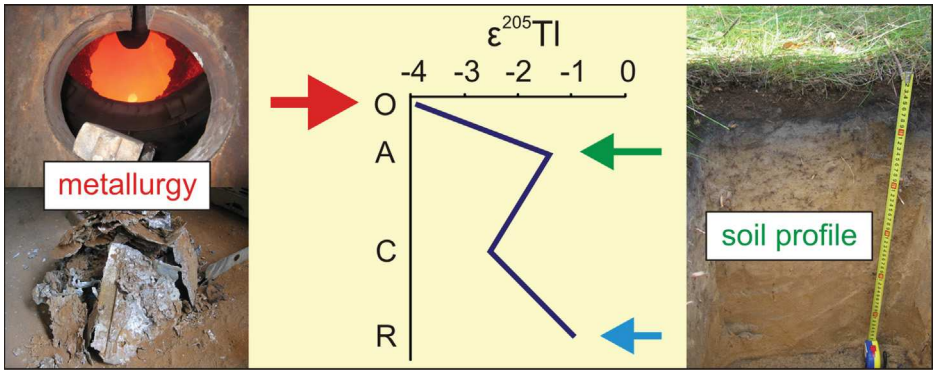

ARTICLE INFO

Article history:
Received 24 May 2017
Received in revised form 22 August 2017
Accepted 12 September 2017
Available online 12 September 2017

Keywords:
Thallium
Waste
Soil
Isotopes
Fractionation

ABSTRACT

Thallium (Tl) concentration and isotope data have been recorded for contaminated soils and a set of industrial wastes that were produced within different stages of Zn ore mining and metallurgical processing of Zn-rich materials. Despite large differences in Tl levels of the waste materials (1–500 mg kg^{-1}), generally small changes in ε^{205}Tl values have been observed. However, isotopically lighter Tl was recorded in fly ash (ε^{205}Tl ~ −4.1) than in slag (ε^{205}Tl ~ −3.3), implying partial isotope fractionation during material processing. Thallium isotope compositions in the studied soils reflected the Tl contamination (ε^{205}Tl ~ −3.8), despite the fact that the major pollution period ended more than 30 years ago. Therefore, we assume that former industrial Tl inputs into soils, if significant, can potentially be traced using the isotope tracing method. We also suggest that the isotope redistributions occurred in some soil (subsurface) horizons, with Tl being isotopically heavier than the pollution source, due to specific sorption and/or precipitation processes, which complicates the discrimination of

* Corresponding author.
E-mail address: vaneka@af.czu.cz (A. Vaněk).

http://dx.doi.org/10.1016/j.jhazmat.2017.09.020

primary Tl. Thallium isotope analysis proved to be a promising tool to aid our understanding of Tl behavior within the smelting process, as well as its post-depositional dynamics in the environmental systems (soils).

1. Introduction

Anthropogenic sources of thallium (Tl) include emissions and solid wastes from ferrous/non-ferrous mining and metallurgy, coal combustion, or possibly cement production. Complex processing of Tl-bearing ores/sulfides (FeS_2, ZnS etc.) probably dominates in areas where extreme pollution levels of this element have been recorded [1–7]. Since most Tl compounds are volatile at high temperatures, its removal from the metallurgical emissions using bag and/or electrostatic filters may be difficult. Hence, a large Tl portion could potentially enter the atmosphere and affect surrounding environmental compartments [2,4]. It should be highlighted that apart from the chalcophile nature of Tl(I), monovalent Tl(I) can also substitute K in K-silicates (feldspars, micas, etc.) [8,9]. Efficient sorbents for Tl in soils and sediments include Mn(III,IV) oxides (mainly birnessite, δ-MnO_2) and illite [10–14], which may bind Tl through specific adsorption resulting from Tl(I)–K replacement reactions within the mineral (inter)layers. Manganese oxides may also bind Tl via Tl(I) oxidation to Tl(III) and complexation of the Tl(III) [14].

Despite the achievements in Tl isotope geochemistry during the last decade, little is still known about the processes that influence the isotope fractionation of Tl of anthropogenic origin. The pioneering works of Kersten et al. [15] and Vaněk et al. [16] demonstrate differences in the stable isotope signature between Tl of geogenic and industrial origin. However, to date there are no data available on the isotope signatures of Tl in waste materials and emissions from non-ferrous metal smelters and in surrounding contaminated soils. For example, we do not know to what extent Tl may isotopically fractionate from the primary material to different waste materials during this kind of high-temperature industrial process. Moreover, it is unknown to what extent chemical processes in soils contaminated by smelter emissions affect the Tl isotope composition. Here, we report for the first time, the Tl isotope record in soils heavily contaminated by Zn metallurgy and we attempt to describe the isotope shift from the start to the end of the Tl "life cycle". The presented Tl isotope results can contribute to a better understanding of anthropogenic Tl inputs into soils and the processes that affect all Tl mobility, enrichment and cycling in the environment.

2. Experimental

2.1. Study area, sampling and characterization process

The Olkusz district, situated in the Silesia-Krakow region of southern Poland, is known for extensive mining and processing of Zn ores/sulfides since the early 1950s. The ores are enriched in Tl, and particulate and gaseous emissions from the local primary/secondary Zn smelter (Boleslaw Zn smelter) are considered the predominant source of Tl contamination in the area (Supplementary material, Fig. S1). The smelter has been operational for more than 60 years (opened 1952) and the deposition of pollutants has led to significant inputs of Zn, Pb, Cd and Tl. Average concentrations reported for the forest floor humus or the upper soil layers near the smelter typically exceed 5000 mg kg^{-1} for Zn and 50 mg kg^{-1} for Tl or Cd [17]. Despite the fact that detailed data on Tl emissions/deposition are not available, a comparable trend with historical dust/metal emissions (mainly Zn and Cd) is suggested [18]. Regarding the smelter technology, pyrolytic processes followed by electrolytic Zn extraction are combined throughout the whole history of the plant. All Zn ores, Zn-Fe residues and other Zn-rich materials have been used as raw/feed materials here. After enhancement of the electrolytic section in 1962, the importance of roasted sulfide concentrates originating from local ores was continuously growing in the feed. Apart from the secondary materials, Zn ores from up to six European localities (including the local one) have been used for calcine (ZnO) production since 2012.

For tracing Tl sources in soils, both natural and industrial (including waste) samples from the recycling division of the Zn smelter (Boleslaw Recycling, Ltd.) were investigated:

(i) Local Zn ore (sphalerite, ZnS; Pomorzany mine, mineralogical collection of the University of Silesia).
(ii) Post-flotation Zn-Fe residue.
(iii) Fly ash, collected from the de-dusting system placed on a technological line within the Waelz furnaces (Supplementary material, Fig. S2). In these furnaces, different Zn-bearing waste materials are processed, including Zn-Fe residues from steelmaking, Zn-C batteries, residual slimes from Zn hydrometallurgy, etc.
(iv) Slag from the Waelz furnaces, which occurs as solid agglomerates, containing ash from coke combustion, Fe oxides, etc. (Supplementary material, Fig. S2).
(v) Granulated waste resulting from different stages of hydrometallurgical processing of Zn, containing unwanted components in the electrolytic process, but still incorporating Zn and accompanying metals/metalloids. This material is combined with Zn-Fe residues, granulated and introduced into the smelting furnace as a secondary batch feed.
(vi) Final refinement waste, coming from the wet filtration of $ZnSO_4$ electrolyte in the hydrometallurgical process. This material was collected from Larox filter which is used for the solution purification prior to Zn electrolysis (Supplementary material, Fig. S2). The material typically contains a variety of sulphates (Zn, Pb, Fe, As, etc.) and similarly to granulated waste (sample v), it is recycled within the pyrometallurgical stage.

Historical wastes from the Zn smelter were not available; therefore, we were not able to test these materials for their Tl isotope composition. Similarly, we do not know the exact Tl isotope signature for the initial feed material, which is processed in the recycling plant using the Waelz technology. The problem is that its composition depends on the type of furnace charge, which is heterogeneous and variable, consisting of a variety of Zn- and Zn-Fe-rich materials with different starting Tl concentrations and probably different isotope signatures.

To investigate the fate of Tl in the environment, three profiles of forest and meadow soils (1—forest, 2—meadow and 3—forest) were sampled approximately 1 km S and N of the Zn smelter (Supplementary material, Fig. S1; GPS coordinates in Table 1). Soil samples were collected from 1 × 1 m wide pits according to the natural development of soil horizons, down to the bottom horizon C. Soils were classified as a Haplic Regosol Arenic, a Rendzic Leptosol and an Eutric Arenosol [19]. Soil samples were air-dried, homogenized and sieved through a 2-mm stainless-steel sieve prior to further

Table 1
Physico-chemical characteristics of the studied soils.

Soil profile/ GPS position	Soil type (Land use)	Horizon	Depth (cm)	Clay content (%)	pH KCl	pH H_2O	CEC (cmol kg^{-1})[a]	TOC (%)[a]	S_{tot} (%)[a]	Fe_{ox} (g kg^{-1})[a]	Mn_{ox}	Al_{ox}
1/N50°16.314′ E19°28.379′	Haplic Regosol Arenic (forest)	O	5–0	n.d.	6.1	6.5	31.7	26.3	0.6	2.8	0.8	1.3
		Ap	0–25	3.5	7.2	7.5	23.3	2.3	0.04	1.5	1.8	1.1
		C	25–60	5.1	7.4	7.7	13.9	1.3	0.02	1.4	1.0	0.7
2/N50°17.063′ E19°28.386′	Rendzic Leptosol (meadow)	Ah	0–25	6.0	7.1	7.5	43.2	2.6	0.06	1.7	1.2	1.2
		Cr	25–60	15.9	7.4	7.9	40.7	0.2	<0.01	0.7	0.8	0.7
3/N50°16.910′ E19°29.109′	Eutric Arenosol (forest)	O	2–0	n.d.	6.9	7.0	38.2	21.4	3.1	11.3	1.0	2.0
		Ai	0–4	7.1	7.3	7.6	27.3	2.3	0.3	4.8	0.8	1.4
		C1	4–10	3.6	7.1	7.5	21.5	0.2	<0.01	0.2	0.2	0.3
		C2	10–40	2.8	7.4	7.7	25.9	0.6	<0.01	0.8	0.7	0.8

Fe_{ox}, Mn_{ox}, Al_{ox}: oxalate-extractable Fe, Mn and Al concentrations.
Total inorganic carbon (TIC) detected in the horizon Cr (Profile 2) reached 4.3 wt.%.
n.d.: not determined.
[a] The data are means (n = 3) with RSD ≤ 10%.

Table 2
Total and mobilizable Tl concentrations, Tl isotope compositions (expressed as ε^{205}Tl), and Tl/Zr and Tl/La ratios in the studied soils, bedrocks, and reference/industrial samples, i.e., local Zn ore (ZO), post-flotation Zn-Fe residue (PFR), fly ash (FA), slag (S), granulated waste (GW), final refinement waste (FRW).

Soil profile/Sample (Land use)	Horizon	Total Tl (mg kg^{-1})	Mobilizable Tl (mg kg^{-1})	ε^{205}Tl ± 0.7	Tl/Zr (×10)	Tl/La
1 (forest)	O	11.6 ± 2.3	2.42 ± 0.06	−3.92	1.98	2.53
	Ap	5.84 ± 0.97	0.41 ± 0	−1.45	0.62	0.87
	C	4.91 ± 1.21	0.40 ± 0.06	−2.53	0.64	0.62
	bedrock	1.80 ± 0.46	n.d.	−0.98	0.55	0.58
2 (meadow)	Ah	5.85 ± 0.93	0.89 ± 0.18	−2.69	1.64	7.04
	Cr	4.08 ± 0.42	0.16 ± 0.05	−2.71	0.65	0.57
	bedrock	2.36 ± 0.79	n.d.	−1.88	0.81	1.69
3 (forest)	O	30.1 ± 1.4	5.65 ± 0.52	−3.21	5.23	5.93
	Ai	18.8 ± 0.9	3.06 ± 0.02	−3.04	3.94	2.75
	C1	5.27 ± 0.34	0.48 ± 0.04	−0.63	1.23	0.77
	C2	3.50 ± 0.05	1.24 ± 0.06	0.41	1.60	1.08
ZO		9.95 ± 0.90	n.d.	−3.76	197	132
PFR		27.6 ± 3.0	n.d.	−3.89	154	13.2
FA		15.0 ± 0.5	n.d.	−4.09	135	148
S		1.19 ± 0.30	n.d.	−3.31	n.d.	n.d.
GW		322 ± 55	n.d.	−3.60	5690	19900
FRW		568 ± 72	n.d.	−4.77	1510	7520

Mobilizable Tl concentration was determined using a 0.05 M EDTA extraction procedure.
n.d.: not determined.
The uncertainties for total/mobilizable Tl concentrations are reported at the 2 SD level (n = 3).
The ε^{205}Tl results are assigned an error of ±0.7 ε^{205}Tl (2 SD), which is based on a long term reproducibility of multiple separate analyses (involving sample dissolution, column chemistry and mass spectrometry) of USGS standard reference material AGV-2 (Supplementary material, Table S3).

use or analyses. Data on the physico-chemical properties of the soils are summarized in Table 1. Soil pH was measured in a 1:5 (v/v) ratio of soil and water or 1 M KCl solution using a Handylab pH 11 multimeter (Schott, Germany). The amounts of total organic carbon (TOC), and sulfur (S_{tot}) were determined by catalytic oxidation (1350 °C) using a combination of Metalyt CS 500 and Metalyt CS 530 (ELTRA, Germany) elemental analysers. The cation exchange capacity (CEC) was computed after saturation of the soil sample with 0.1 M $BaCl_2$ followed by Ba^{2+} release using $MgSO_4$ [20]. Acid oxalate extraction (0.2 M ammonium oxalate/oxalic acid at pH 3), used to indicate the presence of amorphous/poorly crystalline Fe, Mn, and Al (hydr)oxides, was performed according to Pansu and Gautheyrou [21]. The mobilizable fraction of Tl in soil samples was determined by means of a single (1 h) extraction at a solid-to-liquid ratio of 1:10 using 0.05 M EDTA [22]. Clay content was estimated by the hydrometer (sedimentary) method. The bulk mineralogy of the soils was dominated by quartz (SiO_2), feldspars ($K/NaAlSi_3O_8$), calcite ($CaCO_3$), dolomite ($CaMg(CO_3)_2$), illite ($(K,H_3O)Al_2(Si,Al)_4O_{10}(OH)_2$), clinochlore ($(Mg,Al)_6(Si,Al)_4O_{10}(OH)_8$) and kaolinite ($Al_2Si_2O_5(OH)_4$), as determined using X-ray diffraction analysis (XRD) within our previous study [23]. Metalliferous phases were represented mainly by traces of goethite (α-FeOOH), sphalerite and galena (PbS), smithsonite ($ZnCO_3$) and cerusite ($PbCO_3$) [23]. XRD analysis was performed using an X'Pert Pro diffractometer (PANalytical, the Netherlands) under the following conditions: CuKα radiation, 40 kV, 30 mA, step scanning at 0.02°/150 s in the range 3–80° 2θ. X-ray absorption near-edge structure (XANES) spectroscopy (SuperXAS beamline, the Swiss Light Source – SLS, Villigen, Switzerland) was applied on the sample of granulated waste to identify Tl speciation within the waste sample matrix (Supplementary material, Fig. S3).

Prior to determining total metal concentrations and Tl isotopes, soils, bedrocks, and reference/waste samples were carefully homogenized, and then finely ground in an agate mill (Pulverisette 0, Fritsch, Germany). Subsequently, a mass of 0.2–0.5 g of each sample was totally decomposed using a hot acid mixture. Concentrated HNO_3 and HF acids (Merck Ultrapure, Germany) mixed in the ratio of 2:1 were added to the sample in a total volume of 20–30 mL, then left in a closed 60-mL PTFE beaker (Savillex, USA) on a hot plate (150 °C) for 48 h. If any organic residue persisted, 2–4 mL of H_2O_2

was added and left overnight at room temperature. The standard reference material, NIST 2711 (Montana Soil) (National Institute of Standards and Technology, USA) was used for QC of quantitative analyses (Supplementary material, Table S1).

2.2. Sample purification

In order to isolate Tl from the sample matrix (i.e., dissolved sample), a three-stage chromatographic separation with an anion exchange resin (Bio-Rad AG1-X8, 200–400 mesh, Cl^- cycle) was performed according to the modified procedure of Baker et al. [24] The sample was evaporated to complete dryness and then re-dissolved in 0.1 M HCl. Subsequently, Br_2 was added so that the reagent had a final concentration of 1% (v/v) in the sample solution (0.1 M HCl). The solution was then left overnight (>12 h) to ensure that all Tl(I) was oxidized to Tl(III). For Tl separation, a sample aliquot was taken so that generally 100–500 ng of total Tl is present. The first stage of chromatography utilized a glass 8-mL Econo-column (Bio-Rad, USA) filled with 2 mL of resin, followed by steps with reagent mixtures and volumes as follows: (i) 5 × 1 mL 0.1 M HCl-SO_2 + 5 × 1 mL 0.1 M HCl, resin cleaning; (ii) 5 × 1.5 mL 0.1 M HCl-1% Br_2, resin treatment; (iii) sample loading (0.1 M HCl-1% Br_2); (iv) 10 × 2 mL 0.01 M HCl-1% Br_2; (v) 6 × 2 mL 0.03 M HBr-0.5 M HNO_3-1% Br_2; (vi) 6 × 2 mL 0.03 M HBr-2M HNO_3-1% Br_2; (vii) 6 × 2 mL 0.1 M HCl-1% Br_2; (viii) 13 × 2 mL 0.1 M HCl-SO_2, Tl/Pb fraction elution. The obtained Tl/Pb fraction was evaporated and redissolved in 200 μL 0.1 M HCl-1% Br_2 (> 12 h), in preparation for the next part of Tl purification. For the second and third chromatographic stage, a PP 1.2-mL micro-column filled with 250 μL of resin was used. Resin cleaning and treatment, as well as sample loading were performed in the same way, with corresponding lower volumes of individual reagent mixtures. Once the final Tl fraction was obtained, the Tl sample was evaporated and diluted in 5 mL 2% HNO_3. Thallium and Pb concentrations were monitored after sample dissolution and Tl separation. Chemicals of ultrapure and suprapure quality (Merck, Germany), and deionized water (MilliQ+, Millipore, USA) were used for separation techniques.

2.3. Analytical measurements

Concentrations of major and trace elements (Al, Fe, Mn, Tl, Zn, Pb, Cd) in the total digests of soils, rocks, and industrial (waste) samples (Supplementary material, Table S2), as well as in various soil extracts were determined in triplicate using either inductively coupled plasma optical emission spectrometry (ICP-OES, iCAP 6500, Thermo Scientific, UK) or quadrupole based inductively coupled plasma mass spectrometry (Q-ICP-MS, Xseries II, Thermo Scientific, Germany) under standard analytical conditions.

Thallium isotope analyses were carried out using MC-ICP-MS (Neptune Plus, Thermo Scientific, Germany) with desolvating nebulizer (Aridus II, CETAC, Thermo Scientific, Germany) at the Laboratories of Mass Spectrometry of the Faculty of Science, Charles University, under the following analytical conditions: The detector configuration was: ^{202}Hg–L3, ^{203}Tl–L2, ^{204}Pb–L1, ^{205}Tl–C, ^{206}Pb–H1, ^{207}Pb–H2, ^{208}Pb–H3. All solutions were measured in 3 runs of 50 cycles. Mass bias drift was eliminated using external normalization and standard sample bracketing (NIST SRM 997). Solutions with Tl concentration were doped with NIST SRM 981 to obtain Pb/Tl 2–3. For inter-element correction, the ratio ^{208}Pb/^{206}Pb was related to the raw ^{205}Tl/^{203}Tl data by the exponential mass dependent fractionation law. The NIST SRM 997 was measured directly before and after each sample, and final data were interpolated between bracketing standards. Thallium isotope composition was reported with an ε notation relative to the NIST SRM 997 (Eq. (1)).

$$\varepsilon^{205}Tl = \frac{^{205}Tl/^{203}Tl_{sample} - {}^{205}Tl/^{203}Tl_{NIST997}}{^{205}Tl/^{203}Tl_{NIST997}} \times 10^4 \quad (1)$$

The NIST SRM 997 was used as ε^{205}Tl = 0 standard throughout. Repeated analyses of the Sigma-Alrich standard solution (for ICP analysis) confirmed very good consistency with reported ε^{205}Tl = −0.81 ± 0.33 (2 SD, n = 133) [25], corresponding to a value of ε^{205}Tl = −0.88 ± 0.40 (2 SD, n = 3). The total procedural Tl blank was <15 pg Tl, corresponding to less than 0.1% of the indigenous element budget (3–25 ng mL^{-1}). An external reproducibility of Tl isotope analyses carried out in our laboratories yielded a value of ± 0.7 ε^{205}Tl (2 SD), and is based on 8 separate dissolutions (2 for this study) of USGS standard reference material AGV-2 of known Tl isotope composition (Supplementary material, Table S3). This value represents an estimated error for the presented dataset because such an uncertainty accounts for all possible sources of error including sample dissolution, ion exchange chromatography and mass spectrometric procedures.

3. Results and discussion

3.1. Thallium in industrial samples

We identified a large difference in Tl concentrations in industrial samples, with a maximum for final refinement and granulated wastes (568 and 322 mg kg^{-1}) and minimum for the slag (1.19 mg kg^{-1}). Comparison of the Tl concentrations in the fly ash (15.0 mg kg^{-1}) and the slag indicates that the latter is highly depleted of this trace element (Table 2). As Tl is supposed to readily enter the smelter emissions due to its volatile nature [2,4], we predict preferential concentration of Tl in the vapor/gas phase followed by its (rapid) condensation onto the surface of solid microparticles [26]. The overall Tl isotope composition, expressed as ε^{205}Tl in the studied materials, varied from −4.8 to −3.3 (Table 2). The detected isotope signatures for both Zn ore and post-flotation Zn-Fe residue were very close with an average ε^{205}Tl of ∼−3.8. Given the fact that processing of local ores has been linked with extreme emissions from the 1950s to the 1970s [18], this value can be considered as the reference isotope composition of historical Tl contamination in the area. The ε^{205}Tl values for fly ash (−4.1) and slag (−3.3), point to isotopically lighter Tl in the fly ash, but it should be noted that the difference was not statistically significant (i.e., using 2σ error) (Table 2). On the other hand, an analogous observation has been reported by Bigalke et al. [27] for Zn isotopes in fly ash (δ^{66}Zn, −0.41‰) in relation to heavier Zn in slag or solid waste from copper metallurgy (0.18‰ and 0.25‰, respectively), implying that kinetic isotope fractionation during Zn evaporation could be a controlling process. Likewise, this isotope pattern was documented for Tl in wastes from a coal-fired power plant within our previous study [16], where the lighter Tl fraction was present in fly ash, contrary to the heavier Tl in bottom ash. However, there was a significant difference in ε^{205}Tl (up to 3 units) between these two materials, compared to the present metallurgical samples with apparently less isotope variability. At this point, it should be noted that substantial Tl evaporation from the Tl-rich pyrite, subjected to the controlled high-temperature (oxidizing) conditions, was observed within that work [16]. This model experiment favors the tendency of Tl to readily enter the smelter emissions, i.e., during ore or other Zn-bearing material roasting.

The lowest ε^{205}Tl value was found for final refinement waste (−4.77, Table 2) and might be related to Tl co-precipitation with the newly-formed (secondary) precipitates (e.g., $ZnSO_4$(s), $FeSO_4$, $KFe_3(SO_4)_2(OH)_6$) abundant in the Zn electrolyte slurry reported for

the Boleslaw plant [28]. Light Tl isotopes, which usually react faster, possibly become concentrated in these phases. Similar behavior has been reported for Hg in a study by Smith et al. [29], who identified lighter Hg isotopes enriched in all sulfide and Hg(II) oxide precipitates relative to the dissolved Hg. The authors stated that light Hg in the solid phases reflects both kinetic and equilibrium isotope effects, and they emphasized the importance of Hg solution speciation in the process [29]. We do not expect any redox (oxidation) reactions for Tl throughout the Zn refining stage, which in that case would be probably the major control of the Tl isotope shift toward the heavy fraction. Moreover, the presence of Tl(III) species is not probable, given the need for highly oxidative conditions. As far as the pyrolytic process is concerned, the formation of Tl(I) phases is also favored, due to limited thermal stability of Tl(III) compounds [30]. For example, $TlCl_3$ tends to degrade from its melting point (150–160 °C), leading to the formation of more stable TlCl. Similarly, Tl_2O_3 decomposes in the range of 100–500 °C with Tl_2O as a final product [31]. On the basis of thermodynamic data available for different Tl species [32,33], Tl(I) chloride is assumed to be a major component of volatile Tl species (boiling temperature, 806 °C) present in the smelter-derived flue gas, respecting the well-known affinity of Tl to Cl^- anion, similar to Pb [15]. It should be noted that the operation temperature for the Waelz process reaches ~1100 °C. For the granulated waste, characterization of Tl by Tl L_{III}-edge X-ray absorption near-edge structure (XANES) spectroscopy confirmed the predominance of Tl(I) (Supplementary material, Fig. S3). Comparison of the spectrum with reference spectra further allowed to exclude substantial formation of Tl(I)-jarosite, which can form in ore processing wastes [34]. The sample spectrum closely matched the spectrum of lorandite ($TlAsS_2$), suggesting that Tl(I) may be associated with sulfide phases. On the other hand, the low signal quality and the lack of reference spectra for other potential host phases, namely TlCl or Tl_2O, did not allow to further specify the speciation of Tl based on the XANES results. Since granulated waste represents a complex mixture of different materials from pyro- and hydrometallurgy, its signature with $\varepsilon^{205}Tl = -3.6$ (Table 2) mimics the average isotope composition of Tl derived by the total process of secondary Zn smelting at the time of sampling (2011). Unfortunately, as mentioned above, due to the heterogeneity in Tl distribution (or nature) in the feed material and in materials produced by hydrometallurgical separations, we were not able to calculate both Tl mass and Tl isotope mass balances for the studied smelter.

3.2. Distribution and mobility of Tl in soils

A comparable trend in Tl concentrations showing a depth dependent decrease was observed in all studied soil profiles (Fig. 1), indicating Tl migration through the soils. The anthropogenic input of Tl into the soils is consistent with the Tl values normalized by Zr and La (Table 2), representing geogenic elements with typically very low levels for industrial wastes. High Tl concentrations were detected in surface (organic) horizons O of forest soils, with a maximum for the profile 3 (~30 mg kg^{-1}) (Table 2). An important role of the forest floor layer in the retention of Tl (presumably in the form of smelter-derived particulates) is thus apparent. The mobilizable fraction of Tl (EDTA extractable), corresponding to up to 20% of total Tl content, also indicated preferential accumulation of "labile" Tl in these TOC-rich layers (Tables 1 and 2). This finding confirms an interaction of Tl containing phases with soil organic matter (SOM) and suggests that Tl can be potentially released and enter the underlying mineral layers. The ability of the SOM to contribute to Tl release from mineral solids has already been reported [35] and possibly results from the acidic attack of the SOM. Nevertheless, Ettler et al. [36] highlighted that not only H^+-promoted reactions but also the nature of simple organic acids and fulvic or humic substances are responsible for enhanced reactivity of anthropogenic dusts, including fly ash, followed by trace element release in organic soils. Considering the available data on Tl binding to SOM [11,12], formation of organic complexes with Tl and/or its strong specific adsorption onto the SOM cannot be expected. Therefore, we assume that the capacity of the SOM to stabilize Tl is much lower, as com-

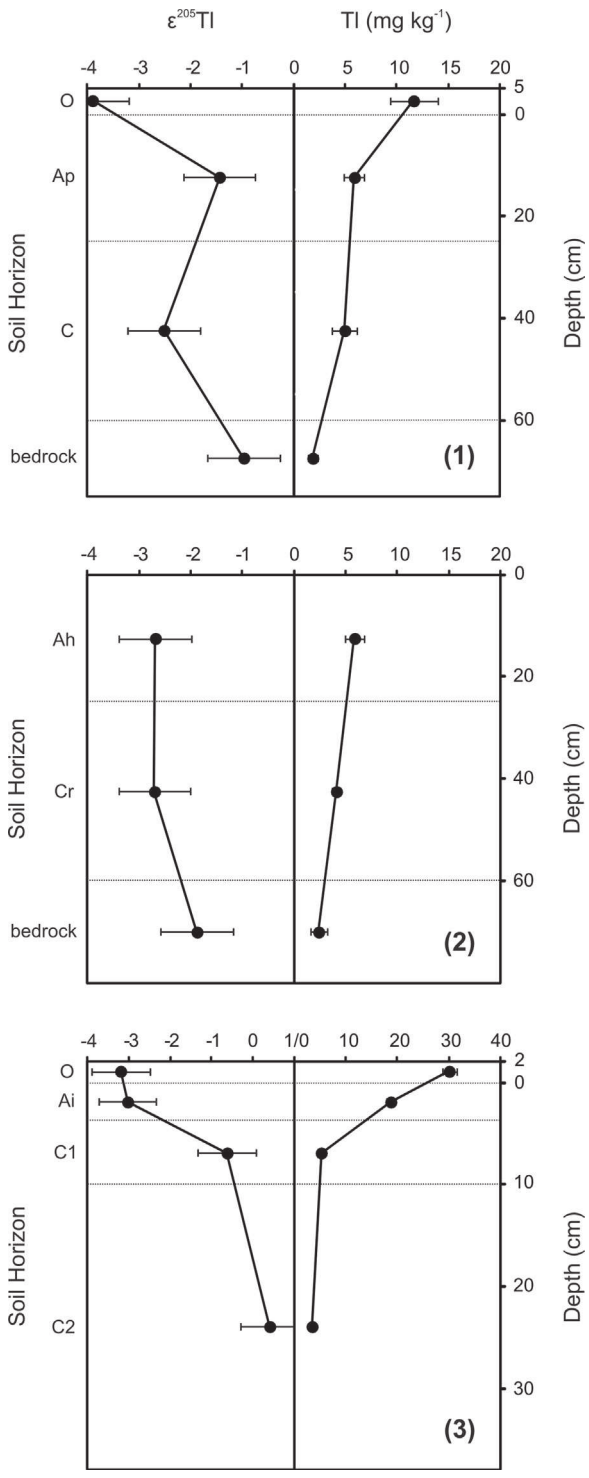

Fig. 1. Vertical evolution of Tl isotope composition ($\varepsilon^{205}Tl$) and Tl concentration in the studied soil profiles – 1 (forest), 2 (meadow) and 3 (forest). The $\varepsilon^{205}Tl$ results are assigned an error of ±0.7 $\varepsilon^{205}Tl$ (2 SD), which is based on a long term reproducibility of multiple separate analyses (including sample dissolution, column chemistry and mass spectrometry) of USGS standard reference material AGV-2 (Supplementary material, Table S3). The concentration values depict means ± 2 SD (n = 3).

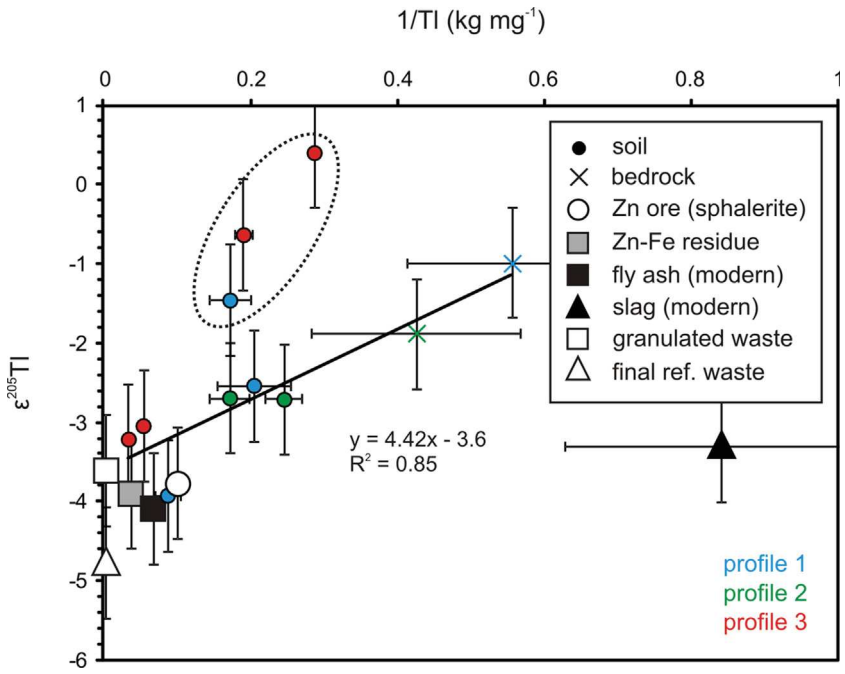

Fig. 2. The Tl isotope composition of soils, bedrocks and reference/industrial samples, expressed as ε^{205}Tl value against 1/Tl concentration. The Tl isotope data are assigned an estimated error of ±0.7 ε^{205}Tl (2 SD). Thallium concentrations depict means ± 2 SD (n = 3). The dotted oval shows the soil samples (Ap, C1 and C2) in which Tl is fractionated, being isotopically heavier than the prevailing (contamination) source probably due to soil sorption processes. The linearity and the R^2 value were calculated from the soil and bedrock data only, i.e., except for the Ap, C1 and C2 horizons.

pared to its role in the Tl mobilization, which tends to prevail [35,37]. Although we were not able to distinguish between both the nature and origin (i.e., anthropogenic vs. natural) of mineral phases containing Tl, we hypothesize that Tl could be concentrated in specific sulfides, silicates (mainly illite) and/or secondary oxides (potentially of Mn), which have been detected by XRD in tested soils [23] and exhibit documented affinities for Tl [4–8,12–14]. The transport of Tl in soils in colloidal and/or microparticulate form, i.e., associated with these phases, must therefore be considered. On the other hand, in the case of organic and subsurface horizons of forest soils, representing "highly reactive" soil layers, simple migration of dissolved Tl seems to be more probable.

3.3. Thallium isotopes in soils

All studied soil profiles exhibited variations in the Tl isotope signature between the upper and lower soil horizons (or bedrocks), with ε^{205}Tl values generally increasing with depth (Fig. 1, Table 2). The Tl isotope composition of the surface (organic or organo-mineral) layers clearly reflected isotopically lighter Tl of anthropogenic origin, represented by appropriate reference samples (Zn ore, post-flotation Zn-Fe residue; ε^{205}Tl ~−3.8) (Table 2). The lighter Tl derived from vegetation [15] also cannot be omitted. However, it should form only a minor part of the topsoil Tl amount and thus its isotope effect seems to be limited for such heavily Tl-impacted soils. From the long-term point of view, the contribution of this Tl portion (i.e., associated with the primary biomass) having low ε^{205}Tl signature is potentially more pronounced. Even though Tl in soil is an isotope mixture derived from two different reservoirs (Fig. 1), with the predominance of the anthropogenic pool relative to the geogenic one, we detected partial Tl isotope fractionations in the studied profiles. The increase in ε^{205}Tl in the horizons Ap (profile 1), C1 and C2 (profile 3), up to the value of +0.4 (Table 2), cannot reflect the input of geogenic Tl (enriched in ^{205}Tl). The reason is that the layers have near-surface positions and/or higher Tl concentrations, as compared to the underlying soils. Therefore, this isotope variation matches better to specific sorption processes onto soil constituents and/or precipitation reactions. Preferential retention of the heavier isotope fraction and leaching of the lighter fraction is well documented for Cu and Cd [27,38], although it should be noted that their chemical behavior markedly differs from that of Tl. The origin of increased ε^{205}Tl in the Ap horizon (Fig. 1) might be theoretically ascribed to Tl retention onto secondary phases, such as oxides, which are indicated by the oxalate-extractable increase in Mn (Table 1). For example, Nielsen et al. [39] document a systematic increase in the fraction of heavier ^{205}Tl during Tl sorption onto the Mn(III,IV) oxide (hexagonal birnessite) using model sorption experiments; the magnitude of fractionation (α) accounted for ~1.0002 to 1.0015. The authors hypothesized that this isotope fractionation comes from the combined effect of the oxidation of Tl(I) to Tl(III), which is then adsorbed on top of Mn vacancy sites in the octahedral phyllomanganate sheets of birnessite (δ-MnO_2). In the case of C1 and C2 horizons, the post-depositional Tl isotope behavior is more difficult to explain, as no indications in physico-chemical properties and bulk mineralogy were recorded in these layers.

Further evidence for the proposed anthropogenic origin of Tl enrichment in soils is provided by positive linear relationship (R^2 = 0.85) between 1/Tl and the isotope record, as determined for soil and bedrock samples only (i.e., except for the Ap, C1 and C2 horizons), indicative of binary Tl mixing (Fig. 2). Assuming that anthropogenic (ε^{205}Tl ~ −3.8) and geogenic Tl (ε^{205}Tl ≤ −1.0) would not be subjected to any isotope fractionation in the soils, the fraction of anthropogenic Tl (X) can be roughly estimated based on Eq. (2):

$$X = \frac{\varepsilon^{205}Tl_s - \varepsilon^{205}Tl_B}{\varepsilon^{205}Tl_C - \varepsilon^{205}Tl_B} \quad (2)$$

where $\varepsilon^{205}Tl_S$, $\varepsilon^{205}Tl_B$ and $\varepsilon^{205}Tl_C$ refer to the isotope composition of the soil sample, the corresponding bedrock, and the local

historical Tl contamination source, respectively. The calculated smelter-derived Tl load for the uppermost forest soil layers equals to up to the total (soil) Tl content. In contrast, for the meadow soil profile (profile 2), the calculation suggests that only about half of the total Tl in all soil horizons is smelter-derived.

4. Conclusions

In general, the Tl isotope signatures of waste products from different stages of Zn ore mining and metallurgical processing of Zn-bearing materials varied only insignificantly, despite large variations in total Tl contents. Nevertheless, the lower ε^{205}Tl value of fly ash than slag may indicate that kinetic isotope fractionation during Tl evaporation could occur. Our findings demonstrate that Tl isotope compositions in the studied soils reflected the isotope signature of the contamination source, despite the fact that the major pollution period ended more than 30 years ago. Therefore, it is evident that historical Tl input, if significant, can be traced using this method and the Tl isotope record in soils (or sediments) is likely to be preserved for a relatively long time. We also observed some Tl isotope fractionations in our soils, with Tl being isotopically heavier than its dominant (anthropogenic) source. These fractionation processes generally complicate the tracing of pollution sources in soils or sediments based on Tl isotope signature. On the other hand, Tl isotope fractionation due to soil chemical processes can be exploited, in order to contribute to a better understanding of the reactions that control the fate and cycling of Tl in subsurface environments. Here, we simply interpret these Tl isotope shifts as a result of unidentified sorption processes of Tl onto soil constituents and/or precipitation reactions. To gain further insight into Tl isotope fractionation due to chemical and biological processes in soils, laboratory experiments under well-defined conditions need to be carried out in the future.

Acknowledgements

This research was funded by the grants of the Czech Science Foundation (17-03211S and 16-13142S). Part of the equipment used for this study was purchased from the Operational Programme Prague – Competitiveness (Project CZ.2.16/3.1.00/21516). We kindly thank Dr. Miroslaw Fatyga and Eng. Jacek Jakubowski (Boleslaw Recycling Ltd.) for their help with industrial issues. The Swiss Light Source (Paul Scherrer Institute, Switzerland) is acknowledged for the provision of beamtime at the SuperXAS beamline. We would also like to thank three anonymous reviewers for their suggestions which significantly improved the quality of the paper.

Appendix A. Supplementary data

Supplementary data associated with this article can be found, in the online version, at http://dx.doi.org/10.1016/j.jhazmat.2017.09.020.

References

[1] T. Xiao, J. Guha, D. Boyle, C.Q. Liu, J. Chen, Environmental concerns related to high thallium levels in soils and thallium uptake by plants in southwest Guizhou, China, Sci. Total Environ. 318 (2004) 223–244.
[2] A.L. John Peter, T. Viraraghavan, Thallium: a review of public health and environmental concerns, Environ. Int. 31 (2005) 493–501.
[3] G. Kazantzis, Thallium in the environment and health effects, Environ. Geochem. Health 22 (2000) 275–280.
[4] J. Liu, J. Wang, Y. Chen, X. Xie, J. Qi, H. Lippold, D. Luo, C. Wang, L. Su, L. He, Q. Wu, Thallium transformation and partitioning during Pb – Zn smelting and environmental implications, Environ. Pollut. 212 (2016) 77–89.
[5] T. Xiao, F. Yang, S. Li, B. Zheng, Z. Ning, Thallium pollution in China: a geo-environmental perspective, Sci. Total Environ. 421–422 (2012) 51–58.
[6] M. Jakubowska, A. Pasieczna, W. Zembrzuski, Z. Swit, Z. Lukaszewski, Thallium in fractions of soil formed on floodplain terraces, Chemosphere 66 (2007) 611–618.
[7] B. Karbowska, W. Zembrzuski, M. Jakubowska, T. Wojtkowiak, A. Pasieczna, Z. Lukaszewski, Translocation and mobility of thallium from zinc–lead ores, J. Geochem. Explor. 143 (2014) 127–135.
[8] V. Jović, Thallium, in: C.P. Marshall, R.W. Fairbridge (Eds.), Encyclopedia of Geochemistry, Kluwer Academic Publishers, Dordrecht, Germany, 1998, pp. 622–623.
[9] A. Tremel, P. Masson, T. Sterckeman, D. Baize, M. Mench, Thallium in French agrosystems–I. Thallium contents in arable soils, Environ. Pollut. 95 (1997) 293–302.
[10] A.R. Jacobson, M.B. McBride, P. Baveye, T.S. Steenhuis, Environmental factors determining the trace-level sorption of silver and thallium to soils, Sci. Total Environ. 345 (2005) 191–205.
[11] A.R. Jacobson, S. Klitzke, M.B. McBride, P. Baveye, T.S. Steenhuis, The desorption of silver and thallium from soils in the presence of a chelating resin with thiol functional groups, Water Air Soil Pollut. 160 (2005) 41–54.
[12] A. Vaněk, M. Mihaljevič, I. Galušková, V. Chrastný, M. Komárek, V. Penížek, T. Zádorová, O. Drábek, Phase-dependent phytoavailability of thallium – a synthetic soil experiment, J. Hazard. Mater. 250–251 (2013) 265–271.
[13] A. Vaněk, M. Komárek, P. Vokurková, M. Mihaljevič, O. Šebek, G. Panušková, V. Chrastný, O. Drábek, Effect of illite and birnessite on thallium retention and bioavailability in contaminated soils, J. Hazard. Mater. 191 (2011) 190–196.
[14] A. Voegelin, N. Pfenninger, J. Petrikis, J. Majzlan, M. Plötze, A.C. Senn, S. Mangold, R. Steininger, J. Göttlicher, Thallium speciation and extractability in a thallium- and arsenic-rich soil developed from mineralized carbonate rock, Environ. Sci. Technol. 49 (2015) 5390–5398.
[15] M. Kersten, T. Xiao, K. Kreissig, A. Brett, B.J. Coles, M. Rehkämper, Tracing anthropogenic thallium in soil using stable isotope compositions, Environ. Sci. Technol. 48 (2014) 9030–9036.
[16] A. Vaněk, Z. Grösslová, M. Mihaljevič, J. Trubač, V. Ettler, L. Teper, J. Cabala, J. Rohovec, T. Zádorová, V. Penížek, L. Pavlů, O. Holubík, K. Němeček, J. Houška, O. Drábek, C. Ash, Isotopic tracing of thallium contamination in soils affected by emissions from coal-fired power plants, Environ. Sci. Technol 50 (2016) 9864–9871.
[17] J. Cabala, L. Teper, Metalliferous constituents of rhizosphere soils contaminated by Zn–Pb mining in southern Poland, Water Air Soil Pollut. 178 (2007) 351–362.
[18] A. Vaněk, V. Chrastný, L. Teper, J. Cabala, V. Penížek, M. Komárek, Distribution of thallium and accompanying metals in tree rings of Scots pine (*Pinus sylvestris* L.) from a smelter-affected area, J. Geochem. Explor. 108 (2011) 73–80.
[19] Food and Agriculture Organization of the United Nations (FAO), World Reference Base for Soil Resources, Food and Agriculture Organization of the United Nations (FAO), Rome, 2014.
[20] International Organization of Standardization, Standard of Soil Quality – Determination of Effective Cation Exchange Capacity and Base Saturation Level Using Barium Chloride Solution (ISO 11260:1994).
[21] M. Pansu, J. Gautheyrou, Handbook of Soil Analysis, Mineralogical, Organic and Inorganic Methods, Springer-Verlag, Berlin, Heidelberg, 2006.
[22] Ph. Quevauviller, Operationally defined extraction procedures for soil and sediment analysis I. Standardization, Trends Anal. Chem. 17 (1998) 289–298.
[23] V. Chrastný, A. Vaněk, L. Teper, J. Cabala, J. Procházka, L. Pechar, P. Drahota, V. Penížek, M. Komárek, M. Novák, Geochemical position of Pb, Zn and Cd in soils near the Olkusz mine/smelter, South Poland: effects of land use, type of contamination and distance from pollution source, Environ. Monit. Assess. 184 (2012) 2517–2536.
[24] R.G.A. Baker, M. Rehkämper, T.K. Hinkley, S.G. Nielsen, J.P. Toutain, Investigation of thallium fluxes from subaerial volcanism–implications for the present and past mass balance of thallium in the oceans, Geochim. Cosmochim. Acta 73 (2009) 6340–6359.
[25] J. Prytulak, S.G. Nielsen, T. Plank, M. Barker, T. Elliot, Assessing the utility of thallium and thallium isotopes for tracing subduction zone inputs to the Mariana arc, Chem. Geol. 345 (2013) 139–149.
[26] R. Meij, Trace element behavior in coal/fired power plants, Fuel Process. Technol. 39 (1994) 199–217.
[27] M. Bigalke, S. Weyer, J. Kobza, W. Wilcke, Stable Cu and Zn isotope ratios as tracers of sources and transport of Cu and Zn in contaminated soil, Geochim. Cosmochim. Acta 74 (2010) 6801–6813.
[28] J. Liszka, E. Świć, E. Dzieje Wydarzenia Ludzie, Zakłady Górniczo-Hutnicze Bolesław S. A., Bukowno, Poland, 2004 (in Polish).
[29] R.S. Smith, J.G. Wiederhold, R. Kretzschmar, Mercury isotope fractionation during precipitation of metacinnabar (β-HgS) and montroydite (HgO), Environ. Sci. Technol. 49 (2015) 4325–4334.
[30] A.F. Holleman, E. Wiberg, N. Wiberg, Lehrbuch der Anorganischen Chemie, Walter de Gruyter & Co., Berlin, New York, 1995.
[31] G. Brauer, Handbuch der Präparativen Anorganischen Chemie, F. Enke Verlag, Stuttgart, Germany, 1954.
[32] D.R. Lide, CRC Handbook of Chemistry and Physics, CRC Press (Taylor and Francis Group), Boca Raton, FL, 2009.
[33] S.L. Phillips, D.L. Perry, Handbook of Inorganic Compounds, CRC Press, Boca Raton, FL, 1995.
[34] J.E. Dutrizac, T.T. Chen, S. Beauchemin, The behavior of thallium(III) during jarosite precipitation, Hydrometallurgy 789 (2005) 138–153.

[35] A. Vaněk, V. Chrastný, M. Mihaljevič, P. Drahota, T. Grygar, M. Komárek, Lithogenic thallium behavior in soils with different land use, J. Geochem. Explor. 102 (2009) 7–12.
[36] V. Ettler, R. Vrtišková, M. Mihaljevič, O. Šebek, T. Grygar, P. Drahota, Cadmium, lead and zinc leaching from smelter fly ash in simple organic acids–simulators of rhizospheric soil solutions, J. Hazard. Mater. 170 (2009) 1264–1268.
[37] A. Vaněk, V. Chrastný, M. Komárek, I. Galušková, P. Drahota, T. Grygar, V. Tejnecký, O. Drábek, Thallium dynamics in contrasting light sandy soils–soil vulnerability assessment to anthropogenic contamination, J. Hazard. Mater. 173 (2010) 717–723.
[38] V. Chrastný, E. Čadková, A. Vaněk, L. Teper, J. Cabala, M. Komárek, Cadmium isotope fractionation within the soil profile complicates source identification in relation to Pb-Zn mining and smelting processes, Chem. Geol. 405 (2015) 1–9.
[39] S.G. Nielsen, L.E. Wasylenki, M. Rehkämper, C.L. Peacock, Z. Xue, E.M. Moon, Towards an understanding of thallium isotope fractionation during adsorption to manganese oxides, Geochim. Cosmochim. Acta 117 (2013) 252–265.

- PŘÍLOHU VI. - Izotopové složení Tl v půdách

Vaněk, A., Voegelin, A., Mihaljevič, M., Ettler, V., Trubač, J., Drahota, P., Vaňková, M., Oborná, V., Vejvodová, K., Penížek, V., Pavlů, L., Drábek, O., Vokurková, P., Zádorová, T., Holubík, O., 2020. Thallium stable isotope ratios in naturally Tl-rich soils. Geoderma 364, 114183. https://doi.org/https://doi.org/10.1016/j.geoderma.2020.114183

Geoderma 364 (2020) 114183

Contents lists available at ScienceDirect

Geoderma

journal homepage: www.elsevier.com/locate/geoderma

Thallium stable isotope ratios in naturally Tl-rich soils

Aleš Vaněk[a,*], Andreas Voegelin[b], Martin Mihaljevič[c], Vojtěch Ettler[c], Jakub Trubač[c], Petr Drahota[c], Maria Vaňková[c], Vendula Oborná[a], Kateřina Vejvodová[a], Vít Penížek[a], Lenka Pavlů[a], Ondřej Drábek[a], Petra Vokurková[a], Tereza Zádorová[a], Ondřej Holubík[a]

[a] Department of Soil Science and Soil Protection, Faculty of Agrobiology, Food and Natural Resources, Czech University of Life Sciences Prague, Kamýcká 129, 165 00 Prague 6, Czech Republic
[b] Eawag, Swiss Federal Institute of Aquatic Science and Technology, Ueberlandstrasse 133, CH-8600 Duebendorf, Switzerland
[c] Institute of Geochemistry, Mineralogy and Mineral Resources, Faculty of Science, Charles University, Albertov 6, 128 00 Prague 2, Czech Republic

ARTICLE INFO

Handling Editor: David Laird

Keywords:
Soil
Thallium
Isotope fractionation
Illite

ABSTRACT

Soils on the Erzmatt (Switzerland) formed on hydrothermally mineralized dolomite rock are naturally Tl-rich. In this study, we investigated if variations in the stable Tl isotope ratios in soil samples from different profiles can be linked to data on the extractability and speciation of soil Tl and whether the isotopic data allow drawing conclusions on the geochemical processes that affected Tl over the course of soil formation. In two soil profiles, we observed a marked accumulation of the heavy ^{205}Tl isotope in the B horizons, with ε^{205}Tl values that were up to 7 higher than in the underlying bedrock. This ^{205}Tl enrichment, however, was neither reflected in the speciation of Tl nor its chemical fractionation. Furthermore, exchangeable soil Tl in the B horizons was found to be much isotopically lighter than the bulk soil Tl. These findings suggest that the observed isotopic shift may be linked to cyclic Tl mobilization and immobilization processes over the period of rock weathering and soil formation. Oxidative Tl uptake by Mn-oxides associated with a ^{205}Tl enrichment, continuous weathering of the Tl (III)-containing phases, followed by a Tl(I) remobilization (leading to enrichment in ^{205}Tl) are suggested to be responsible for the binding of the heavy Tl isotope fraction into other phases, mainly illite (a dominant Tl host), which is not normally expected. Hence, our results show that the Tl isotopic fractionation data measured in a dynamic multi-phase (soil) system can potentially serve as a proxy for tracing redox-controlled processes, but their use for phase or the sorption process identification is much more complicated.

1. Introduction

Thallium (Tl) is a highly toxic trace element and contamination of environmental systems with Tl may represent a serious threat to human and environmental health. The geochemistry of Tl is complex. Monovalent Tl(I) tends to react as lithophile element in analogy to K, but exhibits also chalcophile character and can be bound to S in inorganic and organic compounds. Under highly oxidizing conditions, strongly hydrolyzing and poorly soluble Tl(III) may occur (Peter and Viraraghavan, 2005). Thallium has two stable isotopes, ^{203}Tl and ^{205}Tl, and variations in the stable Tl isotope ratios in soils and at the soil–plant interface may offer insights into the biogeochemical processes that control the environmental fate and impact of Tl (Howarth et al., 2018; Nielsen et al., 2017). In a pioneering study using high-resolution multi-collector inductively coupled plasma mass spectrometry (MC-ICP-MS), Kersten et al. (2014) demonstrated that stable Tl isotope ratios can be used to identify anthropogenic and geogenic Tl inputs into soil and that plants may preferentially accumulate the light ^{203}Tl in plants. Studies with plants grown in soil and hydroponic systems showed systematic plant-specific Tl isotope fractionation patterns, with preferential transfer of light ^{203}Tl from nutrient solutions to roots and further into stems and leaves, resulting in a decrease in the ε^{205}Tl along this transfer path. These isotopic trends were clearly due to Tl translocation and/or specific chemical reactions (Rader et al., 2019; Vaněk et al., 2019). In relation to rock weathering and soil formation, Howarth et al. (2018) showed that intensive weathering in laterite soil profiles may cause enrichment in ^{205}Tl, presumably due to redox/sorption processes and changes in mineralogy, where Tl(I) oxidation to Tl(III) by Mn-oxides is thought to be the key factor (Nielsen et al., 2013; Rehkämper et al., 2004). In relation to anthropogenic activities, we observed Tl isotopic fractionation during both industrial high-temperature processes (coal burning and metallurgy) and post-depositional Tl dynamics in soils, probably related to Tl sorption or (co)precipitation (Vaněk et al., 2016, 2018). Currently available data thus suggest that

* Corresponding author.
E-mail address: vaneka@af.czu.cz (A. Vaněk).

https://doi.org/10.1016/j.geoderma.2020.114183
Received 19 November 2019; Received in revised form 2 January 2020; Accepted 12 January 2020
Available online 20 January 2020

variations in the Tl isotopic signature may act as a proxy for specific geochemical and biological processes/reactions and associated enrichments or chemical alterations of Tl. However, to advance the level of understanding of Tl isotopic patterns in soil systems, information on stable Tl isotope ratios should be evaluated in combination with data on the speciation and fractionation of Tl in soils.

In the Swiss Jura Mountains, soils on the Erzmatt ("ore meadow") contain exceptionally high levels of geogenic Tl of up to several thousand mg/kg, due to soil formation on dolomite rock that hosts weathered hydrothermal Tl-As-Fe sulfide mineralization (Hermann et al., 2018; Voegelin et al., 2015). Using X-ray absorption spectroscopy (XAS), it has been shown that secondary minerals from the weathered mineralization, avicennite (Tl_2O_3) and Tl(I)-bearing jarosite, mainly occur in deeper soil horizons (Voegelin et al., 2015). With respect to pedogenic Tl species, Tl(I) bound to illite (or other micaceous clay minerals) represented the dominant Tl species, but also Tl(III) sorbed onto Mn-oxides was identified (Voegelin et al., 2015).

The present study was performed to evaluate if variations in stable Tl isotope ratios in soil samples from Erzmatt can be linked to data on the extractability and speciation of Tl and whether the data allow drawing conclusions on the geochemical processes that affect Tl over the course of soil formation. For this purpose, one soil profile was sampled on the Erzmatt meadow and one in the adjacent forest. The samples were analyzed for basic soil chemical and mineralogical properties, Tl fractionation (single and sequential batch extractions), Tl speciation (XAS) and Tl isotope ratios (MC-ICP-MS). Data from the two soil profiles were combined with the Tl isotope data on selected soil samples from an earlier study that exhibit substantial variations in Tl speciation (Voegelin et al., 2015).

2. Experimental section

2.1. General site description

The Erzmatt is a meadow situated near the village Buus in the Swiss Jura Mountains (Fig. S1, Supplementary Material). The soils on the Erzmatt contain high levels of Tl, As and Fe due to their formation on the carbonate rock (lower Keuper, triassic dolomite) that locally hosts a weathered hydrothermal Tl-As-Fe mineralization (Hermann et al., 2018; Voegelin et al., 2015). The soils are characterized as Cambisols, with neutral to slightly acidic pH values and exhibit weak redoximorphic features (Voegelin et al., 2015). The Erzmatt site was used as a pasture in the past. In 2016, the agricultural use of the zone with the highest Tl contents has been discontinued and this land is now managed as an ecological compensation area (fallow with native wild herbs). The speciation of soil Tl and the mineralogy of secondary Tl- and As-bearing minerals in soil samples from the Erztmatt were studied in earlier work (Hermann et al., 2018; Voegelin et al., 2015).

2.2. Soil sample collection

Two soil profiles were sampled in this study, one at the meadow (M) and one under the adjacent forest (F) (Figs. S1, S2 and S3, Supplementary Material). Soil samples and one bedrock sample (meadow profile) were collected from individual soil layers in ~1 × 1 m wide pits according to the soil development (1–5 cm). All soil samples were air-dried and sieved through a 2-mm stainless-steel sieve prior to further use/analyses. In addition to the soil samples from the two soil profiles, selected soil samples from that have previously been shown to exhibit large variations in Tl speciation (Voegelin et al., 2015) were analyzed for their stable Tl isotope ratios as well.

2.3. Soil sample characterization

The soil pH (active, exchangeable) was determined at a 1:5 (v/v) ratio of soil to H_2O or 1 M KCl solution. Total carbon (TC) and total sulfur (TS) were identified by catalytic oxidation using a Flash 2000 Series CNS analyzer (Thermo Scientific, Germany). The cation exchange capacity (CEC) was determined by saturating soil cation exchange sites with Ba^{2+} (0.1 M $BaCl_2$) followed by Ba^{2+} exchange with $MgSO_4$. The clay content was estimated by the sedimentary method on mixed sample sets for each soil profile. X-ray diffraction (XRD) data were collected using an X'Pert Pro diffractometer (PANalytical, the Netherlands) under the following conditions: CuKα radiation, 40 kV, 30 mA, step scanning at 0.02°/150 s in the range 3–80° 2θ. Mineral phases were identified using X'Pert HighScore software 1.0 and the JCPDS PDF-2 database.

A single extraction with 1 M NH_4NO_3 at a solid to liquid ratio of 1:2.5 (2 h reaction time) was used to quantify the exchangeable soil Tl fraction. The exchangeable Tl from selected soil samples was also analyzed for its stable Tl isotope signature. Acid oxalate extraction (0.2 M ammonium oxalate/oxalic acid at pH 3.0) (Pansu and Gautheyrou, 2006) was used to quantify oxalate-extractable Fe and Mn and co-extracted Tl. A modified BCR sequential extraction procedure by Rauret et al. (2000) was employed to quantify chemical fractionation of Tl (and Mn) in four extraction steps (with hypothetical interpretation in parentheses): (i) 0.11 M CH_3COOH, pH 3 (acid-extractable); (ii) 0.5 M $NH_2OH{\cdot}HCl$, pH 1.5 (reducible); (iii) 8.8 M H_2O_2/1 M CH_3COONH_4, pH 2 (oxidizable); (iv) hot acid digestion with HNO_3/HCl/HF (residual). Analytical grade chemicals (Lach-Ner, Czech Republic) were used for all the extractions.

To characterize the speciation of Tl in selected samples (Oi, Oe, Ah, Bw2 and C layers/horizons), the dried and powdered samples were prepared as 7-mm pellets for analysis by Tl L_{III}-edge X-ray absorption near-edge structure (XANES) spectroscopy at the SuperXAS beamline at the Swiss Light Source (SLS, Villigen, PSI), using the same setup as in previous works (Vaněk et al., 2018; Wick et al., 2018). The XANES spectra were evaluated by linear combination fitting based on selected reference spectra. Starting from the best one-component fit, fits with more components were considered only if the sum of the squared residuals of the fit decreased by at least 10% (relative). The sum of the fitted fractions was not constrained.

To determine the total element concentrations and Tl isotopic fractionation, the samples were homogenized and finely ground in an agate mill. A mass of 0.2 g of each sample was decomposed using a mixture of concentrated acids. Nitric and HF acids mixed in a ratio of 2:1 were added to the sample in a total volume of ≤20 mL; the dissolution was performed in 60-mL PTFE beakers (Savillex, USA) on a hot plate (150 °C) for 48 h with the subsequent addition of 2–4 mL of H_2O_2 for possible organic residues.

The element concentrations in all the digests and soil extracts were measured in triplicate using either inductively coupled plasma optical emission spectrometry (ICP-OES, iCAP 6500, Thermo Scientific, UK) or quadrupole based inductively coupled plasma mass spectrometry (Q-ICP-MS, Xseries II, Thermo Scientific, Germany). The standard reference material NIST 2711 (Montana Soil) (National Institute of Standards and Technology, USA) was used for QC (Table S1, Supplementary Material).

2.4. Thallium isotope separation

Thallium was isolated from the sample matrix using chromatographic separation with an anion exchange resin (Bio-Rad AG1-X8, 200–400 mesh, Cl^- cycle) as earlier described in detail (Baker et al., 2009; Vaněk et al., 2016, Vaněk et al., 2018). The only exception for this work was the absence of HBr in all the chromatographic stages. The obtained Tl/Pb fraction after the first extraction step was evaporated and redissolved in 0.1 M HCl to be ready for the next part of the Tl purification. Once the final Tl fraction (with no Pb present) was obtained, the Tl sample was transferred to 2% HNO_3. Suprapure chemicals (Merck, Germany) and deionized water (MilliQ+, Millipore, USA) were employed during whole separation procedure.

2.5. Thallium isotope analysis

The MC-ICP-MS (Neptune Plus, Thermo Scientific, Germany) with a desolvating nebulizer (Aridus II, CETAC, USA) was used to measure the Tl isotope ratios. All the solutions were measured in 3 runs of 50 cycles. External normalization/standard sample bracketing (NIST SRM 997) were employed to eliminate the mass bias drift. For inter-element correction, the $^{208}Pb/^{206}Pb$ ratio was used to correct the raw $^{205}Tl/^{203}Tl$ ratio. The Tl isotopic composition was calculated using the following equation with ε notation relative to NIST SRM 997 (Eq. (1)).

$$\varepsilon\ ^{205}Tl = \frac{^{205}Tl/\ ^{203}Tl_{sample} - \ ^{205}Tl/\ ^{203}Tl_{NIST997}}{^{205}Tl/\ ^{203}Tl_{NIST997}} \times 10^4 \quad (1)$$

Repeated analyses of the Sigma-Aldrich standard solution (for ICP analysis) with the mean of ε^{205}Tl between −0.80 and −0.90 (n = 4) were consistent with the reported ε^{205}Tl value (−0.81) (Prytulak et al., 2013). The external reproducibility had a value of ± 0.7 ε^{205}Tl (2 SD), based on long-term separate analyses (3 for this study) of standard reference material AGV-2 (Andesite, USGS, USA) in the same laboratory (Table S2, Supplementary Material), accounting for complete isotope analysis (sample dissolution, ion exchange chromatography and the mass spectrometric procedure).

3. Results and discussion

3.1. Characterization of soil profiles

The studied soils were classified as Eutric Cambisols (Figs. S2 and S3, Supplementary Material). Key physicochemical properties are summarized in Table S3 (Supplementary Material). The soils can be briefly characterized by a medium content of clay fraction (12–15%), increased CEC of the mineral soil horizons (~30 cmol(+)/kg) and a circum-neutral pH value. The organic horizons contain up to 40 wt% of TC, compared to only ~3% in the mineral horizons. The bulk soil mineralogy as determined by XRD is dominated by quartz (SiO_2), K-feldspar ($KAlSi_3O_8$), muscovite ($K,Al_2(AlSi_3O_{10})(F,OH)_2$) and/or illite ($(K,H_3O)Al_2(Si,Al)_4O_{10}(OH)_2$), chlorite and mixed-layered illite/smectite (Fig. S4, Supplementary Material), in accordance with earlier mineralogical results (Hermann et al., 2018; Voegelin et al., 2015).

3.2. Total and extractable Tl in soil profiles

The depth profiles for total Tl, exchangeable Tl, oxalate-extractable Tl and the fractions of the sequential extraction are all shown in Fig. 1 and Tables 1 and S4 (Supplementary Material). In both profiles, the Tl contents were the lowest in the topsoils (~20–200 mg Tl/kg) and increased to ~500–600 mg/kg with depth. The highest fractions of exchangeable and oxalate-extractable Tl were observed in the organic (O) horizons. In combination, these results pointed to the sorption of Tl on soil organic matter (SOM) in a relatively labile form. In the Ah and Bw horizons, only ~5% of the total Tl was exchangeable and ~7% oxalate-extractable. In the sequential extraction, most of the Tl was associated with the residual phase (Fig. 1), in accordance with earlier studies on soil Tl fractionation in soils, sediments or waste materials (Aguilar-Carrillo et al., 2018; Gomez-Gonzalez et al., 2015; Grösslová et al., 2018; Jakubowska et al., 2007; Karbowska et al., 2014; Liu et al., 2016, Liu et al., 2019). In agreement with the large fractions of exchangeable and oxalate-extractable Tl, the largest non-residual Tl fractions were observed in the O horizons. In the Ah and Bw horizons of both profiles, ~90% of the Tl was associated with the residual fraction, ~8% with the reducible fraction, and only minor percentages with the acid-extractable and oxidizable fractions, with a small peak for the topsoils (Oi layers) (Fig. 1 and Table S5, Supplementary Material). Considering the speciation data from an earlier study on the Erzmatt site (Voegelin et al., 2015), and the XANES results provided below (indicating that most Tl in the two soil profiles studied here was associated with micaceous clay minerals), residual Tl in the Ah and Bw horizons probably mostly corresponds to Tl(I) in the interlayers of illite or other micaceous clay minerals. The minor fraction of Tl extracted in the reducible fraction of the sequential extraction may at least partly be Tl(I) or Tl(III) associated with soil Mn-oxides. Molar Tl/Mn ratios from the oxalate extraction (~0.01) and the reducible fractions (~0.02) (Table S4, Supplementary Material) thus point to high Tl loading of Mn-oxides, although it should be noted that both extracts could also mobilize variable proportions of exchangeable Tl (oxalate-extract without prior extraction of exchangeable Tl) or of Tl associated with mica-type minerals (hydroxylamine extract at pH 1.5) (Vaněk et al., 2010).

3.3. Thallium speciation in soil profiles

The Tl L_{III}-edge XANES spectra of selected samples from the soil profile under the meadow are shown in Fig. 2, in comparison with the reference spectra of avicennite (Tl_2O_3) (proxy for Tl(III) in avicennite, adsorbed on Mn-oxides, or organically complexed), aqueous Tl^+ (proxy for (mostly hydrated) Tl(I) adsorbed on the soil minerals or organic matter or in the biomass), and Tl^+ adsorbed at the frayed edges of illite (proxy for dehydrated Tl^+ associated with micaceous clay minerals).

All the soil spectra indicated a clear prevalence of Tl(I) over Tl(III). The spectra of the two organic topsoil samples from the meadow, M-Oi and M-Oe, differed markedly from the spectra of the Ah, Bw and C horizons, and more closely resembled the spectrum of aqueous Tl^+, pointing to a larger fraction of Tl^+ adsorbed on the SOM or associated with the biomass (Vaněk et al., 2019; Wick et al., 2018). The spectra of samples M-Ah, M-Bw2 and M-C resembled the spectrum of Tl^+ adsorbed on illite, but exhibited more pronounced oscillations in the post-edge region than the illite reference spectrum. Considering that less than 10% of the Tl in these soil horizons was bound in exchangeable form (Table 1), we attribute this spectral difference to the presence of non-exchangeable structural Tl in the interlayers of micaceous clay minerals (Voegelin et al., 2015). For quantitative evaluation of the sample spectra by linear combination fitting (LCF), the spectrum of the soil sample M-C rather than the reference spectrum of Tl(I) adsorbed on illite was used to represent Tl associated with micaceous clay minerals. The LCF results (Table 2) pointed to a minor fraction of Tl(III) in the M-Oi sample, possibly organically-complexed Tl(III), in addition to Tl(I). In the Ah and Bw horizons, no species other than Tl(I) associated with micaceous clay minerals were detected by LCF, pointing to nearly uniform Tl speciation. The LCF analysis of the samples from the forest profile revealed only a minor fraction of hydrated Tl^+ in sample F-Oi, whereas Tl in all the other samples (F-Oe, F-Ah, F-Bw2, F-C) appeared to be mainly associated with micaceous clay minerals (Fig. S5, Supplementary Material).

Overall, the spectroscopic results were in agreement with the chemical extractions. The large fractions of residual Tl in sequential extraction of the Ah, Bw and C horizon samples can be attributed to Tl incorporated into the interlayers of micaceous clay minerals (mainly illite); the exchangeable Tl can be interpreted at least partly as Tl adsorbed at the frayed edges of the clay minerals. The increases in the percentages of exchangeable Tl and Tl extracted by H_2O_2 in the organic topsoil samples are in accordance with the detectable fractions of hydrated Tl^+ in LCF and point to the binding of Tl(I) by SOM and probably also association of Tl(I) with the living or dead biomass.

In comparison with the soil samples from the meadow/forest profiles, the soil samples from an earlier study on the Erzmatt site (Voegelin et al., 2015) spanned a wider range in soil Tl contents and Tl speciation (Table 3), with up to ~ 6000 mg Tl/kg, and containing all Tl (I) associated with illite, Tl(I)-jarosite, Tl(III) species like Tl_2O_3 or some other/unidentified Tl(III)-phases.

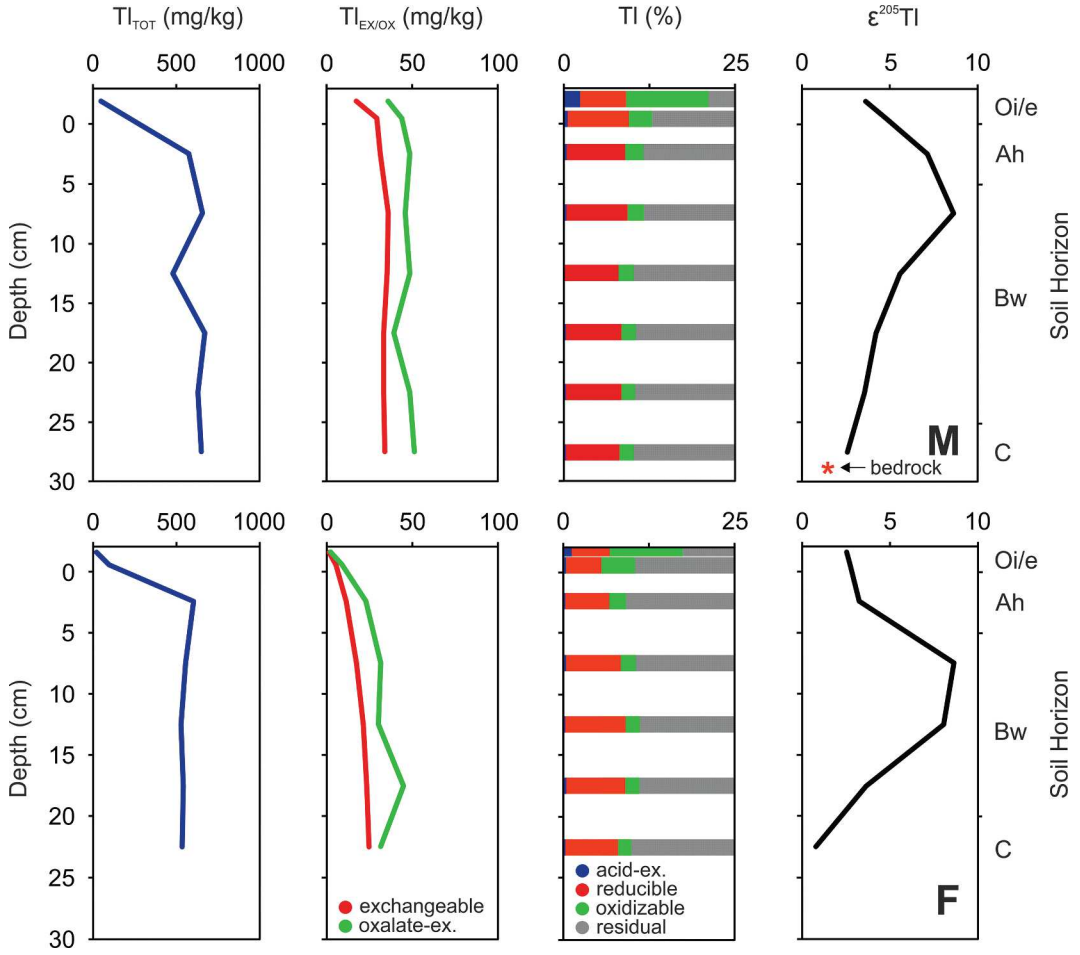

Fig. 1. Vertical evolution of total (Tl_{TOT}), exchangeable and oxalate-extractable Tl concentrations, chemical Tl fractionation (≤25% of total fractionation) and Tl isotopic compositions ($\varepsilon^{205}Tl$) in the studied soils – (M) meadow, (F) forest.

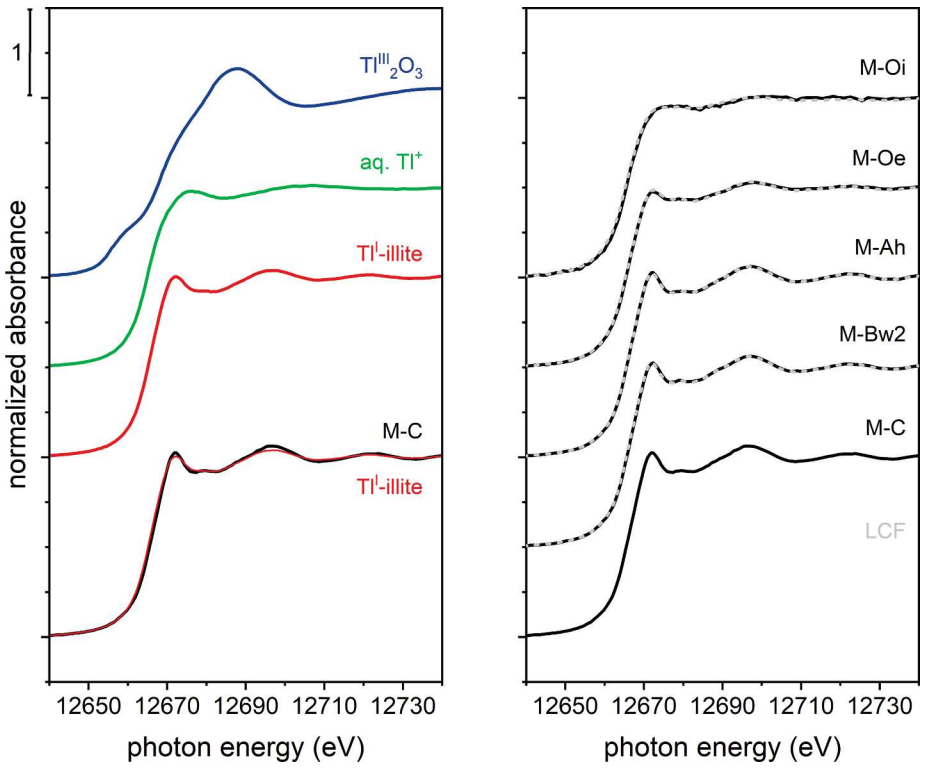

Fig. 2. Tl L_{III}-edge XANES spectra of selected soil samples from the meadow profile (M-Oi, M-Oe, M-Ah, M-Bw2, M-C) and reference spectra $Tl^{III}_2O_3$ (Voegelin et al., 2015), proxy for Tl(III); aqueous Tl^+ (Wick et al., 2018), proxy for hydrated Tl^+; Tl^I-illite (sample with 3800 mg/kg Tl) (Wick et al., 2018), proxy for Tl(I) adsorbed at frayed edge sites or bound in the interlayer of micaceous clay minerals. The gray dashed lines in the right panel represent linear reconstruction spectra based on the LCF results in Table 2. The spectra of selected samples from the forest profile are available in the Fig. S5 (Supplementary Material).

Table 1
Total Tl concentrations (Tl_{TOT}), exchangeable (Tl_{exch}) and oxalate-extractable (Tl_{oxal}) Tl fractions, and stable Tl isotope compositions ($\varepsilon^{205}Tl$) in the studied soils and the reference material.

Profile/Material	Sample	Tl_{TOT} (mg/kg)	Tl_{exch} (%)	Tl_{oxal} (%)	$\varepsilon^{205}Tl \pm 0.7$
Meadow	M-Oi	50.7 ± 0.6	34.7	71.2	+3.62
	M-Oe	220 ± 10	13.5	20.0	+4.84
	M-Ah	570 ± 14	5.5	8.5	+7.18
	M-Bw1	657 ± 22	5.5	7.0	+8.66
	M-Bw2	481 ± 21	7.3	10.0	+5.57
	M-Bw3	670 ± 12	5.0	5.9	+4.23
	M-Bw4	630 ± 13	5.3	7.8	+3.58
	M-C	651 ± 23	5.2	7.8	+2.60
	M-R (bedrock)	231 ± 5	n.d.	n.d.	+1.56
Forest	F-Oi	22.1 ± 0.5	5.3	10.8	+2.53
	F-Oe	92.9 ± 1.3	5.8	9.8	+2.72
	F-Ah	602 ± 25	1.9	3.8	+3.26
	F-Bw1	551 ± 18	3.1	5.8	+8.65
	F-Bw2	526 ± 20	4.0	5.8	+8.06
	F-Bw3	539 ± 17	4.4	8.4	+3.63
	F-C	533 ± 22	4.7	5.9	+0.76
AGV-2		0.25	n.d.	n.d.	−2.57

The uncertainties for total Tl concentrations are reported at the 2 SD level (n = 3). The relative data on exchangeable (1 M NH_4NO_3) and oxalate-extractable Tl are the means (n = 3) with RSD less than 10%. The $\varepsilon^{205}Tl$ results are assigned an error of ± 0.7 $\varepsilon^{205}Tl$ (2 SD), based on the long-term reproducibility of multiple separate analyses (involving sample digestion, column chemistry and mass spectrometry) of standard reference material AGV-2 (Andesite, USGS, USA) (3 for this study) (Table S2, Supplementary Material). n.d.: not determined.

Table 2
Linear combination fit analysis of Tl L_{III}-edge XANES spectra of meadow and forest soil samples. The sample and reconstructed LCF spectra are shown in Figs. 2 and S5 (Supplementary Material). In the LCF, Tl_2O_3 represents Tl(III) in organic or inorganic form, aqueous Tl^+ represents hydrated Tl^+ sorbed on the soil (mineral/organic) components or in the biomass, and soil sample M-C represents Tl(I) in micaceous clay minerals (see text for details).

Sample	Tl_2O_3	aq. Tl^+	M-C	Sum	NSSR[a]
M-Oi	0.08	0.66	0.25	0.99	0.00110
M-Oe	–	0.37	0.63	1.00	0.00020
M-Ah	–	–	1.00	1.00	0.00007
M-Bw2	–	–	1.00	1.00	0.00016
F-Oi	–	0.11	0.88	1.00	0.00058
F-Oe	–	–	1.00	1.00	0.00009
F-Ah	–	–	1.00	1.00	0.00020
F-Bw2	–	–	1.00	1.00	0.00012
F-C	–	–	1.00	1.00	0.00018

[a] NSSR = normalized sum of squared residuals ($\Sigma(data_i\text{-}fit_i)^2/\Sigma data_i^2$).

3.4. Stable Tl isotope ratios in soil samples

The Tl isotopic data for the meadow and forest soil profiles are listed in Table 1 and shown in Fig. 1. The two soil profiles exhibited very similar trends in $\varepsilon^{205}Tl$ over depth. The lowest $\varepsilon^{205}Tl$ values of +0.8 to +2.6 were observed for the bottom C horizons of both soil profiles and the bedrock sample from the meadow profile. The value of $\varepsilon^{205}Tl$ gradually increased to +8.7 from the C horizons to the uppermost Bw horizons. The value of $\varepsilon^{205}Tl$ then decreased to +2.5 from the Bw over the Ah horizon to the overlying O horizons. The increase in $\varepsilon^{205}Tl$ from the C to the Bw horizons was not reflected either in clear trends in Tl fractionation, dominated by residual Tl, or in Tl speciation, dominated by Tl(I) associated with micaceous clays (Tables 1 and 2, Fig. 1). This suggests that the processes resulting in the observed enrichment in the heavy ^{205}Tl in the soil horizons were linked to fractions of total soil Tl that were not readily observable in the extraction and speciation results

Table 3
Total Tl concentrations (Tl_{TOT}) and LCF-derived Tl speciation in selected samples from Voegelin et al. (2015) and corresponding stable Tl isotope data ($\varepsilon^{205}Tl$).

Sample	Tl_{TOT} (mg/kg)	Tl(I)-illite	Tl(I)-jarosite	Tl(III)	$\varepsilon^{205}Tl \pm 0.7$
P1 00–20	119	1.00	–	–	+12.63
P1 20–40	265	0.93	–	0.07	+6.44
P1 60–80	1801	0.32	0.32	0.36	+5.27
P1 65 Ore R	5677	–	0.84	0.17	+1.76
P1 95–115	1120	–	0.48	0.52	+6.01
P2 00–20	438	0.82	0.11	0.07	+7.41
P2 44–64	981	0.46	0.36	0.19	+6.74
P2 60–80	706	0.84	0.16	–	+6.18
P2 95–115	151	1.00	–	–	+7.76
P3 00–20	1142	0.87	–	0.13	+9.78
P3 20–40	3269	0.43	–	0.57	+12.49

Sample names indicate profile number (n = 3) and sampling depth (interval). The samples are averaged bulk samples, except sample P1 65 Ore R, a red weathered ore fragment.

(see the next section). The trend towards lower $\varepsilon^{205}Tl$ values, on the other hand, was reflected in higher fractions of exchangeable, oxalate-extractable and oxidizable Tl fractions in the O horizons of both profiles (Tables 1 and S5, Supplementary Material) and in the observation of hydrated Tl^+ by LCF (as well as a minor fraction of Tl(III) in sample M-Oh) (see the next section) (Table 2).

Regarding exchangeable soil Tl (NH_4NO_3-mobilizable), here we clearly detected isotopically lighter Tl in the B horizons than for the bulk soil Tl in both profiles (Tables 1 and S6, Supplementary Material), suggesting important Tl isotope shift due to the "aging" of secondary Tl (see the next section).

In soil samples from the earlier study (Voegelin et al., 2015), the measured $\varepsilon^{205}Tl$ values ranged from + 1.8 to +12.6 (Table 3) and thus spanned a larger range of Tl isotope ratios than the samples from the meadow and forest soil profiles. The lowest $\varepsilon^{205}Tl$ value of +1.8 was measured in a Tl-rich ore fragment (P1 65 Ore R) with a predominant content of Tl(I)-jarosite (Table 3), a weathering product of primary Tl-bearing sulfide(s) (Hermann et al., 2018; Voegelin et al., 2015). The highest $\varepsilon^{205}Tl$ values of +12.6/+12.5 were measured in two contrasting samples, a topsoil sample (P1 00–20) with relatively low Tl content mainly associated with micaceous clay minerals and a subsoil sample (P3 20–40) with much higher Tl content, with about half Tl(I) associated with micaceous clay minerals and half Tl(III) species (Table 3).

3.5. Relation of stable Tl isotope ratios to Tl fractionation, speciation, and geochemical processes

Because primary Tl-bearing sulfide minerals could not be sampled on the Erzmatt to date, the exact Tl isotopic signature of the hydrothermal mineralization is not exactly known. On the other hand, similar low $\varepsilon^{205}Tl$ values were observed for a Tl-rich weathered ore fragment dominated by Tl(I)-jarosite (+1.8) and the bedrock sample M-R dominated by Tl(I) associated with micaceous minerals (+1.6), which may exhibit $\varepsilon^{205}Tl$ values similar to the primary mineralization due to limited isotope fractionation during (near-quantitative) primary ore weathering. We speculate that the Tl isotopic signature of the Erzmatt mineralization could be similar to that of the Lengenbach deposit (Switzerland), which is genetically similar to the Erzmatt except for the metamorphic processes at Lengenbach. For the Lengenbach site, Hettman et al. (2014) observed relatively low $\varepsilon^{205}Tl$ values in sulfide and sulfosalt samples (−4.1 to +1.9), which probably resulted from isotopically light Tl in the hydrothermal fluid.

Despite the different $\varepsilon^{205}Tl$ values of the bedrock sample (+1.6) and

of the C horizon samples (+2.6/+0.8), in which Tl(I) is similarly associated with mica-type minerals, we do not expect important Tl isotopic fractionation during the (non-oxidative) Tl(I) transfer from weathering sulfide minerals (and jarosite) into pedogenic clay (Nielsen et al., 2017; Schauble, 2007). Moreover, kinetically-promoted (mass dependent) Tl isotopic fractionation during Tl sorption onto clay minerals, if present, should lead to preferential incorporation of ^{203}Tl rather than ^{205}Tl, leading to a shift to a lighter isotopic signature than in the source material (Wiederhold, 2015).

In both the meadow and forest soil profiles, ε^{205}Tl increased from the C horizons (+2.6, +0.8) to the Bw horizons (+8.7) (Fig. 1, Table 1). This trend pointed to preferential accumulation of heavier ^{205}Tl as a result of soil weathering processes. Nielsen et al. (2013) document a substantial increase in the fraction of ^{205}Tl during Tl uptake by hexagonal K-birnessite; the magnitude of fractionation (α) reaching up to 1.0015 at low Tl solution concentrations where oxidative Tl sequestration was assumed to dominate Tl sorption, an assumption confirmed by recent spectroscopic work (Wick et al., 2019). This process has previously been proposed as the origin of highly-positive ε^{205}Tl anomalies in sedimentary or soil systems (Howarth et al., 2018; Kersten et al., 2014; Nielsen et al., 2013; Peacock and Moon, 2012; Rehkämper et al., 2004; Vaněk et al., 2016, 2018). Although Tl(I) may also be adsorbed non-oxidatively on Mn-oxides (Nielsen et al., 2013; Vaněk et al., 2010), non-oxidative Tl uptake is not assumed to cause substantial Tl isotopic fractionation (Nielsen et al., 2013; Schauble, 2007). The chemical extractions (oxalate-extractable Tl; reducible Tl) suggested that less than 10% of the Tl in the Bw and C horizon samples was associated with Mn-oxides. Indeed, oxidative accumulation of Tl in soil Mn-concretions in the Erzmatt soil samples has previously been documented using micro-XAS, but bulk XAS analyses indicated that Tl-binding to Mn-oxides was quantitatively less relevant than Tl sequestration by illite (or other mica-type clay minerals) (Voegelin et al., 2015). We therefore conclude that the process, which resulted in the ^{205}Tl enrichment in the B horizons of the soil profiles is linked to repeated Tl mobilization and immobilization processes linked to regular reduction/oxidation cycles over the period of the parent rock weathering and subsequent soil formation. Such a prediction favors a redoximorphic feature of the studied soils (Voegelin et al., 2015). Oxidative Tl uptake associated with ^{205}Tl enrichment, continual weathering of the Tl(III)-containing phases, including Mn-oxides, followed by Tl(I) remobilization (enriched in ^{205}Tl) are suggested to be responsible for the migration/entry of the heavy Tl isotope fraction into other phases, mainly illite. This is in line with the Tl isotopic data obtained for the exchangeable soil Tl pool (Table S6, Supplementary Material), indicating preferential introduction of the lighter Tl isotope fraction into "labile" soil Tl complex, and again by contrast the accumulation of isotopically heavy Tl in the residual Tl pool, i.e., where Tl is strongly bound (illite).

Although the Erzmatt soils are "young" (10,000 to 100,000 years) relative to lateritic soil profiles for which redox-driven ^{205}Tl accumulation has previously been inferred (Howarth et al., 2018), the process might still be fast enough relative to the period of soil formation. The highest ε^{205}Tl values of +12.5/+12.6 which were measured in the sample P3 20–40 with 50% Tl(III) and the sample P1 00–20 with only Tl(I)-illite (Table 3) clearly support the notion that the redox Tl cycling may control the accumulation of ^{205}Tl in soil and, in parallel, also Tl(I) incorporation into the pedogenic illite.

In both the meadow and forest soil profiles, the ε^{205}Tl value decreased from the Bw over the Ah horizon to the organic soil horizons (Fig. 1). The enrichment in light ^{203}Tl in whole plants or specific plant parts relative to the substrate has already been documented (Kersten et al., 2014; Rader et al., 2019; Vaněk et al., 2019). The observed trend was therefore attributed to preferential uptake of light ^{203}Tl by plants and its accumulation in the topmost soil layers, including its binding to SOM in readily available form (Vaněk et al., 2016, Vaněk et al., 2018). Conversely, preferential uptake of ^{203}Tl by plants and its enrichment in the O and Ah horizons could also contribute to the enrichment of ^{205}Tl in the Bw horizons, in addition to ^{205}Tl enrichment due to redox-driven oxidative Tl uptake by e.g. Mn-oxides.

4. Conclusions

In this study, we combined stable Tl isotope measurements with chemical extractions and XAS speciation data to evaluate whether Tl isotopic patterns can be linked to geochemical processes present in soils (or sediments). Our results show that weathering processes/soil formation may lead to the accumulation of the heavy ^{205}Tl isotope. However, this ^{205}Tl enrichment is not reflected in changes in the Tl chemical extractability and speciation, probably because the isotopic accumulation process is complex, i.e., may be controlled by regular redox Tl cycling over the course of pedogenesis, and thus, unrelated to actual "speciation" data. This probably also allows the accumulation of ^{205}Tl in other phases, such as illite (a dominant Tl host), for which preferential uptake of ^{205}Tl is not expected. Preferential uptake of ^{203}Tl by plants and related effects on vertical enrichment and depletion of ^{203}Tl and ^{205}Tl may further complicate the situation. Accordingly, no simple correlations between Tl isotopic patterns and variations in bulk Tl chemistry and speciation can be observed.

To gain further insights into processes and mechanisms determining Tl isotopic patterns in soils, studies are required to determine the isotopic fractionation factors for individual chemical processes, such as Tl adsorption and incorporation by micaceous clay minerals, carbonates, Fe-oxides or even SOM. The question of the role or degree of these potential soil constituents in the isotopic fractionation during Tl absorption is mostly not fully clear. Therefore, the analysis and interpretation of the isotopic patterns in soils should be extended to the individual Tl host minerals/phases or well-designed chemical extracts targeting these specific Tl pools. However, for example, the approach involving redox-driven Tl mobilization with subsequent Tl isotope analysis in respective solutions, i.e., involving reductive/oxidative Tl leaching, must be omitted, since this would produce artificial isotopic fractionation unrelated to real isotopic data.

Declaration of Competing Interest

The authors declare that they have no known competing financial interests or personal relationships that could have appeared to influence the work reported in this paper.

Acknowledgements

This work was funded by the Czech Science Foundation (Projects 17-03211S and 19-08614S) and the European Regional Development Fund (Project CZ.02.1.01/0.0/0.0/16_019/0000845). Part of the equipment used for this study was purchased from Operational Programme Prague – Competitiveness (Project CZ.2.16/3.1.00/21516). The Charles University team was partly supported by institutional funding from the Center for Geosphere Dynamics (UNCE/SCI/006). The Swiss Light Source (Paul Scherrer Institute, Switzerland) is acknowledged for providing the beamtime at the SuperXAS beamline. Dr. Madeleine Štulíková (a native speaker) is thanked for revision of the English manuscript. We also wish to acknowledge the anonymous three reviewers for their help with the modification of the original manuscript version.

Appendix A. Supplementary data

Supplementary data to this article can be found online at https://doi.org/10.1016/j.geoderma.2020.114183.

References

Aguilar-Carrillo, J., Herrera, L., Gutiérrez, E.J., Reyes-Domínguez, I.A., 2018. Solid-phase distribution and mobility of thallium in mining-metallurgical residues: Environmental hazard implications. Environ. Pollut. 243, 1833–1845. https://doi.org/10.1016/j.envpol.2018.10.014.

Baker, R.G.A., Rehkämper, M., Hinkley, T.K., Nielsen, S.G., Toutain, J.P., 2009. Investigation of thallium fluxes from subaerial volcanism–Implications for the present and past mass balance of thallium in the oceans. Geochim. Cosmochim. Acta 73 (20), 6340–6359. https://doi.org/10.1016/j.gca.2009.07.014.

Gomez-Gonzalez, M.A., Garcia-Guinea, J., Laborda, F., Garrido, F., 2015. Thallium occurrence and partitioning in soils and sediments affected by mining activities in Madrid province (Spain). Sci. Total Environ. 536, 268–278. https://doi.org/10.1016/j.scitotenv.2015.07.033.

Grösslová, Z., Vaněk, A., Oborná, V., Mihaljevič, M., Ettler, V., Trubač, J., Drahota, P., Penížek, V., Pavlu, L., Sracek, O., Kříbek, B., Voegelin, A., Göttlicher, J., Ondřej, D., Tejnecký, V., Houška, J., Mapani, B., Zádorová, T., 2018. Thallium contamination of desert soil in Namibia: chemical, mineralogical and isotopic insights. Environ. Pollut. 239, 272–280. https://doi.org/10.1016/j.envpol.2018.04.006.

Hermann, J., Voegelin, A., Palatinus, L., Mangold, S., Majzlan, J., 2018. Secondary Fe-As-Tl mineralization in soils near Buus in the Swiss Jura Mountains. Eur. J. Mineral. 30, 887–898. https://doi.org/10.1127/ejm/2018/0030-2766.

Hettman, K., Kreissig, K., Rehkämper, M., Wenzel, T., Mertz-Kraus, R., Markl, G., 2014. Thallium geochemistry in the metamorphic Lengenbach sulfide deposit, Switzerland: thallium-isotope fractionation in a sulfide melt. Am. Mineral. 99, 793–803. https://doi.org/10.2138/am.2014.4591.

Howarth, S., Prytulak, J., Little, S.H., Hammond, S.J., Widdowson, M., 2018. Thallium concentration and thallium isotope composition of lateritic terrains. Geochim. Cosmochim. Acta 239, 446–462. https://doi.org/10.1016/j.gca.2018.04.017.

Jakubowska, M., Pasieczna, A., Zembrzuski, W., Swit, Z., Lukaszewski, Z., 2007. Thallium in fractions of soil formed on floodplain terraces. Chemosphere 66, 611–618. https://doi.org/10.1016/j.chemosphere.2006.07.098.

Karbowska, B., Zembrzuski, W., Jakubowska, M., Wojtkowiak, T., Pasieczna, A., Lukaszewski, Z., 2014. Translocation and mobility of thallium from zinc–lead ores. J. Geochem. Explor. 143, 127–135. https://doi.org/10.1016/j.gexplo.2014.03.026.

Kersten, M., Xiao, T., Kreissig, K., Brett, A., Coles, B.J., Rehkämper, M., 2014. Tracing anthropogenic thallium in soil using stable isotope compositions. Environ. Sci. Technol. 48 (16), 9030–9036. https://doi.org/10.1021/es501968d.

Liu, J., Wang, J., Chen, Y., Xie, X., Qi, J., Lippold, H., Luo, D., Wang, C., Su, L., He, L., Wu, Q., 2016. Thallium transformation and partitioning during Pb − Zn smelting and environmental implications. Environ. Pollut. 212, 77–89. https://doi.org/10.1016/j.envpol.2016.01.046.

Liu, J., Yin, M., Luo, X., Xiao, T., Wu, Z., Li, N., Wang, J., Zhang, W., Lippold, H., Belshaw, N.S., Feng, Y., Chen, Y., 2019. The mobility of thallium in sediments and source apportionment by lead isotopes. Chemosphere 219, 864–874. https://doi.org/10.1016/j.chemosphere.2018.12.041.

Nielsen, S.G., Wasylenki, L.E., Rehkämper, M., Peacock, C.L., Xue, Z., Moon, E.M., 2013. Towards an understanding of thallium isotope fractionation during adsorption to manganese oxides. Geochim. Cosmochim. Acta 117, 252–265. https://doi.org/10.1016/j.gca.2013.05.004.

Nielsen, S.G., Rehkämper, M., Prytulak, J., 2017. Investigation and application of thallium isotope fractionation. Rev. Mineral. Geochemistry 82, 759–798. https://doi.org/10.2138/rmg.2017.82.18.

Pansu, M., Gautheyrou, J., 2006. Handbook of Soil Analysis: Mineralogical, Organic and Inorganic Methods. Springer-Verlag:, Berlin, Heidelberg, Germany.

Peacock, C.L., Moon, E.M., 2012. Oxidative scavenging of thallium by birnessite: Explanation for thallium enrichment and stable isotope fractionation in marine ferromanganese precipitates. Geochim. Cosmochim. Acta 84, 297–313. https://doi.org/10.1016/j.gca.2012.01.036.

Peter, A.L.J., Viraraghavan, T., 2005. Thallium: a review of public health and environmental concerns. Environ. Int. 31 (4), 493–501. https://doi.org/10.1016/j.envint.2004.09.003.

Prytulak, J., Nielsen, S.G., Plank, T., Barker, M., Elliot, T., 2013. Assessing the utility of thallium and thallium isotopes for tracing subduction zone inputs to the Mariana arc. Chem. Geol. 345, 139–149. https://doi.org/10.1016/j.chemgeo.2013.03.003.

Rader, S., Maier, R.M., Barton, M., Mazdab, F., 2019. Uptake and fractionation of thallium by Brassica juncea in geogenic thallium-amended substrate. Environ. Sci. Technol. 53 (5), 2441–2449. https://doi.org/10.1021/acs.est.8b06222.

Rauret, G., López-Sánchez, J.F., Sahuquillo, A., Barahona, E., Lachica, M., Ure, A.M., Davidson, C.M., Gomez, A., Lück, D., Bacon, M., Yli-Halla, M., Muntau, H., Quevauviller, Ph., 2000. Application of a modified BCR sequential extraction (three-step) procedure for the determination of extractable trace metal contents in a sewage sludge amended soil reference material (CRM 483), complemented by a three-year stability study of acetic acid and EDTA extractable metal content. J. Environ. Monitor. 2, 228–233. https://doi.org/10.1039/B001496F.

Rehkämper, M., Frank, M., Hein, J.R., Halliday, A., 2004. Cenozoic marine geochemistry of thallium deduced from isotopic studies of ferromanganese crusts and pelagic sediments. Earth Planet. Sci. Lett. 219, 77–91. https://doi.org/10.1016/S0012-821X(03)00703-9.

Schauble, E.A., 2007. Role of nuclear volume in driving equilibrium stable isotope fractionation of mercury, thallium, and other very heavy elements. Geochim. Cosmochim. Acta 71, 2170–2189. https://doi.org/10.1016/j.gca.2007.02.004.

Vaněk, A., Grygar, T., Chrastný, V., Tejnecký, V., Drahota, P., Komárek, M., 2010. Assessment of the BCR sequential extraction procedure for thallium fractionation using synthetic mineral mixtures. J. Hazard. Mater. 176, 913–918. https://doi.org/10.1016/j.jhazmat.2009.11.123.

Vaněk, A., Grösslová, Z., Mihaljevič, M., Trubač, J., Ettler, V., Teper, L., Cabala, J., Rohovec, J., Zádorová, T., Penížek, V., Pavlů, L., Holubík, O., Němeček, K., Houška, J., Drábek, O., Ash, C., 2016. Isotopic tracing of thallium contamination in soils affected by emissions from coal-fired power plants. Environ. Sci. Technol. 50 (18), 9864–9871. https://doi.org/10.1021/acs.est.6b01751.

Vaněk, A., Grösslová, Z., Mihaljevič, M., Ettler, V., Trubač, J., Chrastný, V., Penížek, V., Teper, L., Cabala, J., Voegelin, A., Zádorová, T., Oborná, V., Drábek, O., Holubík, O., Houška, J., Pavlů, L., Ash, C., 2018. Thallium isotopes in metallurgical wastes/contaminated soils: A novel tool to trace metal source and behavior. J. Hazard. Mater. 343, 78–85. https://doi.org/10.1016/j.jhazmat.2017.09.020.

Vaněk, A., Holubík, O., Oborná, V., Mihaljevič, M., Trubač, J., Ettler, V., Pavlů, L., Vokurková, P., Penížek, V., Zádorová, T., Voegelin, A., 2019. Thallium stable isotope fractionation in white mustard: Implications for metal transfers and incorporation in plants. J. Hazard. Mater. 369, 521–527. https://doi.org/10.1016/j.jhazmat.2019.02.060.

Voegelin, A., Pfenninger, N., Petrikis, J., Majzlan, J., Plötze, M., Senn, A.C., Mangold, S., Steininger, R., Göttlicher, J., 2015. Thallium speciation and extractability in a thallium- and arsenic-rich soil developed from mineralized carbonate rock. Environ. Sci. Technol. 49 (9), 5390–5398. https://doi.org/10.1021/acs.est.5b00629.

Wick, S., Baeyens, B., Marques Fernandes, M., Voegelin, A., 2018. Thallium adsorption onto illite. Environ. Sci. Technol. 52 (2), 571–580. https://doi.org/10.1021/acs.est.7b04485.

Wick, S., Peña, J., Voegelin, A., 2019. Thallium sorption onto manganese oxides. Environ. Sci. Technol. 53 (22), 13168–13178. https://doi.org/10.1021/acs.est.9b04454.

Wiederhold, J.G., 2015. Metal stable isotope signatures as tracers in environmental geochemistry. Environ. Sci. Technol. 49, 2606–2624. https://doi.org/10.1021/es504683e.